



FACULTY OF SCIENCES

Antiviral Activity of Camelid Single Domain Antibodies Targeting the Neuraminidase of H5N1 Influenza Virus

Francisco Miguel Lopez Cardoso

Thesis submitted in partial fulfillment of the requirements for the degree of Doctor in Sciences,
Biotechnology

Promotor: Prof. Dr. Xavier Saelens

Co-promotors: Prof. Dr. Ann Depicker², Prof. Dr. Serge Muyldermans

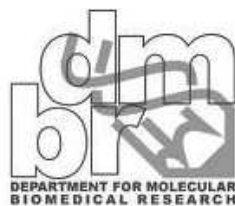
Academic year

2012 – 2013

Faculty of sciences, Ghent university

Department of Biomedical Molecular Biology

Department of Plant Systems Biology



Nothing of this thesis may be reproduced or published in any way without prior permission of the author.

Francisco Miguel Lopez Cardoso

Antiviral Activity of Camelid Single Domain Antibodies Targeting the Neuraminidase of H5N1 Influenza Virus

Francisco Miguel Lopez Cardoso

Unit of Molecular Biology ^{1,2}

Promoter: Prof. Dr. Xavier Saelens ¹

Co-promoters: : Prof. Dr. Ann Depicker ², Prof. Dr. Serge Muyldermans ³

Examination committee:

Chairman:

Prof. Dr. Johan Grooten ¹

Reading commission:

Prof. Dr. Kristien van Reeth ⁴

Dr. Roosmarijn Vandenbrouke ¹

Prof. Dr. Lieve Naesens ⁵

Dr. Peter Vanlandschoot ⁶

Other members:

Prof. Dr. Han Remaut ⁷

Dr. Bert Schepens ¹

¹ Department for Molecular Biomedical Research, VIB, Ghent University

² Department of Plant Systems Biology, VIB, Ghent University

³ Laboratory of Cellular and Molecular Immunology (CMIM), VIB
Free University of Brussels

⁴ Laboratory of Virology, Department Virology, Parasitology and Immunology
Faculty of Veterinary Medicine, Ghent University

⁵ Laboratory of Virology and Chemotherapy, Rega Institute, Catholic University of Leuven, Belgium

⁶ N-Spire, Bellem, Belgium

⁷ VIB Laboratory of Structural and Molecular Microbiology, VIB, Free University of Brussels, Belgium

LIST OF ABBREVIATIONS:

Ab	<u>A</u> ntib <u>o</u> dies
AcNPV	<u>A</u> utogra <u>f</u> a <u>c</u> alifornia <u>N</u> uclear <u>P</u> oliedrosis <u>V</u> irus
AD	<u>A</u> ntigenic <u>D</u> rift
ADCC	<u>A</u> ntibody <u>D</u> ependant <u>C</u> ellular <u>C</u> ytotoxicity
AA	<u>A</u> mino <u>A</u> cid
cRNA	antigenomic <u>c</u> opy <u>R</u> NA
CH1-3	<u>C</u> onstant <u>H</u> eavy Regions 1-3
CDC	<u>C</u> omplement- <u>D</u> ependent <u>C</u> ytotoxicity
CDR	<u>C</u> omplementary <u>D</u> etermining <u>R</u> egion
CL	<u>C</u> onstant <u>L</u> ight region
DRiP	<u>D</u> efective <u>R</u> ibosomal <u>P</u> roducts
FR	<u>F</u> ramework <u>R</u> egion
HA	<u>H</u> emagglutinin
HA ₀	<u>H</u> A precursor
Hap	<u>H</u> ydroxyapatite
HCAb	<u>H</u> eavy <u>C</u> hain <u>A</u> ntib <u>o</u> dies
HPAIV	<u>H</u> ighly <u>P</u> athogenic <u>I</u> nfluenza <u>A</u> <u>V</u> irus
IAV	<u>I</u> nfluenza <u>A</u> <u>V</u> irus
IgG	<u>I</u> mmunoglobulin <u>G</u>
M1	<u>M</u> atrix protein <u>1</u>

M2	<u>M</u> atrix protein <u>2</u>
M2e	<u>M2</u> <u>e</u> xternal domain
moi	<u>m</u> ultiplicity <u>o</u> f <u>i</u> nfection
N1rec	H5 <u>N1</u> A/Crested Eagle/Belgium/09/2004 NA <u>r</u> ecombinant protein
N1-VHHb	Bacteria-produced <u>b</u> ivalent <u>VHH</u> directed against <u>N1</u> rec
N1-VHH-Fc	Plant-produced bivalent <u>Fc</u> linked <u>VHH</u> directed against <u>N1</u> rec
N1-VHHm	<u>m</u> onovalent <u>VHH</u> directed against <u>N1</u> rec
NA	<u>N</u> eur <u>a</u> minidase
NS2	<u>N</u> on <u>S</u> tructural Protein <u>2</u>
NEP	<u>N</u> uclear <u>E</u> xport <u>P</u> rotein
qPCR	<u>q</u> uantitative <u>P</u> CR <u>A</u> c
-ssRNA	negative stranded <u>R</u> NA
Sia	<u>S</u> ialic <u>a</u> cid
Siac	<u>S</u> ialic <u>a</u> cid <u>c</u> onjugates
SPR	<u>S</u> urface <u>P</u> lasmon <u>R</u> esonance
SN	<u>S</u> upernatant
Sf9	<i>Spodoptera frugiperda</i> continuous cell line substrain
TCID ₅₀	<u>T</u> issue <u>C</u> ulture <u>I</u> nfectious <u>D</u> ose 50
VH	<u>V</u> ariable <u>H</u> eavy <u>R</u> egion
VHH	<u>V</u> ariable single <u>H</u> eavy chain domain <u>H</u> CAb
VL	<u>V</u> ariable <u>L</u> ight

Table of contents:

Chapter 1. INTRODUCTION	7
1.1 HISTORICAL IMPACT OF INFLUENZA VIRUS	7
1.2 CLASSIFICATION	9
1.3 GENOME	11
1.4 INFLUENZA VIRUS PROTEINS	14
1.5 REPLICATION CYCLE	15
1.5.1 ENTRY	16
1.5.2 GENOME REPLICATION	16
1.5.3 VIRION RELEASE	17
1.6 HEMAGGLUTININ	20
1.7 NEURAMINIDASE	23
1.8 INFLUENZA ANTIVIRALS	31
1.9 ANTIBODIES	39
1.9.1 CONVENTIONAL ANTIBODIES	39
1.9.2 SINGLE VARIABLE DOMAIN OF THE HEAVY CHAIN ANTIBODIES	40
1.9.3 NEURAMINIDASE-SPECIFIC ANTIBODIES	45
1.9.4 N9 mAb NC41 AND NC10	48
1.9.5 N2 mAb Mem5	50
Chapter 2. AIMS	55
2.1 SCOPE	55
2.2 OBJECTIVES	57
Chapter 3. RESULTS	58
CAMELID SINGLE CHAIN ANTIBODIES TARGETING NEURAMINIDASE PROTECT AGAINST H5N1 CHALLENGE VIRUS	58
ADDITIONAL DATA	130

Chapter 4. GENERAL DISCUSSION	134
PERSPECTIVES	140
Chapter 5. SUMMARY	141

Chapter 1: INTRODUCTION

1.1 HISTORICAL IMPACT OF INFLUENZA VIRUS

The Influenza A Virus (IAV) has caused several pandemics during the 20th century, and continues to cause annual epidemics and pandemics. Both pandemics and epidemics represent a significant economic burden owing to costs of prevention, treatment, absenteeism, and excess hospitalizations. Besides infection in humans, the IAV is also a pathogen in several animals, including pigs and birds. Wild aquatic birds like ducks, geese, terns or gulls (*Anseriformes* and *Charadriiformes*) are considered to be natural reservoirs of IAV. The transmission of IAV to poultry (e.g. *Galliformes*) results in two pathotypes: low pathogenicity IAV and Highly Pathogenic Influenza A Virus (HPAIV). To date, the HPAIV has been caused only by IAV viruses of the H5 and H7 subtypes, resulting in a severe and systemic infection, with close to 100% of lethality in poultry. The first avian HPAIV fatal infections in humans were reported in Hong Kong in 1997 (Claas et al., 1998; Subbarao et al., 1998), where culling was an efficient strategy to control this outbreak. In 2003, the reports of HPAIV human cases resulted in a worldwide alert (60% of mortality rate) but fortunately, human-human transmission did not occur or was extremely rare (Chotpitayasunondh et al., 2005). In 2009, outbreaks of respiratory illness caused by IAV were reported in Mexico (Fraser et al., 2009). Later the IAV identified was a novel swine-origin H1N1, followed by outbreaks globally and leading to an official declaration by the World Health Organization on June of 2009 of a pandemic IAV. Nevertheless, most of patients presented a mild infection and do not required hospitalization.

These data and the fact that the pandemic H1N1 was a triple reassortant, from swine North American H3N2 and H1N2 with Eurasian avian-like H1N1 swine IAV (Garten et al., 2009),

highlighted the importance of zoonotic diseases preparedness. The pandemic swine H1N1 became the first pandemic of this century and caused global alert, since presented a high transmissibility in humans, raising concern about further pathogenicity (Smith et al., 2009; Zimmer and Burke, 2009). Nevertheless, the pandemic H1N1 low lethality seems to be underestimated. From spring 2009 to summer 2010, the pandemic H1N1 death toll was estimated in 18 500, but recent reports contrast significantly, with an estimated 10 – 15 fold higher death toll, according to a recent report (WHO, Pandemic (H1N1) 2009–update 112, www.who.int/csr/don/2010_08_06/en/index.html), (Dawood et al., 2012), highlighting the lack of proper surveillance.

The “Spanish Flu” pandemic during 1918-1919 caused the highest recorded death toll by any infectious disease in the history, with a conservative estimate of 50 million deaths (Johnson and Mueller, 2002). In the 21st century, the work by Taubenberger resulted in the sequence of the genome of the “Spanish Flu” virus that caused the 1918 pandemic (H1N1 A/Brevig Mission/1/1918) (Taubenberger et al., 1997; Taubenberger et al., 2005). Later it was revealed that 1918 pandemic IAV was closer to mammalian than to avian IAV (Taubenberger et al., 2007). These studies resulted into the so called “resurrection” of the 1918 pandemic virus, one of the deadliest infectious agents in history, provoking public and governmental concern, demonstrating the profound effects of one single IAV pandemic in the society even after more than 80 years of occurrence. Three other IAV pandemics took place in the 20th century: the Asian flu (H2N2, 1957), the Hong Kong Flu (H3N2, 1968), and the Russian Flu (H1N1, 1977) (Kawaoka et al., 1989; Horimoto and Kawaoka, 2005; Tumpey et al., 2005). The Asian and Hong Kong pandemic IAV were genetically related to the descendants of the Spanish flu virus but had acquired avian genes by gene reassortment process. Such a reassortment is possible, *i.e.* by co-infection of avian and human IAV in one host (presumably a mammalian host that is susceptible to both human and avian IAV such as the pig), producing a virus with mixed viral

RNA segments of both IAV (Fang et al., 1981). This process generally yields a highly virulent virus to the reassortment host. For example, the IAV of 1957 acquired avian PB1, HA and NA gene segments, and the virus of 1968, the HA and PB1 genes were also from avian origin. The process of reassortment is not the only factor contributing to the virulence of a pandemic IAV, it is suspected that the human to human transmissibility of the “Spanish Flu” 1918 virus was obtained by a mutations in the mutation in the HA gene (E190D and D225) (Glaser et al., 2005; Stevens et al., 2006).

On the other hand, the seasonal IAV epidemics have widespread impacts, infecting 250-500 million people each year, leading to 250.000-500.000 deaths, reaching a peak of morbidity during winter months in moderate climate zones (www.who.int/mediacentre/factsheets/fs211/en/index.html). The elderly (over 65 years), the very young (less than 2 years) and the immuno-compromised patients are particularly susceptible to more severe respiratory disease and death due to IAV infection. A commercial vaccine formulation against the seasonal IAV is available in developed countries, but it is non-optimal and raises polemic about its sustainability. In addition, the possibility of contribution of the HPAIV to seasonal IAV epidemics remains a constant worldwide threat.

1.2 CLASSIFICATION

The influenza virus represents three of the six genera from the *Orthomyxoviridae* family, has a segmented, single-stranded, negative sense RNA genome (-ssRNA) complexed as vRNPs, encapsidated in a matrix shell that is enveloped by a lipid bilayer (see section 1.5), and is subdivided into three different genera: influenza A, B and C viruses (Bouvier and Palese, 2008). This classification is based on the identity of the major internal protein antigens such as Nucleoprotein (NP) and Matrix protein 1 M1 (Horimoto and Kawaoka, 2001). The IAV genera

can be further classified into subtypes according to the serological reactivity of its major surface glycoproteins Neuraminidase (NA) and Hemagglutinin (HA). All different genetic subtypes of IAV, 16 for HA and 9 for NA, are maintained in a vast natural reservoir of wild waterfowls and shorebirds, from which they emerge to cause disease in domestic poultry, horses, pigs and humans (Fouchier et al., 2005). Although all subtypes are continuously replicating usually asymptotically, in the intestines of their natural avian hosts, only four HA (H1, H2, H3 and rarely H5, H7 and H9) and two NA (N1 and N2) subtypes, and are known to cause human IAV infections, since the characterization of isolates in 1933 (Webster et al., 1978; Webster et al., 1992).

In contrast, influenza B and C viruses infect primarily humans, but there have been also examples of transmission to other hosts (influenza B viruses in seals) (Osterhaus et al., 2000; Steinhauer and Skehel, 2002). In contrast to influenza A viruses, influenza B and C viruses do not have a natural reservoir from which they can recruit novel surface antigens. As a consequence, they undergo only gradually antigenic variation. However, the genome of influenza B viruses mutates frequently enough, making long-lasting immunity following infection or vaccination impossible. In addition, strains of one of the two antigenically distinct lineages (Victoria and Yamagata lineage) are currently included in the formulation of influenza vaccines. Influenza C virus is the most stable and outbreaks are typically local and do not become large epidemics or global pandemics. In addition, a standard nomenclature is followed, in which the virus genus is described first, followed by the host species (omitted if human origin), the geographical origin, strain number and year of isolation. For the influenza A viruses, this is followed by the HA and NA subtype between brackets, *i.e.* A/crested eagle/Belgium/01/2004 (H5N1).

In humans, the IAV (H3N2 and H1N1) and B viruses are of epidemiological interest, since they cause recurrent seasonal influenza epidemics, and are therefore also the constituents of the

annual inactivated or live-attenuated influenza vaccines. For example the 2012 - 2013 recommended influenza vaccine composition includes: A/California/7/2009 (H1N1), A/Victoria/361/2011 (H3N2) and B/Wisconsin/1/2010.

1.3 GENOME

The genome of IAV is composed of 8 negative sense single-stranded viral RNA (-ssRNA) segments comprising about 14 kb, which encodes 12 viral proteins, including a newly discovered overlapping protein encoded in the segment 3 of the genome, called PA-X (Jagger et al., 2012). The influenza genome segments contain cis-acting packaging signals that mediate the specific packaging of a full genome in an orderly fashion within the virus particle (Fujii et al., 2003; Hutchinson et al., 2010). The numbering of the different genome segments is based on their decreasing length. These -ssRNAs are transcribed in 8 positive stranded messenger RNAs (mRNAs), which are translated in 12 proteins (Figure 1A) (Wise et al., 2009b). Each -ssRNA segment encodes one or two proteins, making use of alternative splicing or shifted reading frames (Steinhauer and Skehel, 2002).

The viral RNA-dependent RNA-polymerase is error prone with a mutation rate of over 5×10^{-5} average mutation rate per base pair per replication cycle, because it does not have proof-reading activity to prevents replication errors (Drake, 1993). This relatively high mutation rate (almost one nucleotide exchange per genome per replication) leads to the accumulation of point mutations and subsequent amino acid replacements during the virus propagation in the host species. As a result of these mutations, a heterogeneous viral population is produced, and if a selective pressure (*i.e.* antiviral drugs) is present during the replication process, selection of escape-mutants can occur. For example, IAV escape-mutants can present insensitivity to an antiviral drug, antibody binding abolished, or no longer be recognized by cytotoxic CD8 T-cells.

The change of the antigenic properties of the membrane glycoproteins HA and/or NA, mainly due to Ab pressure, is called Antigenic Drift (AD) (Ferguson et al., 2003). Therefore, changes in antigenic properties caused by AD are possible every replication cycle. During AD in HA, a number of AA sequence changes can take place close to the receptor-binding site, which may influence the binding affinity and specificity and lead to adaptation to a new host (Hensley et al., 2009). Genetic recombination between different viral strains infecting the same host may also be a source for antigenic alteration. On the other hand, the replacement of complete RNA segments encoding for HA and NA between different subtypes influenza A viruses leads to abrupt changes in these antigenic determinants and is called Antigenic Shift (AS), resulting in reassortant virus (Rohde and Scholtissek, 1980; Rohm et al., 1996) (Webster and Hulse, 2004). The variation in antibody binding sites in HA and NA created by AD or even AS over time, permits virus evasion from the human immune system. One consequence of this process is the well-known yearly formulation of IAV vaccines for humans. Reassortment in the other six genes also plays a role in the evolution of the IAV, but less is known about their pathogenicity (Lindstrom et al., 1998). In contrast to AD, AS is relatively rare, but is important in the emergence of pandemics in human populations, being able to produce antigenically new viruses in the human population.

The presence of AS in zoonotic human infections poses a potentially pandemic threat. It has been reported that mutations at the receptor-binding site of HA are necessary to cross the interspecies barrier between birds and humans. The human airway epithelium contains receptors for human and avian viruses, the first on non-ciliated cells and the latter on ciliated cells, localized in the upper and lower human respiratory tract, respectively (Matrosovich et al., 2004b). The pigs are candidates to be a potential pandemic intermediate host, since the epithelial cells of pigs trachea co-express α 2,3-linked SA and α 2,6-linked SA on the epithelial cells of their trachea, making them susceptible to co-infection by avian and human IAV

(Scholtissek et al., 1985; Ito et al., 1998; Kobasa et al., 1999; Van Reeth, 2007; Nidom et al., 2010). As mentioned above, the recent pandemic H1N1 swine flu of 2009 evidences the role of animal host as a potential source of pandemic IAV.

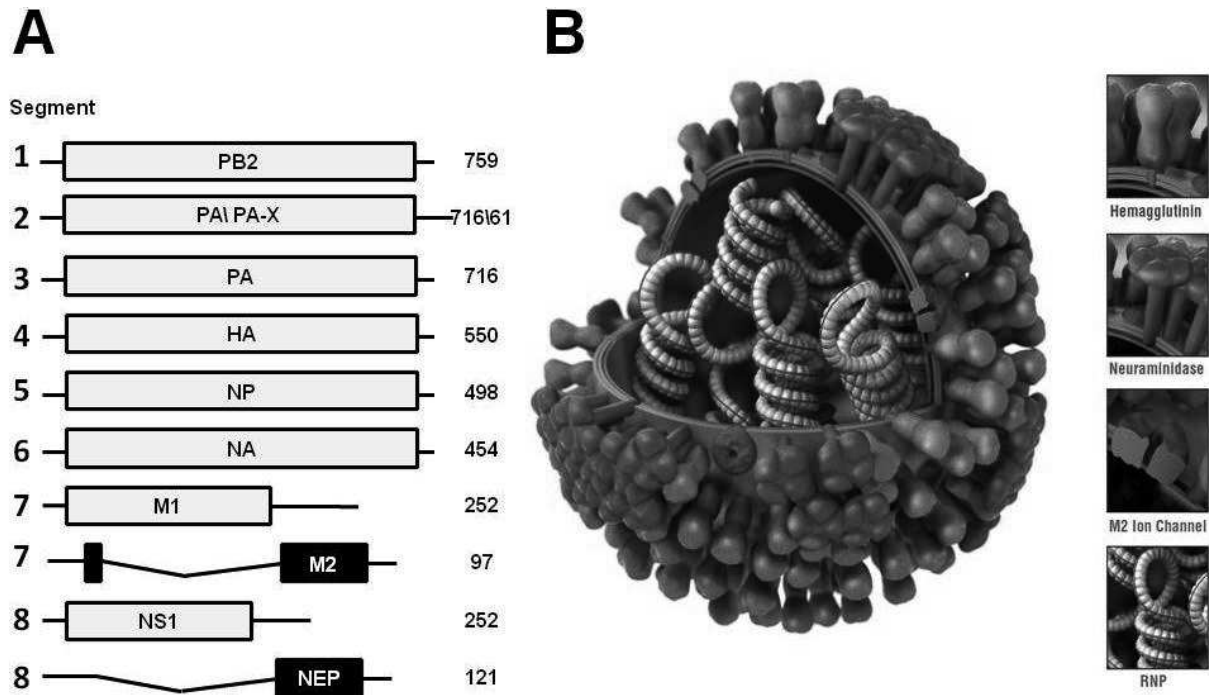


Figure 1. Graphic representation of the Influenza virus protein coding sequences and the virion. **A.** The gray boxes depict the coding sequences for the 12 viral proteins, organized in 8 negative-sense single stranded RNA genomic segments. The numbers at the boxes flanks indicate: (left) the genome segment that encodes the protein; (right) the protein amino acid sequence length. **B.** The virion consists of a core with the RNP-complex, encapsidated by a lipid bilayer with the embedded membrane proteins Hemagglutinin (HA, blue), the sialidase Neuraminidase (NA, red) and the ion channel M2 protein (M2, magenta). The RNP-complex consists of the 8 genomic segments in complex with the proteins M1, PB1, PB2 and PA. (figure 1B taken from <http://www.cdc.gov/media/subtopic/library/diseases.htm> PHIL ID #11822).

1.4 INFLUENZA VIRUS PROTEINS

The three integral membrane proteins are: the receptor binding Hemagglutinin (HA), the sialidase Neuraminidase (NA) and the Matrix ion channel protein 2 (M2). The most abundant membrane protein, HA, is a homotrimeric type I transmembrane glycoprotein and is important early in the viral infection cycle by binding to the N-acetylneuraminic acid or Sialic acid (Sia) residues on the host cell and facilitating fusion between the viral envelope and the endosomal membrane (Wilson et al., 1981). The NA is a homotetrameric type II transmembrane glycoprotein and is critical for the release of virus particles from the cell surface and the spread of the virus (Hogue and Nayak, 1994). The HA and NA proteins are the major antigenic determinants of the influenza viruses. The less abundant matrix M2 ion channel is a small homotetrameric type III transmembrane protein with proton channel activity, enabling activation of the membrane fusion function of HA and uncoating and disassembly of the virus during the initial stages of infection (Pinto et al., 1992). The cytoplasmic tail of the M2 protein also plays a role in virus assembly (Iwatsuki-Horimoto et al., 2006). The viral M1 supports the viral envelope and is the most abundant component of the virion and plays a pivotal role in the process of assembly and budding, and also envelops the viral RiboNucleoProtein-complex (vRNP). The Non Structural Protein 2 (NS2) mediates the export of newly synthesized vRNP from the nucleus, and is therefore also referred to as the Nuclear Export Protein (NEP) (Neumann et al., 2000). The vRNP-complex consists of the arginin-rich NucleoProtein (NP) and a heterotrimeric RNA-dependent RNA polymerase complex (RdRp) consisting of three proteins: two Polymerase Basic (PB1 and PB2) proteins and one Polymerase Acidic (PA), which bind to the terminal helical hairpin of each viral -ssRNA segment (see figure 2D). The PA-PB1-PB2 polymerase complex is responsible for transcribing the mRNA and for synthesizing positive-sense antigenomic copy RNA (cRNA) from which the newly produced -ssRNAs are transcribed and incorporated into new progeny viruses. The rest of the -ssRNA segment is coated with NP,

which has an overall positive charge, enabling it to bind to the negative-charged phosphate backbone from the -ssRNA (Compans et al., 1972; Murti et al., 1988; Baudin et al., 1994). The NP is also necessary for the synthesis of cRNAs and -ssRNAs to be recognized as template for the viral polymerase (Steinhauer and Skehel, 2002). Finally, there are also non structural IAV proteins, involved in cell regulation. The -ssRNA segment encoding PB1 has a small overlapping ORF, that encodes the small non-structural protein PB1-F2 which has a pro-apoptotic function, and the non-essential PB1-N40 protein, which may have an influence on virus replication and whose absence may be detrimental in some genetic backgrounds (Krug and Aramini, 2009; Wise et al., 2009a). The Non-Structural protein 1 (NS1) antagonizes interferon suppression and is abundantly present in the infected cell but is, together with PB1-F2, not incorporated in the virion (Takasuka et al., 2002).

1.5 REPLICATION CYCLE

Human influenza is usually transmitted via air droplets produced by coughs or sneezes, followed by mucosal contamination of the respiratory tract of a new host. In humans, the primary targets for IAV are the epithelial cells from the respiratory tract, and NA promotes virus access to these target cells by mucus degradation in the respiratory tract (Matrosovich et al., 2004a). In addition, decoy receptors on mucins, cilia and the glycocalyx of epithelium cells in human airways are removed by NA, hereby aiding virus invasion of the ciliated epithelium of human airways because these decoy receptors can no longer impede virus access to functional receptors on the surface membrane of target cells (Matrosovich et al., 2004a).

1.5.1 ENTRY

The IAV binds via HA to a Sia residue on the target cell, resulting in the IAV virion entering the infected cell in an endosome via endocytosis (Figure 2A). After attachment, virus particles are internalized by receptor-mediated clathrin-dependent and -independent endocytosis (Rust et al., 2004). After the endosome internalization and detachment of clathrin molecules, the tetrameric M2 ion channel pumps H⁺ ions from the acidic endosome into the interior of the virion, resulting in a pH of ca. 5.0 in the virion core. This causes dissociation of the -ssRNA from M1 by disruption of the low pH-sensitive interaction (Ciampor et al., 1992). This acidification leads to exposure of the buried, highly hydrophobic N-terminal fusion peptide of the HA2 subunit of each HA monomer. The fusion peptide inserts in the endosomal membrane, initiating fusion of viral and endosomal membranes, and the release of the viral RNPs (vRNPs) (Haque et al., 2005; Wagner et al., 2005) (Figure 2B).

1.5.2 GENOME REPLICATION

The vRNPs are released into the cytoplasm and are imported into the nucleus via Nuclear Localization Signals (NLS) into the NP protein, in importin α - β dependent pathway (Ozawa et al., 2007) (Figure 2C), where they are used as template for the production of cRNA and mRNA. Viral mRNA and cRNA synthesis occur by two distinct mechanisms (Nagata et al., 2008). Transcription of mRNA is dependent of a process called 'cap-snatching' from nuclear pre-mRNAs. The viral mRNA synthesis requires capped RNA primers, which are obtained by a process called cap-snatching (Plotch et al., 1979; Plotch et al., 1981). The PB2 subunit of the polymerase is involved in binding to the m⁷GpppXm cap structures from the host cell polymerase II. The PA has a cap-dependent endonuclease activity and cleaves off cap structures from the host cell pre-mRNAs, and thereby shuts down the synthesis of most host

proteins (Yuen and Wong, 2005; Dias et al., 2009). The fragments consist of a cap plus 10-13 extra nucleotides and serve as primers for the initiation of viral mRNA synthesis. Termination of mRNA synthesis occurs by iterative copy of stretch of U residues generating a poly (A) tail (Figure 2E). The viral mRNA shuttles back to the cytoplasm where it is translated into viral proteins. This requires NP to assure the switch from viral mRNA synthesis to cRNA replication (Newcomb et al., 2009). On the other hand, the cRNA in the nucleus serves as a template for the production of genomic –ssRNA. In contrast to viral mRNA synthesis, cRNA and -ssRNA replication is initiated without a primer (Figure 2E). The newly produced vRNP are recognized by the M1 protein, via M1-RNA and M1-NP interactions. The complex vRNP-M1 is recognized by the NLS-containing NEP protein. In a cellular export protein Crm1 (chromosome region maintenance 1) dependent pathway, the vRNP-M1-NEP complexes are transported to cytoplasm (Elton et al., 2001) (Figure 2F). The vRNP-M1 complexes are targeted to assembly sites, lipid rafts enriched by HA and NA proteins, in the cell membrane (Figure 2G).

1.5.3 VIRION RELEASE

The release of viruses from infected cells is promoted by NA, which cleaves the Sia residues from viral and cellular glycoconjugates, to which the newly formed viral particles are attached, thereby preventing HA-mediated self-aggregation and facilitating viral release (Air and Laver, 1989) (Figure 2H). The release of newly produced virions occurs approximately eight hours post-infection, either into the airway to find another cell to infect, or by aerosol droplets (*i.e.* during coughing or sneezing), permitting person-to-person transmission. Virus shedding typically continues for up to one week, after which a virus-specific antibody clearing can be present (Carrat et al., 2008).

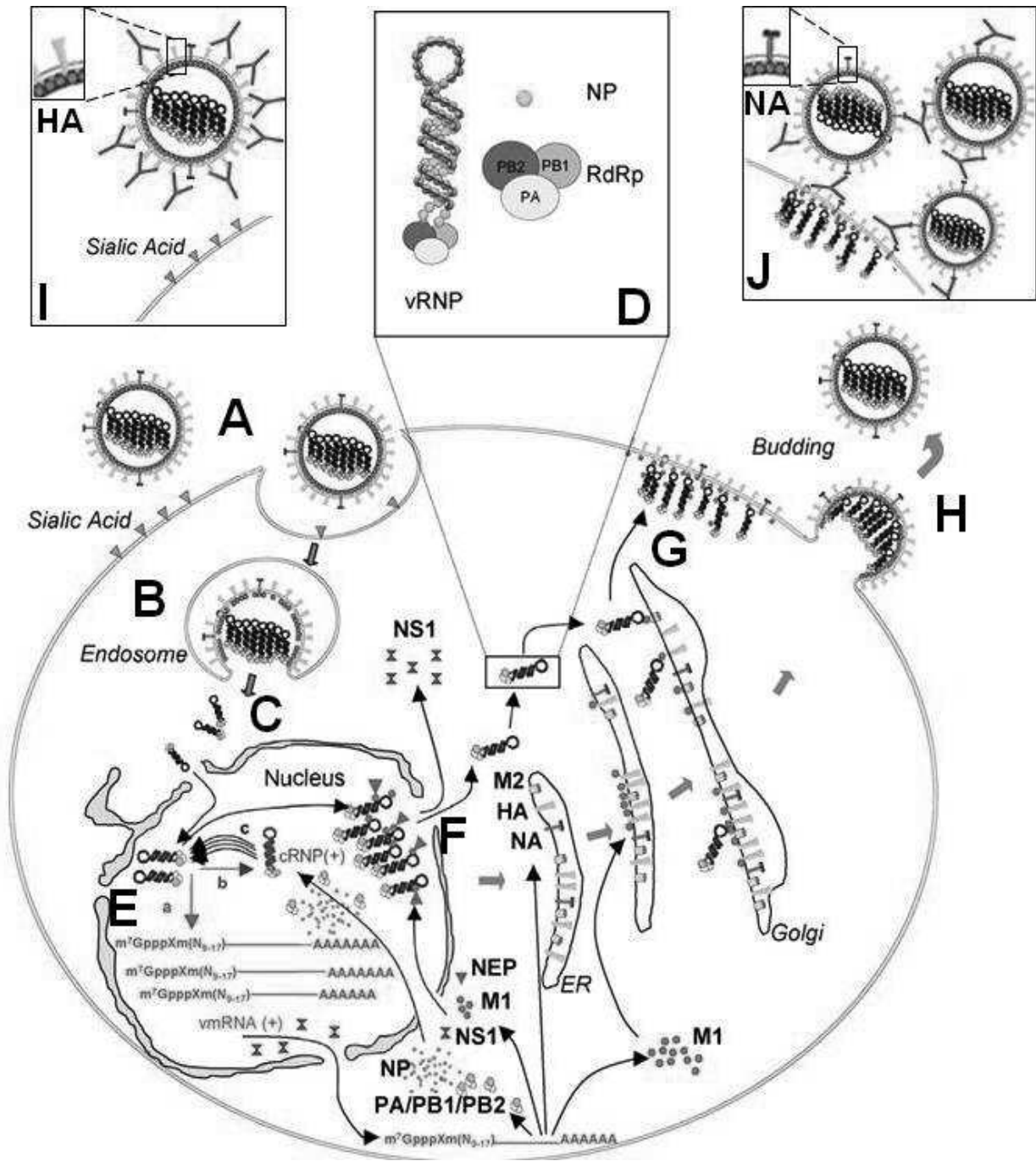


Figure 2. Replication cycle of influenza A viruses and role of HA and NA specific antibodies. **A.** IAV virus entry into the host cell through endocytosis mediated by the attachment of HA to sialylated receptors. **B.** Endosome acidification activates viral M2 ion channel allowing disruption of M1-vRNP interaction and subsequent virus uncoating. The pH dependent conformational rearrangement of HA permits endosomal membrane fusion, the releasing individual vRNPs into the cytoplasm. **C.** Viral genome segments are then transported into the nucleus via Nuclear Localization Signals (NLS) carried by NP protein and the importin alpha–beta mediated pathway. **D.** Schematic organization of vRNP is depicted in the inset. Viral genome consists of negative sense RNA (vRNA) existing as viral ribonucleoprotein (vRNP) complexes associating heterotrimeric RNA dependent RNA polymerase (RdRp, constituted by PB1, PB2, PA proteins) and many copies of nucleoprotein (NP). **E.** An initial round of transcription produces 5' capped and 3' poly (A) viral mRNA efficiently exported towards the cytoplasm to be translated (step a, red). Then vRNA templates are replicated into a perfect positive sense copy RNA (cRNA, step b). This replicative intermediate form is the template for neosynthesis of many copies of vRNA (step c). **F.** After the formation of vRNPs within the nucleus, M1, NEP (Nuclear Export Protein, primary referred to as NS2) and NP catalyze its transport to the cytoplasm via a CRM1-dependent pathway. **G.** M1-vRNP complexes are directed to the virus assembly sites M1 interacts with cytoplasmic tails of H1 and NA, leading to assembly and budding of virions. **H.** Their final release from cell surface relies on the viral NA sialidase activity (Josset et al., 2008). **I.** HA specific antibodies block virus attachment, resulting in the decrease of infected cells. **J.** NA-specific antibodies bind virus to the cell, preventing release of newly produced virions and inducing aggregation

1.6 HEMAGGLUTININ

The two surface glycoproteins HA and NA are the major antigenic determinants of the influenza viruses, but the HA is naturally immunodominant. The HA is the major antigenic determinant, as mentioned above, because it has a key role in the initial stages of infection by its receptor binding and membrane fusion activities (Yoshida et al., 2009). As mentioned above, the HA has an important role in the endosomal membrane fusion during the IAV replication cycle. The HA protein is encoded by the fourth -ssRNA segment, and is synthesized as a single chain precursor (HA0) in the endoplasmic reticulum (ER), where is assembled as a homotrimer of the host cell by the help of chaperones and exported to the cell surface via the Golgi network (Webster et al., 1992). Once in the cell surface, the HA0 can be cleaved into two subunits (HA1 and HA2) by specific host proteases (Kido et al., 1992). Structurally, each HA monomer has a globular head and stalk domain, conformed by two subunits HA1 and HA2. The HA1 domain of each monomer is built up by β -sheets, with a shallow depression conforming the Reportor Binding Domain (RBD), which is responsible for binding to the Sia receptors (Gamblin et al., 2004). The RBD has three structural elements: a 190-helix (HA1 residues 188 – 190); the 130-loop (HA1 residues 134 – 138) and the 220-loop (HA1 residues 221 – 228) (Figure 3B). The HA2 subunit is constituted by a membrane proximal α -helical stalk that functions as an anchor domain, and a fusion peptide, that is responsible for fusion between the viral and the endosomal membrane (Palese and Schulman, 1976) (Figure 3A). The RBD is localized at the membrane distal end of HA1 (Figure 3A-B), and binds to Sia receptors with low affinity (Sauter et al., 1992). Nevertheless, the high density of HA copies on the virion surface, increase the HA avidity to Sia receptors, by multivalent binding. The HA1 globular domain is a preferential target for HA neutralizing antibodies, that block viral attachment (Figure 2I), and contains antibody recognition sites, mapped close to the RBD (Figure 3B). For example, by escape mutants analysis using a

H5-specific camelid single chain antibody, the mutations K154S/D and K189N/E showed to be close to the RBD, and blocked the binding of a H5N1 virus to cells (Ibanez et al., 2011) (Figure 3B). The avian IAV have preferential binding for α 2-6 linked Sia in the intestinal tract, whereas the human-adapted IAV tend to bind to α 2-3 linkage (Parrish and Kawaoka, 2005). The switch of specificity from α 2-3 to α 2-6 is a critical step in the adaptation of avian IAV to human host, and it seems to be an important factor in hindering the avian IAV (including H5) human to human transmission, after avian-human infection. The majority of the HAs have a restricted infection in the lung of the mammals, because of the specific cleavage site (Q/E-X-R) and narrow tissue distribution of relevant proteolytic enzymes. In contrast, the H5 and H7 subtypes have a polybasic sequence that has been associated with high virulence in birds, due enhanced cleavage susceptibility by a broader range of cellular proteases (Hulse et al., 2004). Consequently, H5 IAV present a tissue tropism not only restricted to the lungs, but extends to other organs, including the brain. The H5N1 HA1 C-terminal cleavage site comprises until the proline 324 (Pro³²⁴), not including the QRERRRKKR residues before the N-terminal glycine 1 (Gly¹) of the HA2. The HA2 N-terminus is stabilized by hydrogen bonds from its backbone amide groups to Asp11 and to Ser113 of the adjacent HA2 monomer (Figure 3C) (Stevens et al., 2006). The 17 serological different subtypes are divided into two major phylogenetic groups: group 1 (H1, H2, H5, H6, H8, H9, H11, H12, H13, and H16) and group 2 (H3, H4, H7, H10, H14, and H15). The available HA structures indicate that the two groups differ in their HA stalk region and in the regions that are required for membrane fusion (Steel et al., 2010). In contrast, the Sia-binding site is conserved in all HA subtypes of IAV, throughout antigenic variation (Watowich et al., 1994).

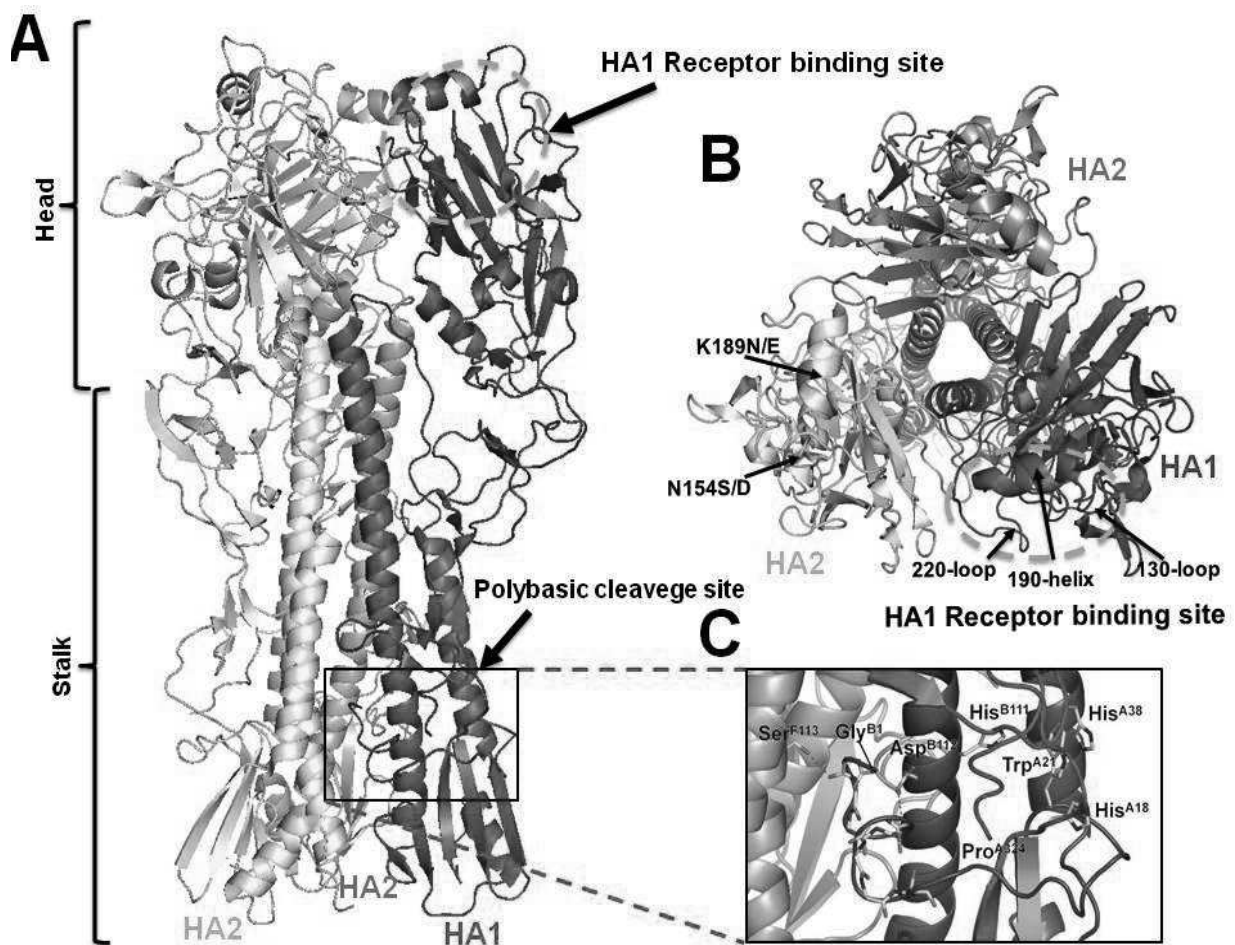
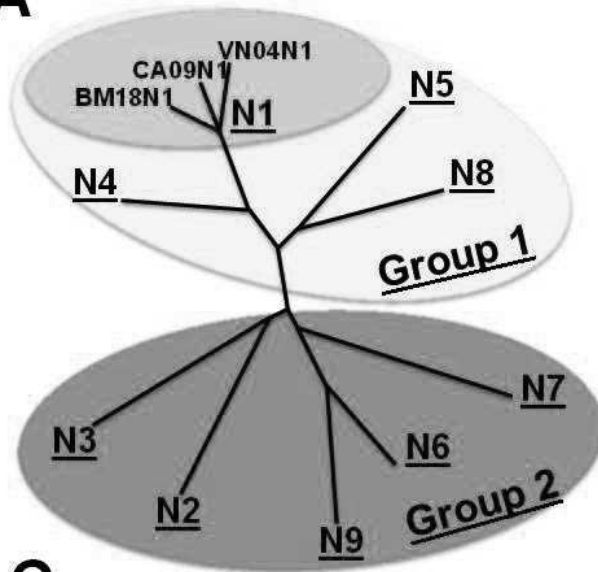
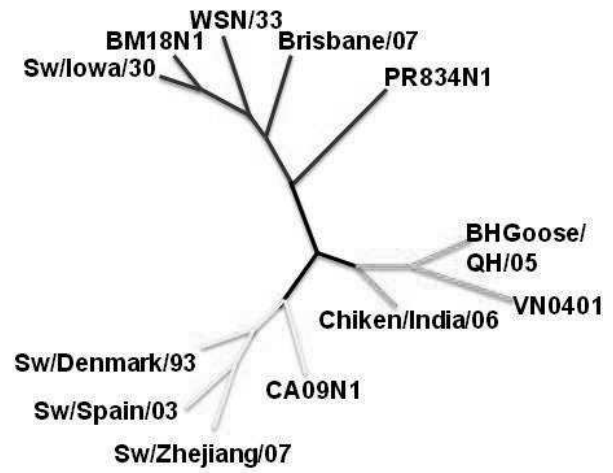
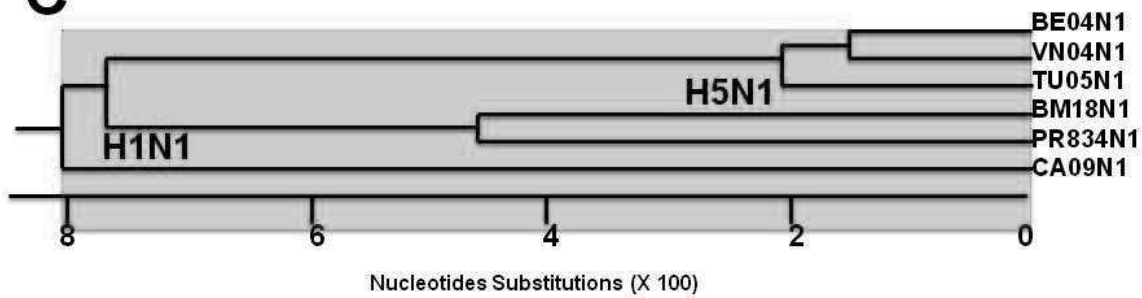


Figure 3. Diagrams of H5N1 HA structure and specific cleavage site. **A.** Side view of a NA trimeric molecule (PDB: 21BX, VN04N1, derived from A/Vietnam/1203/2004). Each monomer has a stalk and head domain (HA1 – HA3). For clarity reasons, each monomer has been colored differently. In one monomer, the HA1 (red) membrane distal receptor binding site (RBD) localization is depicted by the orange dotted line, while the membrane proximal polybasic cleavage site is in the black box. **B.** Top view of the HA trimer. The RCB of HA1 is also depicted in orange dotted line, constituted by the 130 and 220-loops and the 190-helix. The HA1 K154S/D and K189N/E mutations are indicated in green. **C.** Amplification of the HA cleavage site. Cleavage of the polybasic site of HA1 c-terminus from the fusion peptide at the N-terminus of the HA2, which is stabilized by hydrogen bonds from Asp^{B112} and Ser^{F113}, from adjacent monomers (figure 3C taken from Stevens et al., 2006).

1.7 NEURAMINIDASE

There are nine serotypes of NA (N1-N9) that are subdivided into two phylogenetically distinct groups: with group 1 consisting of N1, N4, N5 and N8 and group 2 consisting of N2, N3, N6, N7 and N9 (Thompson et al., 1994) (Figure 4A). Two pandemic H1N1s, the A/BrevigMission/1/1918 (BM18N1) and the A/California/04/2009 (CA09N1) and the emergence of highly HPAIV H5N1 A/Vietnam/1194/2004 (VN04N1), suggest that N1 NA is of major concern. Phylogenetic analysis of the N1 NA sequences reveals three different clusters, co-incident with their human, swine or avian origin (Figure 4B). The VN04N1 NA is a representative of HPAIV H5N1, which shared a high sequence homology (> 95 %) with the NA of A/Crested Eagle/Belgium/01/2004 (BE04N1) and (TU05N1), two HPAIV H5N1 also used in this study. In addition, the VN04N1 and BE04N1 belong to the H5N1 clade 1, separated from the TU05N1 in clade 2 (Figure 4C-D). Depending of the avian or mammal origin, NA substrate specificity varies. As a generality, the NA prefers to cleave α 2-3 linked Sia (3'Sia) (Kobasa et al., 1999). Interestingly, it has been reported that the preference of the NA towards α 2-6 Sia (6'Sia) may be associated with HA binding specificity from avian (3'Sia) to human (6'Sia) (Baum and Paulson, 1991). The preference of the N1 towards 3'Sia over 6'Sia depends of the host, since it varies between species: human 5:1; pigs, 20:1, birds, 50:1 (Mochalova et al., 2007). Several human IAV prefer 6'Sia cleavage more than avian IAV, but still there is a great preference of NA for 3'Sia.

A**B****C****D**

	BE04N1	TU05N1	VN04N1	BM18N1	CA09N1	PR834N1
BE04N1	---	95.5	97.1	87.5	87.3	83.5
TU05N1	4.6	---	96.7	88.0	88.0	84.2
VN04N1	3.0	3.7	---	88.2	87.8	84.0
BM18N1	13.7	13.1	12.9	---	82.9	88.5
CA09N1	13.9	13.1	13.4	16.4	---	78.9
PR834N1	18.2	17.3	17.6	9.1	21.3	---

Figure 4. Phylogenetic analysis of representative neuraminidase genes and N1 proteins. **A.** The IAV neuraminidase genes are divided into group 1 (yellow) and groups 2 (blue), in green are the N1 NA: BM18N1, A/BrevigMission/1/1918 (H1N1); CA09N1, A/California/04/2009 (H1N1); VN04N1, A/Vietnam/1194/2004 (H5N1). **B.** Human, swine, and avian origin N1 genes are depicted in blue, yellow and green, respectively: WSN/33, A/WSN/1933 (H1N1); Brisbane/07, A/Brisbane/59/2007 (H1N1); PR8/34, A/Puerto Rico/8/1934 (H1N1); Sw/Denmark/93, A/Swine/Denmark/WVL9/1993 (H1N1); Sw/Spain/03, A/Swine/Spain/50047/2003 (H1N1); Sw/Zhejiang/07, A/Swine/Zhejiang/1/2007 (H1N1); Ck/India/06, A/Chicken/India/NIV33487/06 (H5N1); BHGoose/QH/05, A/Bar-headed Goose/Qinghai/1/2005 (H5N1). Bootstrapped neighbor-joining analysis (adapted from Li et al., 2010). **C.** Phylogenetic tree of 6 N1 proteins, 3 H1N1: two pandemic, BM18N1 (AAF77036) and CA09N1 (ACP41107), the lab strain PR834N1 (ACF41837); and 3 HPAIV H5N1 analyzed in this project: BE04N1, A/Crested Eagle/Belgium/01/2004 (ABA70757), VN04N1 (ABP52007) and TU05N1, A/turkey/Turkey/8/2005 (ABQ58915). In parenthesis are the protein accession numbers. **D.** Pair distances analysis of the N1 protein sequences of C. Percent of similarity in upper triangle, percent of divergence in lower triangle. Alignment and homology analysis by Clustal W method.

The -ssRNA segment number 6 encodes the NA protein, a homotetrameric type II transmembrane glycoprotein. NA is the second major antigenic determinant and is essential in the spread of the virus by cleaving the SA receptors on the host cell and on the virus itself. Without functional NA-activity, the lack of removal of the Sia residues from the viral and infected cell surfaces resulted in aggregation of the newly produced virus particles on the surface of the infected cell. A major role in this aggregation is the interactions between HA-receptor binding sites and Sia, preventing the release and the spread of the IAV (Palese et al., 1974). The NA protein monomer has a square box-shaped head at the top of a long thin stalk, of variable length, followed by hydrophobic amino acids (AAs) to anchor the NA into the lipid membrane, the transmembrane domain (TMD), and a cytoplasmic domain (CytD) at the N-terminal end (Figure 5 A-B) (Laver and Valentine, 1969; Wrigley et al., 1973; Steinhauer and Skehel, 2002). In the lipid bilayer of the virion, the NA is present as a tetramer composed of four identical NA monomers. Each monomer of the box-shaped fourfold symmetric head consists of six four-stranded antiparallel β -sheets, arranged in a propeller fashion and the active site of the NA is located on top of each monomer, forming the catalytic cleft (Colman et al., 1983; Varghese et

al., 1983; Burmeister et al., 1992) (Figure 5B). The NA CytD has a 6 residues consensus sequence (MNPQKQK), and mutants of this domains present a significant decrease in virion budding. Nevertheless, neither the CytD detailed functions nor its cytoplasmic interaction partners are known (Barman et al., 2004). TMD, varying in length from 7 to 29 residues, contains a signal peptide anchor that redirects the NA into the ER lumen and retains it in the infected cell membrane. Recent studies indicated that the NA tetramer's proper folding and activity depends on the presence of the TMD. The stalk appears to contribute only marginally to NA tetramer formation since as few as 10 AA residues from the NA stalk are enough to allow folding. Nevertheless, TMD is not necessary for the synthesis and trafficking of the NA, but TMD absence compromises NA activity and results in improper folding. Interestingly, the TMD and stalk can be targeted to the ER, pass protein quality control and enter the Golgi complex, and can tetramerize without the head domain (da Silva et al., 2013), highlighting the importance of the role of the TMD during the NA tetramerization. It seems that the NA head domain alone can properly assemble on its own, but when a stalk domain is present, the head domain N-terminus must be stabilized by the TMD to prevent aggregation. The NA stalk domain length is very variable from 32 to 50 residues, and possesses cysteine residues that contribute to the NA stability by intermolecular disulphide bridges (S-S), and also canonical glycosylation sites (N-X-S/T). Deletions in the NA stalk domain are associated with reduced accessibility to Sia complex substrates. Reduced length of the NA stalk is often found in HPAIV that transmitted from ducks to land-based poultry, such as chickens and turkeys (Munier et al., 2010). Unfortunately, only crystallographic structural data of the NA globular head domain are available (Figure 5A).

The NA enzymatic activity was discovered in 1947 (Hirst, 1941), but only 15 years later the sialic acid was identified as its substrate (Figure 5C) (Gottschalk, 1956). The activity of the NA seems to depend on the tetrameric conformation, as it has been reported that protease-extracted NA from crude virus preparations conserved 100 % of activity, suggesting that a

proper folding is necessary for NA activity, the monomeric forms being considered not active (Bucher and Kilbourne, 1972). Several factors are considered to contribute to the NA tetramer stability: i) optimal activity at pH 5.5 – 6.5; ii) head domain residue mutations, i.e. the mutation E119G results in the lack of a salt bridge of E119 with the E156 in a neighbouring monomer, disrupting the tetramer formation; iii) the difference of glycosylation patterns between the NA tetramer and monomers and dimers, suggests that tetramerization is favored in NA molecules with untrimmed mannose residues ($\text{Man}_{5-9}\text{GlcNAc}_2$); iv) the presence of Ca^{2+} molecules in the NA structure, confirmed by crystallographic data, is an important factor for NA tetramerization stability (Lawrenz et al., 2010). The Michaelis constant (K_m) reported for the NA with the small substrate 2'-4-Methylumbelliferyl- α -D-N acetylneuraminic acid (MUNANA) is in the range of 6 – 520 μM ; the K_m for the 3' Sia is 171 – 750 μM . The specific activity of the NA with MUNANA as a substrate is: 100 (N1) and 900 (N9) nmol / sec per mg (Wu et al., 2009; Schmidt et al., 2011). It has been observed that NA has a lower activity for cleaving complex glycoprotein substrates, compared with small substrates like MUNANA. Also the presence of glycans with O-acetylations resulted in lower NA activity, because the O-linked 3'Sia is less efficiently cleaved than the N-linked one (Corfield et al., 1986).

The NA AA residues that are responsible for the active site are highly conserved among the NA subtypes, and can be divided into 3 types for their analysis: residues that have direct contact with the Sia substrate at the catalytic site, active site framework residues, and 150-loop residues. The residues that have contact with Sia are polar and charged: R118, D151, R224, R292, R371 and Y406 (contacting the carboxylate moiety of the Sia), the R152 (contacting the acetamido group of Sia) and E276, which makes hydrogen bonds to the hydroxyl groups of the Sia (Figure 5C). The structure of the active site is stabilized by hydrogen bonds and salt bridges by the framework residues: E119, R156, W178, S179, D198, I222, E227, H274, E277, N294 and E425 (Figure 5D). The group 1 NA 150-loop residues (G147, T148, V149, K150 and D151)

contribute to more extensive interactions with the Sia and the other NA substrates: (Figure 2E-F). The first 3-dimensional structure of any NA solved by X-ray crystallography resulted from pronase-released N2 heads. This first structure was solved at 2.9 Å of resolution, and was a composite of two different Asian origin N2, representing H2N2 (A/R1/5+/57) or H3N2 (A/Tokyo/3/67) (Varghese et al., 1983). Later, the crystal structures of 2 IAV NA (N2, N9), (Tulip et al., 1991; Varghese et al., 1992) and Influenza B NA (Burmeister et al., 1992), were reported. The 2 NA active site rigid structures have been used as an excellent target for drug design, *i.e.* oseltamivir or zanamivir. The first N1 crystal structure was reported by Russell (Russell et al., 2006), from bromelain-extracted NA from crude H5N1 HPAIV preparations (derived from a VN04N1). This N1 structure revealed a main structural difference compared with the group 2 NA reported structures. In the N1, the loop comprising the 147 – 152 residues (called “150-loop”) was able to adopt a closed or open conformation. In addition, oseltamivir binding to the N1 catalytic site occurred in the 150-loop open conformation, resulting in the N1 adopting a closed conformation. This conformational change suggested that the oseltamivir binding favours a 150-loop closed conformation that requires less energy than the open conformation (Figure 2E-F). The NA of N1 and N2 bind oseltamivir with similar affinity suggesting that the difference in energy between the 150-loop open or closed conformations is not very large. The crystal structure of the pandemic 2009 H1N1 NA (09N1) surprisingly showed that the 150-loop was absent in the active site architecture (Li et al., 2010). The NA from CA09N1 was closely related to the NA of Eurasian swine isolates (Figure 4B). The root mean square deviations (rmsd) of the 150-loop residues of the CA09N1 compared to the BM18N1 and a N2 NA was 2.184 and 0.261, respectively, showing the greater similarity of the CA09N1 150-loop residues to the NA of the group 2 than group 1. A possible explanation to this group 2 NA similarity of the CA09N1 is the shared isoleucine at position 149, while the NA of group 1 has a valine at the same position. The isoleucine possess an extra carbon compared with the valine and is oriented towards the

P347, suggesting that in CA09N1, like in some of the group 2 NA, the 430 loop coordinated the closed 150-loop conformation (Li et al., 2010).

A second sialic acid binding site, different to the NA active site had been reported in N9 NA, and is composed of the residues N367, S370, N400, W403 and L432, being called hemadsorption site (HB) (Figure 5D). Notably, this second binding site is only present in NA of birds but not in humans. In avian IAV that infect humans, this HB site is lost. This loss might be necessary for the adaptation of the avian IAV to recognize 6'Sia present in humans, but its function is not completely known (Varghese et al., 1997). Interestingly, the Sia bound to the NA HB is in a boat conformation, in contrast to the Sia in chair conformation in the binding site of HA and NA active site. NA mutants with a +HB site have a higher NA activity than mutants –HB with complex substrates, suggesting that the HB site possibly contributes to stabilize the Sia substrate, or maybe by “feeding” the NA active site.

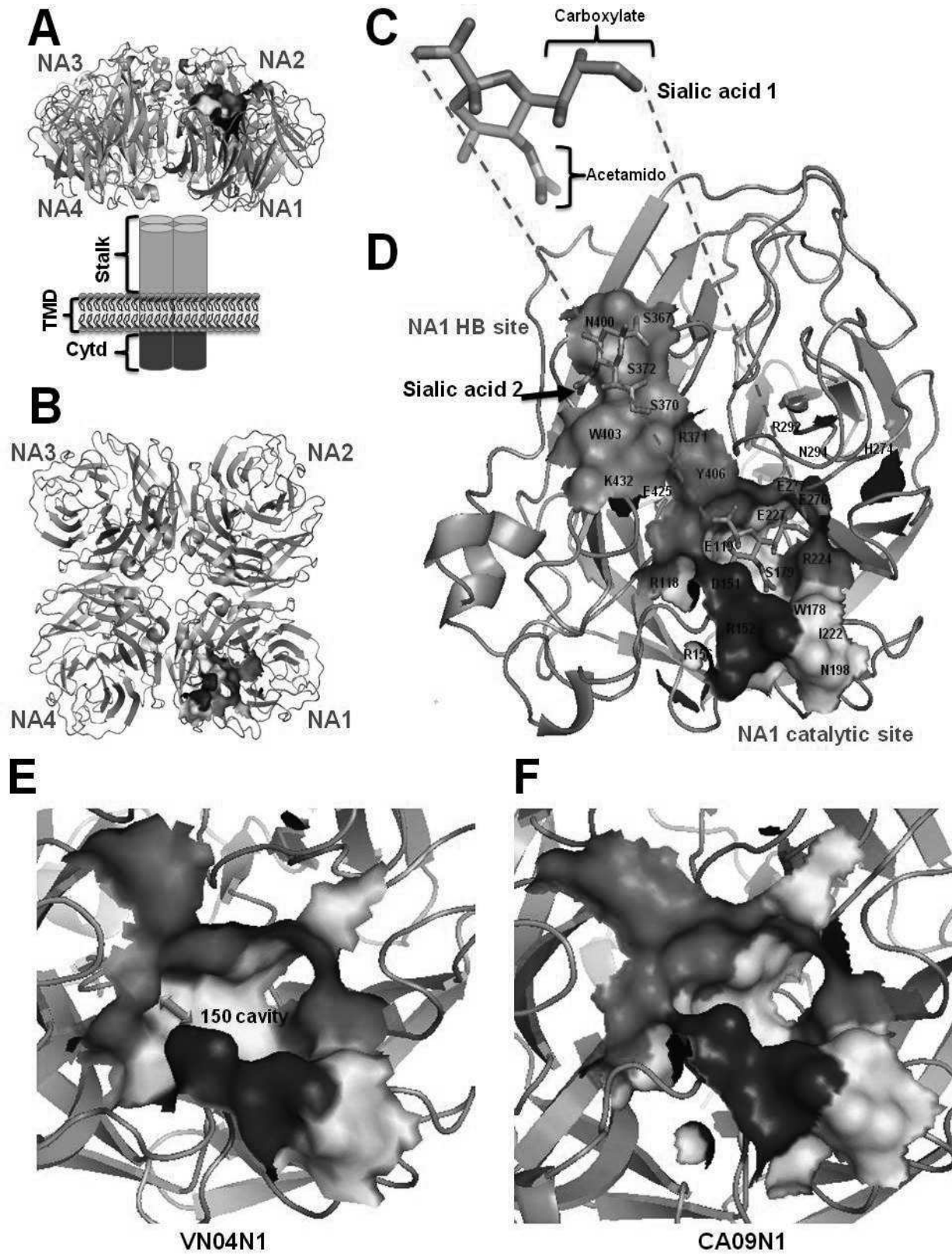


Figure 5. Diagrams of NA structure and its substrate. **A.** Side view of a membrane bound NA tetramer. Each monomer is composed of 4 parts, from N- to C- terminal: a cytoplasmic domain (CytD, purple), a transmembrane domain (TMD, yellow), a stalk domain (light green) and the catalytic globular head domain (green) in ribbon representation (PDB: 2HTY, VN04N1 derived from A/Vietnam/1194/2004). In one of the monomers, the catalytic cleft is in surface and colour presentation: residues that make direct contact with the Sia substrate (red), catalytic site framework (yellow) and the D149 and R150 (blue) as part of the “150 loop”. **B.** Top view of the NA tetramer of A. derived from C. The NA natural substrate is the sialic acid (Sia) (carbon atoms coloured in green) with an acetamido and carboxylate groups at carbons 4 and 6, respectively. **D.** Amplification of one N9 monomer structure, where the catalytic site and a second Sia-binding domain (HB) are depicted. The NA catalytic site is a cleft that harbours a Sia molecule (red dotted lines), with highly conserved residues in both NA groups. As in B, the residues that have direct contact with Sia are in red (R118, R224, E276, R292, R371 and Y406); the framework residues in yellow (E119, R156, W178, S179, D198, I222, E227, H274, E277, N294 and E425). The residues D151 and R152 also make direct contact with the Sia and are represented in blue, as reference residues for the “150-loop” (G147, T148, V149, K150 and D151). The residues of the HB site (present in avian origin IAV) that make contact with a second Sia are in orange (S367, S370, S372, N400, W403 and K432). (PDB: 1MWE; N9 derived from Tern/Australia/G70c/75). **E.** The N1 catalytic site has an extra 150 cavity. A representative 150 cavity of VN04N1 is depicted. The cavity results from the 150-loop adopting an open conformation, and upon substrate binding, the cavity provides extra surface and contacts to NA substrates. **F.** The lack of the 150 cavity in the pandemic CA09N1, resembling the group 2 NA 150-loop in closed conformation (CA09N1 150-loop similar to D), had been subject of recent polemic, and it seems that both conformations can exist in CA09N1 (PDB: 3NSS).

1.8 INFLUENZA ANTIVIRALS

Influenza A and B virus infections can cause local and systemic reactions, including sudden onset of high fever, head ache, chills, myalgia, coughing, sore throat, runny nose, diarrhoea, primary pneumonitis and occasionally secondary bacterial infections (Hubert et al., 1992). The severe morbidity that is often associated with HPAIV infection in humans can be attributed to a high replication rate and a broad cellular tropism that can lead to a systemic spread (see section 1.6). During severe infections, a deregulated induction of pro-inflammatory cytokines and chemokines (sometimes called “cytokine storm”) is associated with HPAIV infections, and can result into an excessive immunological response and autoimmune symptoms (de Jong et al., 2006). The treatments reported and available against HPAIV are far from optimal: treatment

with convalescent plasma for influenza A H5N1 infected patients has been shown to be protective (Zhou et al., 2007); a risky combination of antiviral drugs and immunomodulators can control severe HPAIV infections (White et al., 2009). In addition, bacterial secondary infections are associated with IAV infections that complicate the clinical outcome (Rameix-Welti et al., 2009).

There are two types of antivirals that are licensed for the treatment of human influenza. These drugs target only two viral proteins: the transmembrane domain (TM) of M2, targeted by amantadine and rimantadine; and the inhibitors of the catalytic activity of NA, *i.e.* oseltamivir, zanamivir and peramivir. These drugs are most often used against seasonal influenza and have been applied to try to control disease in patients caused by H5N1 and H7N7 infection. These antiviral drugs present several advantages compared to vaccines: i) administration when the circulating influenza strains do not match the available vaccines; ii) efficient therapeutic effect to reduce morbidity and length of disease; iii) immediately effective and available, can be stockpiled in advance; iv) effective against a broad range of IAV strains. Unfortunately, the use of IAV antiviral drugs is characterized by long term treatment and high concentrations used in clinical cases, causing selective pressure and the appearance of reported and emerging resistant mutants.

The adamantanes, amantadine and rimantadine, are synthetic amines that block the M2 ion channel. The adamantanes are the first generation of IAV antiviral drugs and are effective in both prophylaxis and treatment reducing the duration of illness in healthy individuals by approximately 1 day (Jefferson et al., 1999). These drugs are orally administered, inexpensive, stable and easily stockpiled by their long shelf life (at least two decades). However, adamantanes treatment is frequently complicated by gastrointestinal and central nervous system side effects which significantly limits its wide-scale use (Tominack and Hayden, 1987).

Next to this, M2 inhibitors are effective against IAV while they do not bind to the M2 ion channel of Influenza B viruses. The adamantanes are also limited in their clinical use by the widespread drug resistance (Wenzel, 2000).

The second group of licensed antiviral drugs against influenza are the NA inhibitors, which primarily act by inhibiting viral spread. Inhibition of the viral NA affects several stages of the IAV replicative cycle: i) hindering the passage of the virus through the mucus of the respiratory tract and suppressing infection before virus entry into cells, by a NA-dependent HA-mediated binding to its cellular receptor (Matrosovich et al., 2004a); ii) inhibition of the release of progeny virus on the surface of infected cells, slowing down the spread of the virus.

Analysis of the three-dimensional X-ray structure of the catalytic cleft of the IAV N2 NA has led to the design of the NA inhibitors: zanamivir (Relenza) and oseltamivir (Tamiflu) (Vonitzstein et al., 1993; Kim et al., 1997). These drugs (introduced in 1999 and 2000, respectively) are designed to interfere with the normal function of IAV NA by mimicking Sia (Figure.6A). Although the AA sequence homology between NA from type A and type B virus is only 30%, their NA have a similar topology with a highly conserved active site pocket of the enzyme (Colman et al., 1984; Air et al., 1990). As a consequence, the NA inhibitors are active against both influenza A and B viruses. The first NA inhibitor, zanamivir, is a Sia derivate in which the 4-hydroxyl group of sialic acid is replaced with a guanidinyll group which binds to NA with high affinity (Krug and Aramini, 2009) (Figure 6B). The use of zanamivir is limited by its poor bioavailability, due to a positively charged guanidine group in its structure. Therefore it has to be administered topically as a dry powder by an oral inhalator (Monto et al., 1999). The impractical way of administration of zanamivir, as well as the shortage of supply, limits its wide-scale use.

The other anti-NA drug, oseltamivir is currently the most used available drug for IAV treatment and can be orally administered because of the presence of a lipophilic side chain (Mendel et al.,

1998) (Figure 6B). The oseltamivir oral form is an inactive pro-drug that requires ester-hydrolysis by hepatic esterases for its conversion into its active form, oseltamivir carboxylate. The NA inhibitors reduce the duration of influenza symptoms in average-risk patients by approximately one day, and in high-risk and older patients by 2,5 days (Hayden et al., 1997; 1998; Hayden et al., 1999; Matsumoto et al., 1999; Monto et al., 1999; Treanor et al., 2000; Lalezari et al., 2001). Compared to the M2 inhibitors, the NA inhibitors have the advantage of having lower induction of adverse secondary effects. However, resistant mutants against oseltamivir, and to a lesser extent against zanamivir, have been reported *in vitro*, *in vivo* and also in clinical specimens. In addition, recent polemic has been seen by reports challenging the efficacy of oseltamivir treatment, in biased clinical trials of children and adults IAV infected patients (Jefferson et al., 2012; Wang et al., 2012). The persistent treat of oseltamivir resistant mutants and its efficacy in human patients are pieces of evidences that highlight the necessity of antiviral alternatives for IAV.

Dependent on the specific mutation, a virus can become resistant against oseltamivir but remain sensitive for zanamivir (Carr et al., 2002; Moscona, 2005a, b, 2008). Since both inhibitors bind to the catalytic site of NA, cross-resistance mutations are also found with different drug resistance profiles (Oakley et al., 2010). In addition, some drug-resistant IAV strains permit binding of the drug to the NA, while the fitness is compensated by mutations in or near the HA receptor-binding site, leading to HA reduced binding efficiency to Sia-containing receptors (Gubareva et al., 2000). Since the before mentioned NA inhibitors are based on crystal structures of group 2 NA, there is special interest to design new anti-IAV drugs based on more recently reported N1 NA crystallographic structures (Collins et al., 2008; Li et al., 2010). Among the several oseltamivir-resistance mutations, the H274Y and the R292K (N2 numbering) binding dynamics had been studied in detail (Russell et al., 2006). The H274Y mutation in NA has been isolated in oseltamivir treated human volunteers, but HA mutations in the residues 137 and 225

were reported to affect the fitness of the virus *in vitro* and *in vivo*, by adopting a α 2-6 Sia linkage preference in human respiratory tract (Gubareva et al., 2001). Two factors contributed for the mutant N1 H274Y inability to bind oseltamivir: i) the tyrosine residue at 274 results in a partially displaced E276. The bulkier tyrosine residue in the H274Y mutant pushes the neighbouring E276 carboxylate group into the active site cavity, resulting in the displacement of 2.0 Å of the oseltamivir pentyloxy group, compared to the wild-type NA (Figure 6C). In contrast, the zanamivir glycerol group hydrogen bonds formed by its 8 – 9 hydroxyls with the side chain of the E276 are not affected, conserving hydrogen bonds present (Wang et al., 2002b) (Figure 6D); ii) the group 1 NA, the H274Y mutation cannot accommodate oseltamivir in the active site, due displacement of a bulky and conserved tyrosine residue Y252 just beneath the 274 residue, whereas in group 2 NA, the smaller threonine in the 252 position allows oseltamivir binding in the active site. This observation renders an explanation of why the H274Y mutation in group 1 NA gives resistance to the oseltamivir, but not in the group 2 NA.

In the N294S mutant, the extra hydrogen bond between the S294 with the E276 results in a displacement of the Y347 residue, flipping out from its normal position and being no longer coordinated by a Ca^{2+} molecule (Figure 6E). The appearance of this extra hydrogen bond alters the hydrophobic make up of the N1 substrate-binding site, resulting in weakening the hydrogen bond with the carboxylate of the oseltamivir. On the other hand, the R292K is an oseltamivir-resistance mutation in the group 2 N2, and also results in lack of a hydrogen bond with the carboxylate group of oseltamivir. In the group 1 N1, the tyrosine in the 347 position can compensate the absence of this hydrogen bond, but the N347 in N2 cannot (Mishin et al., 2005). The structures of NA from HPAIV N1 in complex with oseltamivir and zanamivir were solved (Collins et al., 2008), and suggested that the more similar the NA inhibitors to the Sia, the less chances of escape mutant to appear. The *in vitro* enzymatic analysis of H274Y and the N294S mutants showed that the oseltamivir inhibition of the NA activity in the 2 mutants was

negatively affected, by increasing the inhibitory constant (K_i) of the H274Y and the N294S, 285 and 81 fold, respectively (Collins et al, 2008) (Figure 6F). On the contrary, the mutation Y252H, that was reported in human cases in Asia but not associated with oseltamivir treatment (McKimm-Breschkin et al., 2007), decreased the oseltamivir sensitivity by 10 fold. The NA activity (V_m) of these mutants was similar to the N1 WT, suggesting that mutations outside of the residues that make direct contact with the Sia do not affect NA activity. In contrast, none of these mutations affect the zanamivir binding to the NA. The H274Y NA increase in K_i , or sensitivity to oseltamivir, can be explained by an association rate constant (K_{on}) 10 fold smaller than the NA WT, but a dissociation rate constant (K_{off}) 25 fold higher.

There are contradictory reports about the compromised fitness of the H274Y mutant IAV. On one hand, the first reports about this mutation point out severely impaired fitness *in vivo* and *in vitro* posing the H274Y as a not clinically significant threat to human (Ives et al., 2002). On the other hand, later reports showed a not compromised replication efficiency of the H274Y and N294S *in vitro* (only 10X less viable than WT), showed only a slight decreases in morbidity of infected animals (Le et al., 2005; Yen et al., 2007), and most importantly, the H274Y mutation was found viable in human infections (Lackenby et al., 2008; van der Vries et al., 2008).

Compensatory mutations had been proposed to play a major role into the rescue of fitness of the H274Y mutation (Collins et al., 2009; Bloom et al., 2010). For example, the mutation I223R (isolated from an immunosuppressed child) conferred resistance to the oseltamivir and zanamivir (Nguyen et al., 2010). In the pandemic H1N1, the double mutant I223R/H274Y double mutant gives a higher resistance to oseltamivir, and is does not compromise the replicative capacity and transmissibility of the IAV in ferrets (van der Vries et al., 2011). The crystal structure showed the existence of a “223 pocket” within the active site of the WT NA, but in the I223R pocket NA this pocket is absent. In the I223R the pocket harbours 2 water molecules and is occupied by the side chain of the arginine 223, which makes a hydrogen bond with the S247,

which results in a turning of the S247 to make an extra hydrogen bond with E277. These conformational rearrangements resulted in shrinkage of the NA active site, reducing the space that normally accommodates the pentoxyl group of the oseltamivir (Amaro et al., 2011). The mutation S247N also is linked to oseltamivir resistance, and is maybe involved in the shrinkage of the hydrophobic pocket in the NA active site, above mentioned. The double mutant S247N/H274Y fitness is not compromised in ferret models suggesting a normal NA activity (Amaro et al., 2011).

In addition, it has been reported that the mutation H274Y reduced fitness can be rescued by secondary mutations, which are not localized close to the NA active site. In a H1N1 H274Y mutant background, the mutations V234M and R222Q restored the NA protein levels in infected cells to wild-type levels. This findings suggest that IAV that accumulates permissive mutations (like V234M and R222Q), and then acquired the H274Y mutations, can be oseltamivir-resistant, maintaining high level of fitness in the absence of the drug (Bloom et al., 2010).

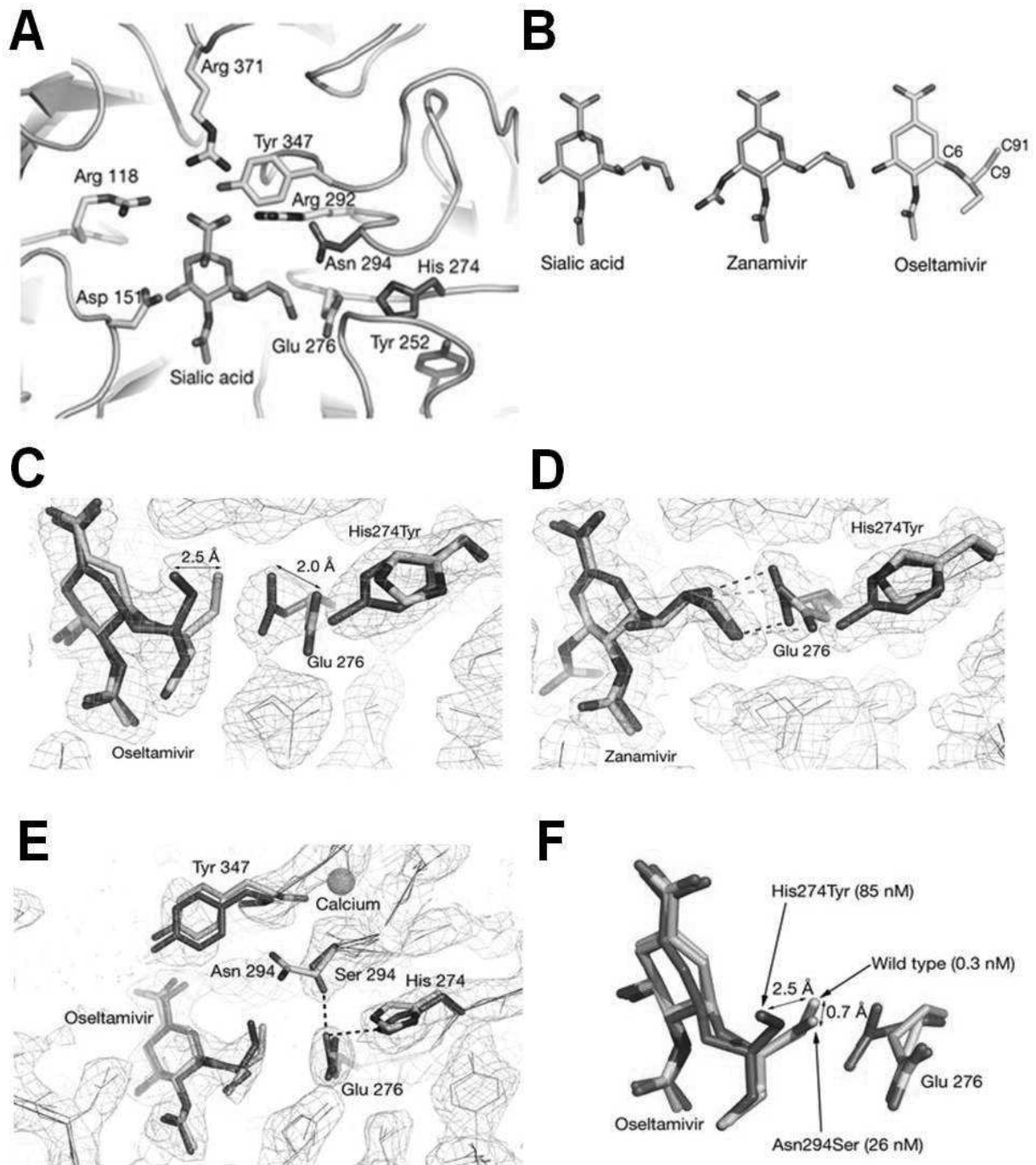


Figure 6. Structure of the N1 neuraminidase complexes. **A.** Sialic acid (blue) docked into the active site of wild-type VN04N1 (yellow) ribbons, from superposition of Sia complex of N2 (Varghese et al., 1992) (PDB: 2BAT). The positions of some key binding residues are shown with carbons coloured yellow, nitrogens blue and oxygens in red. The side chains of three mutations conferring oseltamivir-resistance to IAV: Y252H (Tyr 252), H274Y (His 274) and N294S (Asn 294), are shown as wild type residues depicted with green carbons. **B.** The structures of Sia, zanamivir and oseltamivir with carbons colored in blue, grey and yellow, respectively, are shown in similar orientation with selected carbon atoms numbered. **C – E.** The overlaid structures of the active sites of wild-type (yellow) and mutants N1 NA (green) are shown with bound inhibitors colored similarly; relevant portions of electron density maps are shown. **C.** H274Y in complex with oseltamivir and **D,** with zanamivir. **E.** N294S in complex with oseltamivir. Dashed lines indicate selected hydrogen bonds. **F.** The conformation of oseltamivir and Glu 276 from three complexes is shown after superimposition using protein atoms only; the carbon atoms of the inhibitor from the N1 wild-type are colored yellow, the H274Y in dark green and the N294S in light green. The affinities (KI) oseltamivir to the three NA are given in parenthesis. Modified from Collins et al., 2008.

1.9 ANTIBODIES

1.9.1 CONVENTIONAL ANTIBODIES

Recombinant Antibodies (Ab) are widely regarded as one of the main, if not the most promising tools against cancer and auto-immune, inflammatory, neurodegenerative and infectious diseases (Stiehm et al., 2008). Conventional Abs are relatively complex molecules consisting of pairs of heavy and light chains, whose N-terminal domain is more variable than the rest of the protein sequence. The Ab Heavy chain consists of three Constant domains (C_{H1} , C_{H2} and C_{H3}) and a Variable domain (V_H). The Light chain has only two domains, the Constant domain (C_L) and the Variable domain (V_L). Important glycosylations on the C_{H2} domain are necessary for Ab effector functions, such as Antibody-Dependent Cellular Cytotoxicity (ADCC) and Complement-Dependent Cytolysis (CDC), and for regulating antibody half-time in serum (Figure 4A). Ab binding is determined by the 3 hypervariable Complementary Determining Regions (CDR1, CDR2 and CDR3) present in both the V_H and V_L domains. These regions are located in juxtaposed loops, creating a continuous surface of $\sim 1000 \text{ \AA}^2$ that specifically binds to the

epitope of an antigen. Although all CDRs can potentially make contact with the antigen, CDR3 contacts with the epitope are generally more extensive. The structural diversity of the antigen-binding sites of a conventional Ab depends on the size of the CDR3 in the V_H and the conjunction with the V_L at different angles and distances. These are grouped in 3 different classes, according to the size and type of an antigen: cavities (fitting haptens), grooves (fitting peptides) and planar sites (fitting surface patches of proteins) (Johnson et al., 2010).

1.9.2 SINGLE VARIABLE DOMAIN OF THE HEAVY CHAIN ANTIBODIES

In 1993 a surprising observation was reported for antibodies of the Artiodactyl Tylopoda family (*Camelidae*). Next to conventional Immunoglobulin G Ab (IgG), camelids also naturally produce Heavy Chain Ab (HCAb) that lacks the light chain (Hamers-Casterman et al., 1993). Two years later, similar single chain antibodies were discovered in cartilaginous fish (sharks) (Greenberg et al., 1995). Although the C_H2 and C_H3 of the HCAb and the conventional Ab are highly homologous, there is no C_H1 domain in the camelid HCAb. The HCAb Heavy chain single Variable domain (VHH) is the only domain of HCAb that makes contact with the antigen. Surprisingly, although the VHH have only three CDR regions, their affinity for antigens reaches the low nanomolar to even picomolar range, matching the best affinities of conventional Ab. When expressed as single domains (soluble VHH), the VHH retain their strong epitope specificity and affinity, a feature that might be explained by the VHH architecture (Figure 4B). Just like the VH of conventional Ab, the AA sequence of VHH is organised in CDR1, CDR2 and CDR3, separated by four Framework Regions (FR1-FR4) (Muyldermans et al., 1994). As the AA sequence of the VHH FR is highly similar to those of conventional VH, it was not surprising that the overall architecture of the VHH closely resembles that of VH (Muyldermans et al., 1994). Both VHH and VH domains fold into two β -sheets with the three CDRs that link these two

sheets at one end of the barrel (or domain) (Desmyter et al., 1996; De Genst et al., 2006) (Figure 4C, 4E). However, there are striking structural differences between VHH and conventional VH. Evidently, VHH lack an interacting VL domain. Associated with this lack, the hydrophobic AA present at the V_H surface that is normally interacting with the VL, are substituted by hydrophilic AA (Figure 4D). This enhances the solubility of VHH single domain proteins that usually have an enhanced solubility compared to engineered VH single domain proteins.

Structural features likely compensate the absence of the additional CDR in VHH. First, the CDR3 regions of camelid VHH are generally longer (13-17 AA) than the CDR3 regions of mouse and human V_H (9-12 and 9-17 AA, respectively) (Wu et al., 1993). In contrast to conventional Ab, in which the antigen binding surface is often a flat surface, a cavity or a groove, the long CDR3 loop may extend from the antigen binding surface (Desmyter et al., 1996). This enlarges the paratope surface and hence the potential affinity and repertoire of camelid HCAb. In addition, especially in dromedaries, the CDR1 and CDR3 regions contain a cysteine, which allows formation of a second disulfide bridge next to the single disulfide bridge in conventional VH (Muyldermans et al., 1994). This extra bridge likely stabilizes the CDR loops, thereby reducing their flexibility. This probably also contributes to the affinity (less entropy is lost upon antigen binding) and structural diversity of VHH. Long extending CDR3 loops that are stabilized by an extra disulfide bridge can explain the tendency of VHH to bind to clefts and concave surfaces more readily than conventional Ab do (Figure 4F) (De Genst et al., 2006). Indeed comparison of multiple structures of hen egg white lysozyme interacting with either several conventional human Ab or several camelid VHH clearly illustrated that VHH tends to bind to the concave substrate-binding pocket, whereas conventional antibodies favour epitopes on the "flat" surface of the antigen (Figure 4C). In addition, whereas each of the three CDRs of conventional VH contributes considerably to the interaction with antigen, VHH depended mainly

on the CDR 3 loop for this interaction. Other antigens that are hard to target by conventional antibodies, but can be targeted by camelid VHH are ion channels, GPCRs, haptens and enzymatic sites (Lauwereys et al., 1998; Rasmussen et al., 2011).

Next to an extended CDR3, the AA sequence of the H1 loop that precedes and comprises CDR1 appears to be particularly more variable in camelid VHH than in conventional VH. This might be interpreted as an extension of the VHH CDR1 (Vu et al., 1997). Associated with this high variability in camelid VHH, CH1 loops adopt conformations that deviate from the canonical H1 structures of conventional VH (Barre et al., 1994) (Decanniere et al., 1999; Decanniere et al., 2000). Camelid VHH CH1 loops appear to fold into a more diverse repertoire of structures. The high variability in the AA sequence and conformations of the CH1 loop contribute to the VHH paratope size (850-1150 Å²), which approaches that of conventional antibodies (VH + VL) (Desmyter et al., 2002). Clearly, different biochemical and structural features of camelid VHH compensate for the lack of a V_L domain and allow a broad repertoire of specific high affinity antigen interactions. In addition, due to their small size and typical extruding CDR3 regions, camelid VHH tend to bind in cavities that are not readily accessible for conventional Ab. Next to these particular features, VHH single domain protein is exceptionally stable and soluble, even in stringent conditions. As VHH are small and naturally monomeric, they can be easily formatted. In addition, the small size of VHH allows them to penetrate deeper into tissue (*i.e.* tumor tissue) and to occasionally cross the blood-brain barrier. On the down side, the small size of single domain VHH contributes to their rapid clearance from circulation.

Using display technologies, it is possible to select VHH from large, synthetic or naive libraries (Verheesen et al., 2006). Nevertheless, the phage display generated from an immune VHH repertoire is the most widely and powerful technique used nowadays to rapidly select VHH with the desired specificity (Arbabi Ghahroudi et al., 1997). VHH are easily produced in bacterial or

yeast systems in milligram quantities per litre of culture. The VHH stability, solubility, ease of production and small size make them excellent candidates for multivalent formatting. Tailor-made constructions using VHH as building blocks enhance the avidity of the molecule even in a 3-log scale, and several constructions are being tested in clinical trials (Els Conrath et al., 2001; Hmila et al., 2010). The VHH high potential as therapeutics had prompted the creation in Belgium of the biotechnological company Ablynx in 2001. Because of the publicity surrounding nanotechnology and the small size of the VHH, Ablynx named the VHH as “Nanobody”, and retains full intellectual property rights of the use of VHH in therapeutics and diagnosis. In the field of therapy nowadays only one monoclonal antibody is used against infectious disease (Synagis) (Groothuis and Simoes, 1993).

Several examples of successful VHH treatment against viral infection in vitro and in laboratory mice have been reported (Hultberg et al., 2011; Ibanez et al., 2011; Schepens et al., 2011). These studies were mainly based on the use of VHH (monovalent or bivalent) molecules with virus-neutralizing activity *i.e.* that could prevent viral binding to the host cell in vitro. Another report mentioned the use of a VHH directed against M2 that could suppress replication of amantadine sensitive and resistant IAV strains and protected mice from lethal IAV challenge, and also showed cross-protective potential (Wei et al., 2011). These reports indicate that the VHH cannot only have antiviral capacity by blocking the binding of the IAV virion, but also can be used in other strategies to prevent virus spread. Effective anti-IAV alternatives are needed for the HPAIV treatment, and among them, the VHH technology is a promising tool.

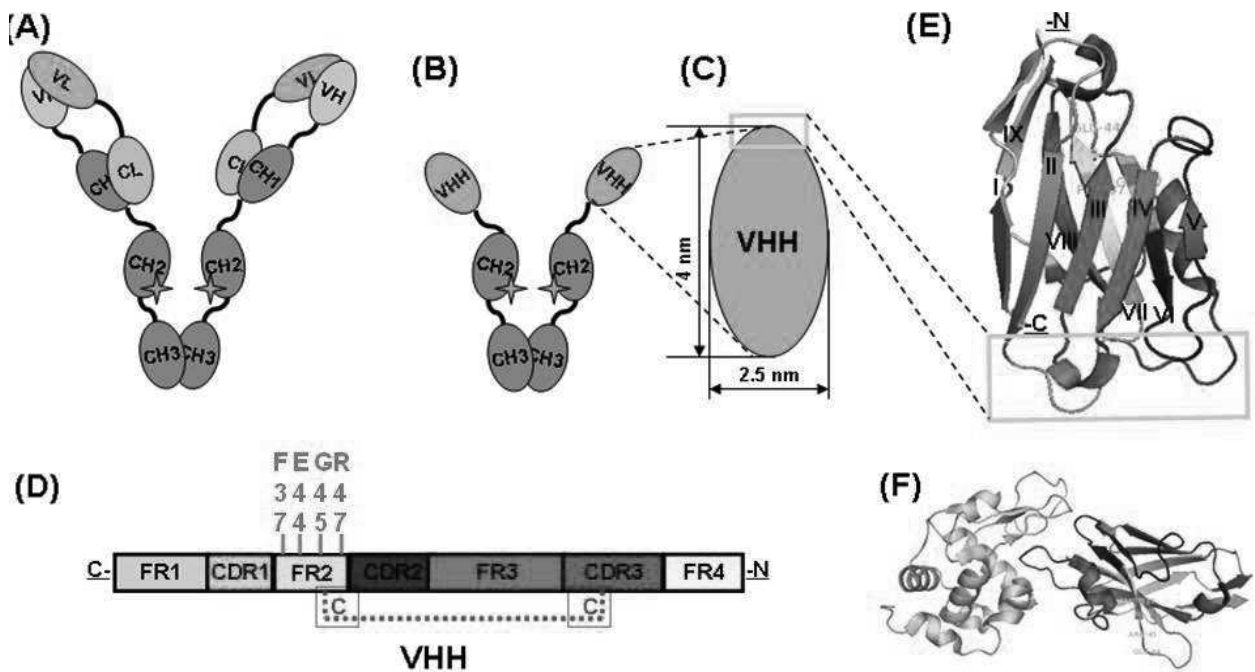


Figure 7. Representative diagrams of a conventional Ab, an HCAb, and a V_{HH} . **A.** A conventional Ab is a dimeric molecule, and each monomer comprising a heavy chain and a light chain. The heavy chain consists of the constant domains (CH1, CH2 and CH3) and the variable domain (V_H). The light chain has only one conserved domain (C_L) and a variable domain (V_L). Important glycosylation sites (orange stars) are present in CH2, which is responsible for effector functions and the flexibility of the molecule. **B.** The HCAb is devoid of the light chain, and the CH1 is the paratope present only in the single variable domain (V_{HH}). **C.** The V_{HH} can be expressed as a prolate-shaped, soluble molecule of ~15 kDa, with. The yellow square shows the antigen-binding site. **D.** The V_{HH} sequence is made of four Framework Regions (FR1, light gray; FR2, cyan; FR3, magenta and FR4, yellow), and three Complementary Determining Regions (CDR1, green; CDR2, blue and CDR3, red). Residues F37, E44, G47 and R45 (orange) are located in the FR2 and mask a hydrophobic patch. The dotted red line represents a disulfide bond between the FR2 and the CDR3; this bond stabilizes the molecule. **E.** A three-dimensional structure of an anti-lysozyme V_{HH} , showing the typical Ig folding of β sheets, five strands in the front (roman numerals: I – V) and four strands in the back (VI – IX). The enlarged yellow square shows the antigen-binding site; formed by juxtaposition of three CDR. **F.** The V_{HH} shown in G, is represented in complex with lysozyme (light blue). A protruding paratope consisting mainly of CDR3 (red) recognizes and binds the catalytic cleft of lysozyme, inhibiting its activity. C-, carboxy - terminal. -N, amino - terminal.

1.9.3 NEURAMINIDASE-SPECIFIC ANTIBODIES

The principal anti-IAV strategy is to induce protective humoral immunity against IAV immunogens by seasonal vaccination, which in turn is mainly based on neutralising Abs against HA. The level of protection against IAV depends on several factors: the composition and formulation of the seasonal vaccine, the circulating IAV in the population, and the level of pre-existing Abs induced by previous vaccination or virus exposure. Antibodies targeting HA can neutralize IAV infectivity, because HA Abs can impede the HA binding into its cellular receptor, resulting in the absence of replication, also known as sterile immunity. Several HA Abs with prophylactic and therapeutic potential have been reported, but until recently the majority of the Abs only conferred protection to homologous or closely related IAV infection.

Besides conventional Abs, also camelid VHH targeting HA were able to inhibit HPAIV infection and rescue challenged mice (Ibanez et al., 2011). In this study, the binding of the VHH close to the receptor-binding domain in the HA membrane distal part, contributed to the binding inhibition properties. However, the continuous antigenic drift of the HA from previous and current IAV vaccine compositions poses a serious challenge towards achieving reliable cross-protection (Carrat and Flahault, 2007). Recent reports had showed the capacity of broadly neutralizing HA antibodies to protect mice and ferrets, posing the importance of antibodies targeting conserved regions in IAV glycoproteins (Corti et al., 2011; Lingwood et al., 2012)

NA-specific Abs are not expected to prevent infection by neutralising the virus, but instead can likely reduce the efficient release of virus from infected cells by blocking the cleavage of the Sia residues to which the newly formed viruses are attached, provided that such Ab have NA inhibition activity (Johansson et al., 1989). Consequently, anti-NA Abs can decrease virus shedding and hence reduce the severity of the IAV infection.

M2e-based vaccination in mice has been found to induce Ab response against the conserved M2e region, offering protection against challenge with different IAV subtypes (Neiryneck et al., 1999; Tompkins et al., 2007). In addition, clinical phase I studies with M2e-vaccine candidates have been completed and demonstrated their safety and immunogenicity in humans (Schotsaert et al., 2009). In addition, a humoral response following infection is also raised against the NP and M1 proteins. However, due to the internal location of these components, the protection conferred has not been proven to be significant (Brugh et al., 1979; Webster et al., 1991). Abs against internal antigens are non-neutralizing and disappear more rapidly. Besides the neutralisation of infectivity or blocking of the release of virus (*i.e.* Abs against HA or NA), Ab can also induce immunological responses like CDC or ADCC.

Nevertheless the NA content in the vaccine formulation is low and variable. In the recent years, the inclusion of the NA into the seasonal formulation of the IAV vaccines had been proposed, in order to increase the immunity of the vaccines and enhance cross-protection (Johansson and Brett, 2008; Bright et al., 2009). The NA Ab response can be easily monitored by NA inhibition assays. Nevertheless, a suitable substrate that can be used effectively is still missing, due to the variant capacity of elicited Ab to inhibit the NA activity using fluorogenic and chromogenic substrates (Sandbulte et al., 2009). The NA had been mutating faster than the HA recently, enforcing the importance of including NA in vaccines. The fact that the NA substrate specificity is not the same as HA specificity, suggested HA-NA substrate affinity mismatch (Gulati et al., 2005).

How could NA-specific Abs suppress influenza virus infectivity?, Abs raised against the NA does not interfere with the IAV binding to the host cell, but it does decrease the release of newly produced virus from infected cells, resulting in plaque size reduction (Kilbourne et al, 1968). Structure determination of antibody-antigen complexes by X-ray crystallography remains the

only definitive way to learn how an Ab recognizes and binds to the surface of its antigen. Specific NA Abs targeting regions close to or in the rim of the catalytic site (Figure 5A) can result in inhibition of the NA catalytic activity. The relevance of the inhibition of the NA catalytic activity in the NA-Ab protection is highlighted by the fact that only Abs with NA inhibitory capacity had been able to select antigenic variants or escape-mutants *in vitro*. Several NA mAbs had been reported, most of them targeting NAs belonging to group 2 (Table 1). In the Ab-antigen complex there is clear shape and biochemical complementarity, hydrogen bonds, van der Waals interactions, salt links or water molecules trapped at the interface, all contribute to the overall binding energy. Surprisingly, despite the growing importance of the NA contribution to the Ab response, only three NA-Ab complexes had been resolved by X-ray, all of them from group 2 N9 (see references in table 1). The information of the location of the NA epitope and a detailed interface structure had played a significant role in the understanding of the NA antigenic drift and catalytic site.

One of the first reports of NA inhibitory Ab, was the panel of 8 mAbs reported by Jackson and Webster (Jackson and Webster, 1982), raised against a H2N2 virus, A/Tokyo/3/67. Seven of these mAbs were able to inhibit the activity of the NA of purified virus, using a macromolecular substrate, such as fetuin (50 kDa) (Table 1). Remarkably, four of those mAbs (23/9, 25/4, S25/3 and S32/3) were able to inhibit the NA activity using the small substrate N-acetylneuraminyl lactose (NAL) (600 Da). Unfortunately, the inhibitory effect of these mAbs was not further characterized, neither an inhibitory concentration (IC_{50}) were reported. Interestingly, it was also reported that a HA Ab (mAb 123/4) partially inhibited the NA activity, suggesting that the binding of a HA Ab can affect the NA access to substrate by steric hindrance (Table 1) (Jackson and Webster, 1982). A much bigger panel of mAbs was used by Webster for the antigenic and biological characterization of a H2N2 NA (R1/5+/57) (Webster et al., 1984). The panel of mAbs was used to map 4 putative overlapping antigenic regions in the pronase-released N2,

according to NA inhibition assays and competitive radioimmunoassay. The putative antigenic regions 1 and 4 appeared far from the NA catalytic site, but different between each other, since region-specific mAb competition was absent. Nevertheless, the mAbs targeting the antigenic regions 1 and 4 failed to inhibit the NA activity using fetuin or NAL substrates. In contrast, the mAbs recognizing the antigenic regions 2 and 3 inhibit the NA activity, using the fetuin substrate. In addition, the mAbs targeting the antigenic region 2 were also subdivided in 4 subgroups, or 4 overlapping epitopes within the region 2, and these mAbs were also able to inhibit the growth of IAV in chick embryos and allowed selection of antigenic variants. Surprisingly, only 2 mAbs recognizing antigenic region 2 (subgroup 2D, 266/4 and 509/3) were able to inhibit 50 – 80 % of the NA activity using NAL as substrate (Table 1). These results suggested that the subgroup 2D epitope is in close proximity to the catalytic site of the NA. An interesting observation in this study was the fact that several NA mAbs inhibited the hemagglutination of crude virus, possibly by proximity of HA and NA protein spikes on the virion, allowing steric inhibition of the HA binding with Abs to NA and vice versa.

1.9.4 N9 mAb NC41 AND NC10

The mAb NC41 was originally part of a panel of 35 mAbs raised against a pronase-released N9 (H11N9, derived from *A/tern/Australia/G70c/75*), and were used to determine N9 antigenic structure by selection of antigenic variants. The N9-NC41 complex was analyzed because NA yielded large protein crystals that were X-ray diffraction quality, and the three-dimensional structure of this complex was obtained (Colman et al., 1987; Colman et al., 1989). The contact residues in N9 responsible for the surface binding in the complex N9-NC41 are: 323 – 350, 368 – 370, 400 – 403, and 430 – 434 (N2 numbering) (Figure 8A) (Tulip et al., 1992). Nineteen AA residues on the N9 are in contact with 17 on the NC41 mAb. The surface areas buried in the

antigen and antibody complex formation are each 800 Å², comprising 12 hydrogen bonds and three ion pairs in the interface (Table 1). Several mAbs of the panel were able to inhibit the N9 activity using fetuin and NAL as substrates. Nevertheless, the 3-D structure of this complex showed that the Fab fragments of the NC41 were not blocking the access of the NAL substrate to the N9 catalytic site. This suggested that the low N9 catalytic activity derives from the displacement of its residue R371, which in the complex N9-NC41, points out directly into the catalytic site (Colman et al., 1987). In addition, the mutation R371K resulted in the loss of 90 % - 95% of NA catalytic activity. The N9-NC41 complex solving was an example of dynamics into antigen-antibody complex formation, due local perturbations of the antigen in the centre of the N9 epitope, challenging the rigid “lock-key” model (Colman et al., 1987). Interestingly, the N329D and I368R mutation in the N9 did not affect greatly the NC41 binding. The structure of the N9 of both mutants with NC41, showed local relaxation of both the Ab and antigen structures (compared to the wild type N9 – NC41 complex) around the mutation, suggesting what was called “promiscuous” aspect of immune surveillance. Mutations within the NC41 binding site had little or no effect in N9 affinity, which could be supported by the flexibility of the VL-VH interface in the Fv fragment of the Ab. In addition, the NC-41 studies showed that the loss of hemagglutination activity in N9 (substitutions in the residues 367, 369, 370, and 372) did not affected the NA activity, leading to propose that the hemagglutination site of the N9 was separated from its catalytic site (Webster et al., 1987).

In similar way that the NC41, the NC10 was also part of a panel of mAbs against a N9, and the N9 -NC10 complex X-ray structure was reported by Malby (Malby et al., 1994; Tulip et al., 1994; Malby et al., 1998). The NC41 and NC10 antigenic epitopes overlap, having approximately 70% of surface residues in common, but different residues were found to make the most critical contributions to the NC41 and NC10 complex stabilities. Compared with NC41 epitope, the NC10 epitope has different energy calculations when complexed with N9, like lower ΔG values

than the NC41 epitope and the major contributions are made by K432, N329 and mannose 200F. Interestingly, the “shape complementarity” (Lawrence and Colman, 1993) measure of the complexes of N9 with NC10 and NC41, is 0.65 or 0.66, respectively (Malby et al., 1994), very similar, suggesting there are another factors to contribute to the differences within the complex interface. On the contrary to the NC41 complex, the NC10 complex posses several water molecules in the interphase, where they increase the surface buried within the complex as well as increasing the shape complementarity. The water molecules in this complex not only help filling the cavity and enhance surface complementarity, but they also serve to bridge hydrogen bonds between the two proteins, therefore acting as adaptors. The role that water molecules play in shaping complementarity may explain why the N9 - NC10 interaction is not mediated by just a subset of critical contacts, as seen in the N9 - NC41 complex, were water is excluded (Lee and Air, 2002, Novotny et al., 1994) (Table 1). It is thus possible, for two different Abs, to recognize the same protein surface in strikingly different ways.

1.9.5 N2 mAb Mem5

The mAb Mem5 recognizes an antigenic site in N2 that is subject to antigenic variation. The Mem5 binds to loops surrounding the N2 active site cavity. In contrast, the Mem5 epitope is in the opposite site to the region bound by the mAbs NC10 and NC41 to N9, which is away from the active site. The Mem5 can inhibit NA activity upon the cleavage of macromolecular substrates (fetuin), but it was only capable of inhibiting the activity of NA small substrates by 40 % (Table 1) (Gulati et al., 2002). The Mem5 CDRs have canonical structures, and 6 CDR are in contact with N2, while only 4 and 5 CDRs are involved in the N9 contact with NC10 and NC41, respectively. The contact surface of the N2 and the Mem5 is 2622 Å, bigger than the N9 complexed with NC10 and NC41 (1413 and 1815 Å, respectively). The epitope of the Mem5 in

the N2 consisted of 4 loops in N2: 146-157 195-202, 216-231 and 243-251 (Figure 8B) (Lee and Air, 2006). This binding of Mem5 partially occludes the N2 active site. The Mem5-N2 contact surface is also contributed by the N200 carbohydrate moiety, which is also important in the N9-NC10 complex, and its lack results in a decreased NA activity probably by misfolding of the NA. There are 33 direct contacts between Mem5 and N2, including 3 salt bridges (D147, H150 and E199), 14 hydrogen bonds and 16 van der Waals interactions. In a similar way that NC41, the N2-Mem5 complex have residues with major contribution to the binding, R249, K221, E199, H150, all of them accounting for the 30 % of the binding surface. In addition, substitutions in the residues 198, 199, 220 and 221 had been identified in Mem5 escape-mutants. This structure also showed a higher level of hydration in the contact surface, (the N9-NC10 complex did not contain any water molecules and the N9-NC41 contained only 3) the N2-Mem5 contains 58 water molecules in the surface (Venkatramani et al., 2006). The water molecules are important because they fill up the gaps where the surfaces do not have shape complementarity, but this is not the case for the Mem5-N9 interface complex. Nevertheless, the residue E199, which contributes greatly to the contact surface and its mutation is present in several escape-mutants but is surrounding in a dry island without any water molecule.

A



B

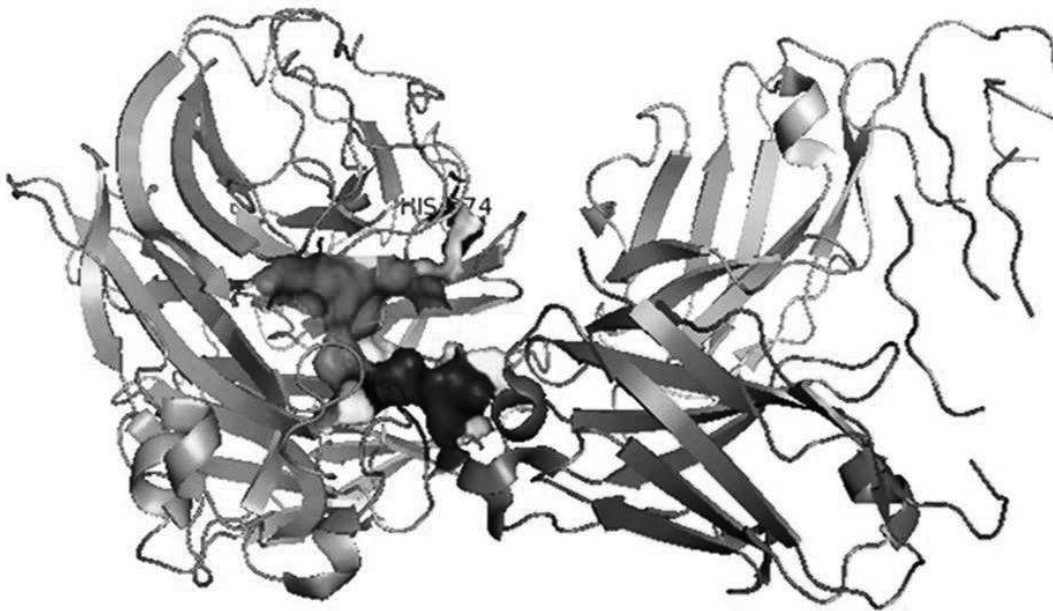


Figure 8. Crystallographic structures of the N9-NC10 and N2-Mem5 complexes. The NA monomers (green ribbons) have the catalytic site in surface representation, sharing the residue colour code of figure 2. The MAb heavy and light chain are in magenta and cyan, respectively. **A.** The N9-NC10 complex. The AA residues in N9 that make contact with NC10 are in orange and are not close to the N9 catalytic site (PDB: 1NMC). **B.** The N2-Mem5 complex. Compared to the NC10, the Mem5 epitope is within the rim of the catalytic site, with several residues of the “150-loop” part of the epitope (PDB: 2AEP).

Table 1. Comparison of NA-specific mAbs

mAb	23/9 *	509/3 *	NC41	NC10	N8-4	N8-10	Mem5
IAV	H2N2 Tokyo/3/67	H2N2 R1/5+/57	H11N9 Tern/Australia/ G70c/75	H11N9 Tern/Australia/ G70c/75	H1N8 WS/duck/Ukraine/1/63	H1N8 WS/duck/Ukraine/1/63	H3N2 Memphis/31/98
NA epitope	ND	ND	323 – 350, 368–370, 400-403, 430–434	328-332, 341-344, 366-370, 400-403	ND	ND	146-157, 195-202, 216-231, 243-251
Escape mut. sites &	221, 253, 344, 368, 370, 403	150, 329, 334, 344, 368, 370, 403	220, 329, 367, 368, 369, 370, 372, 400, 432 §		150, 199, 284, 344, 346, 367, 372, 400 ¶		198, 199, 220, 221
Fetuin Inh. £	+	+ (100 %)	+ (3.25 log ₁₀)	+ (4.5 log ₁₀)	+ (> 4 log ₁₀)	+ (3.6 log ₁₀)	+ (70 – 100 %)
NAL Inh. £	+	+ (50 – 80 %)	+ (3.7 log ₁₀)	-	+ (> 4 log ₁₀)	+ (< 1 log ₁₀)	+ (40 %)
Interface area	ND	ND	1815 Å ²	1413 Å ²	ND	ND	2622 Å ²
PDB	ND	ND	1NCA, 1NCD, 1NMA	1NMC, 1A14, 1NMB	ND	ND	2AEP, 2AEQ
Ref.	Jackson and Webster, 1982	(Webster et al, 1984; Gulati et al, 2002)	Colman, et al., 1987; Webster et al., 1987, Tulip et al., 1992; Tulip et al., 1999	Colman, et al., 1989; Malby et al., 1994. Malby et al., 1998	Saito, et al., 1994	Saito, et al, 1994	Lee and Air, 2005; Gulati et al., 2002 ; Venkatramani et al, 2006

£ Neuraminidase inhibition assay was done with either fetuin or NAL as substrate; antibody titers required for 50 % reduction of the NA activity are expressed in log₁₀ units should be mass over volume. ND Not determined

* Representative Ab of a panel of mAb,

& The escape mutations reported are originated from a panel of mAb, which the specific mAb is part of.

§ Escape mutations shared with NC10, due both mAb are from the same panel.

¶ Escape mutations shared with N8-10, due both mAb are from the same panel.

CHAPTER 2: AIMS

2.1 SCOPE

The huge economical and animal welfare impact as well as the pandemic threat associated with highly pathogenic avian Influenza A virus (HPAIV) H5N1 outbreaks remain a major concern. An enormous economic and social burden was seen in Asiatic countries during 1997 – 2005, where the poultry industry has been devastated, due to the high lethality of HPAIV in chickens and as a result of massive culling of HPAIV infected birds, the prime containment strategy. Moreover, in Hong Kong, in 1997 the first human casualties directly attributed to avian HPAIV were reported (de Jong et al., 1997). Since 2003, more than 600-laboratory confirmed cases of H5N1-infected humans have been reported in 15 countries (www.who.int/influenza/human_animal_interface/H5N1_cumulative_table_archives/en/index.html), where a mortality rate of 60% was seen. Compared with seasonal influenza infections, human HPAIV infection are more severe, presenting a higher replication rate, broader cellular tropism, systemic spread resulting in high levels of circulating proinflammatory cytokines and chemokine (de Jong et al., 2006; Gu et al., 2007; Baskin et al., 2009). Specific antiviral treatment options of hospitalized H5N1-infected patients are largely limited to the NA inhibitor oseltamivir. However, high doses appear to be required for a systemic treatment, and very often drug-resistant viruses emerge in the course of such treatments (Gooskens et al., 2009). In addition, two recent reports provided experimental evidence that H5N1 viruses can likely evolve into variants with human-to-human transmission. Although these studies were performed in ferrets and demonstrated that HPAIV H5N1 viruses can be selected that acquired airborne transmission between ferrets, the findings renewed the concerns of public health care officials that H5N1 viruses may eventually become human-to-human transmissible (Herfst et al., 2012; Imai et al., 2012). Today, the fastest measure against such a pandemic influenza virus outbreak

is still the use of antivirals such as oseltamivir and Relenza to mitigate disease in infected patients.

However, the clinical benefit of the use of e.g. oseltamivir is modest at best and based on meta-analysis of reported clinical trials even uncertain (Jefferson et al., 2012; Wang et al., 2012). Furthermore, to implement small compound drugs such as the NA-inhibitors oseltamivir or Relenza on a vast scale (global population, use in poultry) is unrealistic and too expensive. Despite these shortcomings, even today, oseltamivir (Tamiflu) as a treatment for seasonal influenza represents a blockbuster for Roche.

For this PhD project, the aim was to generate and evaluate a novel strategy to try to control H5N1 virus infections *in vitro* and *in vivo*, the latter in experimental mouse model. First, our aim was to target NA because it is an enzyme that is very important in the viral life cycle. In addition, NA is targeted by the human humoral immune system and is subjected to antigenic drift and shift. Antibodies directed against NA have antiviral activity, which has been best documented for antibodies that block NA activity. Based on this rationale, we proposed a strategy that takes advantage of the potential of camel single chain antibodies (VHH). Our aim was to select VHH antibodies that inhibit NA activity. Ideally the binding of such VHH molecules to NA would involve essential contacts with the conserved residues that make up the catalytic cleft of the enzyme; VHH appear to be uniquely capable of recognizing catalytic clefts in enzymes (De Genst et al., 2006). NA-specific VHH with antiviral potential could possibly also recognize conserved epitopes on the surface of NA. Finally, our aim was to take advantage of two robust expression platforms for these VHH molecules: *E. coli*, allowing the expression of VHH in simple mono- and dimeric format and an *Arabidopsis thaliana* seed-directed expression platform that allows the expression of high amounts of Fc-tailed dimeric VHH-based biologicals. Ultimately, and beyond the scope of this thesis, a seed-based expression system for recombinant NA-

targeting VHH could be explored further as an economical production platform for oral delivery of the antiviral as a crude extract or even as intact seeds, to domesticated birds.

2.2 OBJECTIVES

The first step of the project was to produce recombinant H5N1 Neuraminidase for camelid immunization. NA is a membrane bound tetrameric glycoprotein. NA is enzymatically active as a tetramer. As an immunogen we decided to use soluble recombinant N1 NA, named N1rec, which was engineered as a soluble protein, where the NA cytoplasmic, transmembrane and stalk domains were substituted for a type I secretion signal followed by a yeast-derived tetramerization domain GCN4. A Baculovirus platform was chosen to produce a soluble tetrameric N1rec in insect cells, because is an efficient platform for the production of complex proteins, including mammalian or avian-origin proteins. Purified N1rec, derived from A/crested eagle/Belgium/01/2004, was then used to immunize an alpaca. N1rec-binding VHH (N1-VHH) were selected from an immune phage library by panning with the antigen. The N1-VHH candidates would then be produced in bacteria (*Escherichia coli*) as soluble monovalent proteins for further characterization (N1-VHHm). The inhibitory capacity of the N1-VHH against N1rec was assessed and correlated with antiviral activity in H5N1 infected cells *in vitro*. The N1-VHH that showed the most potent antiviral activity were then formatted as bivalent molecules in order to increase affinity by introduction of avidity, in two different production platforms. As a first approach, the selected N1-VHH genes would be designed in an expression cassette comprising 2 VHH genes in tandem, fused by a flexible linker and produced in bacteria (N1-VHHb). In the second approach, more complex bivalent molecules would be plant-produced, and targeted as seed storage proteins in *Arabidopsis thaliana*. The selected N1-VHH genes would be fused to a mouse IgG2a Fc sequence, resulting in two N1-VHH molecules fused by their Fc moiety (N1-

VHH-Fc). All the bivalent formats of the N1rec-binding VHH were first evaluated *in vitro* and subsequently *in vivo*, in a mouse model of H5N1. Both a clade 1 and a clade 2 H5N1 virus would be used as well as an oseltamivir-resistant virus.

Chapter 3: RESULTS

Camelid single chain antibodies targeting neuraminidase protect against H5N1 challenge virus

Miguel Cardoso^{1,2}, Lorena Itatí Ibañez^{1,2}, Sarah De Baets^{1,2}, Anouk Smet^{1,2}, Bert Schepens^{1,2}, Walter Fiers^{1,2}, Serge Muyldermans³, Ann Depicker^{4,5}, Xavier Saelens^{1,2*}

¹Department for Molecular Biomedical Research, VIB, Technologiepark 927, Ghent, Belgium

²Department of Biomedical Molecular Biology, Ghent University, Technologiepark 927, Ghent, Belgium

³Department of Molecular and Cellular Interactions, VIB, Brussels, Belgium

⁴Department of Plant Systems Biology, VIB, Technologiepark 927, Ghent, Belgium

⁵Department of Biotechnology and Bioinformatics, Technologiepark 927, Ghent, Belgium

ABSTRACT

Although the influenza virus neuraminidase (NA) is the target of several antiviral drugs (*e.g.* oseltamivir) and has a major immunogenic potential, the inclusion of NA in vaccine formulations has been largely neglected. We immunized an alpaca with H5N1 NA recombinant protein, derived from the highly pathogenic influenza virus A/crested eagle/Belgium/09/2004. An immune phage library was constructed and H5N1 NA-binding single chain camelid (N1-VHH) was isolated by panning. Two monovalent N1-VHHs (N1-3-VHHm and N1-5-VHHm) showed strong inhibition of the NA activity, and also antiviral activity in cell-based assays, against clade 1 and 2 H5N1 virus. We introduced bivalency into the N1-3-VHH and N1-5-VHH in two bivalent formats: the bacteria-produced N1-VHHb (two N1-VHH moieties fused by flexible linker); and the plant-produced N1-VHH-Fc (N1-VHH moiety fused to a mouse IgG2a Fc). The *in vitro* antiviral potency of both bivalent formats was increased 10– to 100-fold, compared to their monovalent counterparts. Using a murine model, we assessed the *in vivo* antiviral potential using a single-dose of N1-VHH treatment at 24 hours before a lethal challenge of H5N1 virus. Sixty µg treatment with N1-3-VHHb or N1-5-VHHb rescued Balb/c mice, with a survival of 100%. The plant-produced formats showed an increased protection in mice. The single-dose N1-3-VHH-Fc and N1-5-VHH-Fc treatment of 17 or 3.5 µg, respectively, also rescued 100% of H5N1 challenged mice. The N1-5-VHH-Fc treatment in mice presented a less severe morbidity, compared with N1-3-VHH-Fc, and was dose-dependent. Next, we used a mutant H5N1 virus, carrying the H274Y substitution in the NA (H5N1 H274Y), to assess the antiviral potential of the N1-VHH in an oseltamivir-resistant virus. The single dose treatment N1-3-VHHb and N1-3-VHH-Fc (60 and 84 µg, respectively) rescued 100% of H5N1 H274Y challenged mice, but the morbidity was severe. We did not observe antiviral effects of the N1-5-VHH in any format against the H5N1 H274Y. These pieces of evidence highlight our N1-VHH as a promising alternative to influenza virus treatment, with veterinary and clinical potential.

INTRODUCTION

Zoonotic influenza A virus (IAV) infections are a persistent threat because their pandemic potential. In particular, highly pathogenic avian influenza viruses (HPAIV) of the H5N1 and H7N7 subtypes occasionally cross the species barrier between domesticated birds and human. Whether these viruses could become transmissible between humans through reassortment with circulating swine or human IAV or by gradually accumulating mutations, remains very difficult to predict (Carrat and Flahault, 2007). In the last decade, two zoonotic outbreaks had a major impact on public health: the HPAIV H5N1 (Tran et al., 2004) and the swine flu (H1N1) or “Mexican flu” outbreak in 2009, confirmed the lack of preparedness against pandemic influenza (Ilyushina et al., 2010).

HPAIV H5N1 influenza virus infection in humans leads to an unusual high mortality, reaching a 60% mortality rate (Chotpitayasunondh et al., 2005). The high pathogenicity of HPAIV H5N1 in humans can be attributed to a high replication rate and a broad cellular tropism that can lead to a systemic spread. A deregulated induction of proinflammatory cytokines and chemokines (sometimes called “cytokine storm”) is associated with severe HPAIV H5N1 infections, and can result into an excessive immunological response (de Jong et al., 2006). The treatments reported and available against HPAIV H5N1 are far from been optimal: treatment with convalescent plasma for influenza A (H5N1) infected patients had been shown to be protective (Zhou et al., 2007) as well as a risky combination of antiviral drugs and immunomodulators (White et al., 2009).

Effective anti-influenza alternatives are needed for the HPAIV H5N1 treatment, and among them, the single chain monoclonal antibody technology is a promising tool. Naturally occurring single chain antibodies had been found in sharks (Greenberg et al., 1995; Dooley et al., 2003) and camelids (Hamers-Casterman et al., 1993). The camelid single domain antibodies

represent a new promising alternative in the monoclonal antibody repertoire (Muyldermans et al., 1994). The variable domains of the functional heavy-chain antibodies (VHH) discovered in camels are related to the human VH subgroup III (Nguyen et al., 1998). Their specificity, robustness, ease of production and flexibility had prompted a long lasting research as binding or stabilizing moieties, or building blocks for therapeutics (Coppieters et al., 2006). The VHH tends to target epitopes with concave topology, in contrast with the planar epitopes recognized by “classical” light and heavy chain antibodies (De Genst et al., 2006). The protruding paratope in the Complementary Determining Region 3 (CDR3) had been reported to be a major contributor to the binding contact surface. The VHH small and robust format permits the design of tailor made VHH, boosted by the identification of stable “frameworks” in the VHH structure that allows CDR grafting (Saerens et al., 2005). Some of the most promising described properties of the VHH are inhibitors for several enzymes, and stabilizing moieties for membrane bound proteins that permit their crystallization (Lauwereys et al., 1998; Decanniere et al., 1999; Decanniere et al., 2000; Desmyter et al., 2002; Rasmussen et al., 2011). It has also been reported that the VHH showed an affinity to its antigen even in the nanomolar to picomolar range (Ward et al., 1989), matching the best affinity ever reported into the “classical” antibodies. The reported high affinity and inhibitory properties of the VHH make them an attractive tool against influenza proteins. In addition, several examples of successful VHH treatment against viral diseases have been reported (Hultberg et al., 2011; Ibanez et al., 2011; Schepens et al., 2011). Also, a VHH against M2 resulted in the inhibition of the replication of amantadine-sensitive and -resistant influenza virus strains and protected mice from lethal influenza challenges, with cross protective potential (Wei et al., 2011). All these pieces of evidence indicate that VHH can not only have antiviral efficiency by blocking the binding of the influenza virion (VHH against HA), but also can be used in other ways to prevent virus spread. Here we report on the isolation and characterization of VHH directed against NA from an HPAIV H5N1 virus. We demonstrate the *in*

vitro and *in vivo* antiviral potential of NA-binding VHH (N1-VHH) against oseltamivir-sensitive and -resistant strains.

MATERIALS AND METHODS

H5N1 INFLUENZA VIRUS

H5N1 IAV strains NIBRG-14 and NIBRG-23 were obtained from the UK National Institute for Biological Standards and Control, a center of the Health Protection Agency. NIBRG-14 and NIBRG-23 are 2:6 reverse genetics-derived reassortant of NA and HA derived from A/Vietnam/1194/2004 (H5N1) or A/turkey/Turkey/2005 (H5N1), respectively, and A/PR/8/34 (H1N1) viruses. The H5N1 H274Y is a 1:1:6 reverse genetics-derived reassortant with the NA derived from A/crested eagle/Belgium/09/2004 (Van Borm et al., 2005) (with the H274Y mutation introduced by site-specific mutagenesis), the HA from A/Vietnam/1194/2004 and the remaining six genome segments from A/PR/8/34. All of the HA segments of these H5N1 viruses lack the coding information for the polybasic cleavage site, hence making them acceptable for use in BioSafety Level (BSL-2) facilities. Following adaptation to Balb/c mice, the HA and NA-coding regions of the mouse-adapted NIBRG-14 (NIBRG-14 ma) and H5N1 H274Y (H5N1 H274Yma) were sequenced and found to be identical to those of the parental viruses. The median Tissue Culture Infectious Dose (TCID₅₀) and median Lethal Dose (LD₅₀) of NIBRG-14 ma and H5N1 H274Yma virus were determined using the method of Reed and Muench. All H5N1 IAV experiments above described, were performed in BSL-2 rooms with negative pressure relative to adjoining rooms.

BACULOVIRUS-BASED PRODUCTION OF RECOMBINANT SOLUBLE TETRAMERIC NA

We produced enzymatically active, soluble tetrameric NA (N1rec) derived from A/crested eagle/Belgium/01/2004 (H5N1) using proprietary technology (WO 2002/074795). N1rec was produced using a recombinant baculovirus expression system in Sf9 cells. The N1rec expression cassette (*n1rec*) consisted of: the secretion signal of IAV HA type 1 (ssHA, 16 residues), the leucine zipper, derived from *Saccharomyces cerevisiae*, transcription factor GCN4 (tGCN4, 32 residues) (Harbury et al., 1993) (De Filette et al., 2008) and the extracellular part of the H5N1 NA derived from A/crested eagle/Belgium/09/2004 (53–449 amino acid residues) (Van Borm et al., 2005) (Figure 2). This expression cassette was cloned into a pAcMP2 Baculovirus transfer vector (BD Biosciences®), resulting in the pAcMP2*n1rec* vector. Recombinant baculovirus was generated by co-transfection of pAcMP2*n1rec* with linearized *Autographa californica* Nuclear Polydrosis Virus (AcNPV) DNA, BaculoGold (BD Biosciences®), into Sf9 insect cells (derived from *Spodoptera frugiperda*), using the ESCORT IV Transfection Reagent (Sigma®). The resulting recombinant AcNPVN1rec virus was used for infection of Sf9 cells. Sf9 cells were incubated at 28 °C in rolling bottles in TC-100 medium (Invitrogen®), supplemented with 10% FCS and penicillin/streptomycin. Four days after infection, the supernatant was harvested and clarified by centrifugation (1 hr at 50,000 g).

NEURAMINIDASE ACTIVITY ASSAY

NA activity was quantified by determining the rate of cleavage of the fluorogenic substrate 4-MUNANA (2'-4-Methylumbelliferyl- α -D-N-acetylneuraminic acid, sodium salt hydrate, 50 mM, dissolved in deionized water, Sigma-Aldrich®) into 4-methylumbelliferone. The NA activity reaction was performed in 200 mM NaAc, 2 mM CaCl₂, 1 % butanol and 1 mM 4-MUNANA and measured in a kinetic mode, with excitation at 365 nm and emission at 450 nm in an Optima Fluorostar®. A standard curve of increasing concentrations of soluble 4-methylumbelliferone

was included to correlate the fluorescence intensity with the molar amount of 4-methylumbelliferone. One NA activity unit is defined as 1 nmol of 4-methylumbelliferone / min.

RECOMBINANT NEURAMINIDASE PURIFICATION

Two parts (v:v) of n-butanol were added to 3 parts of cleared AcNPVN1rec infected Sf9 cells supernatant and the resulting mixture was shaken vigorously for 5 minutes. The aqueous phase, containing the soluble N1rec, was separated from the organic phase, and was 2.5 times diluted in 5 mM KH₂PO₄ pH 6.6 and 0.22 µm filtered. The diluted aqueous phase was subsequently applied to a HA Ultrogel® Hydroxyapatite Chromatography Sorbent (Pall®) packed XK26\70 column (GE Healthcare®), and eluted with a gradient of 5 – 400 mM KH₂PO₄ pH 6.6, 4 % butanol. Eluted fractions with NA activity were pooled and loaded onto a Blue Sepharose (Sigma-Aldrich®) column, and equilibrated with 50 mM MES pH 6.6, 5 % glycerol, 8 mM CaCl₂. Bound proteins were eluted by a single step elution with 50 mM MES pH 6.6, 5 % glycerol, 8 mM CaCl₂, 1.5 M NaCl. Eluted fraction with NA-activity were subsequently loaded on a HiLoad 16/60 Superdex 200 (GE Healthcare®) gel filtration column that was equilibrated with 50 mM MES pH 6.6, 5 % glycerol, 8 mM CaCl₂, 150 mM NaCl. Peak fractions containing NA activity were pooled, aliquoted and stored at -80°C for further use. All the chromatography steps were performed using an Akta purification station (GE Healthcare®).

CAMELID IMMUNIZATION AND PHAGE LIBRARY CONSTRUCTION

An alpaca (*Vicugna pacos*) was weekly injected subcutaneously with 125 µg of N1rec during 35 days, in the presence of incomplete Freund's adjuvant emulsions. On day 39, anticoagulated blood was collected for the preparation of lymphocytes. Lymphocytes were isolated using a UNI-SEP density gradient separation kit (NOVAmed®), and total RNA was extracted. cDNA was prepared using oligo (dT) primers, and the VH and VHH genes were amplified with: primer call

01 (GTCCTGGCTGCTCTTCTACAAGG) and primer call 02
(GGTACGTGCTGTTGAACTGTTCC). *Pst*I and *Not*I restriction sites were inserted into the amplified sequences using the primers: A6E (GAT GTG CAG CTG CAG GAG TCT GGR GGA GG) and 38 (GGA CTA GTG CGG CCG CTG GAG ACG GTG ACC TGG GT). The resulting PCR product (550 bp) and the vector pHEN4 were *Pst*I and *Not*I digested and ligated (Arbabi Ghahroudi et al., 1997) and transformed into electrocompetent TGI *E. coli* cells. Transformants were grown in 2xTY medium, (supplemented with 100 µg/ml ampicillin and 1% glucose) into the exponential phase, and the helper phage M13K07 was added. The resulting VHH phage display library was subjected to 4 consecutive rounds of panning, performed with solid-phase coated N1rec. This bio-panning resulted in the isolation of 13 individual N1rec-binding candidates: N1-1-VHH, N1-2-VHH, N1-3-VHH, N1-4-VHH, N1-5-VHH, N1-6-VHH, N1-7-VHH, N1-8-VHH, N1-9-VHH, N1-10-VHH, N1-11-VHH, N1-12-VHH and N1-13-VHH.

N1-VHHm PRODUCTION AND PURIFICATION

The VHH coding information of the selected N1rec-binding phages was amplified by PCR with the primers A6E and 38. A 400 bp PCR product and the pHEN6c vector were *Pst*I and *Bst*EII digested, ligated and used to transform *E. coli* WK6 strain. In the pHEN6c vector, the coding information for the N1rec-binding VHH candidates were cloned downstream of an N-terminal PelB secretion signal sequences and the cloning strategy introduced a carboxyterminal hexahistidine tag (Figure 1). For production and purification of soluble VHH, pHEN6c-transformed WK6 cells were grown in TB medium supplemented with: ampicillin (100 µg/ml), 2 mM CaCl₂ and 0.1% glucose. After 16 hours, VHH production was induced with 1 mM of IPTG, and the periplasmic fraction was extracted by osmotic shock using TES (0.2 M Tris pH 8.0, 0.5 mM EDTA and 0.5 M sucrose). Periplasmic extracts were centrifuged at 8000 rpm at 4 °C and the supernatant was applied to a His Select Nickel Affinity gel (Sigma®). Following loading, the

column was washed with PBS and the soluble VHH was eluted with 0.5 M imidazole and dialyzed at 4 °C against PBS. Monomeric N1-VHH (N1-VHHm) was concentrated with a Vivaspin 5000 MW cutoff filter (Vivascience®). Total protein concentration was determined with BCA protein Assay kit (Thermo Scientific).

ELISA ASSAYS

Ten µg/ml of N1rec or M2e-tGCN4 (De Filette et al., 2008) were coated O/N in 96 well Maxisorp (Nunc®) plates. Dilution series of the 13 N1-VHH candidates (from 10 µM – 0.1 nM) were incubated in the coated plates for 2 hrs at 37 °C, and VHH excess was washed 3X with PBS. The binding of the N1-VHHm to the tGCN4 moiety or to the N1rec NA globular head was assessed by a mouse α-His-tag fused with Horse Radish peroxidase HRP (1:5000). After 3X PBS wash, 100 µl of TMB substrate (Pharmigen BD) was added and absorbance at 565 nm was obtained.

N1-VHHm STRUCTURE PREDICTION AND NA MODELLING

The AA sequences of the 13 N1-VHH were loaded into the ESyPred3D Web Server 1.0 Molecular Biology Research Unit, The University of Namur, Belgium (<http://www.fundp.ac.be/sciences/biologie/urbm/bioinfo/esypred/>), and retrieved as PDB files. The structures of the 13 N1-VHH were modelled with DeepView/Swiss-PdbViewer (<http://spdbv.vital-it.ch/>), and the NA modelling was done using PyMOL Molecular Graphics System (DeLano Scientific).

N1-VHHm SURFACE PLASMON RESONANCE ANALYSIS

The affinity of the monovalent N1-3-VHHm, N1-5-VHHm and N1-7-VHHm directed against N1rec was determined by Surface Plasmon Resonance (SPR) on a Biacore3000 platform. N1rec antigen was first immobilized (2000 RU) into a Series S sensor chip CM5 (GE

Healthcare®) (coupling in 10 mM NaAc pH 4.5), with regeneration in 0.02% SDS. Subsequently, each monovalent N1-VHHm was diluted in HBS buffer (0.01 M HEPES, 0.15 M NaCl, 0.005% Tween 20, pH 6.4) to obtain a N1-VHH gradient between 1.95 and 1000 nM. The different N1-VHHs were injected over the CM5 chip to record their binding kinetics with the N1rec. Binding sensograms were used to calculate the k_{on} and k_{off} values, the equilibrium dissociation constant (K_D) and to perform epitope competition analysis, using the Biacore T100 evaluation software.

CONSTRUCTION OF THE BIVALENT N1-VHH

The coding information of N1-3-VHHm and N1-5-VHHm was amplified with primers MH (CATGCCATGGGAGCTTTGGGAGCTTTGGAGCTGGGGGTCTTCGCTGTGGTGCCTGAGGAGACGGTGACCTGGGT) and A4short (CATGCCATGATCCGCGGCCAGCCGGCCATGGCTGATGTGCAGCTGGTGGAGTCT) to introduce an *Nco*I restriction enzyme site at both extremities of the amplified fragment. The MH primer also added the hinge sequence of llama $\gamma 2c$ (Ala-His-His-Ser-Glu-Asp-Pro-Ser-Ser-Lys-Ala-Pro-Lys-Ala-Pro-Met-Ala) (Hmila et al., 2010) to the 3' end of the N1-VHH. PCR-amplicons were cloned into pHEN6c plasmid containing the *n1-3-vhh* or the *n1-5-vhh* genes, in order to generate the homo-bivalent N1-3-VHHb and N1-5-VHHb expression constructs (Figure 1). These bivalent constructs were expressed and purified as outlined above.

ARABIDOPSIS-BASED EXPRESSION OF N1-VHH-Fc FUSIONS

The *n1-vhh-fc* expression cassette was designed as follows: from 5' to 3': *LB* (left border of T-DNA); 3' *ocs* (3' end of the octopine synthase gene); *npt II* (neomycin phosphotransferase II open reading frame); *Pnos* (nopaline synthase gene promoter); *Pphas* (β -phaseolin gene promoter); 5' utr (5' UTR of *arc5-l* gene); *SS* (signal peptide of the *Arabidopsis thaliana* 2S2 seed storage protein gene); *KDEL* (ER retention signal); *n1-3-vhh* (coding sequence of the N1-3-VHH); 3' *arc* (3' flanking regulatory sequences of the *arc5-l* gene); *n1-3-vhh* (coding sequence

of the N1-3-VHH fused to the mouse CH2 and CH3 IgG2a hinge sequence); RB, T-DNA right border (Figure 1) (De Jaeger et al., 2002) (Van Droogenbroeck et al., 2007). The N1-3-VHH-Fc genetic fusion was synthesized commercially (GenScript®), and cloned into a pPhasGW binary T-DNA vector, resulting in the *pPhasGWn1-vhh-fc* vector. The N1-3-VHH coding information was removed from the N1-3-VHH-Fc construction, and replaced with the N1-5-VHH and N1-7-VHH coding information, using *BstEII* and *PstI* enzymes. Ligation mixtures were transformed into WK6 strain. A plant-produced Coronavirus-Fc fusion protein (GP4) fused to a mouse IgG2a Fc moiety, and was used as an irrelevant control. The GP4-Fc was kindly provided by Robin Piron, from the Gene regulation laboratory, from the Department of Plant Systems Biology, VIB, Technologiepark 927, Ghent University.

PRODUCTION AND PURIFICATION OF N1-VHH-Fc

The *pPhasGWn1-vhh-fc* constructs were used for transformation of *Agrobacterium* C58C1Rif^R (pMP90). This *Agrobacterium* strain was grown on YEB medium supplemented with rifampicin (100 mg/L), gentamycin (40 mg/L), spectinomycin (100 mg/L) and streptomycin (300 mg/L). *Arabidopsis* transformants were subsequently obtained by *Agrobacterium*-mediated floral dip transformation (Clough and Bent, 1998). Seeds from T1 segregating plants were used as the starting material for the isolation of the plant-produced N1-VHH-Fc proteins. One gram of seeds was crushed for total protein extraction in 25 ml of 50 mM Tris-HCl, pH 8.0, 200 mM NaCl, 5 mM EDTA, 0.1% (v/v) of Tween 20 and Complete® protease inhibitor tablets (Roche®). The seed extracts were clarified by centrifugation and applied to a protein G sepharose column (GE Healthcare®). N1-VHH-Fc proteins were eluted with a single step of 0.1 M glycine pH 3.0.

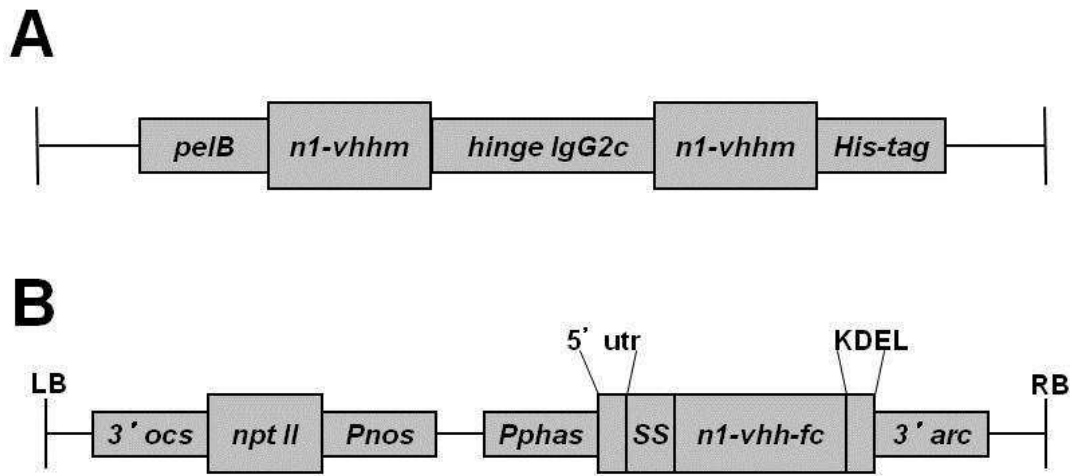


Figure 1. Schematic representation of the expression cassettes of the two bivalent N1rec-binding VHH. **A.** Bacteria-produced N1-VHHb, fused by a flexible linker (IgG2c hinge) and a hexahistidine tag. **B.** The plant-produced N1-VHH-Fc, targeted as a seed storage protein.

H5N1 PLAQUE ASSAY

Monolayers of MDCK cells were grown in DMEM supplemented with 10% Fetal Bovine Serum, 1 % penicillin/streptomycin, 1 % glutamine; at 37 °C with 5% CO₂. MDCK TMPRSS2 (kindly provided by Dr. Wolfgang Garten, Philipps-Universität Marburg, Germany) (Bottcher et al., 2009) were cultured in DMEM supplemented with geneticin (0.3 mg/ml) and puromycin (2 µg/ml) and the expression of TMPRSS2 was induced with doxycycline (0.5 µg/ml). At 70% of confluence, the MCDK cells were infected with a moi of 10 with NIBRG-14, NIBRG-23 or H5N1 H274Y, as indicated. Samples containing N1-VHHm, N1-VHHb, N1-VHH-Fc or oseltamivir were mixed with 0.8% of Avicel RC-591™ as overlay (Matrosovich et al., 2006). After 2-4 days of incubation, the cells were fixed with 4% paraformaldehyde in PBS for 30 min. The cells were permeabilized with 20 mM glycine, 0.5% (v/v) Triton X-100. After blocking, the cells were incubated for 2 hrs with polyclonal α-NIBRG-14 (1:1000) or α-M2e monoclonal antibody (1:5000). After washing, α-

mouse IgG-HRP conjugated was used to visualize plaques using the substrate TrueBlue™ Peroxidase Substrate (KPL®).

IMMUNOFLUORESCENCE

Sixty percent confluent MDCK TMRSS2 cells monolayers were infected with NIBRG-14 at a moi of 10, in serum free medium (SFM). After 2 hrs of adsorption at 37 °C, 5 % CO₂, the inoculum was removed from the monolayer, followed by washes with SFM, and refreshing with DMEM for TMRSS2 culture (see above). After 8 hrs infection; the cells were fixed, permeabilized and blocked. The cells were incubated for 2 hrs with house-made polyclonal α-H5N1 NA recombinant protein (1:1000), washed and incubated for one hour with goat α-mouse IgG-ALEXA Fluor 633 (Invitrogen®), at 1:5000, mounted in glass slides and analysed.

NA SEQUENCE ALIGNMENT

The phylogenetic tree and amino acid substitutions of the aligned sequences of the H5N1 NA of: A/crested eagle/Belgium/01/2004 (accession number: ABP52007), A/Vietnam/1194/2004 (ABA70757) and A/turkey/Turkey/01/2005 (ABQ58915), were obtained by the Clustal W method, using in the MegAlign software (DNASTAR®).

MICE EXPERIMENTS

Specific-pathogen-free female Balb/c mice, 7–9 weeks old, were purchased from Charles River (Germany) and used for all experiments. Mice were housed in ventilated cages with high-efficiency particulate air filters in temperature-controlled, air-conditioned facilities and had food and water *ad libitum*. Mice were anesthetized by intraperitoneal injection of xylazine (10 µg/g) and ketamine (100 µg/g) before intranasal administration of N1-VHHm, N1-VHHb or N1-VHH-Fc. Mice were challenged 4 hours later with 1 or 4 LD₅₀ of the indicated virus (50 µL, divided equally between the nostrils). The N1-VHH in any format were diluted in endotoxin-free

phosphate-buffered saline (PBS) with 1% (wt/vol) bovine serum albumin and dosing ranged from 5 – 0.25 mg/kg, as indicated in the figure legends. To determine the effect of intranasal N1-VHH delivery on lung virus titer production, mice were challenged with 4 LD₅₀ of NIBRG-14 ma IAV. Lung homogenates were prepared in PBS, cleared by centrifugation at 4°C, and used for virus titration. Monolayers of MDCK cells were infected with 50 µL of serial 1:10 dilutions of the lung homogenates, in a 96-well plate in serum-free Dulbecco's modified Eagle medium (Invitrogen®) supplemented with penicillin and streptomycin. After 1 h, the inoculum was replaced by medium containing 2 µg/ml of L-(tosylamido-2-phenyl) ethyl chloromethyl ketone–treated trypsin (Sigma®). End-point virus titers were determined by hemagglutination of chicken red blood cells and expressed as TCID₅₀ per milliliter. IAV RNA levels were determined by quantitative RT-PCR. RNA was isolated from 150 µL of cleared lung homogenate using the Nucleospin RNA virus kit (Machery-Nagel®). The relative amount of NIBRG-14 ma genomic RNA was determined by preparing viral cDNA and performing quantitative PCR with M-genomic segment primers (CGAAAGGAACAGCAGAGT and CCAGCTCTATGCTGACAAAATG) and probe (GGATGCTG) (probe no. 89; Universal ProbeLibrary, Roche®) and the LightCycler 480 Real-Time PCR System (Roche®). To determine the degree of protection against mortality, mice were challenged with 4 LD₅₀ of NIBRG-14 ma virus and subsequently monitored for 14 days. A 30% loss in body weight was the end point at which moribund mice were euthanized. All animal procedures were approved by the Institutional Ethics Committee on Experimental Animals.

MICE EXPERIMENTS STATISTICAL ANALYSIS

Graphpad (Graphpad Prism®, version 5) was used for statistical analysis. Differences between groups were tested using the 2-way ANOVA. When this test demonstrated a significant

difference between groups ($P < .05$), t tests were used to compare 2 groups. Kaplan-Meier survival curves were plotted and evaluated.

SELECTION AND CHARACTERIZATION OF H5N1 N1-VHHm ESCAPE MUTANT VIRUSES

NIBRG-14 ma escape viruses were isolated independently by selection with N1-3-VHHm and N1-5-VHHm *in vitro*. NIBRG-14 ma virus was serially diluted and used to infect MDCK cells in the presence of N1-3-VHHm or H5-VHHb (using a 4.2 or 3.7 μM concentration, respectively, corresponding to 10-fold the median inhibitory concentration NA inhibition assay using N1rec, IC_{50}). Escape mutants were screened by induction of cytopathic effect, and after 12 passages in the presence of N1-VHHm, escape viruses were plaque purified by growth on MDCK cells overlaid with 0.6% low-melting agarose in the presence of N1-3-VHHm or N1-5-VHHm. Only six escape virus isolates obtained by selection with N1-5-VHHm, and were amplified on MDCK cells, still in the presence of the 10-fold IC_{50} of N1-5-VHHm. Total RNA was extracted from the supernatant and used to clone the cDNA corresponding to the NA viral RNA (vRNA) segment (Stech et al., 2008). Deduced amino acid substitutions in the NA sequence of escape viruses were modeled with PyMOL Molecular Graphics System (W. L. DeLano, 2002; DeLano Scientific) using the H5N1 NA structure from A/Vietnam/1194/2004 (PDB code 2HTY).

RESULTS

PRODUCTION OF RECOMBINANT TETRAMERIC NEURAMINIDASE

A Baculovirus Expression Vector System was used to produce a recombinant soluble tetrameric and enzymatically active H5N1 NA derived from A/crested eagle/Belgium/09/2004 (N1rec). The N1rec expression cassette gene (*n1rec*) (Figure 2) was cloned into a pAcMP2 expression vector (pAcMP2*n1rec*), under the control of the AcNPV basic protein promoter, which is an infectious cycle late phase promoter preferred for the production of proteins with post-translational modifications. Infection of *Spodoptera frugiperda* (Sf9) cells with the recombinant baculovirus AcNPVN1rec (containing the N1rec expression cassette) resulted in sialidase activity in the cell supernatant, suggesting that the N1rec product was a soluble and enzymatically active tetrameric NA (Figure 2B). A house-made polyclonal mouse antibody against a recombinant H5N1 NA was used for detection of NA in H5N1 MDCK TMPRSS2 infected cells and further N1rec characterization (Figure 2C). The infected Sf9 SuperNatant (SN) was the starting material for the N1rec protein purification by chromatography. First, the SN was butanol-extracted, separating the SN in an organic phase (fatty acids content) and an aqueous phase, which contained the NA-activity. The aqueous phase was diluted and applied to a hydroxyapatite packed column (Figure 2D). The UV profile of the hydroxyapatite eluted fractions, showed a peak of high protein content, between eluted fractions 20 – 45, corresponding to high NA activity according to a NA activity assay, using the small fluorogenic substrate MUNANA (MW. 469 Da). The hydroxyapatite eluted fractions that scored positive in the NA activity assay and immunoblotting, were pooled and further purified using a Blue Sepharose packed column (Figure 3A-B, 4A). Following a final size exclusion chromatography step by Superdex 200, the tetrameric N1rec containing fractions were eluted after 150 – 180 ml, and the NA activity and immunoblot assays confirmed the catalytic activity of these fractions (Figure 5A-B). On the other

hand, the UV peaks that elute after ca. 190 ml possibly corresponded to N1rec in tri-, di- or monomeric forms, but the NA activity assay confirmed the absence of any NA activity (Figure 5A-B). The N1rec eluted from gel filtration was ca. 90% pure N1rec (Figure 6C-D and Table 1). The theoretical molecular weight of N1rec is 49.5 kDa, but the relative electrophoretic mobility in SDS-PAGE suggested a size of approximately 60 kDa (Figure 6D), presumably due to the presence of glycosylations; there are three N-glycosylation and two O-glycosylation sequences in the N1rec. The purified protein had a specific activity of 56850.9 NA units/mg of total protein and the progressive enrichment of the N1rec production process is depicted in the Table 1.

Table 1. Progressive enrichment of eluted fractions of N1 NA through the purification process

	Volume (ml)	Total NA units\mg total protein ^a	Relative purity
AcNPVN1rec infected Sf9 supernatant	1650	20605.92	ND ^b
Butanol extracted aqueous phase	1450	13115.45	ND
Hydroxyapatite Elution	555	12080.01	35%
Blue sepharose Elution	15	21801.24	80%
Superdex 200 Elution	11	56850.90	90%

^a Based in a NA inhibition assay, using the substrate 2'-(4-methylumbelliferyl)-a-D-N acetylneuraminic acid (MUNANA), expressed in NA units (1 unit neuraminidase = nmoles 4-methylumbelliferone/min).

^b ND, Not determined

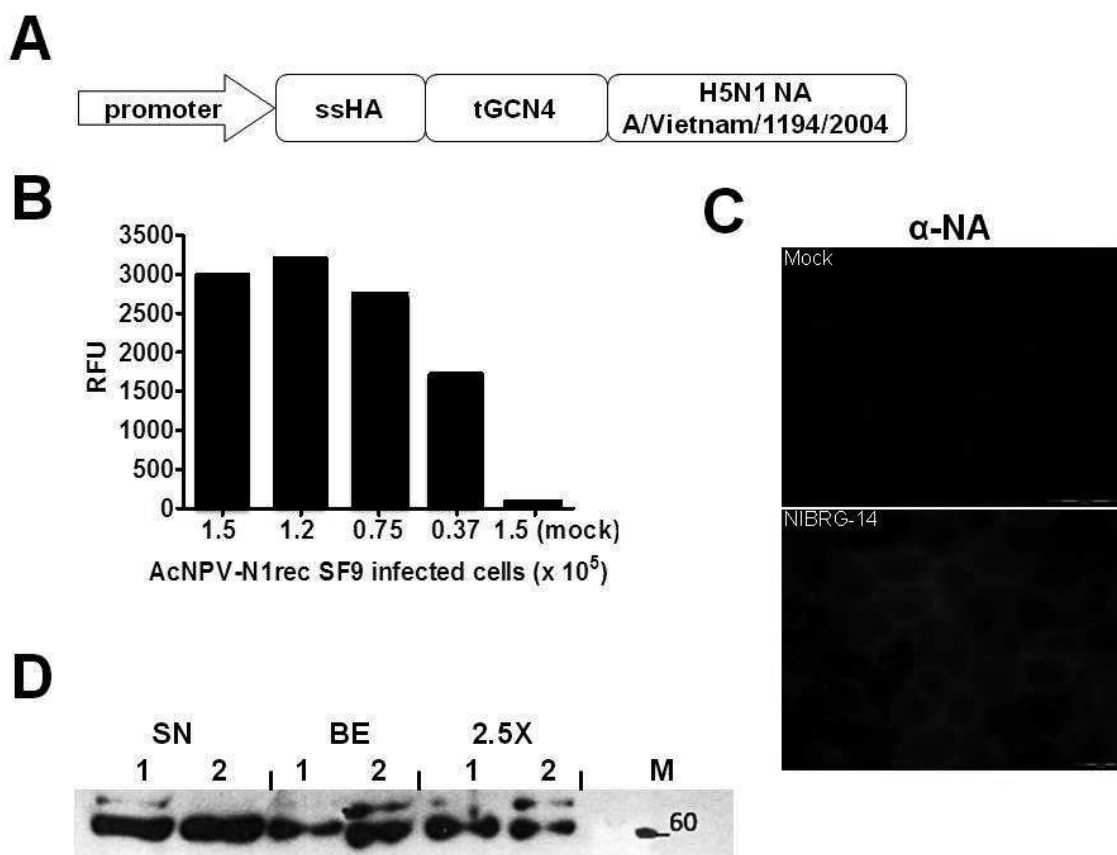


Figure 2. Design and initial steps of production of recombinant N1. Soluble recombinant NA (N1rec) derived from H5N1 A/crested eagle/Belgium/01/2004 was produced in Sf9 cells using the Baculovirus expression platform. **A.** Diagram of the *n1rec* expression cassette in the pACMP2 vector: promoter, Baculovirus basic protein promoter; ssHA, secretion signal of HA; tGCN4, tetramerizing leucine zipper; H5N1 NA, extracellular domain of the N1rec. **B.** Neuraminidase activity in crude cleared culture supernatant (SN) of infected Sf9 cells. Supernatants of different amounts of AcNPV-N1rec infected cells or mock infected cells were measured in a NA activity assay (MUNANA substrate). **C.** MDCK TMRSS2 cells were mock or NIBRG-14 infected, fixed and stained against NA, using a house-made mouse polyclonal α-NA. There is a specific signal in the cell membrane corresponding to NA expression in NIBRG-14 infected cells, which is not present in mock infected cells. The scale in the right lower corner represents 20 μm. **D.** Immunoblot of the initial purification process of N1rec is depicted, before chromatography and using a mouse polyclonal Ab against a recombinant H5N1 NA. SN, crude cleared culture supernatant of infected Sf9; BE, butanol-extracted SN; 2.5X, 2.5 times dilution of BE before the first chromatography step. The numbers 1 and 2 denote two different batches produced. The theoretical molecular weight of monomeric N1rec is 49.5 kDa, but migrates close to 60 kDa, due to possible glycosylations.

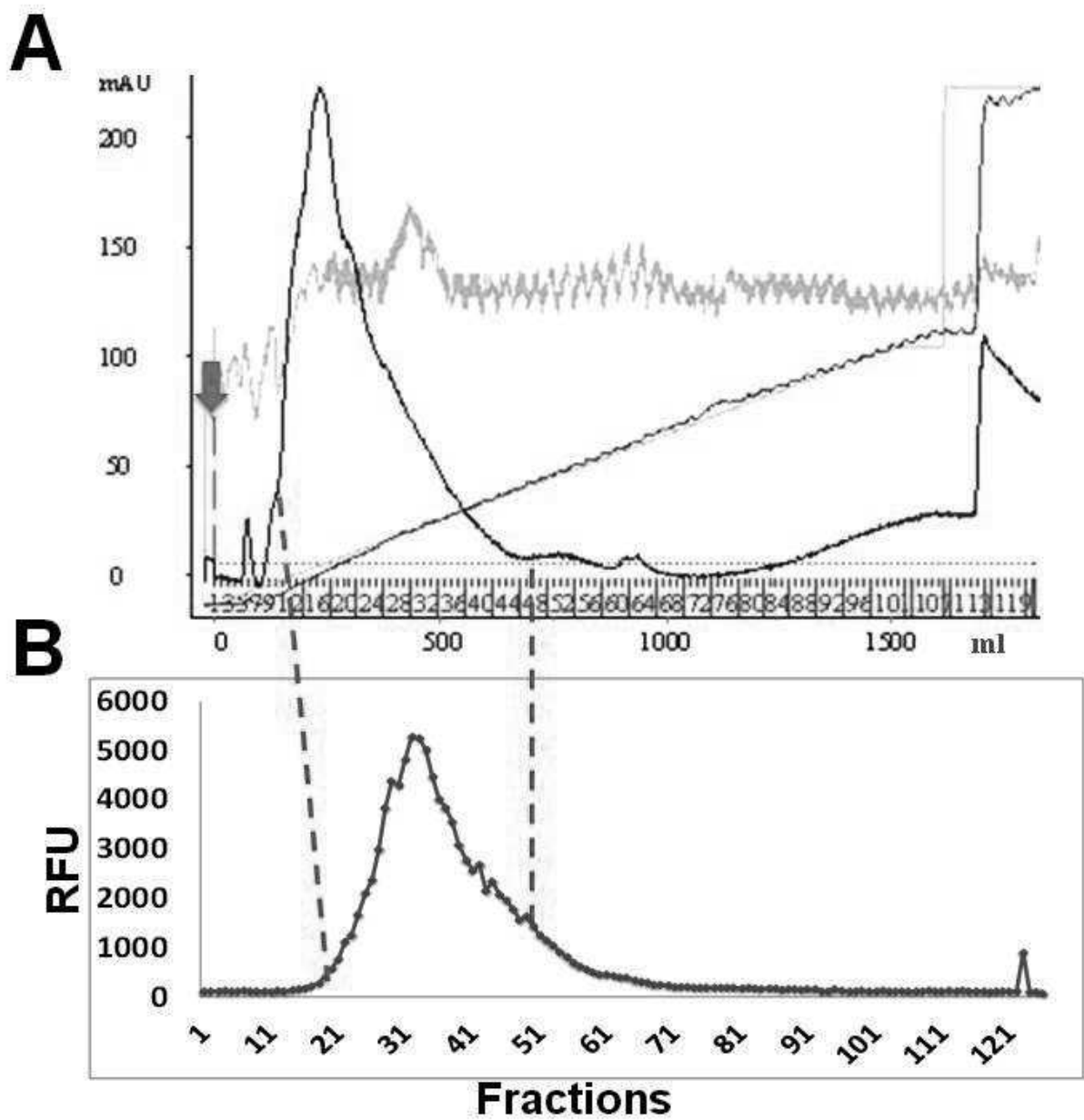


Figure 3. Representative hydroxyapatite elution profile and NA activity characterization of eluted N1rec-containing fractions. **A.** The butanol-extracted and 2.5X diluted SN was applied to a hydroxyapatite column, and the eluted F20 – F45 showed a major protein content peak, according to their UV profile. Eluted fractions (red); SN injection (magenta arrow); mAU, UV 280 nm (blue); Conductivity (brown); pH (grey); ml, eluted volume in milliliters. **B.** NA activity analysis of all the eluted fractions of A. The F20 – F 45 UV peak corresponds with the highest NA activity fractions (dotted red lines). RFU, relative fluorescence units.

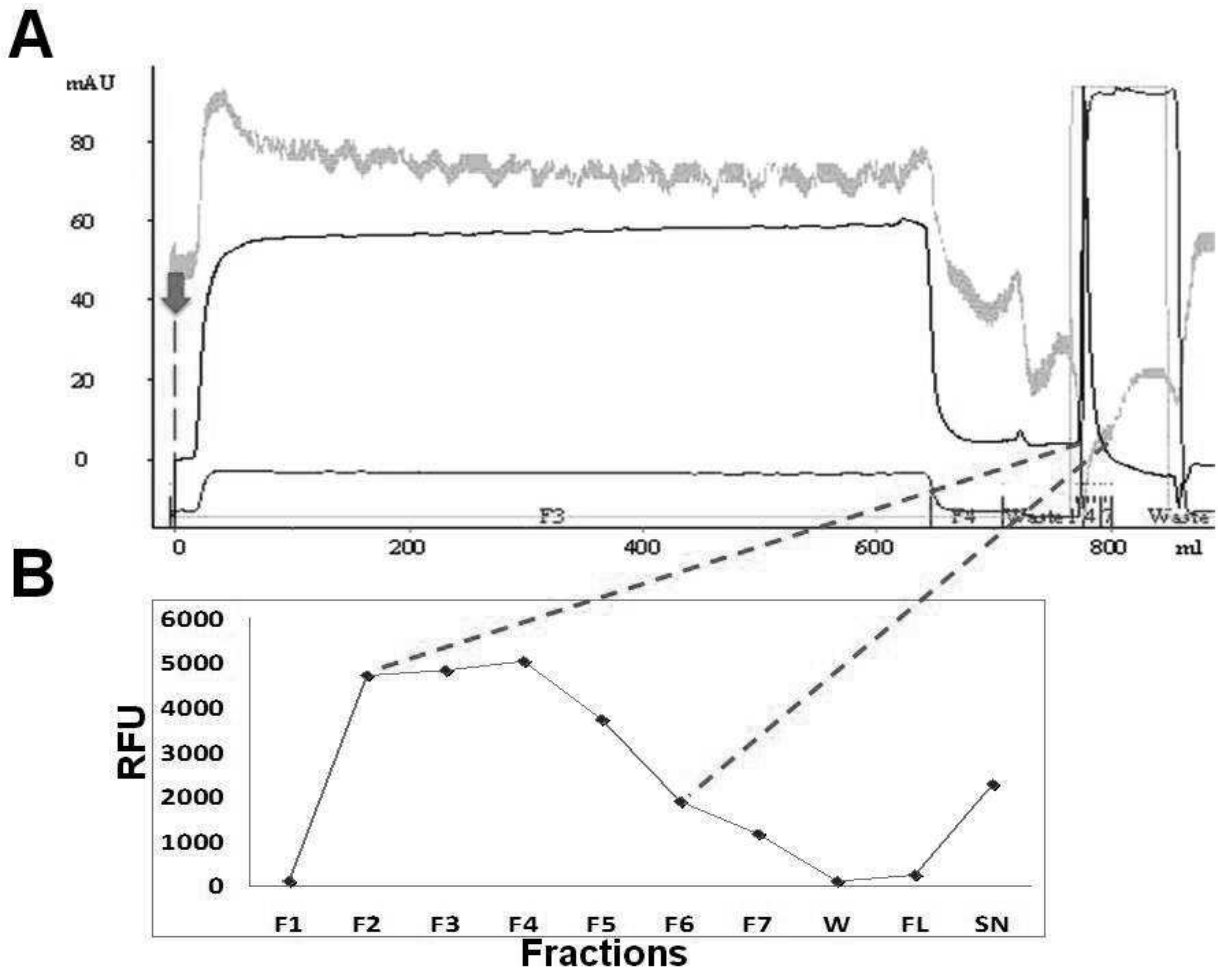


Figure 4. A representative N1rec second chromatographic purification step by Blue Sepharose. **A.** The elution from the Blue Sepharose column resulted in concentrated N1rec fractions (F2 – F5), with a single UV peak. Eluted fractions (red); Hydroxyapatite eluted pooled fractions injection (magenta arrow) mAU, UV 280 nm (blue); Conductivity (brown); pH (grey), ml, eluted volume in milliliters. **B.** NA activity analysis of the eluted fractions of A. The F2 – F 5 protein content peak corresponds with the highest NA activity fractions (dotted red lines). RFU, relative fluorescence units.

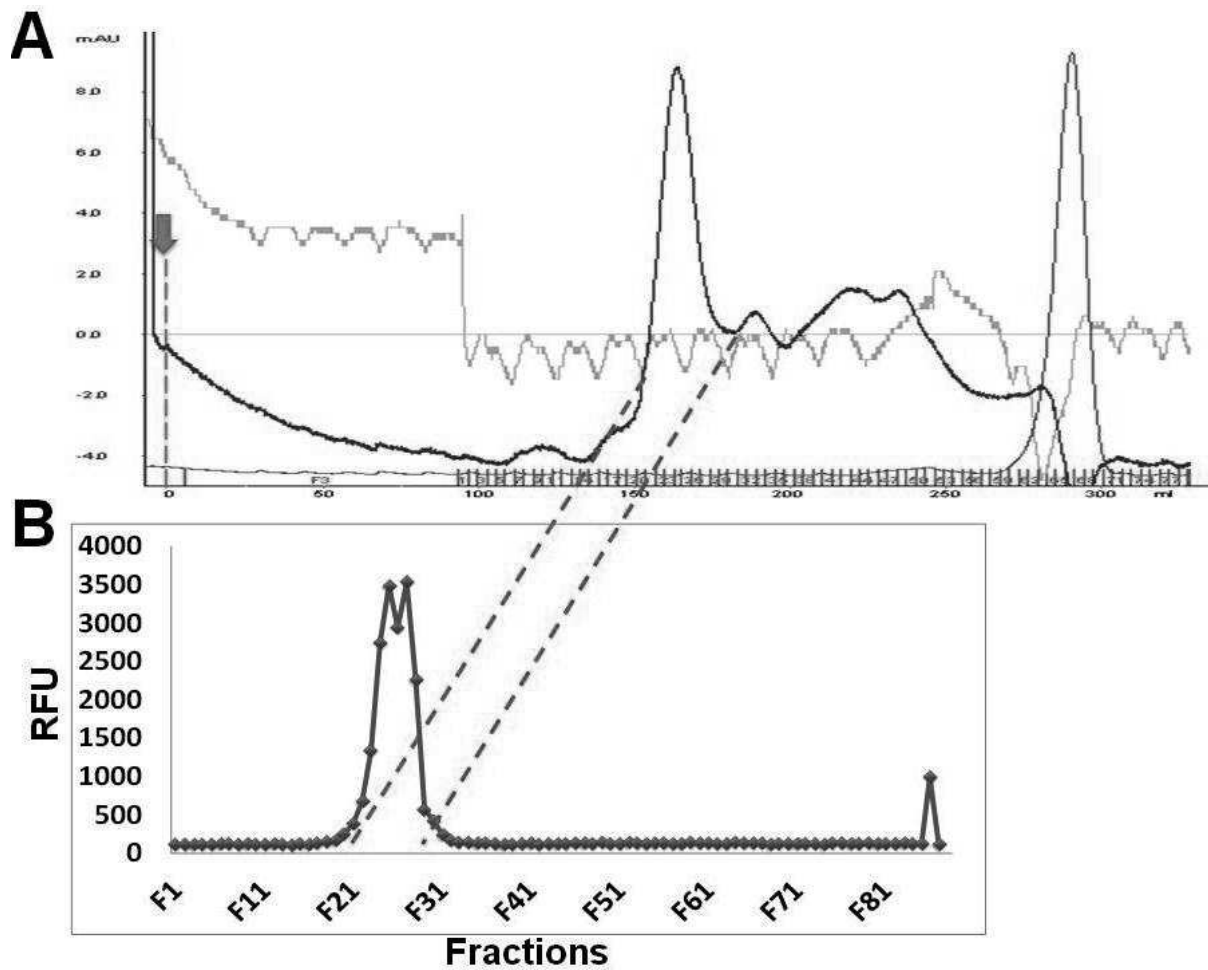


Figure 5. Representative N1rec purification final gel filtration process. **A.** The eluted pooled fractions after Blue Sepharose purification from figure 4 (magenta arrow) were applied to a Superdex 200 column. After ca. 150- 190 ml (F20 – F30) of eluted volume, a major UV peak corresponded to the size of tetrameric N1rec, while the following minor UV peaks possibly represent N1rec trimers, dimers or monomers. Eluted fractions (red); mAU, UV 280 nm (blue); Conductivity (brown); pH (grey), ml, eluted volume in milliliters. **B.** The NA activity revealed that the major UV peak (F20 – F30) corresponded with the fractions with NA activity (red dotted lines). In contrast the other minor peaks did not present any NA activity, suggesting that only the N1rec in tetrameric form is active. RFU, relative fluorescence units.

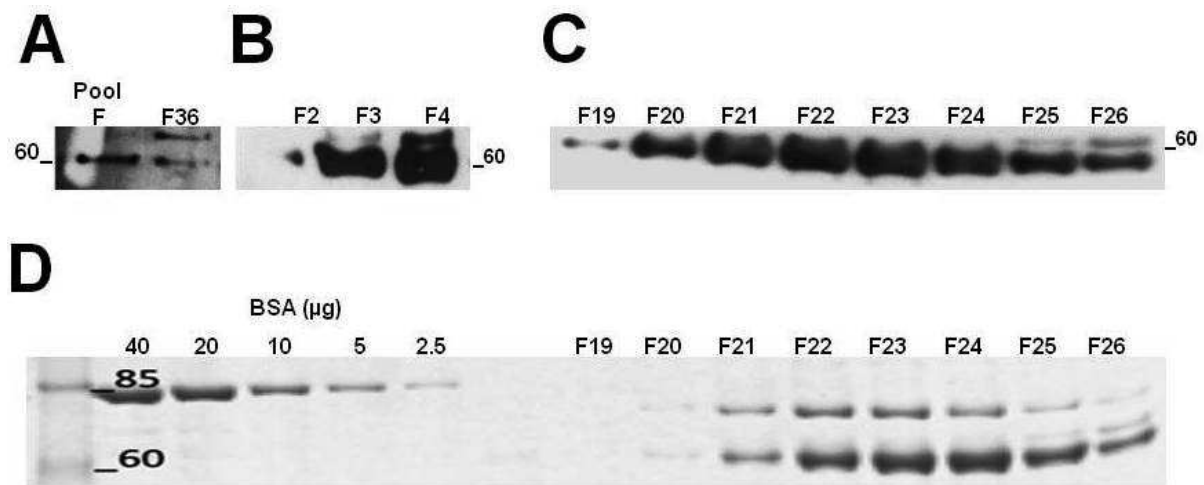


Figure 6. Analysis of the N1rec during and after the chromatography purification. Sequential N1rec purification and enrichment of the eluted fractions of the 3 different N1rec chromatography purification processes, by immunoblotting: **A**, Hydroxyapatite; **B**, Blue Sepharose; and **C**, Superdex 200. In the Superdex 200, 9 μ l of F19 – F26 were loaded per lane. All the blots were obtained using a mouse polyclonal Ab, against H5N1 NA recombinant protein. **D**. Coomassie stained reducing SDS-PAGE of the Superdex 200 eluted fraction F19 - F26 of C (18 μ l of each fraction were resolved). BSA, Bovine Serum Albumin protein standards.

IMMUNIZATION AND VHH PHAGE LIBRARY CONSTRUCTION

Next, N1rec was used as an antigen for the generation and selection of NA-specific VHH. An alpaca (*Llama alpacos*) was immunized at day 0 with 125 μ g of N1rec, followed by 6 weekly boosts (Figure 7A). One week after the last immunization, blood was collected and peripheral blood lymphocytes were isolated (Figure 7B). From the lymphocytes, total RNA was extracted and used as template for cDNA synthesis (Figure 7C). The VH and VHH genes were amplified by PCR, and the VHH genes were isolated and cloned into the phagemid vector pHEN4 (Figure 7D-E, 8A) (Arbabi Ghahroudi et al., 1997). We obtained a VHH phage library of 2×10^8 independent transformants. Fifty-seven percent of these transformants harbored a pHEN4 with a VHH cDNA insert of the correct size (550 bp) (Figure 7F-G). The VHH phage display library

was then subjected to four consecutive rounds of panning, performed on solid-phase coated N1rec antigen (Figure 7H-I). Seventy-eight positive clones were selected and isolated from the eluted phages and were sequenced (Figure 7J). Subsequent restriction fragment length polyphorphism analysis narrowed down the N1rec-binding VHH candidates to 24 colonies, encoding 13 unique and different VHH sequences. These sequences were cloned into the bacterial expression vector pHEN6 (pHEN6*n1-vhh*) under the control of a lac promoter, for expression and purifications purposes (Figure 7K, 8B) (Kang et al., 1991).

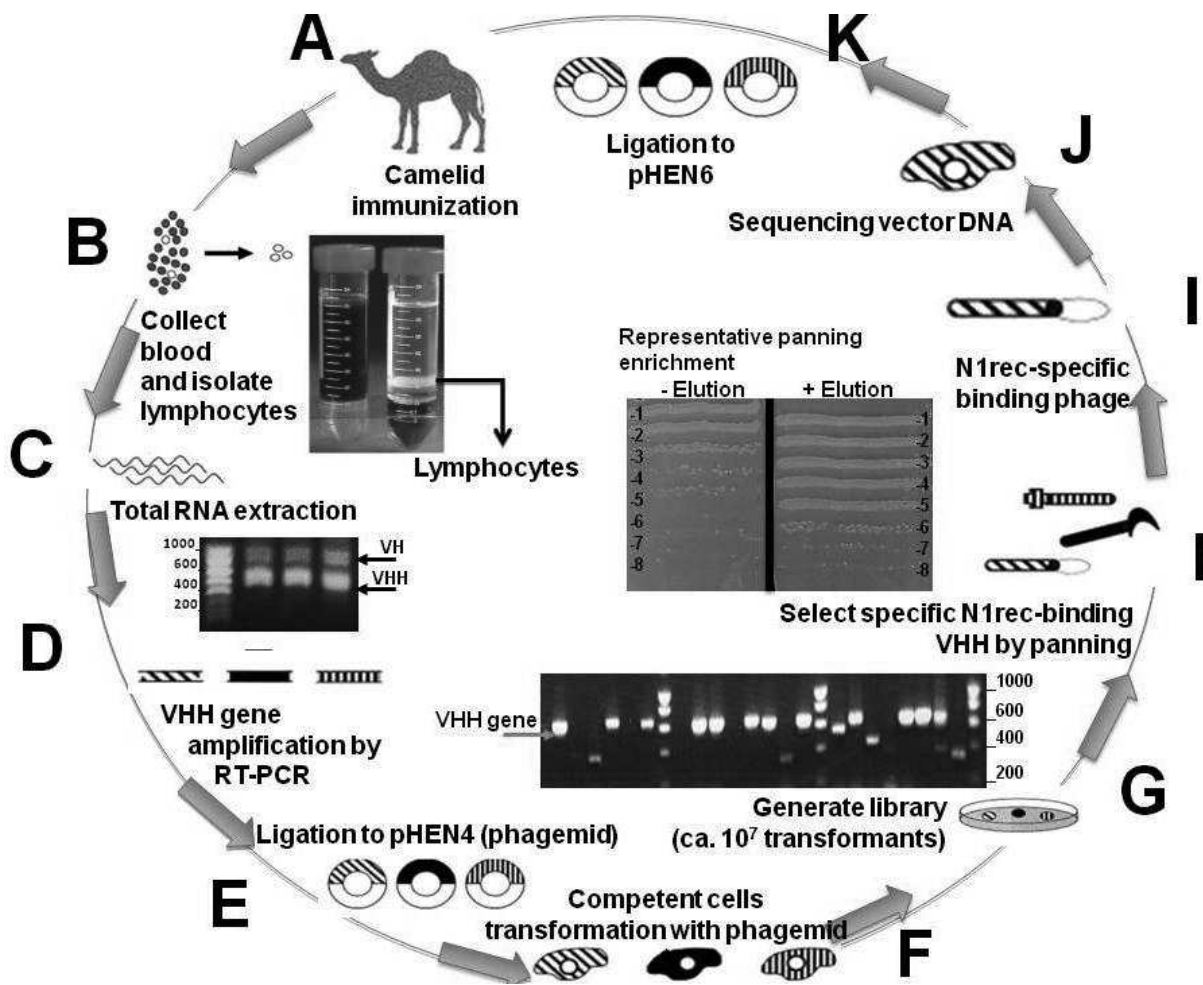


Figure 7. Flow chart of the phage library production and panning process of the N1rec-binding VHH production. **A.** Purified N1rec was used to immunize an alpaca (*Llama alpacos*). **B.** Eight weeks after immunization, peripheral blood was extracted and the lymphocytes were isolated by a sucrose gradient. **C.** cDNA was obtained from total RNA extracted from isolated lymphocytes. **D.** VH and VHH genes were amplified from cDNA, and the VHH genes were isolated and purified. **E.** The VHH genes were cloned and inserted into the pHEN4 vector, where the VHH gene is fused to the phage protein III gene, resulting into a phagemid. **F.** TG1 competent cells were co-transformed with the phagemid and the helper phage M13, in order to produce viable and infective phages. **G.** A library of ca. 10^7 transformants was generated; an insert of 597 bp (VHH gene) was present in approximately 57% of the transformants. **H.** Purified phages from the library were used for panning N1rec-binding phages using N1rec as bait. A representative panning enrichment is depicted, showing specific enrichment through a dilution series, measured by the growing of bacteria infected with eluted phages from panning (conferring an antibiotic resistance gene, + Elution), compared with the negative control (- Elution). **I.** After 4 rounds of panning enrichment, eluted phages were isolated, and **J.** sequenced. **K.** The VHH genes of the selected sequenced phages were cloned into the vector pHEN6c, resulting into the VHH expression cassette (5'-pelB-VHH gene-hexahistidine-3') in order to produce soluble VHH.

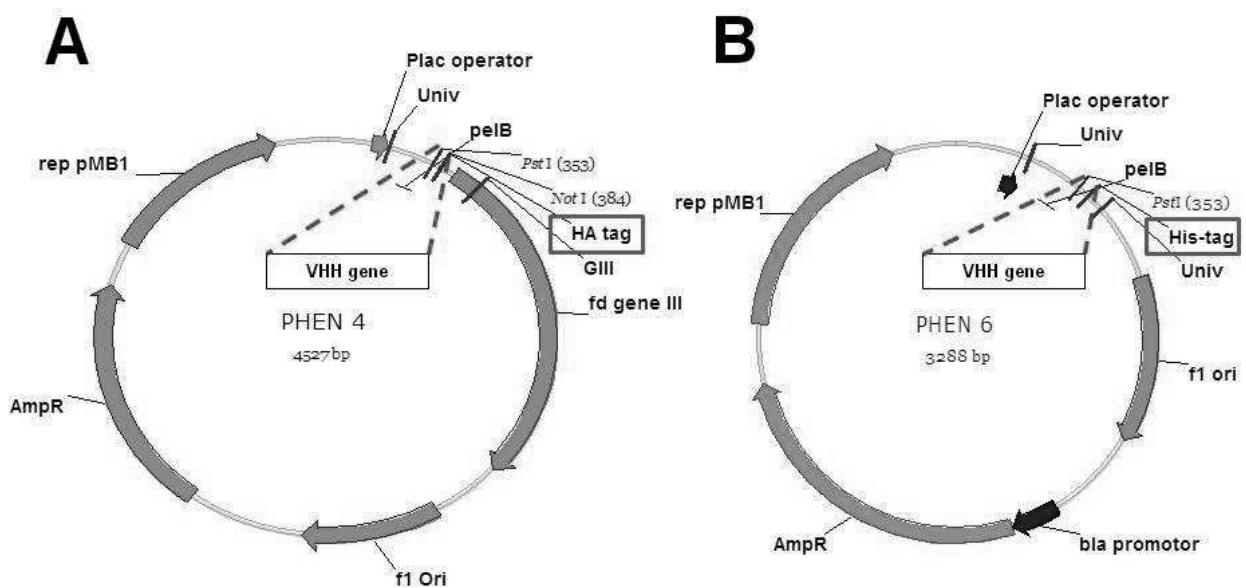


Figure 8. Schematic diagrams of the phagemid vector pHEN4 and the production vector pHEN6. **A.** The VHH genes from the phage library were cloned into the pHEN4 vector (4527 bp), resulting in an expression cassette encoding the VHH gene (red dotted lines) fused to the phage gene III, resulting in a phagemid. Plac operator, lacUV5 promoter; Univ, universal primer recognition site; peIB, signal peptide for periplasmic targeting; HA tag, hemagglutinin tag for screening purposes (dark red box); GIII, GII primer recognition site; fd gene III, phage protein III gene; f1 origin; AmpR, ampicillin resistance gene; rep pMB1; origin of replication starts at 4347 bp (+/- 1). **B.** The selected VHH genes were cloned for soluble protein production into the vector pHEN6 (3288 bp). In this vector, the VHH gene is fused to a hexahistidine tag (His-tag, dark red box), that substituted the HA tag and the phage protein III gene.

PRODUCTION AND CHARACTERIZATION OF SOLUBLE MONOMERIC N1-VHH

The sequences of the 13 N1rec-specific candidates are shown in Figure 9, containing four framework regions (FR1-FR4) and three complementary determining regions (CDR1-CDR3). The transformation of amber suppressor *E. coli* strain WK6 with the pHEN6n1-vhh vector resulted in the production a monomeric soluble N1rec-binding VHH (N1-VHHm) that is targeted to the periplasm and C-terminally tagged with hexahistidine. Following osmotic shock, periplasmic extracts were prepared and loaded into a nickel sepharose column, to purify each of the 13 different N1-VHHm proteins (Figure 10A-C). *In silico* structure prediction of the 13 N1-VHHm showed a typical VHH structure, and interestingly, the CDR3 of N1-1-VHHm, N1-3-VHHm, N1-4-VHHm, N1-5-VHHm and N1-6-VHHm presented an electronegative protruding paratope, not present in the rest of the N1-VHHm (Figure 11). The binding of the 13 N1-VHHm proteins to the NA moiety of N1rec, but not to its tGCN4 moiety was assessed by ELISA assay. The majority of the N1-VHHm did not present significant binding to a recombinant M2e-tGCN4 protein, which contains the same tetramerizing leucine zipper (Figure 12). We next assessed the capacity of the N1-VHHm candidates to inhibit the enzymatic activity of N1rec, by using a small MUNANA substrate. Interestingly, four candidates, N1-1-VHHm, N1-3-VHHm, N1-5-VHHm and N1-6-VHHm, could inhibit the N1rec catalytic activity (Figure 13; Table 2). N1-3-VHHm and the N1-5-VHHm were the most potent inhibitors of the N1rec catalytic activity (Table 3), and together with N1-7-VHHm, were analyzed by SPR using immobilized N1rec. The N1-7-VHHm protein was included in this analysis as a binding but non-inhibitory N1-VHHm control. Both N1-3-VHHm and N1-5-VHHm presented a high affinity for N1rec, with equilibrium dissociation constant (K_D) in the low nanomolar (N1-5-VHHm) to picomolar (N1-3-VHHm) range. N1-7-VHHm showed an approximately 10- to 100-fold lower affinity K_D than N1-5-VHHm and N1-3-VHHm, respectively (Table 2). These binding affinities of N1-3-VHHm and N1-5-VHHm for N1rec are comparable to affinities reported for an enzymatic monomeric VHH that inhibits the

activity of lysozyme (De Genst et al., 2006). Competitive SPR analysis also showed that prior binding of N1-3-VHHm to N1rec abolished subsequent binding of N1-5-VHHm and *vice versa*. On the other hand, N1-7-VHHm binding to N1rec was not affected by prior binding of N1-3-VHHm or N1-5-VHHm to N1rec (Figure 14). This observation suggests that N1-3-VHHm and N1-5-VHHm bind an overlapping epitope in N1rec, while N1-7-VHHm targets a different epitope. We next analyzed the antiviral potential of the N1rec inhibitory VHH N1-3-VHHm and N1-5-VHHm. Therefore, we used the IAV laboratory strain NIBRG-14, generated by reverse genetics and containing NA and HA (lacking the polybasic maturation sequence) segments derived from A/Vietnam/1194/2004. The sequences of the NA of NIBRG-14 and the NA derived from the A/crested eagle/Belgium/09/2004 (used for the alpaca immunization) are highly homologous, with only 13 AA differences. In the presence of N1-3-VHHm or N1-5-VHHm the size of NIBRG-14 plaques in monolayers of infected MDCK cells was reduced in a concentration dependent manner (Table 3, Figure 16A). In contrast, N1-7-VHHm did not affect the size or number of NIBRG-14 plaques in this assay (Table 3). These results suggest that the *in vitro* antiviral potential of N1-3-VHHm and N1-5-VHHm depends on their NA-inhibitory activity.

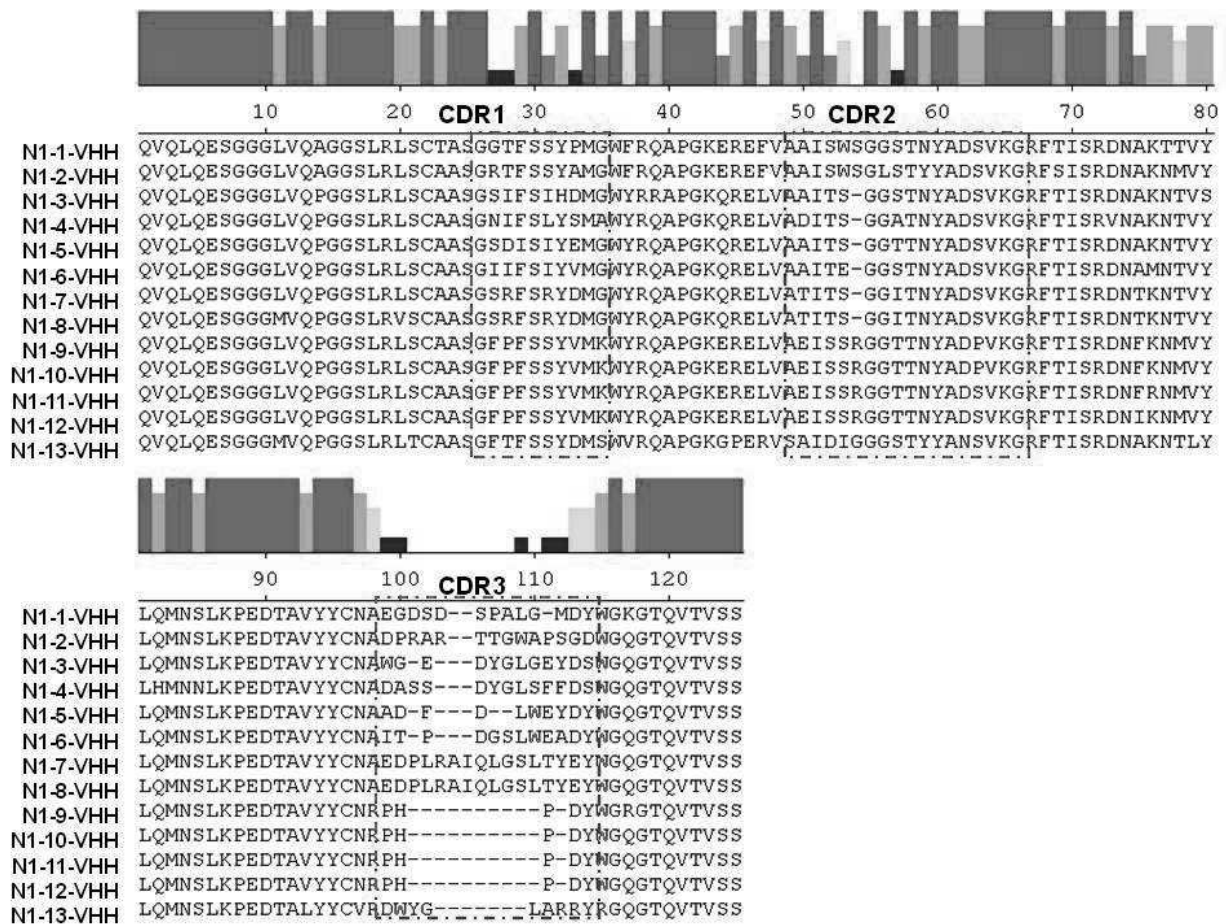


Figure 9. Sequence of the 13 N1rec-binding VHH candidates. Alignment of the amino acid sequences of the 13 N1-VHH, isolated by panning, from the phage library generated from an N1rec-immunized alpaca. Four framework sequences are separated by 3 diverse Complementary Determining Regions (CDR1, CDR2 and CDR3). The VHH CDR3 is the most variable region in the VHH candidate's sequences. The colored histogram denotes the homology between the sequences: red, 100 %; orange 60 – 80%; green 40 – 60 %; light blue 20 – 40 %, dark blue < 20%.

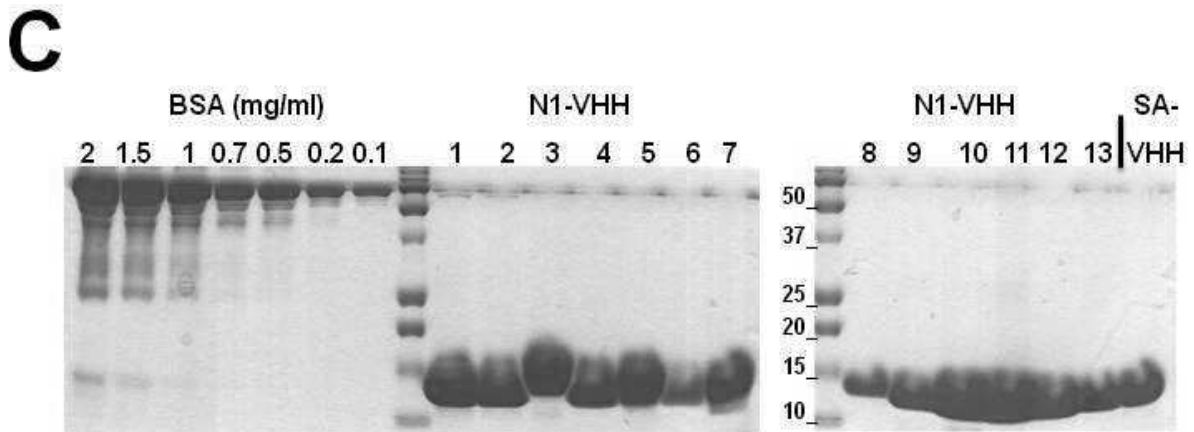
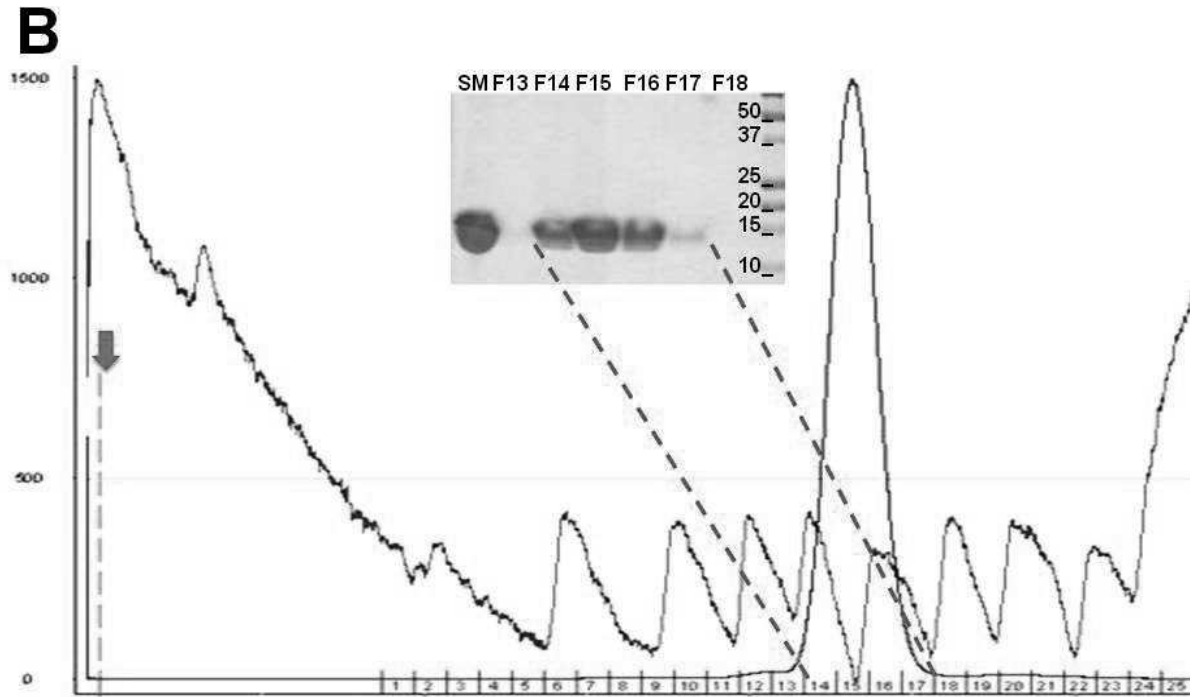
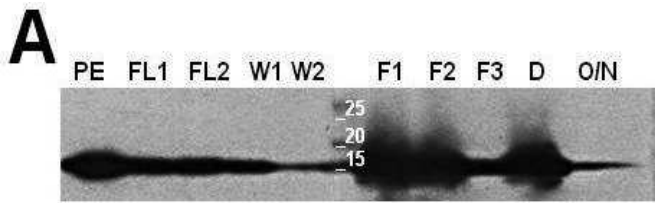


Figure 10. Production of soluble monomeric N1-VHH (N1-VHHm). **A.** Anti-hexahistidine immunoblot of the sequential purification and enrichment process of N1-VHHm production. Periplasmic Extracts (PE), His-select column Flow through (FL1, FL2), Washes (W1, W2), eluted Fractions (F1, F2, F3), Dialyzed eluted pooled fractions (D), and His-select resin incubated OverNight after elution (O/N). **B.** Elution profile of the dialyzed eluted pooled fractions from A (magenta arrow), were gel filtrated by Superdex 200 column. The eluted fractions F14 - F17 single UV peak corresponded to a single band of ca. 15 kDa (red dotted lines), resolved by Coomassie stained reducing SDS-PAGE. Eluted fractions (pink, x axis); mAU, UV 280 nm (blue, y axis); Conductivity (brown). **C.** Coomassie-blue stained reducing SDS-PAGE of the 13 purified *E. coli*-produced soluble N1-VHHm candidates. Twenty μ g of monomeric SA-VHH was loaded as a non N1rec-binding control V_{HH} . The V_{HH} size ranges from 14 – 15 kDa. Purified BSA standards were loaded for quantification and comparison. BSA, Bovine serum Albumin. SA-VHH, Seed Albumin binding V_{HH} .

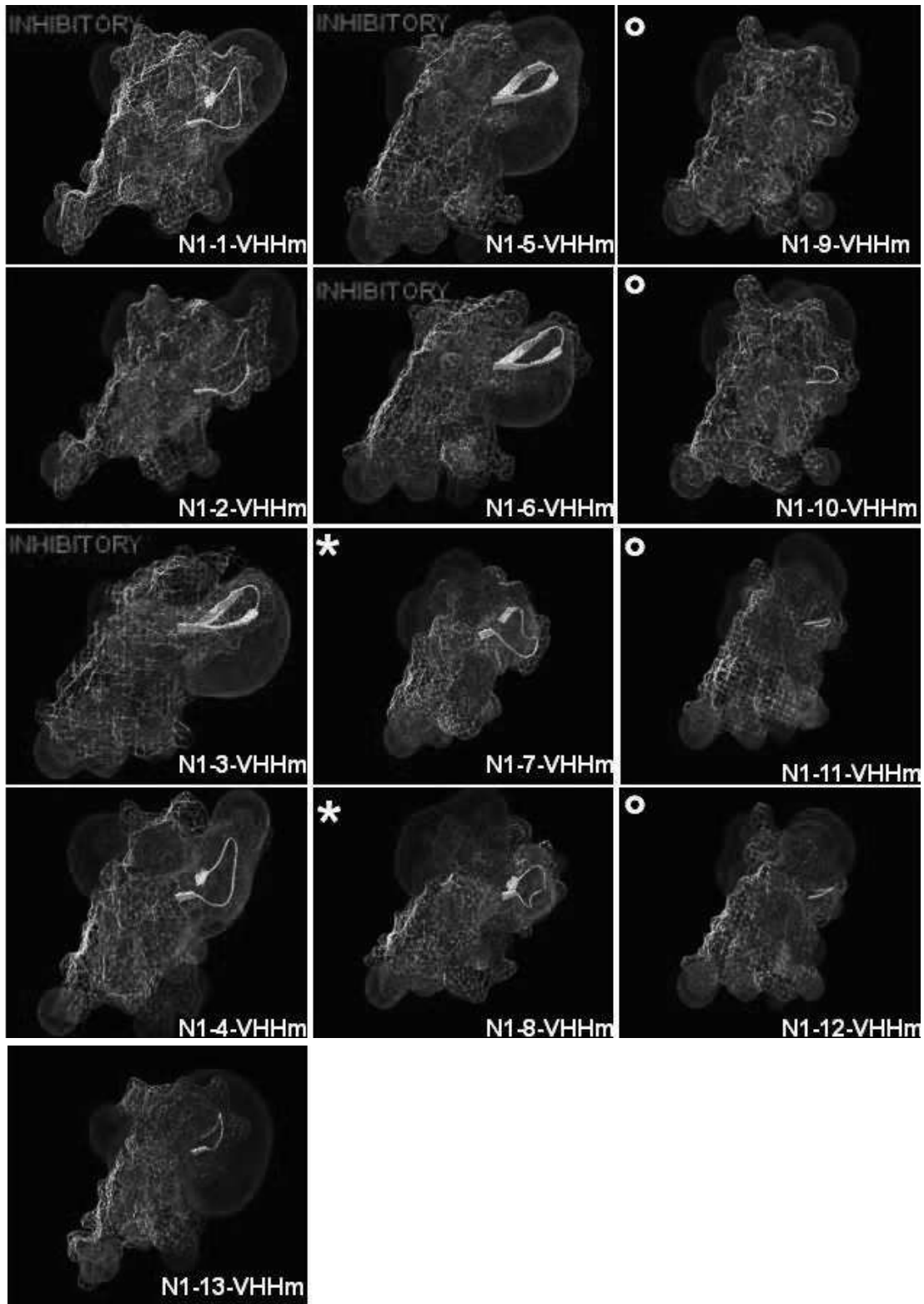


Figure 11. *In silico* prediction of the 3D-structure of the monomeric N1rec-VHH (N1-VHHm). The N1-VHHm surface depicts the positive and negative electro-potential, as blue and red clouds, respectively. The VHH CDR3 is represented in a white ribbon structure. Note that N1-1-VHH, N1-3-VHH, N1-4-VHH, N1-5-VHH and N1-6-VHH CDR3 present an electronegative protruding topology. The asterisk (*) and circle (°) indicate N1-VHHm from the same clonal family.

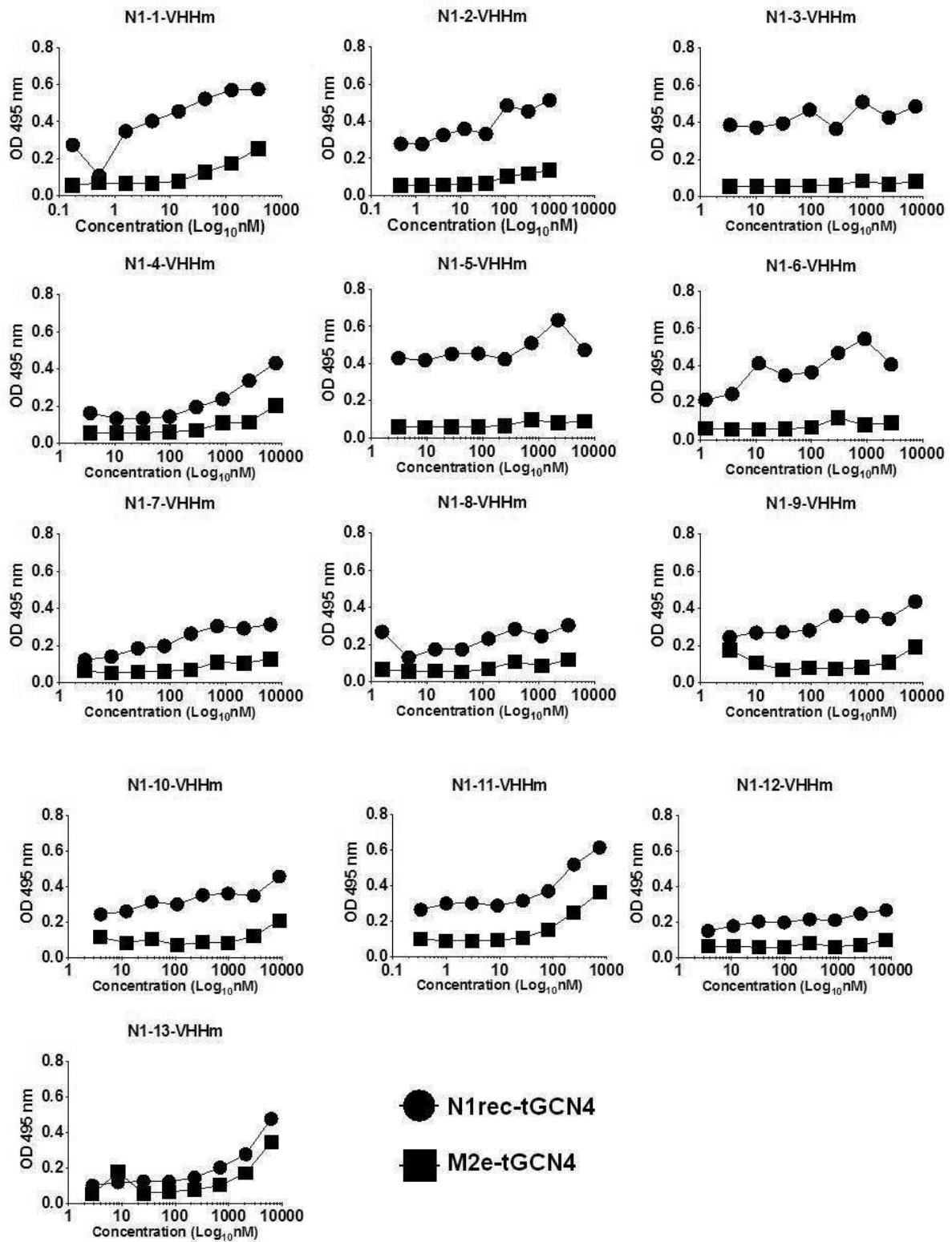
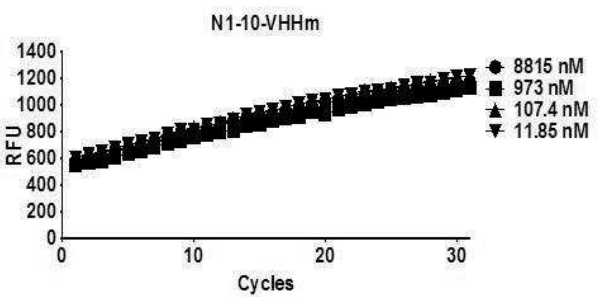
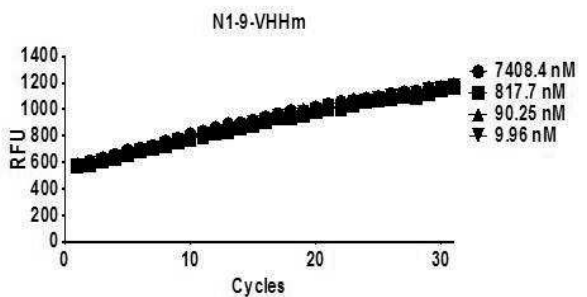
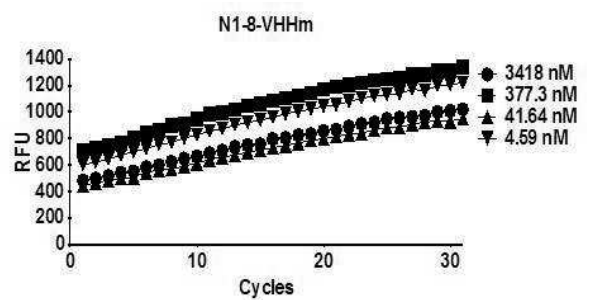
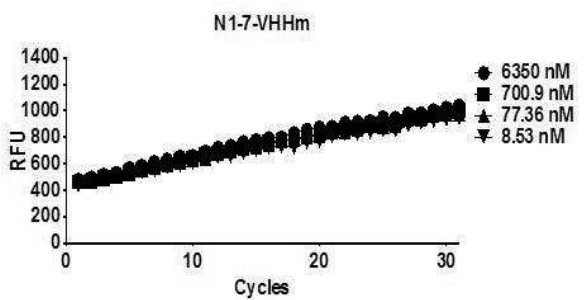
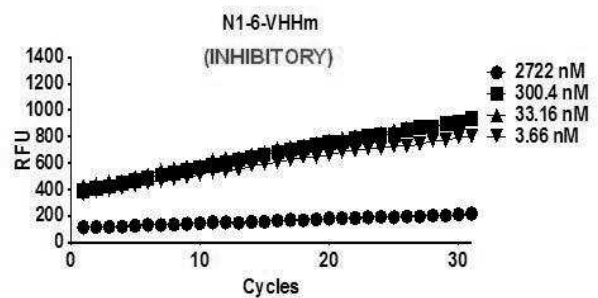
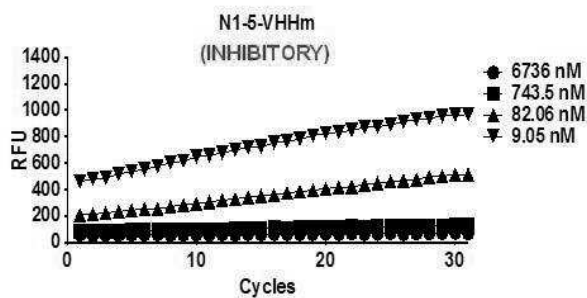
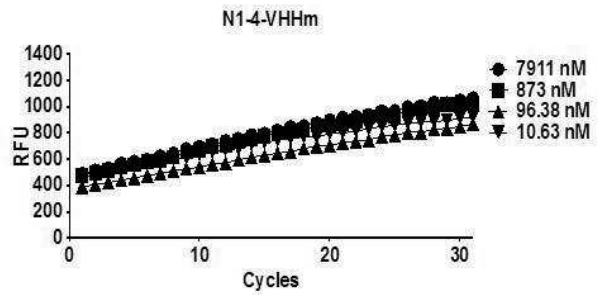
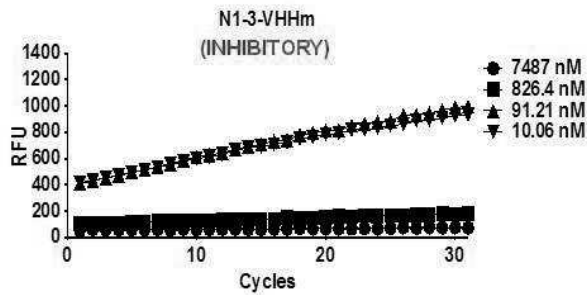
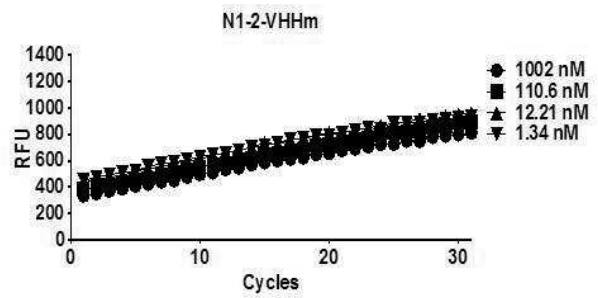
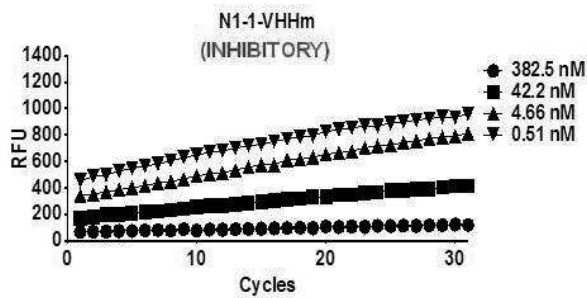


Figure 12. Binding capacity of the 13 N1-VHHm candidates to the N1rec protein by ELISA. Ten µg/ml of N1rec (N1rec-tGCN4.) or IAV recombinant protein M2 (M2-tGCN4) was used for coating O/N 96-well plate. Dilution series of the 13 N1-VHHm were incubated in the N1rec coated plates, and a mouse α-His-tag-HRP was used to measure the binding between both proteins. All the 13 N1-VHHm showed binding to the N1rec in a dose dependent-manner, but the binding to the M2 coated plates was minor or absent. In the N1-1-VHHm, N-11-VHHm and N1-13-VHHm, the M2 binding was more than 0.2 units (OD495 nm) in the lowest dilutions. Interestingly, the binding of the N1-3-VHHm and N1-5-VHHm appeared not be affected by the dilution series.



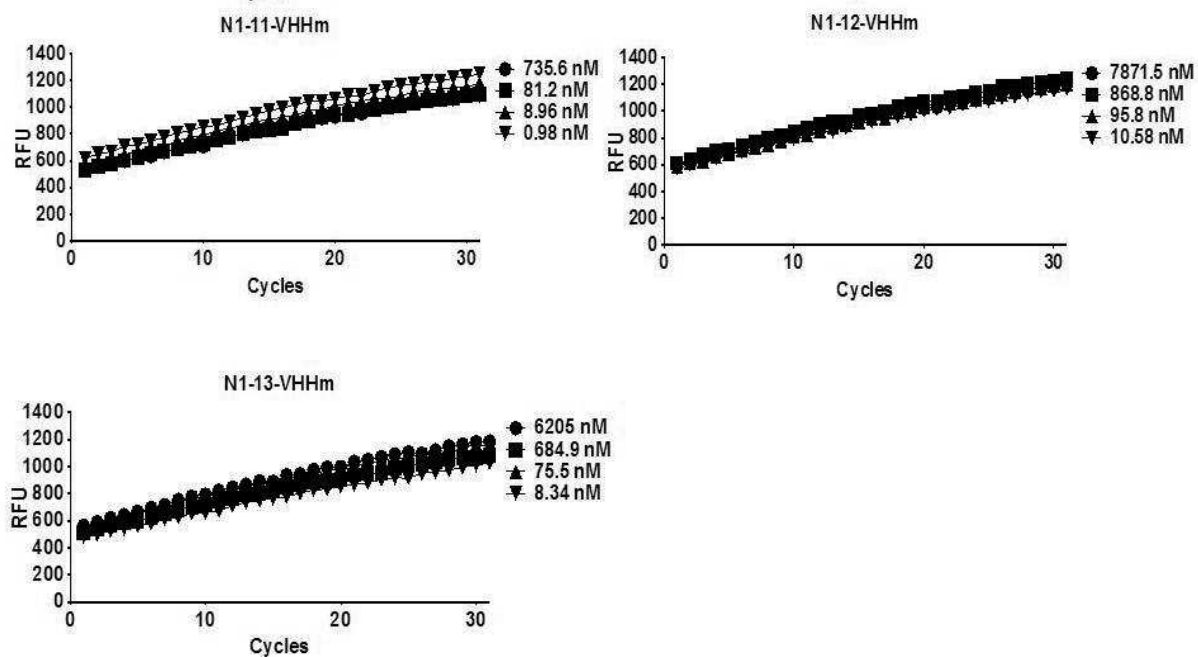


Figure 13. N1rec inhibitory potential of the 13 N1-VHHm. From each N1-VHH, dilution series were incubated with 160 ng of N1rec at 37 °C, in the presence of 1 mM of MUNANA substrate. Readings at 365 nm (excitation) and 450 nm (emission) were taken every 2 min. Only the N1-1-VHHm, N1-3-VHHm, N1-5-VHHm and N1-6-VHHm presented inhibition of the N1rec catalytic activity. The N1-3-VHHm and the N1-5-VHHm seemed to be the most potent NA inhibitors.

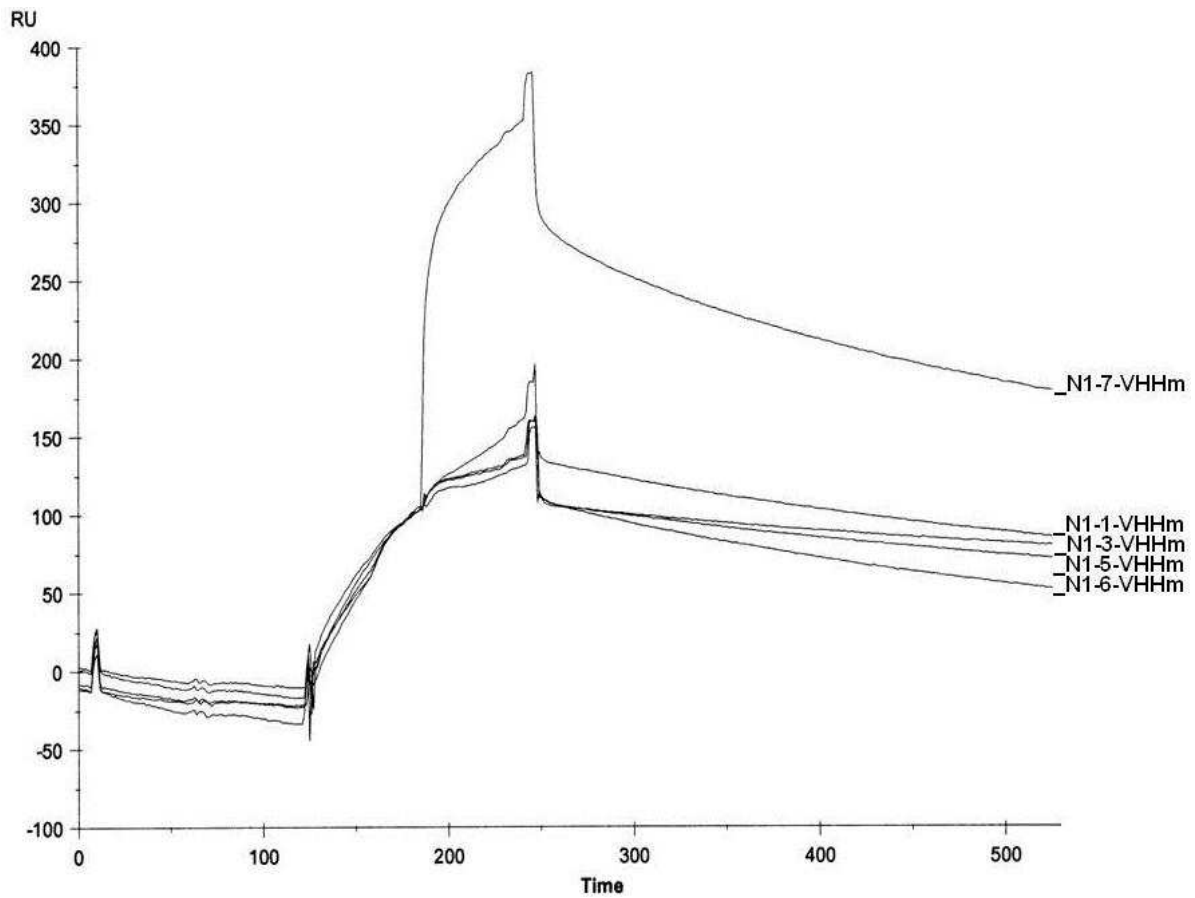


Figure 14. Sensogram of the N1-VHHm binding to the N1rec, by SPR analysis. In the “x” axis is the time (seconds), and in the “y” axis is Resonance Units (RU), that reflects the increase in mass into the N1rec covalently linked into the circuit. The binding of N1-3-VHHm to the N1rec abolished the subsequent binding of the N1-1-VHHm, N1-5-VHHm and N1-6-VHHm, but did not avoid the N1-7-VHHm binding. In this last case, an increase of RU corresponded with an increase of mass into the bound complex, indicating N1-7-VHHm binding to N1rec.

Table 2. Binding and affinities of the N1-VHHm to N1rec by ELISA and Surface Plasmon Resonance

N1-VHHm	Binding to N1rec ^a	Inhibition of N1rec	K_{on} ($M^{-1} \cdot s^{-1}$) ^b	K_{off} (s^{-1}) ^c	K_D (M) ^d
1	+	+	ND ^e	ND	ND
2	+	-	ND	ND	ND
3	+	+	$3.6 E^{+6}$	$1.3 E^{-3}$	$3.7 E^{-10}$
4	+	-	ND	ND	ND
5	+	+	$1.2 E^{+5}$	$5.8 E^{-4}$	$4.7 E^{-9}$
6	+	+	ND	ND	ND
7	+	-	$4.4 E^{+4}$	$2.8 E^{-3}$	$6.3 E^{-8}$
8	+	-	ND	ND	ND
9	+	-	ND	ND	ND
10	+	-	ND	ND	ND
11	+	-	ND	ND	ND
12	+	-	ND	ND	ND
13	+	-	ND	ND	ND

^a N1rec, tetrameric recombinant N1 Neuraminidase

^b Equilibrium dissociation constant K_D (k_{off}/k_{on}),

^c Association rate constant k_{on}

^d Dissociation constant k_{off} , ^e ND, not determined

ENHANCED INHIBITORY AND ANTIVIRAL POTENTIAL OF BIVALENT N1-VHH FORMATS

It has been reported that multivalent formats of VHH increase their affinity, by introducing avidity for their viral target antigen (Hultberg et al., 2011; Ibanez et al., 2011; Schepens et al., 2011). For example, the introduction of avidity drastically decreased the dissociation constant (K_{off}) of the VHH molecules directed against lysozyme, and significantly improved their enzyme inhibitory activity as compared to their monovalent counterparts format (Els Conrath et al., 2001) (Hmila et al., 2010). To increase the avidity of the N1-VHHm, two different bivalent formats were produced.

BACTERIA-PRODUCED N1-VHHb

As a first approach to obtain bivalent VHH, we used the llama IgG2c hinge (17 AA residues) as a flexible linker to fuse two identical N1-VHHm moieties in a tandem configuration, resulting in the bivalent N1-3-VHHb and N1-5-VHHb (Figure 15A, C and D). The complete sequence of the N1-VHHb is shown in Table 4. N1-3-VHHb and N1-5-VHHb were expressed and purified from *E. coli* in the same way as N1-VHHm. The *in vitro* N1-VHHb NA-inhibitory and antiviral activities were compared with those of their monovalent counterparts. We found that N1-3-VHHb and N1-5-VHHb displayed a 500- and 2000-fold enhanced N1rec inhibition activity as compared with the corresponding monovalent N1-3-VHHm and N1-5-VHHm format (Table 3). Surprisingly, in a plaque assay using NIBRG-14 virus infected MDCK cells, both N1-3-VHHb and N1-5-VHHb had an antiviral activity that was comparable to the levels of their monovalent counterparts. We reasoned that the integrity of the bivalent format is necessary to present enhanced antiviral potency in both N1-VHHb. However, in the plaque assay with H5N1 infected MDCK cells, exogenous trypsin is used to facilitate maturation of HA in newly produced virions to allow multicycle replication of the recombinant NIBRG-14 virus. We found that the dimerizing llama IgG2c hinge linker in the N1-VHHb was sensitive to trypsin cleavage (Figure 15D). Therefore, in

the presence of trypsin (< 10 µg/ml), N1-3-VHHb and N1-5-VHHb were effectively severed into monovalent VHH. To circumvent the use of exogenously added trypsin we took advantage of the TMPRSS2 MDCK cells, which are transformed with the doxycycline-inducible serine protease TMPRSS2 and allow multicycle replication of IAV in the absence of trypsin (Bottcher et al., 2009). Using monolayers of TMPRSS2 MDCK cells for infection with NIBRG-14, the antiviral effect of N1-3-VHHb and N1-5-VHHb was 240- and 58-fold increased, respectively, compared with their monovalent format (Table 3). These results obtained with N1-VHHb indicate that: (i) there is a significantly enhanced NA-inhibitory and antiviral activity of both N1-VHHb compared with the N1-VHHm format; and (ii) the 10-fold difference between the increase of the N1rec inhibition compared to the plaque assay, suggests that there are other factors that account for the *in vitro* antiviral effect of the N1-VHHb than just their NA inhibitory potential (*i.e.* NA enhanced aggregation in the infected cell membrane).

Table 3. N1-3-VHH and N1-5-VHH formats inhibition of the catalytic N1 NA activity (IC₅₀, nM)^a and plaque size reduction in H5N1 virus infected cells (PIC₅₀, nM)^b

VHH format	Enzymatic assay		Plaque size reduction assay (cell-based)					
	N1rec ^c	Fold ^d	NIBRG-14 ^e	Fold	H5N1 H274Y ^f	Fold	NIBRG-23 ^g	Fold
N1-3-VHHm	425,2 +/- 149,4	-	1844 +/- 344,3	-	6440 +/- 1247,0	-	4295 +/- 2835,4	-
N1-5-VHHm	374,9 +/- 118,5	-	848,5 +/- 380,2	-	>26500	-	3492 +/- 2967,6	-
N1-7-VHHm	>15448	-	>32896	-	>32896	-	>32896	-
N1-3-VHHb	0,157 +/- 0,206	2708	7,6 +/- 3,0	240	52,2 +/- 36,8	123	24,6 +/- 31,9	174
N1-5-VHHb	0,69 +/- 0,231	543	14,5 +/- 11,1	58	>707.5	-	23,6 +/- 3,8	148
N1-3-VHH-Fc	1.31 +/- 0.605	324	23,08 ^h	79	89,4 +/- 7,8	71	24,2 +/- 3,7	177
N1-5-VHH-Fc	1.49 +/- 0.746	251	28,14 ^h	30	>17083	-	27,03	129
N1-7-VHH-Fc	>7900	-	>5260	-	>5260	-	>5260	-
Oseta mivir	586.1 +/- 120.5	-	15030 +/- 10039	-	>243000	-	73000 ^h	-

^a Mean IC₅₀ of NA inhibition assay using the substrate 2'-(4-methylumbelliferyl)-a-D-N acetylneuraminic acid (MUNANA), using 160 ng of N1rec, in 3 independent experiments.

^b Mean PIC₅₀ of duplicates plaque assays, in which VHH concentration reduced the 50 % of plaque size, compared to control VHH (at least 2 independent experiments.)

^c N1rec, tetrameric recombinant N1 Neuraminidase.

^d Fold increase inhibitory potency of the bivalent format compared to the monovalent format.

^e H5N1 NIBRG-14.

^f H5N1 H274Y.

^g H5N1 NIBRG-23.

^h Mean of single experiment.

TRANSGENIC PLANT-PRODUCED N1-VHH-Fc

The previously described N1-VHH monovalent or bivalent molecules are relatively simple molecules that are stable and small sized, feasible for production in prokaryotic systems. Nevertheless, for more complex protein molecules, other production platforms were available and considered. We used a plant-based approach, with reported promising high-end yield results for recombinant antibodies (Van Droogenbroeck et al., 2007). By targeting the N1-VHH-Fc as a seed storage protein, we were able to produce a second bivalent N1-VHH format. For this, the *n1-3-vhh*, *n1-5-vhh* and the *n1-7-vhh* genes were fused to the sequence encoding the hinge and Fc tail of a mouse IgG2a (*n1-vhh-fc*). The resulting protein, N1-VHH-Fc consists of two identical N1-VHH-Fc moieties linked by a disulphide bridge (Figure 15B, Table 4). These *n1-vhh-fc* constructs were cloned into the binary vector pPhas as a T-DNA expression cassette (Figure 15B, C and E). Subsequently, transgenic *Arabidopsis thaliana* plants were generated by *Agrobacterium*-mediated floral dip transformation. Seed extracts of segregating T3 *Arabidopsis* transformants were screened for the best expressors of the recombinant dimeric protein N1-VHH-Fc. We also found a good correlation between a high expression of N1-VHH-Fc and NA inhibitory activity in crude seed extracts from different T3 transformants. N1-3-VHH-Fc, N1-5-VHH-Fc and N1-7-VHH-Fc were purified from seed extracts by protein G affinity chromatography, and Coomassie stained reducing SDS-PAGE analysis showed that the N1-VHH-Fc monomers migrated at ca. 42 kDa (Figure 15E). We found a clear enhancement of the N1rec inhibition and *in vitro* antiviral activity of N1-3-VHH-Fc and N1-5-VHH-Fc compared with the monovalent N1-3-VHHm and N1-5-VHHm (Table 3). The inhibition of replication of NIBRG-14 virus by either N1-3-VHH-Fc or N1-5-VHH-Fc was 80- and 30-fold stronger compared with their monovalent counterparts (Table 3). These results indicated that the *in vitro* NA inhibition and antiviral activity against NIBRG-14 virus is enhanced 1 - 2 log fold in the N1-VHHb and N1-VHH-Fc formats, compared with N1-VHHm.

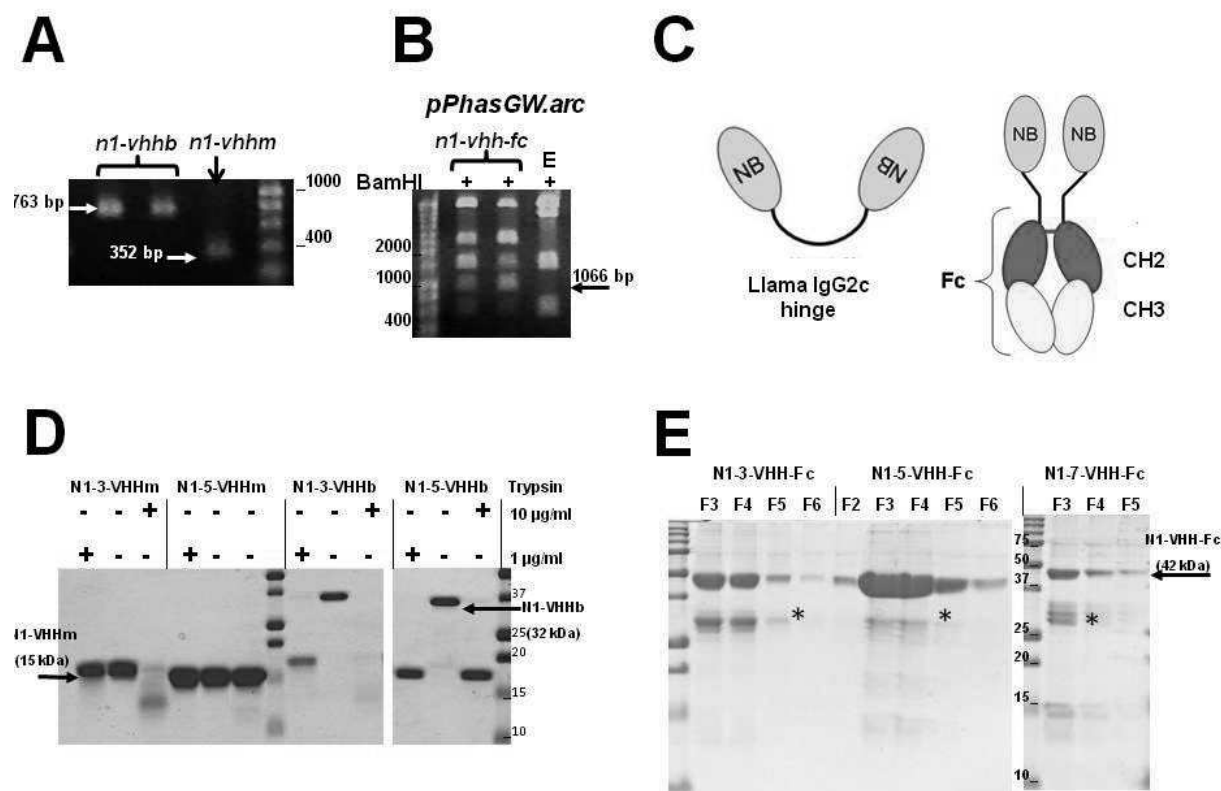


Figure 15. Bivalent formats of the N1-3-VHH and N1-5-VHH. **A.** PCR amplification of the *n1-vhhb* (763 bp) and the *n1-vhhm* (352 bp) genes inserted in the pHEN6c vector, resolved in agarose 1%. **B.** *Bam*HI digested empty (E) or *n1-vhh-fc* gene inserted pPhasGW.arc vector. The 1066 bp band indicates an *n1-vhh-fc* gene insert. **C.** Cartoon representation of the two N1-VHH bivalent formats. The bacteria-produced N1-VHHb consists of two moieties in tandem of N1-VHHm linked by a llama IgG2c hinge of 17 amino acid residues. The plant-produced bivalent N1-VHH-Fc comprises two N1-VHH-Fc moieties, each consist of one N1-VHHm fused to a mouse IgG2a Fc, dimerized through a disulphide bond (red line). **D.** The llama IgG2c-derived hinge is sensitive to trypsin. Coomassie stained reducing SDS-PAGE of purified N1-3-VHHm, N1-5-VHHm, N1-3-VHHb and N1-5-VHHb incubated for 60 min at 37 °C in the presence or absence of 1 µg/ml or 10 µg/ml trypsin. The N1-VHHb molecules migrate at ca. 32 kDa, and the N1-VHHm and the cleavage products of N1-VHHb migrate as bands of ca. 17 kDa (arrows). **E.** Coomassie stained reducing SDS-PAGE of the eluted fractions from a protein G column purification step using seed extracts of pPhas transformed *A. thaliana* T3 plants. The N1-VHH-Fc constructs migrate at ca. 42 kDa (arrow). A degradation product (*) of ca. 28 kDa corresponds to the Fc moiety only, as was confirmed by immunoblotting.

Table 4. Sequences of the N1-VHH bivalent formats

Bivalent Molecule	Amino acid sequence
N1-3-VHHb	<p>LQESGGGLVQPGGSLRLSCAASGSIFSIHDMGWYRRAPGKQRELVAAITSGGSTNYADSVKGRFTISRDNAK NTVSLQMNSLKPEDTAVYYCNAWGEDYGLGEYDSWGQGTQVTVSS<u>AHHS</u>EDPSSKAPKAPMAQVQLQESG GGLVQPGGSLRLSCAASGSIFSIHDMGWYRRAPGKQRELVAAITSGGSTNYADSVKGRFTISRDNAKNTVSLQ MNSLKPEDTAVYYCNAWGEDYGLGEYDSWGQGTQVTVSSHHHHHH</p>
N1-5-VHHb	<p>LQESGGGLVQPGGSLRLSCAASGSDISIYEMGWYRQAPGKQRELVAAITSGGTTNYADSVKGRFTISRDNAK NTVYLQMNSLKPEDTAVYYCNAADFDLWEYDYWGQGTQVTVSS<u>AHHS</u>EDPSSKAPKAPMALQESGGGLVQPG GGSRLSCAASGSDISIYEMGWYRQAPGKQRELVAAITSGGTTNYADSVKGRFTISRDNAKNTVYLQMNSLK EDTAVYYCNAADFDLWEYDYWGQGTQVTVSSHHHHH</p>
N1-3-VHH-Fc	<p>LQESGGGLVQPGGSLRLSCAASGSIFSIHDMGWYRRRPGKQRELVAAITSGGSTNYADSVKGRFTISRDNAK NTVSLQMNSLKPEDTAVYYCNAWGEDYGLGEYDSWGQGTQVTVSS<u>PRGPTIKPCPPCKCPAPNLLGGPSVFI</u> <i>FPPKIKDVLMSLSPIVTCVVVDVSEDDPDVQISWVNNVEVHTAQTQTHREDYNSTLRVVSALPIQHQDWMSGK</i> <i>EFKCKVNNKDLPAPIERTISKPKGSVRAPQVYVLPPEEEMTKKQVTLTCMVTDMPEDIYVEWTNNGKTELNYK</i> <i>NTEPVLDSGGSYFMYSKLRVEKKNWVERNSYSCSVVHEGLHNHHTTKSFSRTPGKKDEL</i></p>
N1-5-VHH-Fc	<p>LQESGGGLVQPGGSLRLSCAASGSDISIYEMGWYRQAPGKQRELVAAITSGGTTNYADSVKGRFTISRDNAK NTVYLQMNSLKPEDTAVYYCNAADFDLWEYDYWGQGTQVTVSS<u>PRGPTIKPCPPCKCPAPNLLGGPSVFI</u><i>FPP</i> <i>KIKDVLMSLSPIVTCVVVDVSEDDPDVQISWVNNVEVHTAQTQTHREDYNSTLRVVSALPIQHQDWMSGKEFK</i> <i>CKVNNKDLPAPIERTISKPKGSVRAPQVYVLPPEEEMTKKQVTLTCMVTDMPEDIYVEWTNNGKTELNYK</i> <i>NTEPVLDSGGSYFMYSKLRVEKKNWVERNSYSCSVVHEGLHNHHTTKSFSRTPGKKDEL</i></p>
N1-7-VHH-Fc	<p>LQESGGGLVQPGGSLRLSCAASGSRFSRYDMGWYRQAPGKQRELVAITITSGGITNYADSVKGRFTISRDNTK NTVYLQMNSLKPEDTAVYYCNAEDPLRAIQLGSLTYEYWGQGTQVTVSS<u>PRGPTIKPCPPCKCPAPNLLGGPS</u> <i>VFIFPPKIKDVLMSLSPIVTCVVVDVSEDDPDVQISWVNNVEVHTAQTQTHREDYNSTLRVVSALPIQHQDWMS</i> <i>GKEFKCKVNNKDLPAPIERTISKPKGSVRAPQVYVLPPEEEMTKKQVTLTCMVTDMPEDIYVEWTNNGKTEL</i> <i>NYKNTEPVLDSGGSYFMYSKLRVEKKNWVERNSYSCSVVHEGLHNHHTTKSFSRTPGKKDEL</i></p>

Bold: N1-VHHm sequence

Underlined: linker or tag

Italics: IgGa mouse Fc

IN VITRO ANTIVIRAL ACTIVITY OF N1-VHH AGAINST H5N1 CLADE 2.2 AND OSELTAMIVIR-RESISTANT IAV

The N1rec NA is derived from the A/crested eagle/Belgium/01/2004 and belongs to the clade 1 of the H5N1 NAs, as well as the NA of the NIBRG-14 (derived from A/Vietnam/1194/2004). In contrast, the H5N1 virus NIBRG-23 NA is derived from A/turkey/Turkey/01/2005, belonging to the clade 2.2. These three different NA used in this study, shared a high amino acid sequence homology (> 95%). Although the number of laboratory-confirmed human cases of H5N1 virus infection remain limited, it appears that clade 2 H5N1 viruses comprise a majority of these zoonotic infections with HPAIV (Poland et al., 2007). We therefore evaluated the antiviral potential of N1-3-VHH and N1-5-VHH in the three formats available (*i.e.* monovalent, bivalent without and with Fc) against the clade 2.2 virus NIBRG-23 (Table 3, Figure 16B). Monovalent N1-3-VHHm and N1-5-VHHm reduced *in vitro* growth of NIBRG-23 virus on MDCK with an IC₅₀ in the low micromolar range (Table 3). Both bivalent formats of these NA-inhibitory VHHs (N1-3-VHHb, N1-5-VHHb, N1-3-VHH-Fc and N1-5-VHH-Fc) displayed an approximately 150-fold higher *in vitro* antiviral activity against this clade 2 virus, as judged by a plaque size reduction assay. Based on these findings, we conclude that the two NA-inhibitory VHHs can inhibit representative H5N1 IAV from clade 1 and 2, with a comparable efficiency *in vitro*, suggesting that they target a common epitope of the NA of these viruses.

Oseltamivir-resistant IAV frequently emerge and spread in the human population. Several mutations have been reported to contribute to oseltamivir-resistance but among these, the H274Y mutation (N2 numbering) is the most commonly found in oseltamivir-resistant viruses (Wang et al., 2002a). We used reverse genetics (Hoffmann et al., 2000) to generate a clade 1 H5N1 virus harboring the H274Y mutation in NA derived from A/crested eagle/Belgium/09/2004 (the HA segment from NIBRG-14 and the remaining 6 segments from PR/8), resulting in the

H5N1 H274Y virus used in this study. Next, we determined if our N1-3-VHHm, N1-5-VHHm, N1-3-VHHb, N1-5-VHHb, N1-3-VHH-Fc and N1-5-VHH-Fc would be active against this oseltamivir-resistant H5N1 virus that carries the H274Y mutation. Given that all of our formats of N1-3-VHH and N1-5-VHH performed similar in biochemical and *in vitro* antiviral activity assays, we were surprised to observe that only the N1-3-VHH in monovalent and both bivalent formats, but not any format of N1-5-VHH, reduced the growth of oseltamivir-resistant H5N1 H274Y virus (Table 3, Figure 16C). Compared to NIBRG-14 as a target, the H5N1 H274Y IC₅₀ values were 3- to 7-fold higher, but still in the low nM range. Even though the competitive SPR analysis suggested that the N1-3-VHHm and N1-5-VHHm epitopes in NA overlap, the contact residues necessary for their binding are probably not the same. The H274Y mutation seems to be sufficient to abolish the *in vitro* antiviral effect of the N1-5-VHH formats during the infection with the H5N1 H274Y mutant virus used in this study. We conclude that N1-3-VHHm, N1-3-VHHb and N1-3-VHH-Fc can inhibit growth of H5N1 viruses *in vitro*, and that their antiviral protection is enhanced in both bivalent formats.

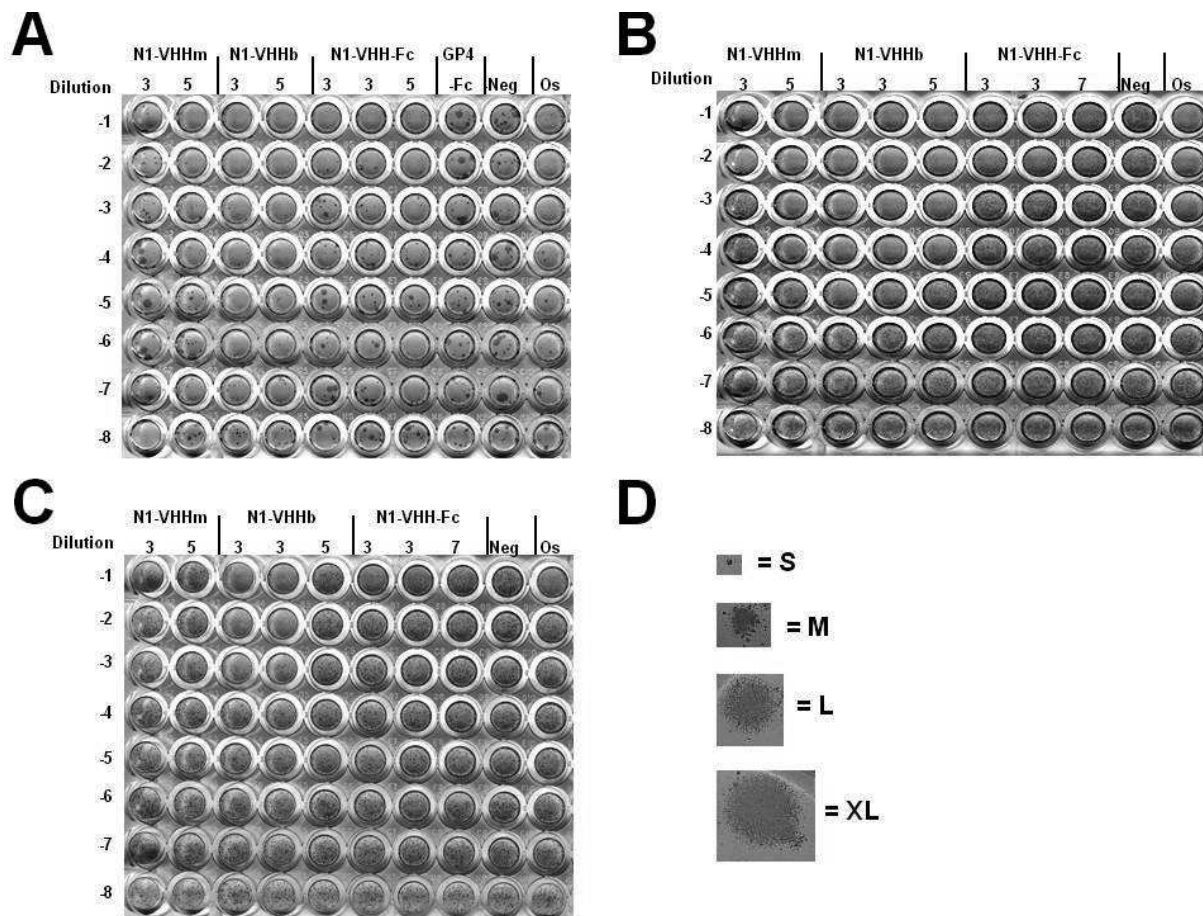
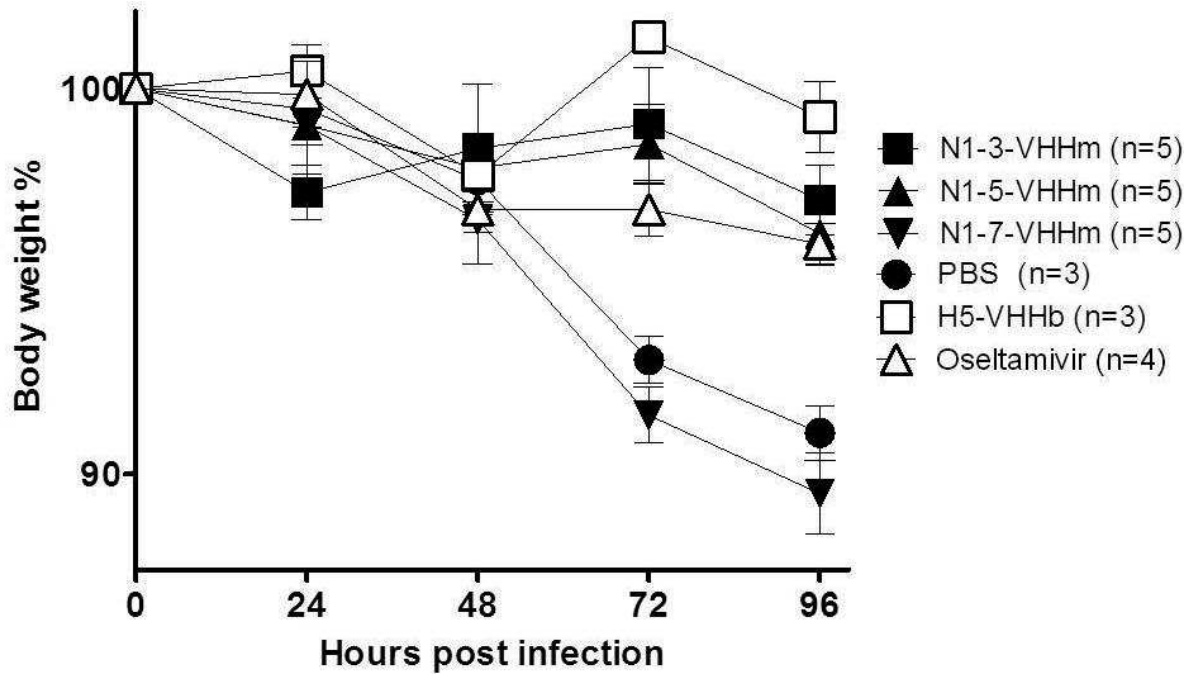


Figure 16. Comparative antiviral effect of the monovalent and bivalent formats of the N1-VHH in representative plaque assays. Dilution series of VHH (Dilution left column) were incubated 1 hr at 37 °C with the indicated virus, and then TMPRSS2 MDCK cells were infected with **A.** NIBRG-14, **B.** NIBRG-23 or **C.** H5N1 H274Y. After 1 hr of adsorption, fresh medium containing the corresponding diluted VHH was added to the washed cells. The infected cells were incubated for 24 hrs and immunostained against M2 protein. The antiviral effect was dose-dependent as indicated in the dilution series. **D.** Representative sizes of the average plaque sizes (amplified 10X, compared with plaques in A, B and C) visualized by immunostaining. -VHH, absence of N1-VHH treatment; Oseltamivir, Os.

N1-3-VHHm AND N1-5-VHHm TREATMENT REDUCES MORBIDITY IN H5N1-CHALLENGED MICE

We next evaluated the *in vivo* antiviral effect of N1-3-VHHm and N1-5-VHHm. In a first experiment we administered intranasally 100 µg of N1-3-VHHm, N1-5-VHHm, and N1-7-VHHm to Balb/c mice at 4 hours before challenge with 4 LD₅₀ of mouse-adapted NIBRG-14 virus (NIBRG-14 ma). As positive controls we included a group of mice that received 30 µg of H5-VHHb, a bivalent NIBRG-14 ma HA neutralizing VHH (Ibanez et al., 2011), as well as daily oral administration of oseltamivir at a high dose of (45 mg/kg/day). The body weight was followed daily, and the groups treated with the inhibitory N1-3-VHHm or N1-5-VHHm showed a significant difference in morbidity at 72 and 96 hours after infection, compared with the groups treated with the N1-7-VHHm and PBS ($P < 0.001$) (Figure 17A). Four days after infection, the mice were sacrificed to determine lung virus titers. Assessment of the lung virus load by endpoint dilution in a TCID₅₀ assay revealed that all mice had a high virus load between -4.75 to -6.48 TCID₅₀/ml approximately in the lung homogenates (including the oseltamivir-treated group), except for the H5-VHHb treated group, which had lung virus titres below detection level (Figure 17B). We therefore decided to quantify the amount of viral RNA in the lung homogenates using a genome strand-specific RT-qPCR method. Except for the samples derived from the H5-VHHb treated mice, all the N1-VHH treated groups showed high viral RNA levels at 96 h after infection, comparable to those in the PBS-treated group, even so for the high oseltamivir-treated mice, although this group differed significantly from the single dose N1-VHHm treated animals ($P < 0.05$) (Figure 17C). We conclude that intranasal administration of N1-3-VHHm and N1-5-VHHm prevents body weight loss after challenge with NIBR-14 ma virus during the early stage of infection.

A**B**

Treatment	TCID ₅₀ /ml
N1-3-VHHm	-6.48
N1-5-VHHm	-5.62
N1-3-VHHb	-5.48
N1-5-VHHb	-4.75
BL-VHHb	-6.48
N1-3-VHH-Fc	-5.75
N1-5-VHH-Fc	-6.48
GP4-Fc	-5.75
Oseltamivir	-4.75
PBS	-6.48
H5-VHHb	ND

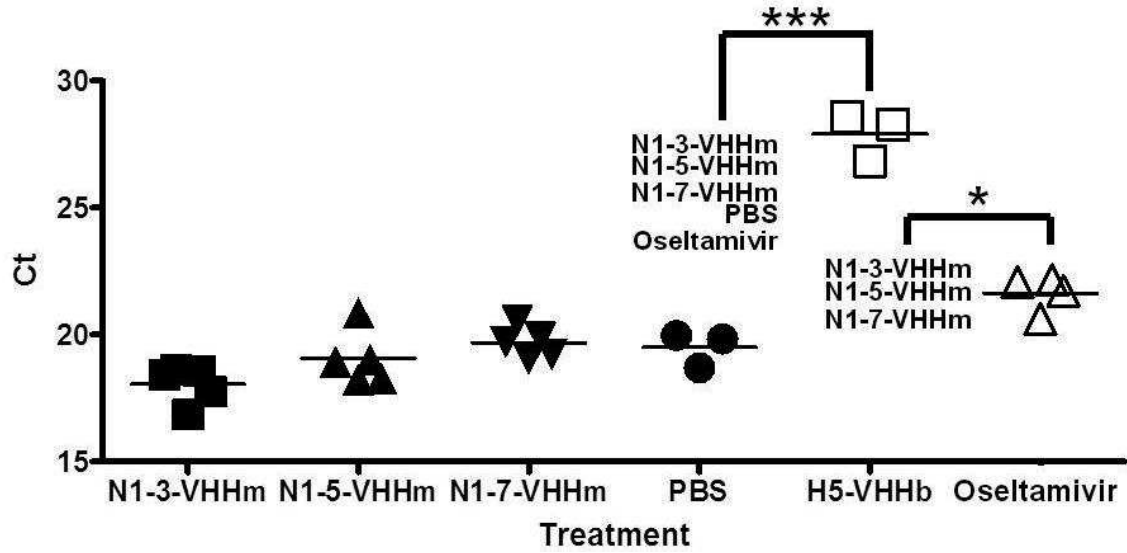
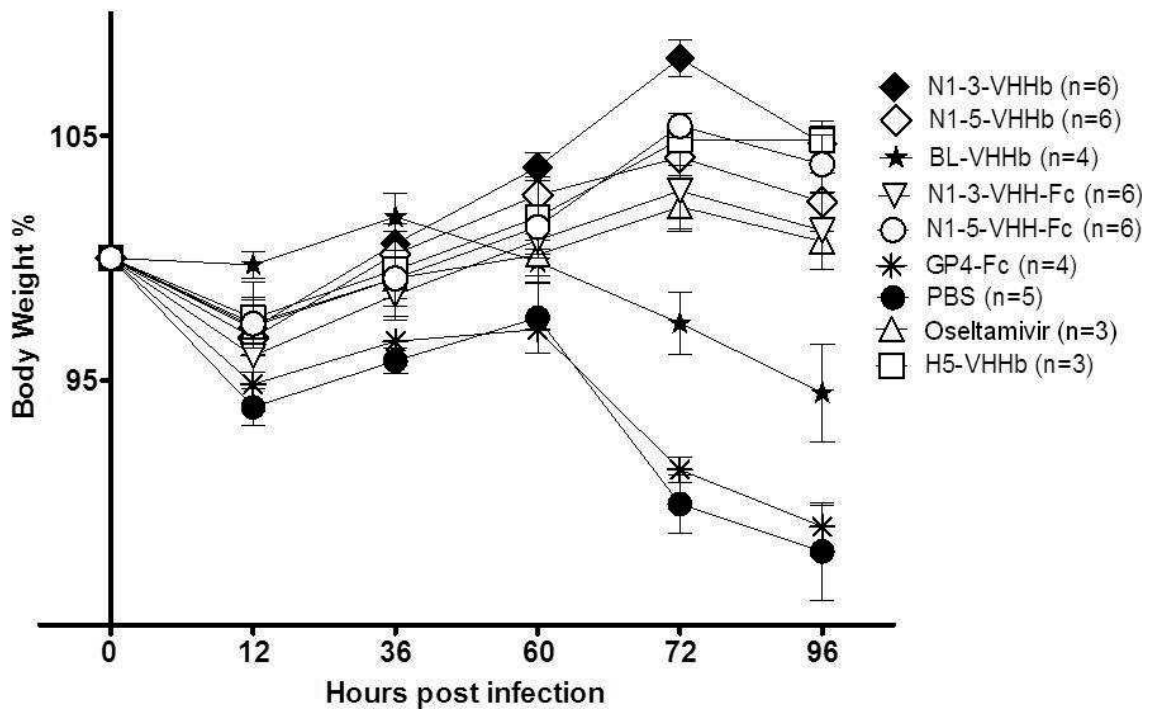
C**D**

Figure 17. Single intranasal administration of N1-3-VHHm, N1-5-VHHm, N1-3-VHHb and N1-5-VHHb decrease the morbidity during the first four days after challenge with H5N1 virus. **A.** Groups of 6-8 week-old Balb/c mice were given 100 µg of indicated VHH, administered intranasally at 4 hours before challenge with 4 LD₅₀ of NIBRG-14ma virus. Thirty µg of intranasal administered H5-VHHb and daily oral administration of oseltamivir (45/kg/day, from 4 hrs before challenge) were included as positive controls. Body weight was monitored daily after challenge and expressed as the percentage of initial body weight. The groups of mice treated with N1-3-VHHm and N1-5-VHHm displayed significantly less morbidity than the groups treated with PBS ($P < 0.001$), N1-7-VHHm ($P < 0.001$) at 72 and 96 hours post infection. Mice were sacrificed on day 4 after challenge and lung homogenates were prepared. **B.** Assessment of the lung virus load by endpoint dilution of the NIBRG-14 infected mice treated with N1-VHH (TCID₅₀/ml). **C.** A viral genome specific RT-qPCR was used as readout for the viral load. The obtained Ct values for the individual mice are plotted and a horizontal line indicates the mean. The Ct value H5-VHHb group was significantly different (indicative for lower virus load), compared to all other groups (***: $P < 0.001$). The oseltamivir-treated group was only slightly different from the groups treated with the N1-3-VHHm, N1-5-VHHm and N1-7-VHHm (*: $P < 0.05$). **D.** The bivalent format of the N1-3-VHH and N1-5-VHH increases the potency to reduce the morbidity in H5N1-challenged mice. Four hours before challenge with 4 LD₅₀ of NIBRG-14 ma, groups of Balb/c mice were treated intranasally with 60 µg of VHHb (N1-3-VHHb, N1-5-VHHb or BL-VHHb), 84 µg of VHH-Fc (N1-3-VHH-Fc, N1-5-VHH-Fc or GP4-Fc). Mice treated with neutralizing H5-VHHb (30 µg) or oseltamivir (45 mg/kg/day, daily by gavage) were included as positive controls. The groups treated with both bivalent formats of the N1-3-VHH and N1-5-VHH were significantly different compared with groups treated with: BL-VHHb and GP4-Fc at 60 hpi ($P < 0.05$), 72 and 96 hpi ($P < 0.001$); PBS, 36 and 60 hpi ($P < 0.05$), and at 72 and 96 hpi ($P < 0.001$).

BIVALENT N1-VHH PROTECTION AGAINST H5N1 CHALLENGE

The *in vitro* results indicated that the bivalent formats of the inhibitory N1-VHHs increased their potency against the tested H5N1 viruses between 30- to 240-fold compared to their monovalent counterparts (Table 3). We therefore assessed if this increased antiviral effect would also be reflected in an *in vivo* challenge experiment. We first determined the protective potential during the early stages of viral infection. Four hours prior to challenge with 4 LD₅₀ of NIBRG-14 ma, groups of Balb/c mice were intranasally given 60 µg of N1-3-VHHb, 60 µg of N1-5-VHHb, 60 µg of BL-VHHb (a bivalent VHH directed against the irrelevant bacterial target β-lactamase), 84 µg of N1-3-VHH-Fc, 84 µg of N1-5-VHH-Fc or 84 µg of GP4-Fc (a plant-produced Coronavirus-Fc fusion protein with an IgG2a Fc moiety, used here as an irrelevant control). Treatment with N1-

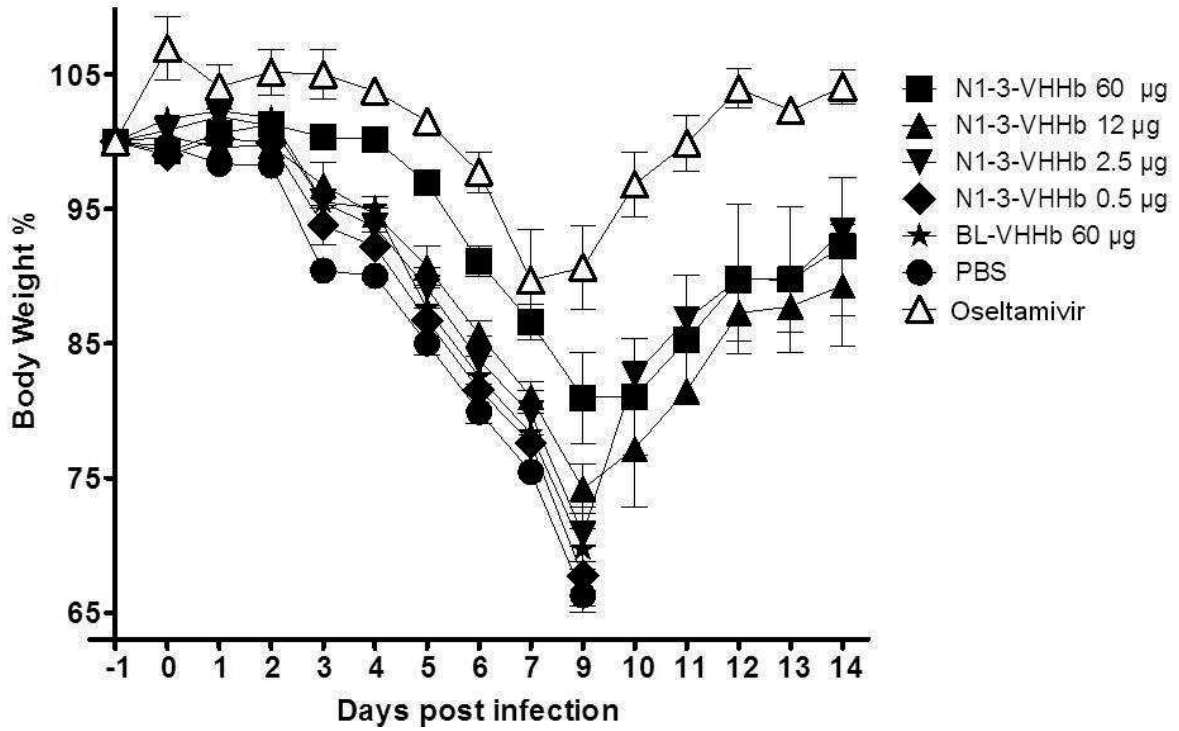
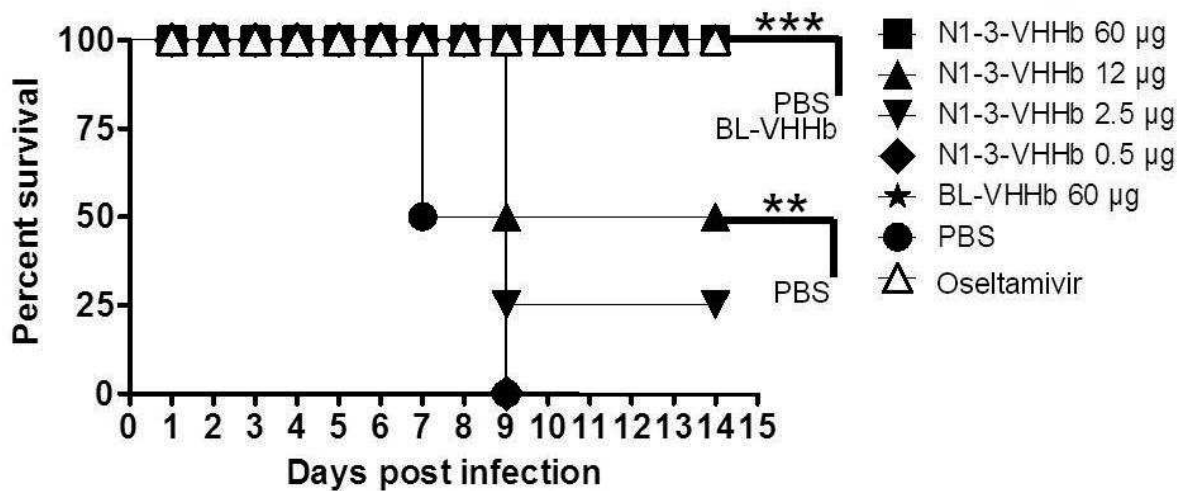
3-VHHb or N1-3-VHH-Fc significantly improved morbidity at 72 and 96 hours after infection (hpi) compared with the negative control groups GP4-Fc and PBS ($P < 0.001$). The protection against weight loss was comparable to that observed with the positive controls (H5-VHHb and oseltamivir, the latter given daily at 45 mg/kg/day, by gavage) (Figure 17D). Treatment with the bivalent formats of N1-5-VHH resulted in a decrease in morbidity that was significant at 60, 72 and 96 hpi compared with the negative controls ($P < 0.001$) (Figure 17D). Determination of the lung virus load on the fourth day after challenge by a TCID₅₀-based assay using lung homogenates from sacrificed mice revealed that all challenged groups, except the H5-VHHb-treated mice (no virus detectable), had a comparable lung virus load (Figure 17B). Taken together, both bivalent formats (tandem repeats and Fc-mediated) of N1-inhibitory N1-3-VHH and N1-5-VHH improve protection during the first four days following NIBRG-14 ma challenge, but did not decrease significantly the viral load in H5N1-infected mice lungs.

BIVALENT N1-VHH PROTECTION AGAINST A LETHAL CHALLENGE WITH H5N1 VIRUS IS DOSE-DEPENDENT

In order to see if mice that have been challenged with 4 LD₅₀ of NIBRG-14 ma virus can be rescued by prior administration of N1-3-VHHb, N1-3-VHH-Fc, N1-5-VHHb or N1-5-VHH-Fc, we followed the morbidity and mortality over a 2-week period. For this, we focussed on the bivalent formats and first assessed their protective efficacy in a dose-response experiment. Groups of four Balb/c mice were treated intranasally with 60, 12, 2.5 or 0.5 µg of N1-3-VHHb or N1-5-VHHb. In parallel, another group was treated by oral administration of oseltamivir (45 mg/kg/day). Negative control groups were treated with 60 µg of BL-VHHb or with PBS prior to challenge. In this experiment, mice that had received 60 µg of N1-3-VHHb, N1-5-VHHb or BL-VHHb prior to the challenge received a second intranasal dose with 60 µg of the same bivalent

VHH at day 6 after the challenge. All mice from the PBS and BL-VHHb treatment groups succumbed at 9 -10 days after the challenge. In contrast, oseltamivir and intranasal high dose N1-3-VHHb or N1-5-VHHb (60 µg) treatment displayed clear body weight loss following challenge (Figure 18A and C), but protected the mice against lethality (Figure 18B and D). The surviving N1-3-VHHb 60 µg treated group, but not the N1-5-VHHb 60 µg treated group, displayed a significant delay in recovery from weight loss after the challenge compared with the oseltamivir treated group (Figure 18A and C). A single intranasal dose of 12 µg or 2.5 µg of either N1-3-VHHb or N1-5-VHHb provided partial protection against mortality but failed to reduce morbidity (Figure 18A-D).

We next evaluated protection against a potentially lethal NIBRG-14 ma challenge by prior single intranasal administration of the plant-produced N1-3-VHH-Fc and N1-5-VHH-Fc formats. Eighty-four and 17 µg of N1-3-VHH-Fc as well as oseltamivir treatment provided full protection against NIBRG-14 ma challenge and the survival of the mice treated with 3.5 and 0.7 µg was dose-dependent (Figure 19B and D). Nevertheless this protection was associated with significant body weight loss for all dosages used, including the oseltamivir group (Figure 19A and C). All PBS and GP4-Fc treated animals died at day 9 after the challenge. On the other hand, the body weight loss was less severe in all N1-5-VHH-Fc treated groups, and only in the group treated with 0.7 µg some of the mice died (Figure 19B and D). Finally, when comparing the protective efficacy of the two bivalent formats of N1-3-VHH and N1-5-VHH, it appears that the Fc moiety in the N1-VHH-Fc formats provides an extra protective effect against morbidity and mortality following NIBRG-14 ma challenge. Taken together, we conclude that bivalent formats of N1-3-VHH and N1-5-VHH can protect mice against a potentially lethal challenge with an H5N1 virus, although this protection does not completely eliminate morbidity.

A**B**

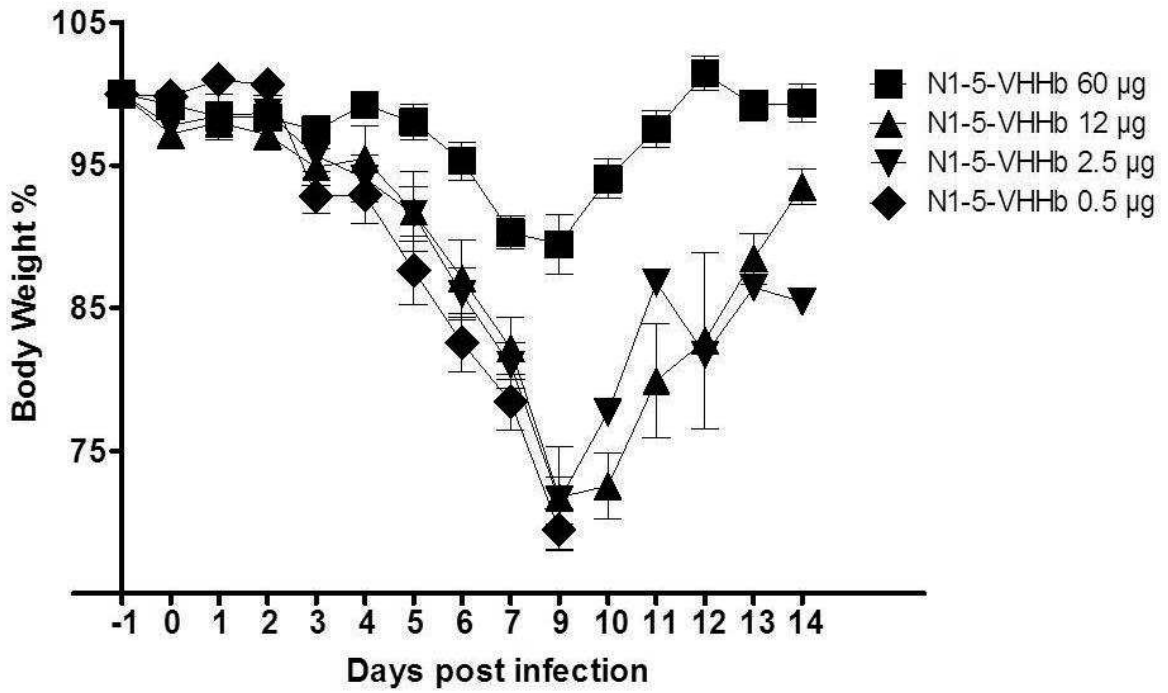
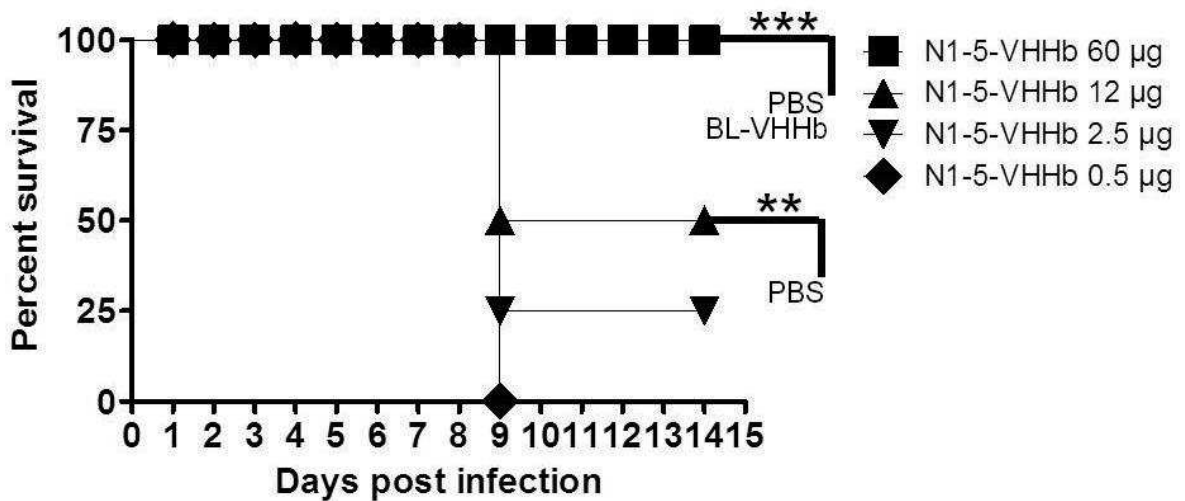
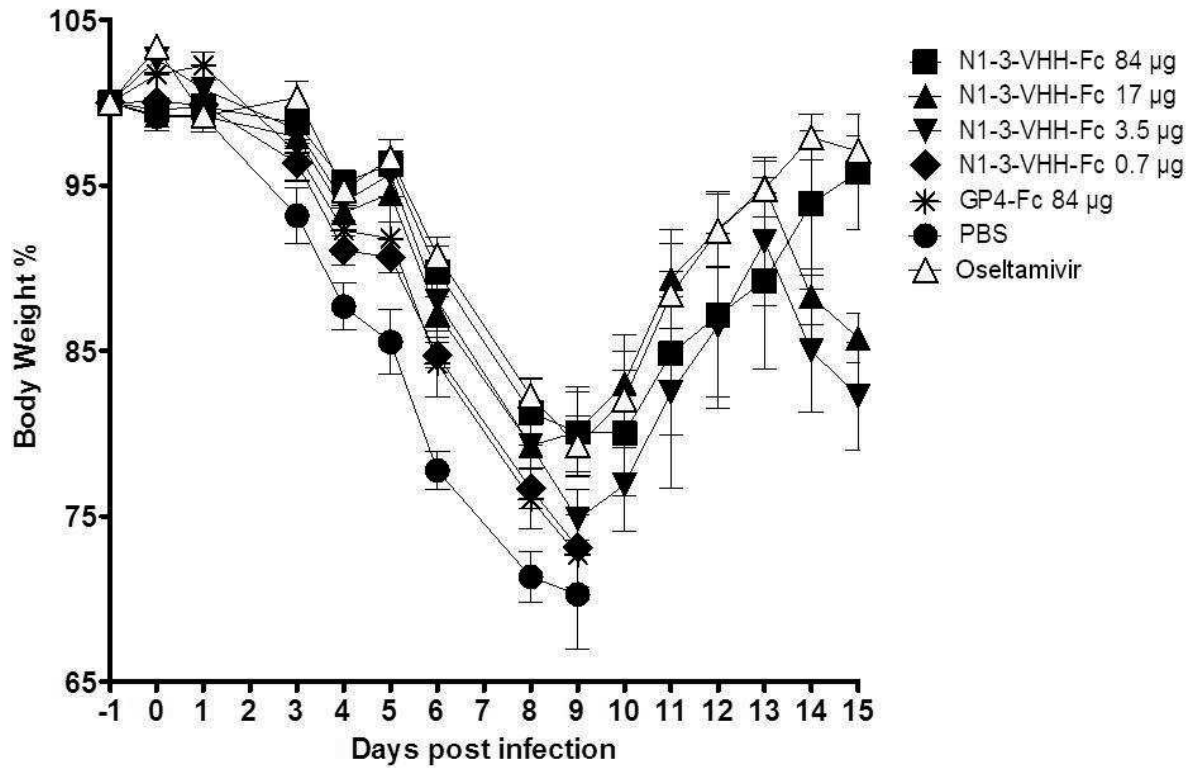
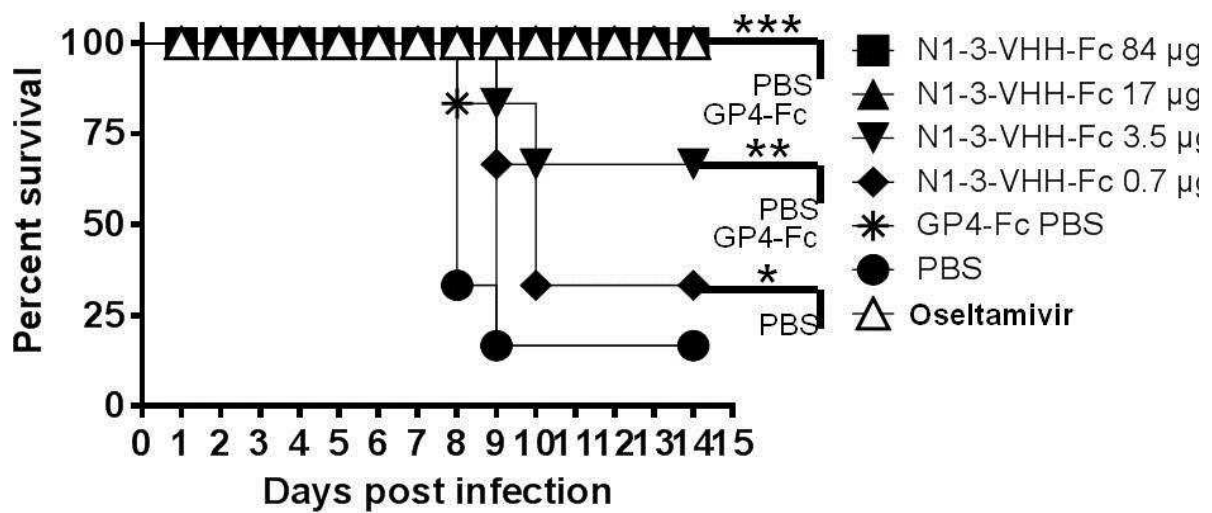
C**D**

Figure 18. The bacteria-produced N1-VHHb formats protect against morbidity and mortality in a dose-dependent way in H5N1-challenged mice. Unless is stated, groups of 4 Balb/c mice were given the indicated amount of N1-VHH and administered 24 hours before challenge with 4 LD50 of NIBRG-14ma virus. One group of mice was treated with one dose of oseltamivir (45 mg/day/kg) as positive control at 24 hrs before challenge, followed by daily boost from 6-14 days after challenge. A boost of N1-VHHb was given at 6 dpi only to the highest doses of each treatment. **A.** The group of mice treated with 60 µg of N1-3-VHHb presented significant increase in morbidity compared to the oseltamivir group at: 10 – 11 dpi ($P < 0.001$), 12-13 dpi ($P < 0.01$) and 14 dpi ($P < 0.05$). The difference of the morbidity between the different N1-3-VHHb treated groups was not significant ($P > 0.05$). **B.** The survival of the N1-3-VHHb 60 µg group was 100 %, being highly significant compared to the control groups BL-VHHb 60µg and PBS (***, $P < 0.001$). The group N1-3-VHHb 12 µg survival was of 50%, but still significant compared to the PBS groups (**, $P < 0.01$). The survival of the groups treated with N1-3-VHHb 2.5 µg (25 %) and 0.5 µg (0 %) was not different to the control groups ($P > 0.05$). **C.** The morbidity of the N1-5-VHHb 60 µg treated group was different to the N1-5-VHHb 12, 2.5 and 0.5 µg groups at days 10 – 14 ($P < 0.001$), but not different to the oseltamivir group ($P > 0.05$). **D.** The survival and significance of the N1-5-VHHb treated groups was the same as the N1-3-VHHb treatment in C. dpi, days post infection.

A**B**

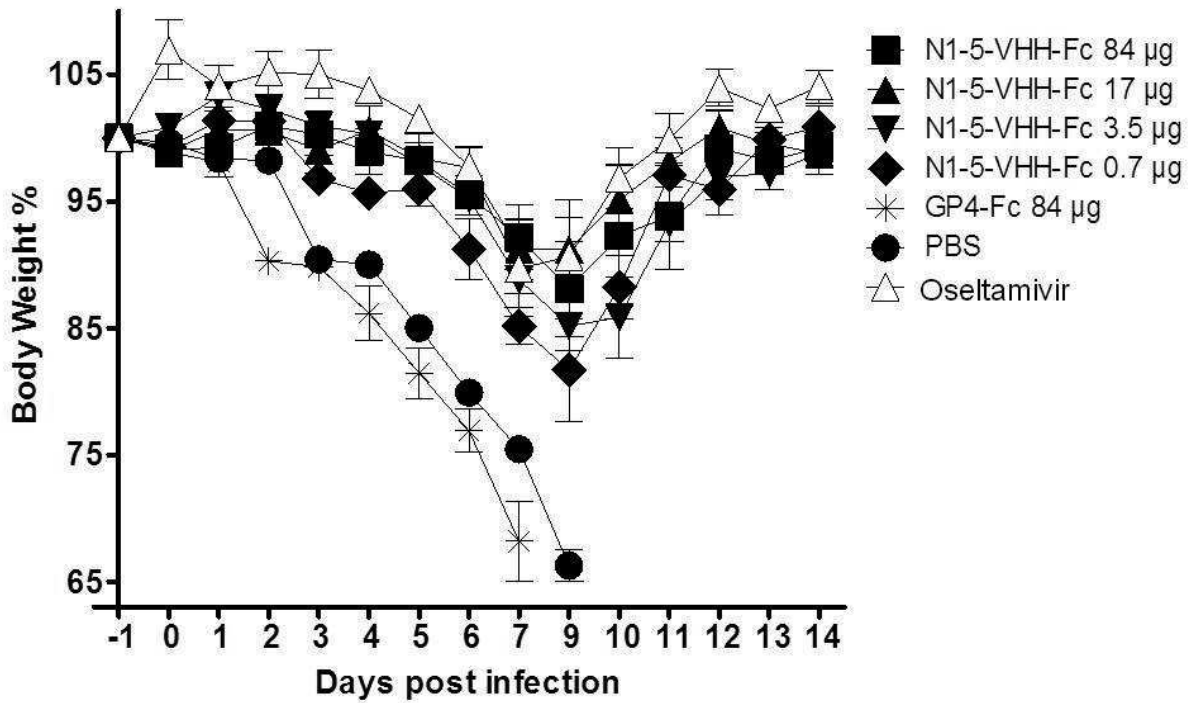
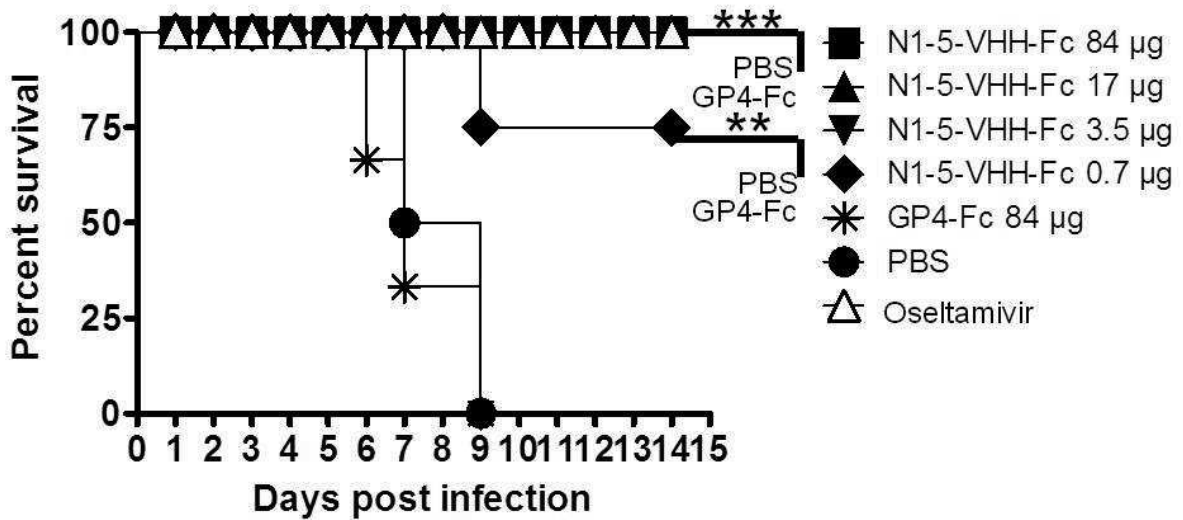
C**D**

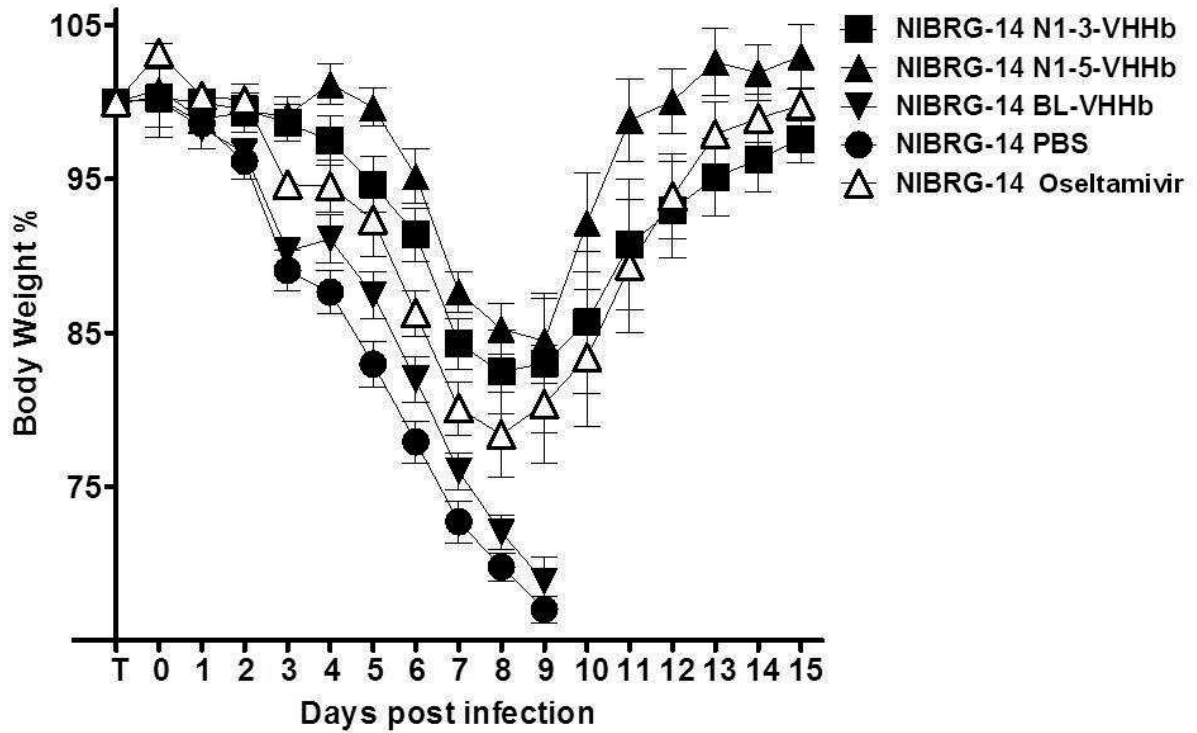
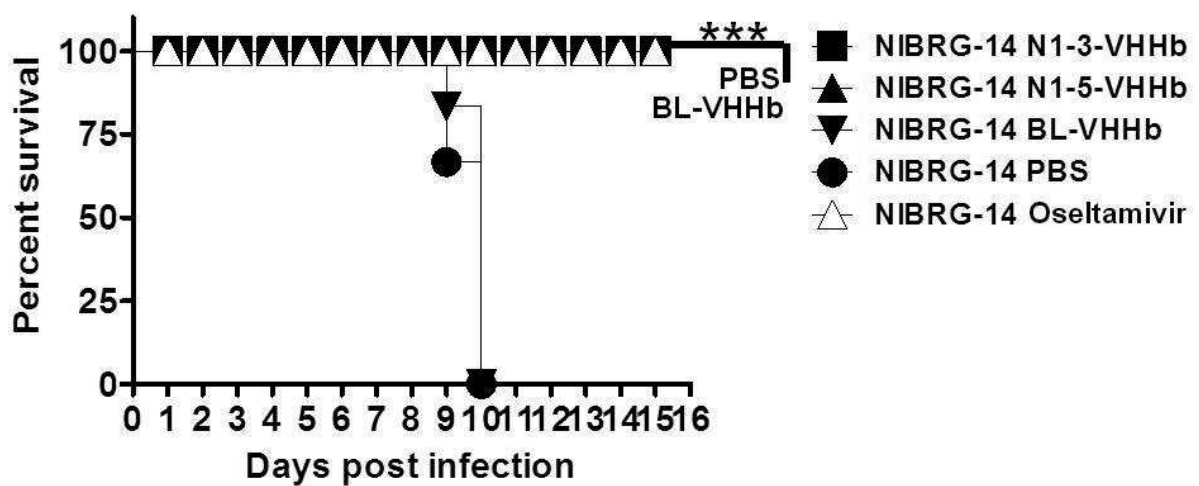
Figure 19. The plant-produced N1-VHH-Fc treatment gave better protection against morbidity and lethality than the N1-VHHb treatment in H5N1-challenged mice. Groups of Balb/c mice were given the indicated amount of N1-VHH-Fc and administered 24 hours before challenge with 4 LD₅₀ of NIBRG-14ma virus. One group of mice was treated with one dose of oseltamivir (45 mg/day/kg) as positive control at 24 hrs before challenge, followed by daily boost from 6-14 days after challenge. A boost of N1-VHH-Fc was given at 6 dpi only to the highest doses of each treatment, including the oseltamivir. **A.** Groups of 6 Balb/c mice were treated with different amounts of N1-3-VHH-Fc, but the difference in morbidity was not significant between them or compared with the oseltamivir treated group ($P > 0.05$). **B.** The survival of the N1-3-VHH-Fc treated groups is dose-dependent, and is significant compared to the control groups PBS and GP4-Fc 84 µg: N1-3-VHH-Fc 84 µg and 17 µg, 100% (both ***, $P < 0.001$); N1-3-VHH-Fc 3.5 µg, 66.6 % (**, $P < 0.01$); 0.7 µg, 33.3 % (PBS only *, $P < 0.05$,). **C.** The morbidity of the groups treated with N1-5-VHH-Fc was not significant different between them and to the oseltamivir-treated group. **D.** The survival of the groups treated with N1-5-VHH-Fc 84, 17 and 3.5 µg was 100%, being highly significant compared with the groups GP4-Fc 84 µg and PBS (both ***, $P < 0.001$). The treatment with N1-5-VHH-Fc 0.7 µg resulted in a survival of 75 %, different from the groups GP4-Fc 84 µg and PBS (**, $P < 0.01$).

N1-3-VHHB AND N1-3-VHH-FC PROTECT AGAINST A CHALLENGE WITH AN OSELTAMIVIR-RESISTANT H5N1 VIRUS

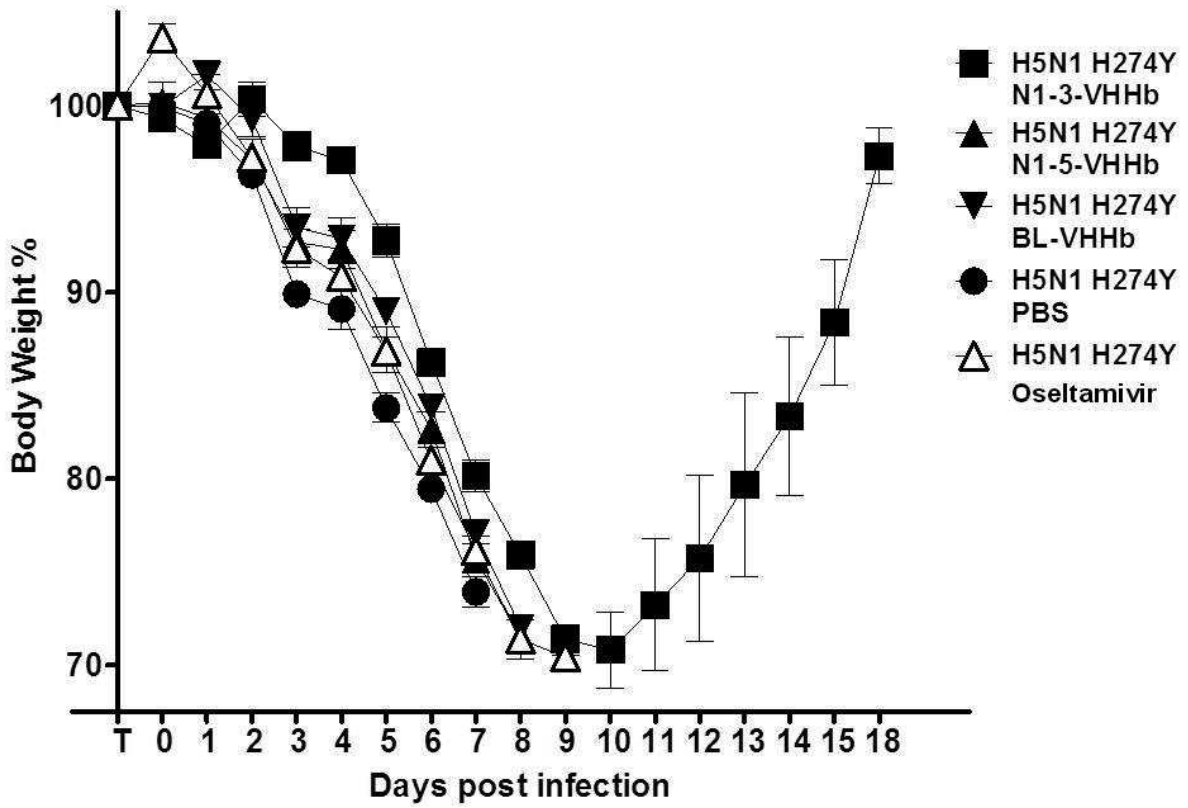
In vitro analysis demonstrated that N1-3-VHH, but not N1-5-VHH, in monovalent or bivalent format could reduce the growth of oseltamivir-resistant H5N1 H274Y virus (Table 3). To try to extrapolate these findings to an *in vivo* challenge model, groups of six Balb/c mice received 30 µg of N1-3-VHHb, N1-5-VHHb or BL-VHHb, by intranasal administration 24 hours before the challenge with 4 LD₅₀ of either NIBRG-14 ma or H5N1 H274Y virus. A PBS recipient group was included as negative control. In parallel, a group was treated by daily oral administration of oseltamivir (1 mg/kg/day), a dose that has been reported to protect laboratory mice against a challenge with an H5N1 virus (Govorkova et al., 2001). All N1-3-VHHb, N1-5-VHHb and oseltamivir treated mice survived the challenge with NIBRG-14 ma virus whereas PBS and BL-VHHb recipient mice succumbed (Figure 20A and B). This result demonstrates that a single intranasal administration of N1-3-VHHb or N1-5-VHHb is sufficient to protect against a subsequent (24 h later) potentially lethal challenge with an H5N1 virus that has an antigenically matching NA. Again all surviving mice suffered from substantial but transient weight loss after

the challenge (Figure 20A). From the mice that had been similarly treated as above but challenged with H5N1 H274Y virus, only those that had received N1-3-VHHb prior to the challenge survived. All other groups, including those that had been treated with an oseltamivir dose that fully protected against a NIBRG-14 ma challenge, died following the challenge with the H5N1 H274Y virus (Figure 20C and D).

Finally, we evaluated the effect of prior intranasal instillation of N1-3-VHH-Fc, N1-5-VHH-Fc, including also N1-7-VHH-Fc in our lethal challenge model. We again included PBS and oseltamivir treatment groups as well as GP4-Fc recipients. Following challenge with 4 LD₅₀ of NIBRG-14 ma, all mice except one in the PBS and one in the GP4-Fc group died. In the N1-7-VHH-Fc group, only one of the six mice died after challenge. In contrast, all mice in the N1-3-VHH-Fc, N1-5-VHH-Fc and oseltamivir groups survived this challenge, all displaying significant body weight loss, except for the mice that had received N1-5-VHH-Fc appearing to be fully protected from morbidity following the NIBRG-14 ma challenge (Figure 21A and B). A challenge with H5N1 H274Y virus proved lethal to all mice except for those that had been treated in advance with N1-3-VHH-Fc (all mice survived) or N1-7-VHH-Fc (4 out of 6 mice survived) although all animals suffered from substantial body weight loss (Figure 21C and D). We conclude that bivalent NA-specific VHH can protect against a potentially lethal challenge with oseltamivir-resistant H5N1 virus.

A**B**

C



D

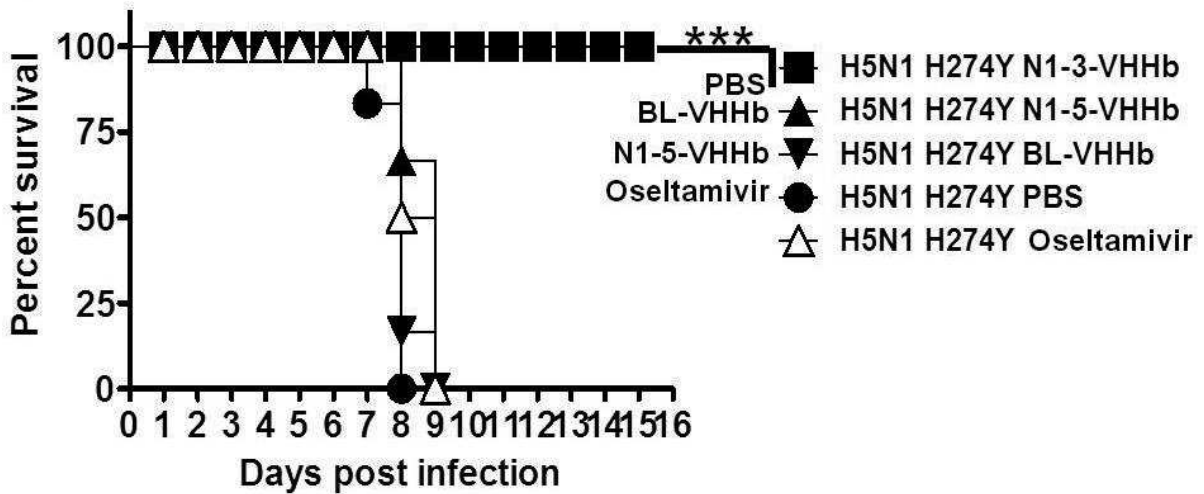
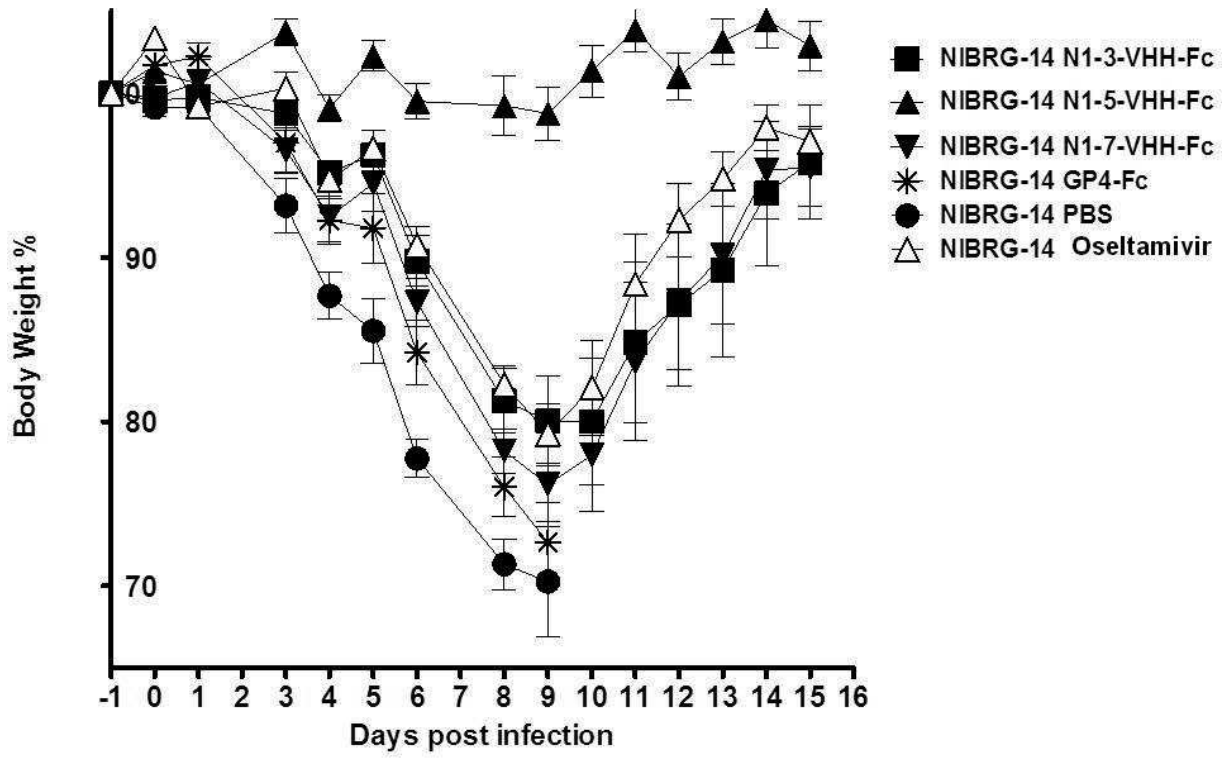
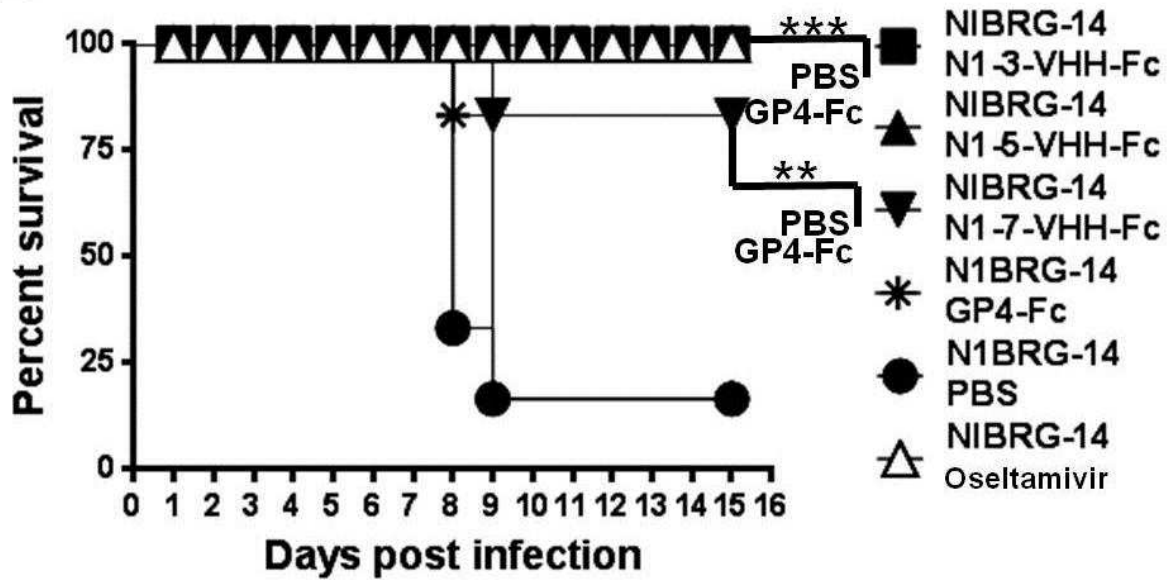


Figure 20. Single-dose treatment with N1-3-VHHb, but not with N1-5-VHHb, rescued mice from a H5N1 H274Y lethal challenge. Twenty-four hours before challenge with 4 LD₅₀ of NIBRG-14 ma or 1 LD₅₀ H274Y H5N1 virus, groups of 6 Balb/c were given: 60 µg of N1-3-VHHb, N1-5-VHHb or BL-VHHb. A group of 6 mice was treated with oseltamivir (1 mg/day/kg) as positive control. **A.** There was no significant difference in the morbidity between the groups treated with N1-3-VHHb and N1-5-VHHb, or compared to the oseltamivir group during the NIBRG-14 infection ($P > 0.05$). In contrast there was an increased morbidity in the irrelevant bivalent VHH BL-VHHb and the PBS treated groups until 9 day post infection. **B.** In NIBRG-14 ma infected mice, the N1-3-VHHb, N1-5-VHHb and oseltamivir-treated groups showed a survival of 100%, being significantly different from the control groups BL-VHHb and PBS (***, $P < 0.001$), where all the mice were dead at 10 days post infection. **C.** The morbidity of H5N1 H274Y treated group was severe and only slightly delayed compared with all other groups. The maximal body weight loss of all groups was close to 70 % at 9 days post infection, but only the N1-3-VHHb treated group showed an increase of body weight at and after 10 dpi. **D.** The treatment with N1-3-VHHb rescued all the H5N1 H274Y infected mice (survival of 100 %), with high significance compared with the rest of the groups (***, $P < 0.001$). The N1-5-VHHb, oseltamivir, BL-VHHb and PBS treatments failed to rescue H5N1 H274Y infected mice.

A**B**

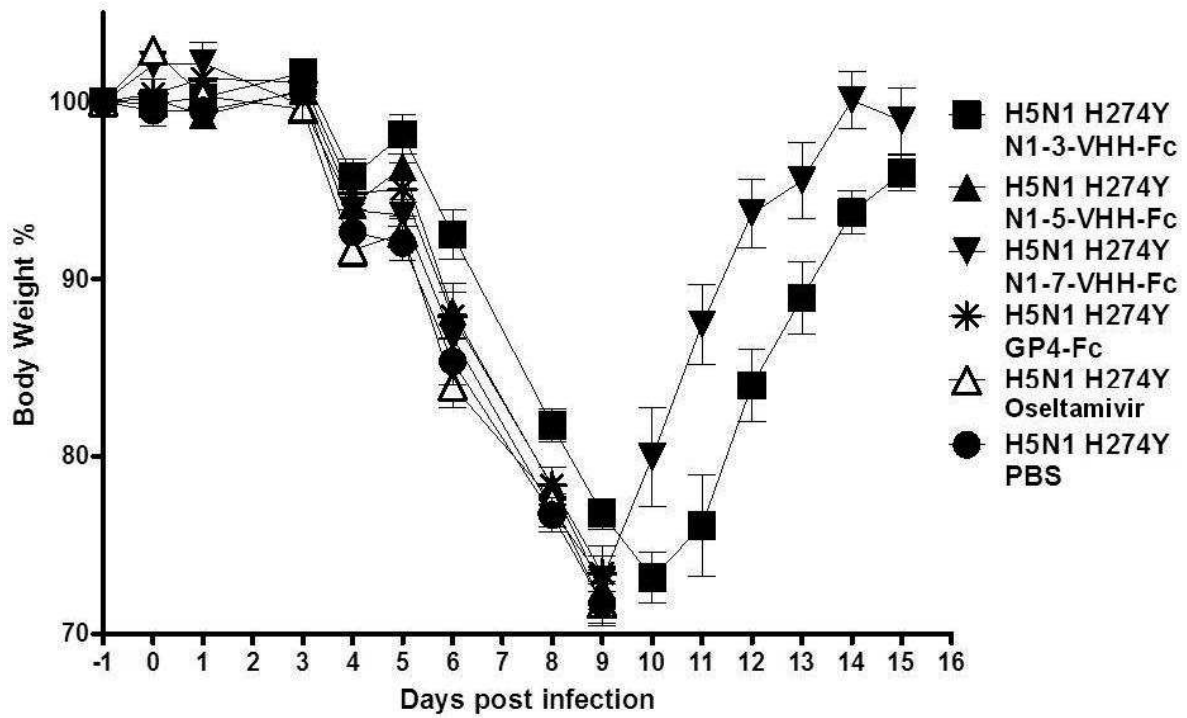
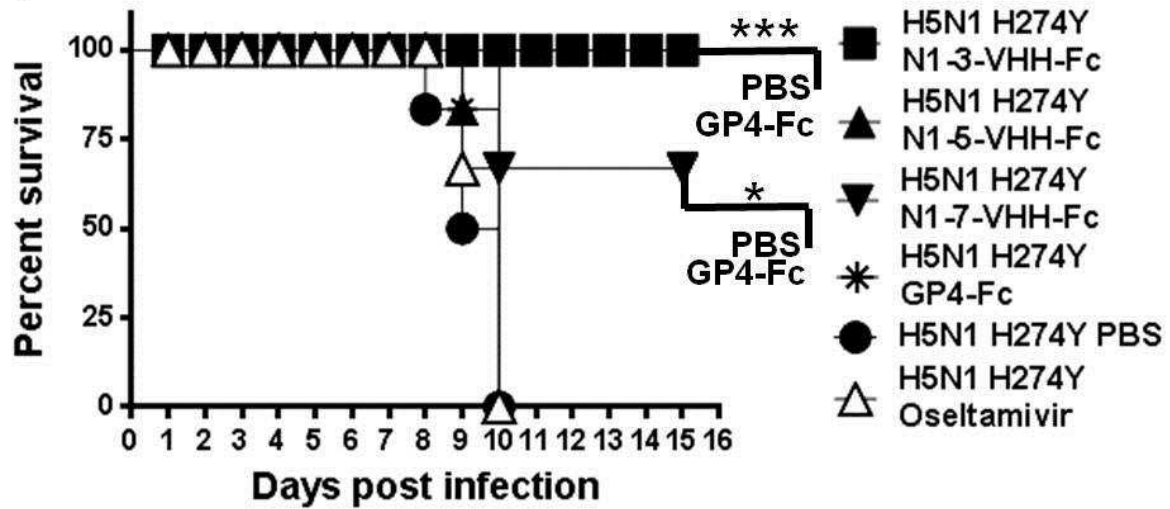
C**D**

Figure 21. The single-dose treatment with N1-3-VHH-Fc and N1-7-VHH-Fc rescued mice from a H5N1 H274Y 1 LD₅₀ challenge, but not with N1-5-VHH-Fc. Twenty-four hours before challenge with 4 LD₅₀ of N1-5-VHH-Fc or 1 LD₅₀ H274Y H5N1 virus, groups of 6 Balb/c were given: 84 µg of the N1-3-VHH-Fc, N1-5-VHH-Fc, N1-7-VHH-Fc or GP4-Fc. A group of 6 mice was treated with oseltamivir (1 mg/day/kg) as positive control. **A.** In N1-5-VHH-Fc infected mice, the difference in morbidity of the N1-5-VHH-Fc group compared with the N1-3-VHH-Fc, N1-7-VHH-Fc or oseltamivir groups is significant at days: 8 -13 dpi ($P < 0.001$) and 14 dpi ($P < 0.01$). The difference in morbidity between N1-3-VHH-Fc, N1-7-VHH-Fc or oseltamivir groups was not significant, and the maximal peak of weight loss was 9 days post infection. **B.** In N1-7-VHH-Fc infected mice, the treatment of N1-3-VHH-Fc, N1-5-VHH-Fc and oseltamivir results in a highly significant survival of 100%, when compared to PBS and GP4-Fc ($***, P < 0.001$). The group treated with N1-7-VHH-Fc presented a survival of 83.3 %, and is significantly different compared to PBS and GP4-Fc ($** , P < 0.01$). **C.** In a similar way as in figure 20C, in the H5N1 H274Y infected mice treated with N1-3-VHH-Fc and N1-7-VHH-Fc presented severe body weight loss, but a positive gain was seen at 10 days post infection in this two groups. The N1-5-VHH-Fc, oseltamivir, GP4-Fc and PBS groups did not present any body weight gain. **D.** In H5N1 H274Y infected mice, the survival of the groups treated with N1-3-VHH-Fc and N1-7-VHH-Fc was significant, 100 % ($***, P < 0.001$) and 66.6 % ($* , P < 0.05$), respectively. The N1-5-VHH-Fc, oseltamivir, GP4-Fc and PBS treatments failed to rescue any H5N1 H274Y infected mice.

DISCUSSION

As commented in the introduction, for several years the vaccine-induced Ab efficacy has been focused rather on HA immunogenicity than NA. NA Abs exert their effects further downstream in the IAV infection process, cannot neutralize the viral infectivity, but they can sharply inhibit replication efficiency and reduce the disease severity upon infection (Schulman et al., 1968; Johansson et al., 1987). There is evidence that the NA Ab response during vaccination can be correlated with the NA activity, which is in turn dependent on the NA amount present in the vaccine formulation. Elderly subjects, immunized with trivalent inactivated vaccines containing H1N1 or H3N2 IAV, presented high titers of NA Ab, after a high dose of vaccine. Ab titers against N1 or N2 had been associated with high NA enzymatic activity in the vaccine preparation, suggesting that the NA content and activity in IAV vaccines is a predictive marker for immunogenicity (Cate et al., 2010). Nevertheless, the HA immunodominancy over NA, and the low NA antigen content in vaccines are factors that contribute to the lack of conclusive

evidence in order to determine the amount of NA antigen necessary to elicit a protective response. During the last decade, growing evidence of the importance in the NA-dependent immune response resulted in the proposal to standardize the NA content in the seasonal vaccine formulation (Johansson et al., 1998; Kilbourne et al., 2004; Marcelin et al., 2012). Besides the immunogenic and viral protein aggregation, there are other NA roles reported: cleavage of decoy receptors of mucins, a process that may be necessary during the initiation of infection (Matrosovich et al., 2004a), limitation of IAV superinfections and reassortment (Huang et al., 2008), and the possibility of increased IAV infectivity (Goto and Kawaoka, 1998). Interestingly, in replicative H5N1 IAVs that are sensitive to NA-inhibitory drugs, a crippled or absent NA activity had been observed. For example, introduction of the mutation R156K decreased 90% of NA activity in H5N1 IAV, under peramivir pressure. The lack of peramivir selective pressure results in the disappearance of this mutant IAV, in culture (Ilyushina et al., 2012). Other reports have shown that the fitness of mutant IAV virus lacking the NA gene or NA activity can be rescued, by decreased HA binding to Sia receptors, due to insertions of mutations or glycosylations in the HA, that affect the receptor-binding site (Gubareva et al., 2002). The compensatory effect in the HA and NA activities towards fitness had been widely reported (Mitnaul et al., 2000; Gubareva et al., 2002; Nedyalkova et al., 2002), demonstrating that the NA activity can be compromised, but not necessarily results in a replication-deficient IAV. These pieces of evidence highlight the IAV mutants' complicate escape mechanism, under selective pressure. There are also important roles of the NA function that seem not to depend on the catalytic site: enhancement of neurovirulence (*i.e.* the glycan at position 130) (Li, et al. 1993); enhanced pathogenicity (length of NA stalk), (Yamada et al., 2006; Matsuoka et al., 2009). Taken together, these data demonstrate the major importance of NA during IAV infection, and targeting NA is a rational choice to generate an effective antiviral strategy, dependent or independent of the NA-catalytic activity.

Our N1-VHHs are not the first inhibitory mAb against a H5N1 NA. Recently, the IgG2bk mAb 2B9 derived from A/Vietnam/1203/04 (H5N1), showed H5N1 interclade and oseltamivir-resistant mutant inhibition (N294S) *in vitro* (Shoji et al., 2011). In a MUNANA and NA-Star (Applied Biosystems) based NA activity assay in live viruses, the 2B9 mAb inhibited the H5N1 clade 1 A/Vietnam/1203/04, the clade 2.1 A/Indonesia/05/05 and the oseltamivir-resistant double mutant A/Vietnam/HN/30408/05 (H274Y and N294S, N2 numbering) with a 2B9 IC₅₀ concentration of approximately 1, 8 and 1 µg/ml, respectively to each IAV. In our study, we used our panel of inhibitory N1-VHH in their three formats (N1-VHHm, N1-VHHb and N1-VHH-Fc) to assess their NA inhibitory and antiviral potential, by NA inhibition assays (using our purified N1rec), and also in cell-based plaque reduction assays. Both of our assays cannot be compared directly with the NA inhibition assays performed by Shoji and coworkers (2011). Our N1rec inhibition assay relies on purified protein, and the NA total protein used in our assays (160 ng) is likely to be higher than the NA molecules copies in live virus preparations. In addition, our MDCK TMPRSS2-based assay measured the capacity of our N1-VHH formats to inhibit the spreading of the H5N1 viruses in a cell monolayer, where other factors than NA inhibition can play a role in the virus spreading (*i.e.* aggregation of viral proteins in the cell membrane). Nevertheless, our N1rec inhibition assay results using the N1-3-VHHm and N1-5-VHHm as inhibitors, showed that their IC₅₀ of 425 nM (6.3 µg/ml) and 374 nM (5.6 µg/ml), respectively, are increased 2 – 3 log fold by the introduction of bivalency, in both bivalent formats (N1-VHHb and N1-VHH-Fc) (Table 3). In addition, an enhanced but more modest antiviral effect by the bivalent formats was also seen in the cell-based assays (Table 3). In NIBRG-14 (NA derived from A/Vietnam/1194/04) infected cells, the concentration necessary to inhibit 50% of plaque size (PIC₅₀, table 3) using N1-3-VHHm and N1-5-VHHm was 1.8 µM (27.3 µg/ml) or 0.8 µM (12.7 µg/ml), respectively, which represents a 30- and 240-fold decrease, respectively when compared with their bivalent formats. Interestingly, we also documented *in vitro* plaque size reduction for the clade 2 H5N1

virus NIBRG-23 (NA derived from A/turkey/Turkey/2005, clade 2.2), where N1-3-VHHm and N1-5-VHHm treatment presented a PIC_{50} of 4.2 μ M (63.6 μ g/ml) and 3.4 μ M (52.3 μ g/ml), respectively, resulting in an increase of the inhibitory potential of 130- and 170-fold, respectively in both bivalent formats (Table 3). The NAs of NIBRG-14 and NIBRG-23 belong to different H5N1 clades but share an homology of 96.7%, and the substitutions in their NA sequences do not affect any of the NA catalytic site residues (substrate direct-contact or framework residues). These results suggest that the epitope recognized by both N1-3-VHHm and N1-5-VHHm is conserved between the H5N1 clades 1 and 2.

In a murine model, the mAb 2B9 failed to give total protection against the H5N1 A/Vietnam/1194/2004 challenge. Intravenous administration of 500 μ g of 2B9 1 hour before 10 LD_{50} of H5N1 IAV, and a daily boost for 5 days, could only protect 50% of mice from mortality, and surviving mice displayed a body weight loss peak of ca. 10% on day 9 after infection (Shoji, et al. 2011). In our study, we are reporting that a single dose of intranasally administered 60 μ g of the bacteria-produced N1-3-VHHb or N1-5-VHHb 24 hours before a H5N1 4 LD_{50} challenge can protect 100% of the mice (Figure 18B and D), but a body weight loss peak of 10 – 20% at 9 days post infection was also observed (Figure 18A and C). The most important difference between a conventional mouse mAb and bacteria-produced N1-3-VHHb and N1-5-VHHb is the lack of an Fc domain in VHH. Therefore, we also evaluated plant-produced bivalent formats of N1-VHH-Fc. For a similar molar amount, N1-VHH-Fc displayed a better protection in H5N1 challenged mice than the bacteria-produced bivalent N1-VHH. Furthermore, a single dose of 17 or 3.5 μ g of N1-3-VHH-Fc or N1-5-VHH-Fc, respectively, also resulted in 100% of survival in mice (Figure 19B and D), and the treatment of N1-5-VHH-Fc decreased significantly or even prevented morbidity (Figures 18A and 19C). By comparing the molar ratio necessary to give 100% survival of H5N1 challenged mice in N1-3-VHH-Fc or N1-5-VHH-Fc treatments

(compared to N1-3-VHHb or N1-5-VHHb), we found that approximately 10 or 50 times lower amounts of the plant-produced formats are necessary.

Compared with the 2B9 treatment in order to rescue 100% of H5N1 challenged mice, the single dose treatment with our N1-3-VHHb/N1-5-VHHb or N1-3-Fc/N1-5-VHH-Fc requires a 10- or 150-fold, respectively, lower amount of Ab needed at the beginning of the treatment. Our bivalent N1-VHH formats gave 100% survival without any boost, showing better protection compared with the 50% survival rate conferred by 2B9 treatment of 500 µg with 5 daily boosts. The intravenous administration of 2B9 in the work of Shoji and colleagues (2011) could be an important factor that can contribute to the superior protection of our N1-VHH formats, whose administration was intranasally. The study of Shoji and colleagues (2011) also evaluated protection by mAb 2B9 in the ferret model. The individual viral titers in nasal wash samples of H5N1 challenged ferrets treated with 2B9 4 days after infection showed a maximal difference of half to one log₁₀ of difference, compared to a PBS treated group. N1-VHH treatment did not seem to suppress lung virus titers in our model (Figure 17B and C). This finding is in line with the paradigm that NA Abs or NA-inhibitory drugs do not prevent infection and that NA-specific immunity is infection permissive.

The observation that the N1-5-VHHm, N1-5-VHHb and N1-5-VHH-Fc treatments did not have any antiviral activity against the oseltamivir-resistant H5N1 H274Y virus *in vitro* was surprising. Not even the highest dilution of any N1-5-VHH format diminished the size or number of the plaques (Table 3). In contrast, the N1-3-VHHm treatment presented an antiviral effect in H5N1 H274Y infected cells, but its PIC₅₀ was approximately 3.5-fold higher when compared to NIBRG-14 infected cells. The introduction of bivalency in the N1-3-VHH also increased the antiviral effect in H5N1 H274Y, by a decrease of 70- to 120-fold in the PIC₅₀ (Table 3). In a H5N1 H274Y challenged mice model, we found confirmation of our *in vitro* results. As previously mentioned,

N1-5-VHHb or N1-5-VHH-Fc had a potent antiviral effect and rescued NIBRG-14 ma challenged mice (Figure 20A and B, 21A and B), but failed completely to rescue H5N1 H274Y challenged mice (Figure 20C and D, 21C and D). The mortality and morbidity presented by these two N1-5-VHH format treatments during H5N1 H274Y infection was the same as PBS, the irrelevant bivalent VHH or oseltamivir groups. In contrast, single dose of N1-3-VHHb or N1-3-VHH-Fc in separate treatments, abolished completely mortality but largely failed to control morbidity (Figure 20 and 21). An unexpected result was the finding that N1-7-VHH-Fc had *in vivo* antiviral activity. Throughout this project, N1-7-VHH was chosen as an NA-binding but not inhibitory N1-VHH. Unfortunately, due to cloning difficulties, we did not obtain the bivalent format N1-7-VHHb, but the N1-7-VHH-Fc was successfully produced and purified. In our *in vitro* assays we could not observe any antiviral effect of the N1-7-VHHm or N1-7-VHH-Fc. Nevertheless, the N1-7-VHH-Fc treatment in NIBRG-14 ma or H5N1 H274Y challenged mice gave 83.3% or 66% of survival, respectively, even when a NA inhibitory potential is absent in the N1-7-VHH-Fc (Figure 21B and D). Like the N1-3-VHH-Fc treatment, the N1-7-VHH-Fc treatment was associated with severe morbidity (Figure 21A and C). These results suggest that the *in vivo* antiviral potential of the N1-VHH-Fc format is enhanced when the VHH moiety has NA-activity inhibition (like in N1-3-VHH-Fc and N1-5-VHH-Fc), but does not depend entirely on the NA inhibition potential.

ADDITIONAL DATA

N1-5-VHHb AND N1-5-VHH-Fc PROTECT AGAINST MORBIDITY IN H5N1 CHALLENGED FcγRI / FcγRIII K.O. MICE

Our previous *in vivo* results indicated that N1-3-VHH-Fc and N1-5-VHH-Fc treatments needed lower amounts to give full protection and decrease morbidity, compared to N1-3-VHHb or N1-5-VHHb (compare figure 18B and D with Figure 19B and D). These results suggest that bivalent format N1-VHH-Fc treatment protection is more potent to rescue H5N1 challenged mice than the bivalent N1-VHHb that lacks the Fc moiety. The enhanced protection by the Fc moiety in the N1-VHH-Fc can be attributed to the induction of ADCC or CDC, as well as an increased half life in the lungs, compared to N1-VHHb formats. On the other hand, the better protection given by the treatment of N1-5-VHH-Fc compared to the N1-3-VHH-Fc in H5N1 challenge mice could be partially explained by a higher proteolytic stability of the N1-5-VHHm compared to N1-3-VHHm (see figure 15D). We therefore decided to choose the N1-5-VHH-Fc over the N1-3-VHH-Fc to test the contribution of protection of the Fc moiety, comparing it with N1-5-VHHb. Groups of four 16-week-old double knockout FcγRI / FcγRIII K.O. mice were treated with 60 µg of N1-5-VHHb, or 84 µg of N1-5-VHH-Fc, N1-7-VHH-Fc or GP4-Fc 24 hours before the challenge with 4 LD₅₀ NIBRG-14 ma, and the weight loss was followed daily. The N1-5-VHH-Fc treatment completely abolished morbidity, in contrast with the N1-5-VHHb and N1-7-VHH-Fc, of which the treatment reached a peak of 17% and 25% weight loss, respectively, at 8 dpi (Figure 22). The control treated groups of GP4-Fc and PBS showed a weight loss close to 30% (Figure 22). The N1-5-VHH-Fc was able to fully protect mice against morbidity, even with the lack of the FcγRI and FcγRIII Fc receptors, suggesting the absence of a major role of these receptors in the rescue by the N1-5-VHH-Fc in H5N1 challenged mice. Possibly, the presence of the FcγRIV in these

double K.O. mice could partially rescue the Fc moiety contribution to the N1-5-VHH-Fc protection.

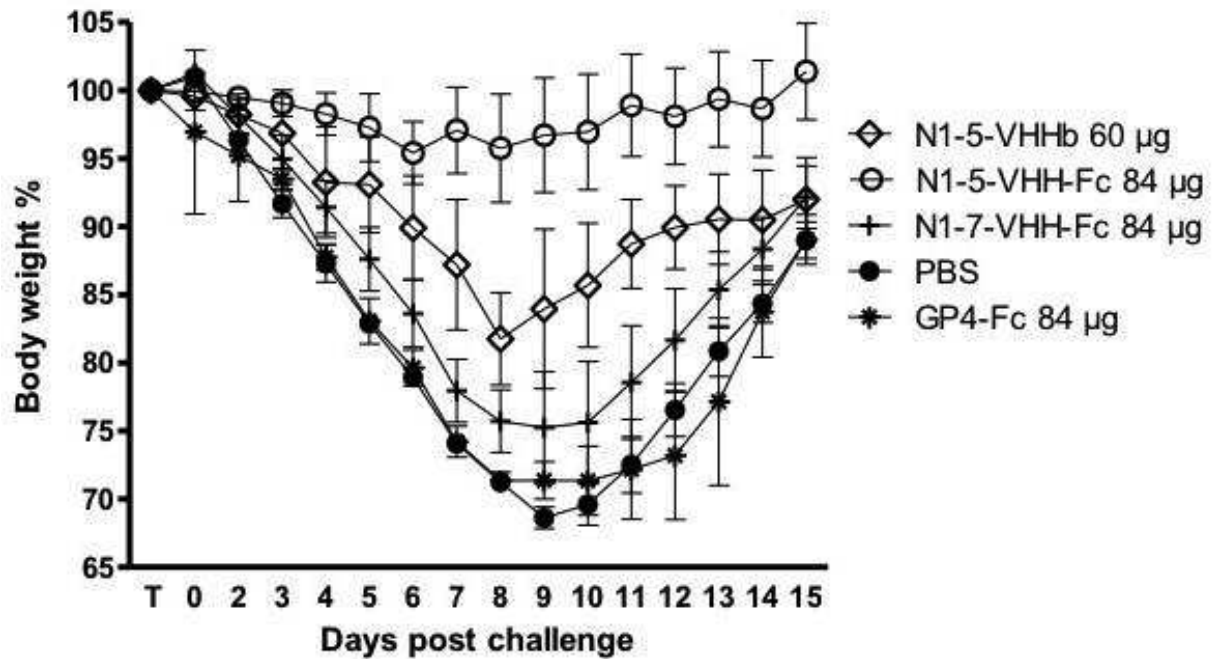


Figure 22. The treatment with N1-5-VHHb and N1-5-VHH-Fc decrease significantly the morbidity in H5N1 challenged FcγRI / FcγRIII K.O. mice. Twenty-four hours before challenge with 4 LD₅₀ of NIBRG-14 ma virus, groups of 4 FcγRI / FcγRIII K.O. mice were given: 60 µg of N1-5-VHHb or 84 µg of the N1-5-VHH-Fc, N1-7-VHH-Fc or GP4-Fc. The N1-5-VHH-Fc treated group showed no morbidity and was statistically different to: the N1-5-VHHb group at 8 dpi ($P < 0.01$) and 9 dpi ($P < 0.05$); the N1-7-VHH-Fc group at 7- 11 dpi ($P < 0.001$), 12 dpi ($P < 0.01$) and 13 dpi ($P < 0.05$). The morbidity of the N1-5-VHHb treated group was statistically different to: GP4-Fc group, at 9 dpi ($P < 0.05$), 10 dpi ($P < 0.01$) and 11–12 dpi ($P < 0.001$) and 13 dpi ($P < 0.05$); PBS group, at 9-10 dpi ($P < 0.01$), 11 dpi ($P < 0.01$) and 12 dpi ($P < 0.05$). The morbidity between the N1-5-VHHb and the N1-7-VHH-Fc groups was not statistically different

N1-5-VHHm ESCAPE MUTANTS

In order to identify the amino acid residues involved in the N1-3-VHHm or N1-5-VHHm binding to H5N1 NA, mutant escape viruses were selected and plaque purified from serial passages of NIBRG-14 virus in MDCK cells, in the presence of 10 IC₅₀ of N1-3-VHHm or N1-5-VHHm (Table

3). Unfortunately, 12 passages in the presence of N1-3-VHHm in NIBRG-14 infected MDCK cells did not yield any escape mutant virus. In contrast, after 12 passages, the NA sequences of four independently isolated N1-5-VHHm escape mutants revealed four mutations that resulted in amino acid residue substitution in the following positions (N2 numbering): one clone with a single substitution of tryptophan to arginine at 379 (W379R); one clone with a double substitution, glycine to valine at the 324 position (G324V) and threonine to tyrosine at 377 (T377Y); another clone with the substitutions G324V, W379R and threonine to alanine at 418 (T418A); and finally another double substitution, W379R and T418A, was found in the last clone. All the above substitutions, except G324V, are localized in the NA surface residues. The T377Y and W379R substitutions are close to the 330-loop, which is restrained by a disulfide bridge by C336, and has been identified as one N2 NA antigenic site contributing to the binding of the mAb NC10 and NC41 by escape mutants and crystal structure analysis (Tulip et al., 1992; Malby et al., 1994) (Figure 23). On the other hand, the T418A substitution seems to be closer to the epitope recognized by the mAb Mem5, which is closer to the NA catalytic site than the NC10 epitope (Figure 23). Nevertheless, the substitutions T377Y, W379R and T418A are not affecting the substrate-contact or framework residues of the NA catalytic site (Figure 23). From the NA surface substitutions, the W379R was the most abundant, presented in three independent clones. These results suggest that several substitutions in the surface of the NA are favored to be present in N1-5-VHHm escape mutants.

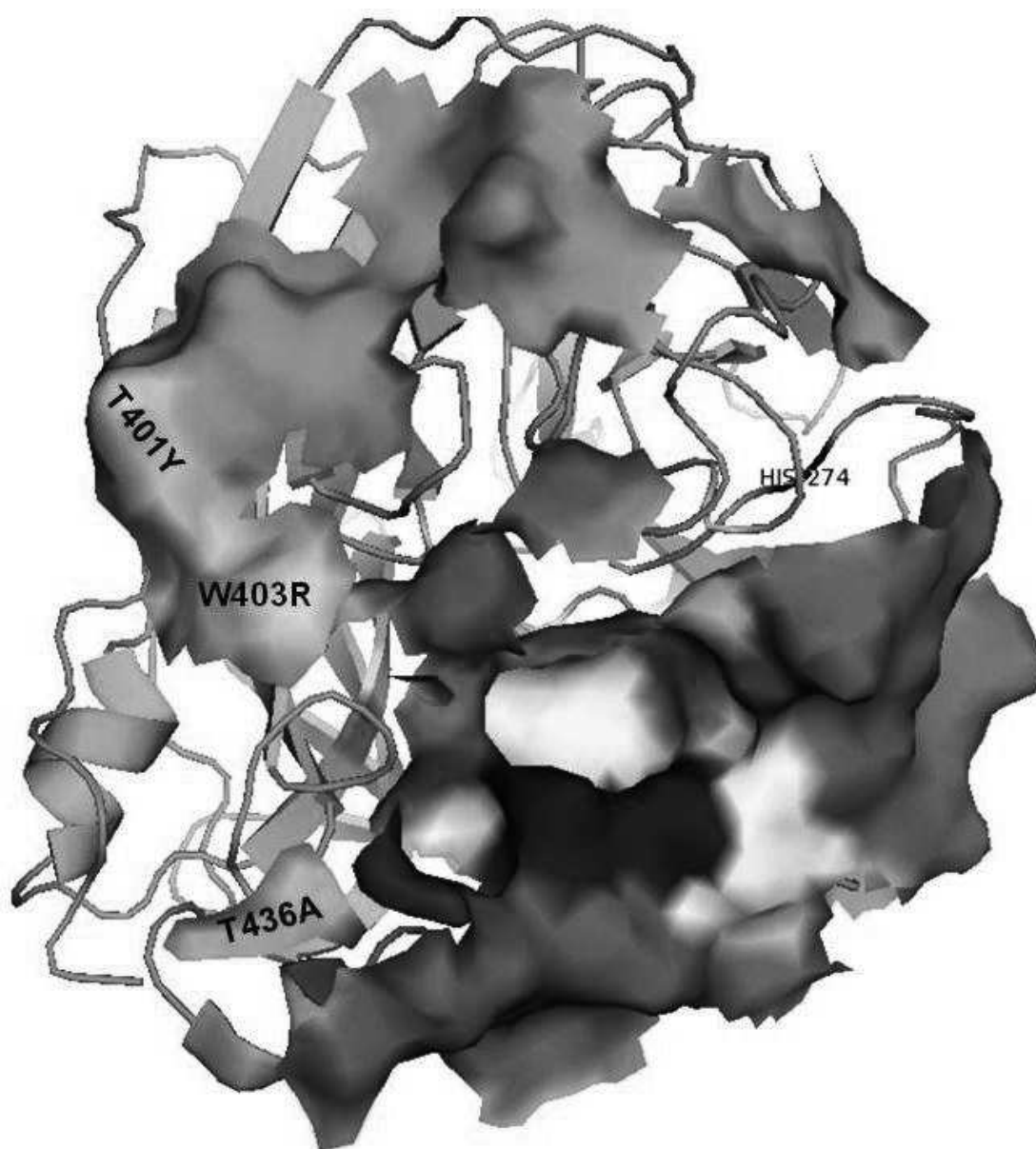


Figure 23. Epitope mapping in the A/Vietnam/1194/2004 H5N1 NA (VN04N1) by escape-mutants using N1-5-VHHm. NIBRG-14 infected TMPRSS2 MDCK cells were passed 10 – 12 times in the presence of a high concentration of N1-5-VHHm (10 IC₅₀, from table 3). Resistant mutants were screened by induction of cytopathic effect in infected cells and single plaque purified. The NA gene of the escape mutants was subsequently sequenced. The catalytic cleft is depicted in surface and color presentation: residues that make direct contact with the Sia substrate (red), catalytic site framework (yellow) and the D149 and R150 (blue) as part of the “150 loop”. In addition, the epitope loops of the mAb NC10 and Mem5 are depicted in orange and purple, respectively (the N2 numbering of the mAb epitopes had been adjusted to fit the N1 numbering). Three mutations, T401Y, W403R and T436A were identified in the surface of the NA of N1-5-VHHm escape mutants. These mutations are not in close proximity of the NA catalytic site, and are closer to the mAb NC10 epitope rather than the Mem5 epitope.

Chapter 4. GENERAL DISCUSSION AND PERSPECTIVES

DISCUSSION

The antibody-dependent cell mediated cytotoxicity (ADCC) is a cytolytic effector mechanism of antibodies in which the antigen-specific Ab initiates and directs the immune effector cell (typically natural killer cells, NKs) in the process of innate immunity by killing antigen-displaying cells. This mechanism involves the Fcγ receptors (FcγRs) and the recruitment of immune effector cells in an Fc-dependent manner, and destruction of the target cells by exocytosis of cytolytic cytokines by NKs. The complement-dependent cytotoxicity (CDC) is like ADCC, a cytolytic cascade known as “classical pathway” of the complement system, which is mediated by a series of complement proteins (C1-C9), abundantly present in the serum. It is triggered by binding of C1q to the Fc domain of immune complexes bound to the cellular surface. The mouse IgG2a-derived Fc moiety in the N1-VHH-Fc molecules is able to bind to Fc receptors and triggers Fc-dependent immune responses (like ADCC or CDC), likely contributing to the protective potential of N1-VHH-Fc treatment. We performed a pilot experiment to further explore this hypothesis, using FcγRI / FcγRIII double K.O. mice. We chose to compare the protection given by N1-VHH-Fc treatment (our most protective N1-VHH-Fc against a NIBRG-14 ma challenge) with N1-5-VHHb and N1-7-VHH-Fc treatments. In NIBRG-14 ma challenged FcγRI / FcγRIII double K.O. mice, the N1-5-VHH-Fc treatment was able to protect them completely from morbidity. This N1-5-VHH-Fc weight loss was significantly different from that of N1-5-VHHb at the 2 peak days of body weight loss, and that of N1-7-VHH-Fc at 7 – 13 days post infection, indicating a severe morbidity in this last treatment, similar to the negative control PBS or GP4-Fc groups (Figure 22). Nevertheless, the morbidity presented during the treatment of N1-7-VHH-Fc in NIBRG-14 ma challenged FcγRI / FcγRIII double K.O. or Balb/c mice is similar in both cases (compare Figure 21A with 22). Nevertheless, is necessary to mention that in our experiment the FcγRI /

FcγRIII double K.O. mice were substantially older (14 weeks instead of 7 weeks) compared with the wild-type Balb/c mice that were used in all the other *in vivo* experiments reported in this PhD. This age difference may explain why only a severe morbidity, but not mortality, was observed even in PBS-treated knockout mice that had been challenged with NIBRG-14 virus. However, their levels of morbidity revealed an interesting tendency of N1-5-VHH-Fc to confer higher degrees of protection, even in the absence of FcγRI / FcγRIII receptors. The mouse IgG2a is known as one of the most potent Ab isotypes to induce ADCC or CDC, due to a high affinity for FcγRIII and especially for FcγRI (K_A : $10^8 - 10^9 \text{ M}^{-1}$), which binds exclusively to IgG2a. Nevertheless, this IgG2a high affinity for FcγRI has a downside: normal serum levels of monomeric IgG2a can constantly bind to FcγRI, limiting the access of IgG2a immunocomplexes to FcγRI. IgG2a has an intermediate affinity for FcγRIV (K_D : $2-3 \times 10^7 \text{ M}^{-1}$), which is one order of magnitude higher than its affinity to the inhibitor receptor FcγRIIB (Nimmerjahn and Ravetch, 2006, 2008). Due to the high conservation and high expression of FcγRIV on neutrophils, monocytes, macrophages and dendritic cells, the activation of FcγR effector functions upon Ab binding is differentially regulated by the low affinity inhibitory FcγRIIB (Nimmerjahn and Ravetch, 2006). The IgG2a activation/inhibition ratio (based on individual Fc receptors' affinities for their respective Ab isotypes) of FcγRIII/FcγRIIB is 1.6, in contrast to that of FcγRIV/FcγRIIB which is 70, indicating a more potent *in vivo* effector function of the IgG2a than IgG1 or IgG3 (Nimmerjahn and Ravetch, 2006) (Figure 22). The presence of FcγRIV and the higher availability of soluble IgG2a (due the absence of FcγRI) in our double K.O. mouse model (Figure 22), could partially rescue a IgG2a activation potential of Fc-dependent effector functions in our H5N1 challenged mice model (Figure 22).

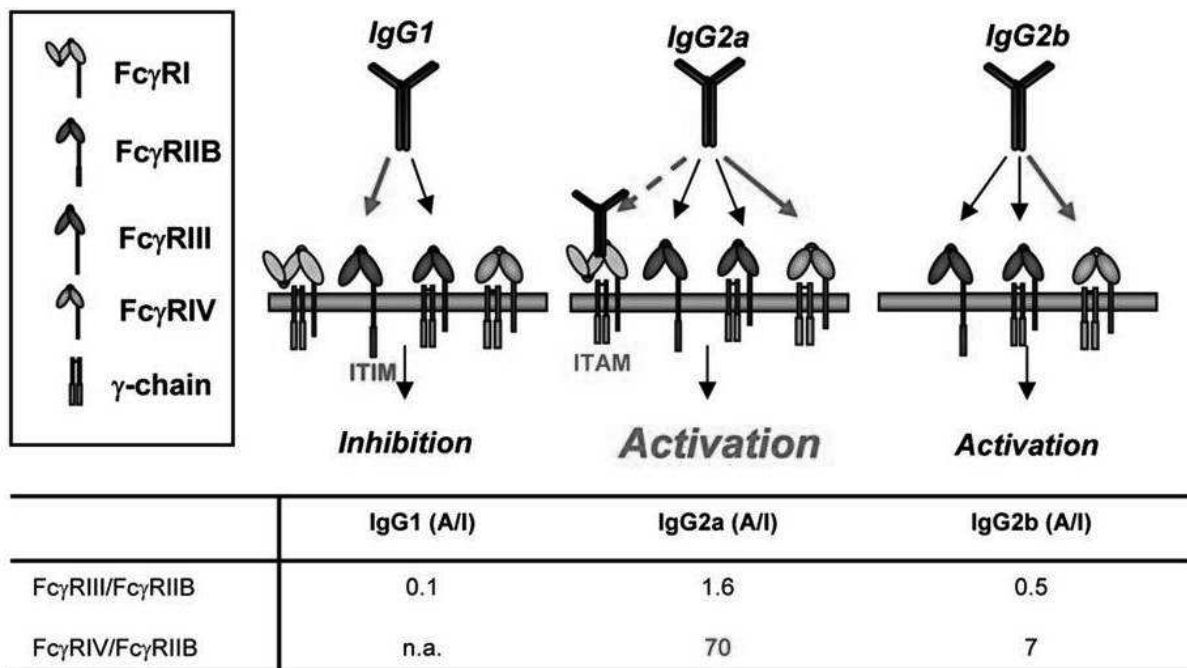


Figure 22. Individual Ab isotypes have different affinities for activating and inhibitory Fc receptors. Red arrows indicate preferential interactions of the indicated antibody isotypes with cellular Fc receptors; black arrows indicate lower affinity interactions. In the case of IgG2a, the broken red arrow indicates that the interaction might be blocked as Fc γ R1 is continuously occupied with monomeric IgG2a. The table summarizes the actual activation/inhibition ratios based on the affinities of the individual Fc receptors for the respective antibody isotypes (taken from (Nimmerjahn and Ravetch, 2006)).

To our knowledge, our N1-VHH formats are the first VHH in any format reported to target any IAV NA. Despite the fact that several IAV NA inhibitory “classical” Abs (light and heavy chain) have been reported, their reported NA inhibitory capacity and antiviral effect was variable, depending on several factors: the animal model used, route of administration or NA substrate. The NA inhibitory mAb NC41, NC10 and Mem5 were able to inhibit the cleavage of macromolecular substrates like fetuin, but NC10 failed to prevent the cleavage of the small substrate NAL (Chapter 1; table 1). The ability to inhibit NA activity using small substrates like NAL or MUNANA seems to characterize Abs that bind close enough to the NA active site (Chapter 1; figure 5B), resulting in a possible full occlusion of the NA catalytic site. Given that

the VHH CDR3 has been proved to be the major factor responsible in the contact of the VHH with its antigen (Desmyter et al., 1996; Desmyter et al., 2002), the N1-3-VHH and N1-5-VHH CDR3 sequences of 10 and 12 residues long, respectively, are possibly involved in the direct contact with their antigen. In addition, as mentioned before, all NA inhibitory N1-VHHs found in this study (N1-1-VHH, N1-3-VHH, N1-5-VHH and N1-6-VHH) presented a predicted electronegatively charged protruding paratope that corresponds to their CDR3 (Chapter 3; figure 11). Nevertheless, the presence of such protruding electronegative CDR3 does not guarantee NA inhibition. The N1-4-VHH CDR3 is similar to the inhibitory N1-VHH CDR3 (Chapter 3; figure 11), but failed to inhibit NA activity. Interestingly, our most potent N1-VHHs, N1-3-VHH and N1-5-VHH, share similarities in their CDR3. Both of them have a highly electronegative CDR3 sequence, composed of mainly hydrophobic and electronegative amino acid residues. The CDR3 motifs of N1-3-VHH (hGXXhGhGXhX) and N1-5-VHH (hXhXhhXhXh), where h is a hydrophobic residue and X is an aspartic or glutamic acid, resulted in a protruding paratope that is electronegatively charged, according to the N1-VHH 3D structure simulation (Figure 11). On the other hand, even when the N1-5-VHHm escape mutants cannot yield a complete map of the epitope, the amino acid residue substitutions observed (Chapter 1; figure 23) can give valuable information about the N1-5-VHHm epitope localization. As mentioned in chapter 1, the available crystal structures of mAb in complex with NA are all from the group 2 NA, specifically N2 and N9. These structures showed that these mAb epitopes rarely include conserved amino acid residues from the catalytic site; rather they are targeting amino acids in loops surrounding the NA catalytic site (Chapter 1; Table 1, Figure 5), which are described as major antigenic regions of the NA. The N1-5-VHHm escape mutants results (Chapter 4) showed that the amino acid substitutions T377Y and W379R are found in the NA surface, close to the 330-loop, which is part of the NC10 and NC41 epitope. Interestingly, the other surface substitution, T418A, is localized closer to the Mem5 than to the NC10 epitope, suggesting that the N1-5-VHHm epitope

is overlapping a small part of both mAb epitopes. Although the distance of the T377, W379 or T418 residues to the catalytic site is bigger than the residues conforming the Mem5 epitope, it is enough to inhibit the catalysis of the small substrate MUNANA. It seems that the N1-5-VHHm epitope is, similarly to previously reported mAb (Chapter 1; table 1), in the loops adjacent to the NA catalytic cleft.

It is likely that the epitope recognized by the non-inhibitory N1-7-VHHm is not shared with the inhibitory N1-3-VHHm or N1-5-VHHm (Chapter 3; figure 14). In line with this observation, our *in vivo* results showed that N1-7-VHH-Fc was able to rescue mice from NIBRG-14 ma and H5N1 H274Y challenges (Chapter 3; figure 20 and 21), suggesting that the H274Y mutation (within the NA catalytic site) does not affect the N1-7-VHH-Fc antiviral effect, pointing out the possibility of a non-shared epitope with N1-3-VHH-Fc or N1-5-VHH-Fc, in line with the SPR analysis.

Plant-produced Abs have been considered as a promising and powerful alternative for Abs production and our N1-VHH-Fc is the first reported plant-produced Ab against the IAV NA. The scalability, robustness and speed of production are major advantages, even when the glycosylation patterns of the plant-produced Abs (rich in high mannose residues) are different than those of the Abs produced in mammalian expression platforms (De Muyck et al., 2010). The use of plants for Ab production also presents an interesting approach for less economically-developed countries: the long-lived storage, relative ease of purification or delivery and the use of established agricultural techniques are very attractive. To our knowledge, to date there are only four VHH Abs produced in plants: three studies were performed as stably transformed lines (Jobling et al., 2003; Ismaili et al., 2007; Winichayakul et al., 2009), but their yield was reported very low. The best VHH expression and accumulation was obtained using transient expression in tobacco leaves (Teh and Kavanagh, 2010). These reports confirmed that the yield of the plant-produced Abs is variable, and depends on several factors: the fusion tag to the

recombinant protein, codon optimization and the subcellular compartment targeted. Results from our lab demonstrated that the Fc moiety improved significantly the VHH accumulation in seeds (compared to the monomeric VHH alone). We observed that in our transformed *Arabidopsis thaliana* seeds, 16% of total seed protein was N1-VHH-Fc (data not published), which represents a very good yield for a plant-produced Ab. The VHH technology is widely known and praised for the advantages of production, efficacy and versatility for tailor-made constructions (Muyldermans S, 2008). This promising technology is currently used and exploited by the biotechnological company Ablynx. Previously, the antiviral potential of the VHH has been reported *in vitro* (Hultberg et al., 2011) and *in vivo* (Ibanez et al., 2011) against IAV, and also against another important viral disease, RSV (Schepens et al., 2011). These reports highlight the potential of the VHH as antiviral tool.

Recent significant reports shed light on the complex and concerning situation of HPAIV H5N1 and pandemic H1N1 epidemiology in humans, situations that highlight the necessity for IAV antiviral alternatives. The experimental adaptation of H5N1 virus for airborne transmission in ferrets, with mutations in the HA and PB2, warns for the possibility of human-to-human transmission of zoonotic HPAIV (Herfst et al., 2012; Imai et al., 2012). Should the HPAIV H5N1 present human-to-human transmission, the NA targeting could be part of an effective strategy to mitigate disease caused by such a virus, which would likely spread globally. Finally an interesting prophylactic and therapeutic approach that deserves further validation, is the combination of VHH targeting IAV NA, HA or M2 proteins in cocktails or biparatopic bivalent constructions, that could diminish the antigenic drift in IAV, and lead to much less selective pressure against IAV VHH.

PERSPECTIVES

The *in vitro* inhibition of other HPAIV H5N1 viruses (*i.e.* A/Indonesia/05/05) and NIBRG-23 *in vivo* validation are necessary to contribute the elucidation of the inhibitory potential and epitope conservation of our inhibitory N1-VHH in H5N1 NA. In addition, *in vitro* escape virus selection of NIBRG-23 virus in the presence of N1-3-VHHm and N1-5-VHHm would be an interesting future experiment to perform that would confirm or disprove that an identical epitope in the NA is targeted by these N1-VHH.

The potency of the inhibitory N1-VHHb and N1-VHH-Fc (100 % protection, single dose) and broadness of protection (HPAIV clade 2.2, oseltamivir- resistance) should be validated in another than the murine model, *i.e.* natural host for influenza viruses. The chicken model is an attractive candidate for the validation of our N1-VHH, not only for the avian origin of the HPAIV, but also for the veterinary and economic importance of this avian model.

It would be interesting to compare the humoral and cellular adaptive immune responses following H5N1 infection of mice that had been treated with neutralizing VHH (Ibanez et al., 2011), N1-VHHb and N1-VHH-Fc. In particular the level of CD8 T cell immunity directed against the conserved internal gene products of IAV is considered important in providing a baseline level of cross-protection that may be vital during a pandemic outbreak (Schotsaert et al., 2012).

In addition, a repeat experiment with larger and younger groups of FcγRI/FcγRIII double knockout mice (*e.g.* groups of 7 mice of 7 weeks old) and including age-matched wild-type mice in parallel will be required to elucidate the real contribution of the IgG2a-Fc to the N1-VHH-Fc protection. Also, a double knockout mice model lacking FcγRIV and FcγRIII could be more useful to dissect the exact contribution of the Fc moiety in N1-VHH-Fc protection of H5N1 challenged mice.

Chapter 5. SUMMARY

The N1-3-VHHm and N1-5-VHHm showed antiviral activity *in vitro*, which was enhanced by bivalency. We observed that the inhibitory potential of N1-3-VHHm and N1-5-VHHm was similar to the commercial drug oseltamivir, and resulted in an antiviral effect in cell-based assays (Chapter 3; table 3). The high affinity of both N1-3-VHHm and N1-5-VHHm (Chapter 3; table 2) likely contributes to their inhibitory potential. In addition, the introduction of avidity in both bivalent formats (bacteria and plant-produced) contributed to an increase in their N1rec inhibitory and antiviral potential, compared with their monovalent formats *in vitro*, surpassing the oseltamivir inhibitory potential. H5N1 cross-clade inhibition was also found, but only the N1-3-VHH was able to show antiviral activity against H5N1 H274Y. In addition to their high antiviral potential against a clade 1 H5N1 virus, a cross-clade antiviral effect was also observed in the three inhibitory N1-VHH formats. The *in vitro* inhibition of the clade 2 NIBRG-23 and the oseltamivir-resistant mutant H5N1 H274Y, illustrates a cross-clade antiviral potential of our N1-VHH (Chapter 3; table 3). These results suggest that the H274 residue is necessary for the binding of N1-5-VHH to the NA. Furthermore, the SPR epitope mapping assay showed that N1-3-VHH and N1-5-VHH recognized an overlapping epitope, but it is probable that their amino acid residues involved in the binding to the NA epitope are not shared between both inhibitory N1-VHHs.

Rescue of H5N1 challenged mice by N1-VHH-Fc was enhanced by the inhibitory capacity of N1-VHH, but it is likely that the Fc moiety contributes to the protection (rescue by N1-7-VHH-Fc). In line with our *in vitro* results, the bivalent formats of N1-3-VHH were able to protect mice against a challenge with H5N1 H274Y. It is possible that morbidity in the H5N1 challenged mice can be prevented by a boost of the N1-VHH treatment in future experiments. The treatment with

bacteria-produced inhibitory N1-VHHb rescues against H5N1 challenge, but depends on their inhibitory potential. It is interesting to point out that the *in vitro* antiviral potential against the HPAIV of the bacteria-produced mono- and bivalent formats, corresponded to the degree of protection in HPAIV challenged mice. This is supported by the observation that N1-3-VHHm, N1-3-VHHb, N1-5-VHHm and N1-5-VHHb showed antiviral activity *in vivo*, which was absent in N1-7-VHH. In line with the *in vitro* results, N1-3-VHHb and N1-5-VHHb were more potent than the monovalent counterparts *in vivo*.

As previously reported with VHH targeting HA HPAIV, selective pressure can give rise to escape mutants (Ibanez et al., 2010). The HA mutations present in the escape mutants affected the receptor binding site of the HA, possibly impairing the binding to the SA moiety into the cellular receptor. As previously described, the H274Y mutation in NA was sufficient to impede the antiviral effect of the N1-5-VHH. This mutation occurs in an amino acid that contributes to the amino acid framework of the catalytic site of the NA, which is conserved among the NA groups 1 and 2. If N1-3-VHH or N15-VHH inhibits the NA activity by occluding the NA catalytic cleft, avoiding the substrate docking, it is possible that their binding contacts occur in the amino acid framework of the surface exposed NA active site. So then, mutations into or close to the framework or substrate-contact amino acids (exposed at the surface of the NA catalytic cleft) are likely to impair the binding of N1-3-VHH or N15-VHH to the NA.

Nowadays, the antiviral strategies for HPAIV human infections rely heavily on antiviral drugs, mainly NA inhibitors. There is an increasing concern about the tendency of high dose-administration of oseltamivir to patients. The most evident is the emergence of drug resistant mutants, *i.e.* wide use of oseltamivir had been correlated with resistant mutants in several countries (de Jong et al., 2005; Lackenby et al., 2008). A possible alternative to the treatment of HPAIV infections could be the administration of cocktails of monoclonal Abs mixed with antiviral drugs. Both treatments can contribute synergistically to the protection, the Ab inducing

an immune response in the host, and the drugs hampering the spreading of the virus by the NA inhibition. Our N1-VHHs are excellent candidates for a proof of concept synergistic effect. The protective effect of the HA-binding VHH demonstrated by Ibanez and colleagues (2011), and the NA-binding reported in this study, raise the interesting concept of the design of heterobivalent VHHs against HPAIV. By fusing two different VHHs targeting different IAV proteins, *e.g.* HA and NA, the binding and release of the virion could be inhibited simultaneously, also decreasing the probability of the occurrence of escape mutants. In addition, broad protection (cross-clade or even cross-subtype) by the VHHs, give them extra attractive and cost effective interests.

Chapter 6. REFERENCES

- (1998). Randomised trial of efficacy and safety of inhaled zanamivir in treatment of influenza A and B virus infections. The MIST (Management of Influenza in the Southern Hemisphere Trialists) Study Group. *Lancet* **352**, 1877-1881.
- Air, G.M., and Laver, W.G.** (1989). The neuraminidase of influenza virus. *Proteins* **6**, 341-356.
- Air, G.M., Laver, W.G., Luo, M., Stray, S.J., Legrone, G., and Webster, R.G.** (1990). Antigenic, Sequence, and Crystal Variation in Influenza-B Neuraminidase. *Virology* **177**, 578-587.
- Amaro, R.E., Swift, R.V., Votapka, L., Li, W.W., Walker, R.C., and Bush, R.M.** (2011). Mechanism of 150-cavity formation in influenza neuraminidase. *Nat Commun* **2**, 388.
- Arbabi Ghahroudi, M., Desmyter, A., Wyns, L., Hamers, R., and Muyldermans, S.** (1997). Selection and identification of single domain antibody fragments from camel heavy-chain antibodies. *FEBS Lett* **414**, 521-526.
- Barman, S., Adhikary, L., Chakrabarti, A.K., Bernas, C., Kawaoka, Y., and Nayak, D.P.** (2004). Role of transmembrane domain and cytoplasmic tail amino acid sequences of influenza a virus neuraminidase in raft association and virus budding. *J Virol* **78**, 5258-5269.
- Barre, S., Greenberg, A.S., Flajnik, M.F., and Chothia, C.** (1994). Structural conservation of hypervariable regions in immunoglobulins evolution. In *Nat Struct Biol*, pp. 915-920.
- Baskin, C.R., Bielefeldt-Ohmann, H., Tumpey, T.M., Sabourin, P.J., Long, J.P., Garcia-Sastre, A., Tolnay, A.E., Albrecht, R., Pyles, J.A., Olson, P.H., Aicher, L.D., Rosenzweig, E.R., Murali-Krishna, K., Clark, E.A., Kotur, M.S., Fornek, J.L., Proll, S., Palermo, R.E., Sabourin, C.L., and Katze, M.G.** (2009). Early and sustained innate immune response defines pathology and death in nonhuman primates infected by highly pathogenic influenza virus. *Proc Natl Acad Sci U S A* **106**, 3455-3460.
- Baudin, F., Bach, C., Cusack, S., and Ruigrok, R.W.** (1994). Structure of influenza virus RNP. I. Influenza virus nucleoprotein melts secondary structure in panhandle RNA and exposes the bases to the solvent. *Embo J* **13**, 3158-3165.
- Baum, L.G., and Paulson, J.C.** (1991). The N2 neuraminidase of human influenza virus has acquired a substrate specificity complementary to the hemagglutinin receptor specificity. *Virology* **180**, 10-15.
- Benmansour, A., Leblois, H., Coulon, P., Tuffereau, C., Gaudin, Y., Flamand, A., and Lafay, F.** (1991). Antigenicity of rabies virus glycoprotein. In *J Virol*, pp. 4198-4203.
- Bloom, J.D., Gong, L.I., and Baltimore, D.** (2010). Permissive secondary mutations enable the evolution of influenza oseltamivir resistance. *Science* **328**, 1272-1275.
- Bottcher, E., Freuer, C., Steinmetzer, T., Klenk, H.D., and Garten, W.** (2009). MDCK cells that express proteases TMPRSS2 and HAT provide a cell system to propagate influenza viruses in the absence of trypsin and to study cleavage of HA and its inhibition. *Vaccine* **27**, 6324-6329.
- Bouvier, N.M., and Palese, P.** (2008). The biology of influenza viruses. *Vaccine* **26 Suppl 4**, D49-53.
- Boyce, T.G., Mellen, B.G., Mitchel, E.F., Wright, P.F., and Griffin, M.R.** (2000). Rates of hospitalization for respiratory syncytial virus infection among children in medicaid. In *J Pediatr*, pp. 865-870.
- Bright, R.A., Neuzil, K.M., Pervikov, Y., and Palkonyay, L.** (2009). WHO meeting on the role of neuraminidase in inducing protective immunity against influenza infection, Vilamoura, Portugal, September 14, 2008. *Vaccine* **27**, 6366-6369.
- Brugh, M., Beard, C.W., and Stone, H.D.** (1979). Immunization of chickens and turkeys against avian influenza with monovalent and polyvalent oil emulsion vaccines. *Am J Vet Res* **40**, 165-169.

- Bucher, D.J., and Kilbourne, E.D.** (1972). A 2 (N2) neuraminidase of the X-7 influenza virus recombinant: determination of molecular size and subunit composition of the active unit. *J Virol* **10**, 60-66.
- Burmeister, W.P., Ruigrok, R.W., and Cusack, S.** (1992). The 2.2 Å resolution crystal structure of influenza B neuraminidase and its complex with sialic acid. *Embo J* **11**, 49-56.
- Carr, J., Ives, J., Kelly, L., Lambkin, R., Oxford, J., Mendel, D., Tai, L., and Roberts, N.** (2002). Influenza virus carrying neuraminidase with reduced sensitivity to oseltamivir carboxylate has altered properties in vitro and is compromised for infectivity and replicative ability in vivo. *Antiviral Res* **54**, 79-88.
- Carrat, F., and Flahault, A.** (2007). Influenza vaccine: the challenge of antigenic drift. *Vaccine* **25**, 6852-6862.
- Carrat, F., Vergu, E., Ferguson, N.M., Lemaître, M., Cauchemez, S., Leach, S., and Valleron, A.J.** (2008). Time lines of infection and disease in human influenza: a review of volunteer challenge studies. *Am J Epidemiol* **167**, 775-785.
- Cate, T.R., Rayford, Y., Nino, D., Winokur, P., Brady, R., Belshe, R., Chen, W., Atmar, R.L., and Couch, R.B.** (2010). A high dosage influenza vaccine induced significantly more neuraminidase antibody than standard vaccine among elderly subjects. *Vaccine* **28**, 2076-2079.
- Chotpitayasunondh, T., Ungchusak, K., Hanshaoworakul, W., Chunsuthiwat, S., Sawanpanyalert, P., Kijphati, R., Lochindarat, S., Srisan, P., Suwan, P., Osotthanakorn, Y., Anantasetagoon, T., Kanjanawasri, S., Tanupattarachai, S., Weerakul, J., Chaiwirattana, R., Maneerattanaporn, M., Poolsavathitikool, R., Chokephaibulkit, K., Apisarnthanarak, A., and Dowell, S.F.** (2005). Human disease from influenza A (H5N1), Thailand, 2004. *Emerg Infect Dis* **11**, 201-209.
- Ciampor, F., Thompson, C.A., Grambas, S., and Hay, A.J.** (1992). Regulation of pH by the M2 protein of influenza A viruses. *Virus Res* **22**, 247-258.
- Cibulski, S.P., Sinigaglia, M., Rigo, M.M., Antunes, D.A., Vieira, G.F., Fulber, C.C., Chies, J.A.B., Franco, A.C., and Roehe, P.M.** (2009). Structure modelling of Rabies Virus Glycoprotein. In 5th International Conference of the Brazilian Association for Bioinformatics and Computational Biology. (Rio de Janeiro).
- Claas, E.C., Osterhaus, A.D., van Beek, R., De Jong, J.C., Rimmelzwaan, G.F., Senne, D.A., Krauss, S., Shortridge, K.F., and Webster, R.G.** (1998). Human influenza A H5N1 virus related to a highly pathogenic avian influenza virus. *Lancet* **351**, 472-477.
- Clough, S.J., and Bent, A.F.** (1998). Floral dip: a simplified method for *Agrobacterium*-mediated transformation of *Arabidopsis thaliana*. *The Plant journal : for cell and molecular biology* **16**, 735-743.
- Collins, P.J., Haire, L.F., Lin, Y.P., Liu, J., Russell, R.J., Walker, P.A., Skehel, J.J., Martin, S.R., Hay, A.J., and Gamblin, S.J.** (2008). Crystal structures of oseltamivir-resistant influenza virus neuraminidase mutants. *Nature* **453**, 1258-1261.
- Collins, P.J., Haire, L.F., Lin, Y.P., Liu, J., Russell, R.J., Walker, P.A., Martin, S.R., Daniels, R.S., Gregory, V., Skehel, J.J., Gamblin, S.J., and Hay, A.J.** (2009). Structural basis for oseltamivir resistance of influenza viruses. *Vaccine* **27**, 6317-6323.
- Colman, P.M., Varghese, J.N., and Laver, W.G.** (1983). Structure of the catalytic and antigenic sites in influenza virus neuraminidase. *Nature* **303**, 41-44.
- Colman, P.M., Varghese, J.N., and Laver, W.G.** (1984). The Structure of Neuraminidase. *Acta Crystallogr A* **40**, C23-C23.
- Colman, P.M., Laver, W.G., Varghese, J.N., Baker, A.T., Tulloch, P.A., Air, G.M., and Webster, R.G.** (1987). Three-dimensional structure of a complex of antibody with influenza virus neuraminidase. *Nature* **326**, 358-363.

- Colman, P.M., Tulip, W.R., Varghese, J.N., Tulloch, P.A., Baker, A.T., Laver, W.G., Air, G.M., and Webster, R.G.** (1989). Three-dimensional structures of influenza virus neuraminidase-antibody complexes. *Philos Trans R Soc Lond B Biol Sci* **323**, 511-518.
- Compans, R.W., Content, J., and Duesberg, P.H.** (1972). Structure of the ribonucleoprotein of influenza virus. *J Virol* **10**, 795-800.
- Coppieters, K., Dreier, T., Silence, K., de Haard, H., Lauwereys, M., Casteels, P., Beirnaert, E., Jonckheere, H., Van de Wiele, C., Staelens, L., Hostens, J., Revets, H., Remaut, E., Elewaut, D., and Rottiers, P.** (2006). Formatted anti-tumor necrosis factor alpha VHH proteins derived from camelids show superior potency and targeting to inflamed joints in a murine model of collagen-induced arthritis. *Arthritis Rheum* **54**, 1856-1866.
- Corfield, A.P., Sander-Wewer, M., Veh, R.W., Wember, M., and Schauer, R.** (1986). The action of sialidases on substrates containing O-acetylsialic acids. *Biol Chem Hoppe Seyler* **367**, 433-439.
- Corti, D., Voss, J., Gamblin, S.J., Codoni, G., Macagno, A., Jarrossay, D., Vachieri, S.G., Pinna, D., Minola, A., Vanzetta, F., Silacci, C., Fernandez-Rodriguez, B.M., Agatic, G., Bianchi, S., Giacchetto-Sasselli, I., Calder, L., Sallusto, F., Collins, P., Haire, L.F., Temperton, N., Langedijk, J.P., Skehel, J.J., and Lanzavecchia, A.** (2011). A neutralizing antibody selected from plasma cells that binds to group 1 and group 2 influenza A hemagglutinins. *Science* **333**, 850-856.
- Crowe, J.E., Firestone, C.Y., Crim, R., Beeler, J.A., Coelingh, K.L., Barbas, C.F., Burton, D.R., Chanock, R.M., and Murphy, B.R.** (1998). Monoclonal antibody-resistant mutants selected with a respiratory syncytial virus-neutralizing human antibody fab fragment (Fab 19) define a unique epitope on the fusion (F) glycoprotein. *Virology* **252**, 373-375.
- da Silva, D.V., Nordholm, J., Madjo, U., Pfeiffer, A., and Daniels, R.** (2013). Assembly of subtype 1 influenza neuraminidase is driven by both the transmembrane and head domains. *J Biol Chem* **288**, 644-653.
- Dawood, F.S., Iuliano, A.D., Reed, C., Meltzer, M.I., Shay, D.K., Cheng, P.Y., Bandaranayake, D., Breiman, R.F., Brooks, W.A., Buchy, P., Feikin, D.R., Fowler, K.B., Gordon, A., Hien, N.T., Horby, P., Huang, Q.S., Katz, M.A., Krishnan, A., Lal, R., Montgomery, J.M., Molbak, K., Pebody, R., Presanis, A.M., Razuri, H., Steens, A., Tinoco, Y.O., Wallinga, J., Yu, H., Vong, S., Bresee, J., and Widdowson, M.A.** (2012). Estimated global mortality associated with the first 12 months of 2009 pandemic influenza A H1N1 virus circulation: a modelling study. *The Lancet infectious diseases* **12**, 687-695.
- De Filette, M., Martens, W., Roose, K., Deroo, T., Vervalle, F., Bentahir, M., Vandekerckhove, J., Fiers, W., and Saelens, X.** (2008). An influenza A vaccine based on tetrameric ectodomain of matrix protein 2. *J Biol Chem* **283**, 11382-11387.
- De Genst, E., Silence, K., Decanniere, K., Conrath, K., Loris, R., Kinne, J., Muyldermans, S., and Wyns, L.** (2006). Molecular basis for the preferential cleft recognition by dromedary heavy-chain antibodies. In *Proc Natl Acad Sci*, pp. 4586-4591.
- De Jaeger, G., Scheffer, S., Jacobs, A., Zambre, M., Zobell, O., Goossens, A., Depicker, A., and Angenon, G.** (2002). Boosting heterologous protein production in transgenic dicotyledonous seeds using *Phaseolus vulgaris* regulatory sequences. *Nature biotechnology* **20**, 1265-1268.
- de Jong, J.C., Claas, E.C., Osterhaus, A.D., Webster, R.G., and Lim, W.L.** (1997). A pandemic warning? *Nature* **389**, 554.
- de Jong, M.D., Bach, V.C., Phan, T.Q., Vo, M.H., Tran, T.T., Nguyen, B.H., Beld, M., Le, T.P., Truong, H.K., Nguyen, V.V., Tran, T.H., Do, Q.H., and Farrar, J.** (2005). Fatal avian influenza A (H5N1) in a child presenting with diarrhea followed by coma. *N Engl J Med* **352**, 686-691.
- de Jong, M.D., Simmons, C.P., Thanh, T.T., Hien, V.M., Smith, G.J., Chau, T.N., Hoang, D.M., Chau, N.V., Khanh, T.H., Dong, V.C., Qui, P.T., Cam, B.V., Ha do, Q., Guan, Y., Peiris, J.S., Chinh, N.T., Hien,**

- T.T., and Farrar, J.** (2006). Fatal outcome of human influenza A (H5N1) is associated with high viral load and hypercytokinemia. In *Nat Med*, pp. 1203-1207.
- De Muynck, B., Navarre, C., and Boutry, M.** (2010). Production of antibodies in plants: status after twenty years. *Plant Biotechnol J* **8**, 529-563.
- Decanniere, K., Muyldermans, S., and Wyns, L.** (2000). Canonical antigen-binding loop structures in immunoglobulins: more structures, more canonical classes? In *J Mol Biol*, pp. 83-91.
- Decanniere, K., Desmyter, A., Lauwereys, M., Ghahroudi, M.A., Muyldermans, S., and Wyns, L.** (1999). A single-domain antibody fragment in complex with RNase A: non-canonical loop structures and nanomolar affinity using two CDR loops. In *Structure*, pp. 361-370.
- Desmyter, A., Spinelli, S., Payan, F., Lauwereys, M., Wyns, L., Muyldermans, S., and Cambillau, C.** (2002). Three camelid VHH domains in complex with porcine pancreatic alpha-amylase. Inhibition and versatility of binding topology. In *J Biol Chem*, pp. 23645-23650.
- Desmyter, A., Transue, T.R., Ghahroudi, M.A., Thi, M.H., Poortmans, F., Hamers, R., Muyldermans, S., and Wyns, L.** (1996). Crystal structure of a camel single-domain VH antibody fragment in complex with lysozyme. In *Nat Struct Biol*, pp. 803-811.
- Dias, A., Bouvier, D., Crepin, T., McCarthy, A.A., Hart, D.J., Baudin, F., Cusack, S., and Ruigrok, R.W.** (2009). The cap-snatching endonuclease of influenza virus polymerase resides in the PA subunit. *Nature* **458**, 914-918.
- Dooley, H., Flajnik, M.F., and Porter, A.J.** (2003). Selection and characterization of naturally occurring single-domain (IgNAR) antibody fragments from immunized sharks by phage display. *Mol Immunol* **40**, 25-33.
- Drake, J.W.** (1993). Rates of Spontaneous Mutation among Rna Viruses. *P Natl Acad Sci USA* **90**, 4171-4175.
- Els Conrath, K., Lauwereys, M., Wyns, L., and Muyldermans, S.** (2001). Camel single-domain antibodies as modular building units in bispecific and bivalent antibody constructs. *J Biol Chem* **276**, 7346-7350.
- Elton, D., Simpson-Holley, M., Archer, K., Medcalf, L., Hallam, R., McCauley, J., and Digard, P.** (2001). Interaction of the influenza virus nucleoprotein with the cellular CRM1-mediated nuclear export pathway. *J Virol* **75**, 408-419.
- Falsey, A.R., Hennessey, P.A., Formica, M.A., Cox, C., and Walsh, E.E.** (2005). Respiratory syncytial virus infection in elderly and high-risk adults. In *N Engl J Med*, pp. 1749-1759.
- Fang, R., Min Jou, W., Huylebroeck, D., Devos, R., and Fiers, W.** (1981). Complete structure of A/duck/Ukraine/63 influenza hemagglutinin gene: animal virus as progenitor of human H3 Hong Kong 1968 influenza hemagglutinin. *Cell* **25**, 315-323.
- Ferguson, N.M., Galvani, A.P., and Bush, R.M.** (2003). Ecological and immunological determinants of influenza evolution. *Nature* **422**, 428-433.
- Fouchier, R.A., Munster, V., Wallensten, A., Bestebroer, T.M., Herfst, S., Smith, D., Rimmelzwaan, G.F., Olsen, B., and Osterhaus, A.D.** (2005). Characterization of a novel influenza A virus hemagglutinin subtype (H16) obtained from black-headed gulls. *J Virol* **79**, 2814-2822.
- Fraser, C., Donnelly, C.A., Cauchemez, S., Hanage, W.P., Van Kerkhove, M.D., Hollingsworth, T.D., Griffin, J., Baggaley, R.F., Jenkins, H.E., Lyons, E.J., Jombart, T., Hinsley, W.R., Grassly, N.C., Balloux, F., Ghani, A.C., Ferguson, N.M., Rambaut, A., Pybus, O.G., Lopez-Gatell, H., Alpujch-Aranda, C.M., Chapela, I.B., Zavala, E.P., Guevara, D.M., Checchi, F., Garcia, E., Hugonnet, S., Roth, C., and Collaboration, W.H.O.R.P.A.** (2009). Pandemic potential of a strain of influenza A (H1N1): early findings. *Science* **324**, 1557-1561.
- Fujii, Y., Goto, H., Watanabe, T., Yoshida, T., and Kawaoka, Y.** (2003). Selective incorporation of influenza virus RNA segments into virions. *P Natl Acad Sci USA* **100**, 2002-2007.

- Gamblin, S.J., Haire, L.F., Russell, R.J., Stevens, D.J., Xiao, B., Ha, Y., Vasisht, N., Steinhauer, D.A., Daniels, R.S., Elliot, A., Wiley, D.C., and Skehel, J.J.** (2004). The structure and receptor binding properties of the 1918 influenza hemagglutinin. *Science* **303**, 1838-1842.
- Garten, R.J., Davis, C.T., Russell, C.A., Shu, B., Lindstrom, S., Balish, A., Sessions, W.M., Xu, X., Skepner, E., Deyde, V., Okomo-Adhiambo, M., Gubareva, L., Barnes, J., Smith, C.B., Emery, S.L., Hillman, M.J., Rivaviller, P., Smagala, J., de Graaf, M., Burke, D.F., Fouchier, R.A., Pappas, C., Alpuche-Aranda, C.M., Lopez-Gatell, H., Olivera, H., Lopez, I., Myers, C.A., Faix, D., Blair, P.J., Yu, C., Keene, K.M., Dotson, P.D., Jr., Boxrud, D., Sambol, A.R., Abid, S.H., St George, K., Bannerman, T., Moore, A.L., Stringer, D.J., Blevins, P., Demmler-Harrison, G.J., Ginsberg, M., Kriner, P., Waterman, S., Smole, S., Guevara, H.F., Belongia, E.A., Clark, P.A., Beatrice, S.T., Donis, R., Katz, J., Finelli, L., Bridges, C.B., Shaw, M., Jernigan, D.B., Uyeki, T.M., Smith, D.J., Klimov, A.I., and Cox, N.J.** (2009). Antigenic and genetic characteristics of swine-origin 2009 A(H1N1) influenza viruses circulating in humans. *Science* **325**, 197-201.
- Glaser, L., Stevens, J., Zamarin, D., Wilson, I.A., Garcia-Sastre, A., Tumpey, T.M., Basler, C.F., Taubenberger, J.K., and Palese, P.** (2005). A single amino acid substitution in 1918 influenza virus hemagglutinin changes receptor binding specificity. *J Virol* **79**, 11533-11536.
- Glezen, W.P., Paredes, A., Allison, J.E., Taber, L.H., and Frank, A.L.** (1981). Risk of respiratory syncytial virus infection for infants from low-income families in relationship to age, sex, ethnic group, and maternal antibody level. In *J Pediatr*.
- Gooskens, J., Jonges, M., Claas, E.C., Meijer, A., and Kroes, A.C.** (2009). Prolonged influenza virus infection during lymphocytopenia and frequent detection of drug-resistant viruses. *J Infect Dis* **199**, 1435-1441.
- Goto, H., and Kawaoka, Y.** (1998). A novel mechanism for the acquisition of virulence by a human influenza A virus. *Proc Natl Acad Sci U S A* **95**, 10224-10228.
- Gottschalk, A.** (1956). Neuraminic acid; the functional group of some biologically active mucoproteins. *Yale J Biol Med* **28**, 525-537.
- Govorkova, E.A., Leneva, I.A., Goloubeva, O.G., Bush, K., and Webster, R.G.** (2001). Comparison of efficacies of RWJ-270201, zanamivir, and oseltamivir against H5N1, H9N2, and other avian influenza viruses. *Antimicrob Agents Chemother* **45**, 2723-2732.
- Greenberg, A.S., Avila, D., Hughes, M., Hughes, A., McKinney, E.C., and Flajnik, M.F.** (1995). A new antigen receptor gene family that undergoes rearrangement and extensive somatic diversification in sharks. *Nature* **374**, 168-173.
- Groothuis, J.R., and Simoes, E.A.** (1993). Immunoprophylaxis and immunotherapy: role in the prevention and treatment of respiratory syncytial virus. In *Int J Antimicrob Agents*, pp. 97-103.
- Gu, J., Xie, Z., Gao, Z., Liu, J., Korteweg, C., Ye, J., Lau, L.T., Lu, J., Zhang, B., McNutt, M.A., Lu, M., Anderson, V.M., Gong, E., Yu, A.C., and Lipkin, W.I.** (2007). H5N1 infection of the respiratory tract and beyond: a molecular pathology study. *Lancet* **370**, 1137-1145.
- Gubareva, L.V., Kaiser, L., and Hayden, F.G.** (2000). Influenza virus neuraminidase inhibitors. *Lancet* **355**, 827-835.
- Gubareva, L.V., Kaiser, L., Matrosovich, M.N., Soo-Hoo, Y., and Hayden, F.G.** (2001). Selection of influenza virus mutants in experimentally infected volunteers treated with oseltamivir. *J Infect Dis* **183**, 523-531.
- Gubareva, L.V., Nedyalkova, M.S., Novikov, D.V., Murti, K.G., Hoffmann, E., and Hayden, F.G.** (2002). A release-competent influenza A virus mutant lacking the coding capacity for the neuraminidase active site. *The Journal of general virology* **83**, 2683-2692.
- Gulati, U., Wu, W., Gulati, S., Kumari, K., Waner, J.L., and Air, G.M.** (2005). Mismatched hemagglutinin and neuraminidase specificities in recent human H3N2 influenza viruses. *Virology* **339**, 12-20.

- Gulati, U., Hwang, C.C., Venkatramani, L., Gulati, S., Stray, S.J., Lee, J.T., Laver, W.G., Bochkarev, A., Zlotnick, A., and Air, G.M.** (2002). Antibody epitopes on the neuraminidase of a recent H3N2 influenza virus (A/Memphis/31/98). *J Virol* **76**, 12274-12280.
- Hamers-Casterman, C., Atarhouch, T., Muyldermans, S., Robinson, G., Hamers, C., Songa, E.B., Bendahman, N., and Hamers, R.** (1993). Naturally occurring antibodies devoid of light chains. *Nature* **363**, 446-448.
- Haque, M.E., Koppaka, V., Axelsen, P.H., and Lentz, B.R.** (2005). Properties and structures of the influenza and HIV fusion peptides on lipid membranes: Implications for a role in fusion. *Biophys J* **89**, 3183-3194.
- Harbury, P.B., Zhang, T., Kim, P.S., and Alber, T.** (1993). A switch between two-, three-, and four-stranded coiled coils in GCN4 leucine zipper mutants. *Science* **262**, 1401-1407.
- Hayden, F.G., Osterhaus, A.D., Treanor, J.J., Fleming, D.M., Aoki, F.Y., Nicholson, K.G., Bohnen, A.M., Hirst, H.M., Keene, O., and Wightman, K.** (1997). Efficacy and safety of the neuraminidase inhibitor zanamivir in the treatment of influenza virus infections. GG167 Influenza Study Group. *N Engl J Med* **337**, 874-880.
- Hayden, F.G., Atmar, R.L., Schilling, M., Johnson, C., Poretz, D., Paar, D., Huson, L., Ward, P., Mills, R.G., and Grp, O.S.** (1999). Use of the selective oral neuraminidase inhibitor oseltamivir to prevent influenza. *New Engl J Med* **341**, 1336-1343.
- Hensley, S.E., Das, S.R., Bailey, A.L., Schmidt, L.M., Hickman, H.D., Jayaraman, A., Viswanathan, K., Raman, R., Sasisekharan, R., Bennink, J.R., and Yewdell, J.W.** (2009). Hemagglutinin receptor binding avidity drives influenza A virus antigenic drift. *Science* **326**, 734-736.
- Herfst, S., Schrauwen, E.J., Linster, M., Chutinimitkul, S., de Wit, E., Munster, V.J., Sorrell, E.M., Bestebroer, T.M., Burke, D.F., Smith, D.J., Rimmelzwaan, G.F., Osterhaus, A.D., and Fouchier, R.A.** (2012). Airborne transmission of influenza A/H5N1 virus between ferrets. *Science* **336**, 1534-1541.
- Hirst, G.K.** (1941). The Agglutination of Red Cells by Allantoic Fluid of Chick Embryos Infected with Influenza Virus. *Science* **94**, 22-23.
- Hmila, I., Saerens, D., Ben Abderrazek, R., Vincke, C., Abidi, N., Benlasfar, Z., Govaert, J., El Ayeb, M., Bouhaouala-Zahar, B., and Muyldermans, S.** (2010). A bispecific nanobody to provide full protection against lethal scorpion envenoming. *Faseb J* **24**, 3479-3489.
- Hoffmann, E., Neumann, G., Kawaoka, Y., Hobom, G., and Webster, R.G.** (2000). A DNA transfection system for generation of influenza A virus from eight plasmids. *Proc Natl Acad Sci U S A* **97**, 6108-6113.
- Hogue, B.G., and Nayak, D.P.** (1994). Deletion Mutation in the Signal Anchor Domain Activates Cleavage of the Influenza-Virus Neuraminidase, a Type-II Transmembrane Protein. *Journal of General Virology* **75**, 1015-1022.
- Horimoto, T., and Kawaoka, Y.** (2001). Pandemic threat posed by avian influenza A viruses. *Clin Microbiol Rev* **14**, 129-149.
- Horimoto, T., and Kawaoka, Y.** (2005). Influenza: lessons from past pandemics, warnings from current incidents. *Nature reviews. Microbiology* **3**, 591-600.
- Huang, I.C., Li, W., Sui, J., Marasco, W., Choe, H., and Farzan, M.** (2008). Influenza A virus neuraminidase limits viral superinfection. *J Virol* **82**, 4834-4843.
- Huang, K., Incognito, L., Cheng, X., Ulbrandt, N.D., and Wu, H.** (2010). Respiratory syncytial virus-neutralizing monoclonal antibodies motavizumab and palivizumab inhibit fusion. In *J Virol*, pp. 8132-8140.
- Hubert, B., Watier, L., Garnerin, P., and Richardson, S.** (1992). Meningococcal disease and influenza-like syndrome: a new approach to an old question. *J Infect Dis* **166**, 542-545.

- Hulse, D.J., Webster, R.G., Russell, R.J., and Perez, D.R.** (2004). Molecular determinants within the surface proteins involved in the pathogenicity of H5N1 influenza viruses in chickens. *J Virol* **78**, 9954-9964.
- Hultberg, A., Temperton, N.J., Rosseels, V., Koenders, M., Gonzalez-Pajuelo, M., Schepens, B., Ibanez, L.I., Vanlandschoot, P., Schillemans, J., Saunders, M., Weiss, R.A., Saelens, X., Melero, J.A., Verrips, C.T., Van Gucht, S., and de Haard, H.J.** (2011). Llama-derived single domain antibodies to build multivalent, superpotent and broadened neutralizing anti-viral molecules. *PLoS One* **6**, e17665.
- Hutchinson, E.C., von Kirchbach, J.C., Gog, J.R., and Digard, P.** (2010). Genome packaging in influenza A virus. *J Gen Virol* **91**, 313-328.
- Ibanez, L.I., De Filette, M., Hultberg, A., Verrips, T., Temperton, N., Weiss, R.A., Vandeveld, W., Schepens, B., Vanlandschoot, P., and Saelens, X.** (2011). Nanobodies with in vitro neutralizing activity protect mice against H5N1 influenza virus infection. *J Infect Dis* **203**, 1063-1072.
- Ilyushina, N.A., Bovin, N.V., and Webster, R.G.** (2012). Decreased neuraminidase activity is important for the adaptation of H5N1 influenza virus to human airway epithelium. *J Virol* **86**, 4724-4733.
- Ilyushina, N.A., Ducatez, M.F., Rehg, J.E., Marathe, B.M., Marjuki, H., Bovin, N.V., Webster, R.G., and Webby, R.J.** (2010). Does pandemic A/H1N1 virus have the potential to become more pathogenic? *mBio* **1**.
- Imai, M., Watanabe, T., Hatta, M., Das, S.C., Ozawa, M., Shinya, K., Zhong, G., Hanson, A., Katsura, H., Watanabe, S., Li, C., Kawakami, E., Yamada, S., Kiso, M., Suzuki, Y., Maher, E.A., Neumann, G., and Kawaoka, Y.** (2012). Experimental adaptation of an influenza H5 HA confers respiratory droplet transmission to a reassortant H5 HA/H1N1 virus in ferrets. *Nature* **486**, 420-428.
- Ismaili, A., Jalali-Javaran, M., Rasaee, M.J., Rahbarizadeh, F., Forouzandeh-Moghadam, M., and Memari, H.R.** (2007). Production and characterization of anti-(mucin MUC1) single-domain antibody in tobacco (*Nicotiana tabacum* cultivar Xanthi). *Biotechnology and applied biochemistry* **47**, 11-19.
- Ito, T., Couceiro, J.N., Kelm, S., Baum, L.G., Krauss, S., Castrucci, M.R., Donatelli, I., Kida, H., Paulson, J.C., Webster, R.G., and Kawaoka, Y.** (1998). Molecular basis for the generation in pigs of influenza A viruses with pandemic potential. *J Virol* **72**, 7367-7373.
- Ives, J.A., Carr, J.A., Mendel, D.B., Tai, C.Y., Lambkin, R., Kelly, L., Oxford, J.S., Hayden, F.G., and Roberts, N.A.** (2002). The H274Y mutation in the influenza A/H1N1 neuraminidase active site following oseltamivir phosphate treatment leave virus severely compromised both in vitro and in vivo. *Antiviral Res* **55**, 307-317.
- Iwatsuki-Horimoto, K., Horimoto, T., Noda, T., Kiso, M., Maeda, J., Watanabe, S., Muramoto, Y., Fujii, K., and Kawaoka, Y.** (2006). The cytoplasmic tail of the influenza A virus M2 protein plays a role in viral assembly. *J Virol* **80**, 5233-5240.
- Jackson, D.C., and Webster, R.G.** (1982). A topographic map of the enzyme active center and antigenic sites on the neuraminidase of influenza virus A/Tokyo/3/67 (H2N2). *Virology* **123**, 69-77.
- Jagger, B.W., Wise, H.M., Kash, J.C., Walters, K.A., Wills, N.M., Xiao, Y.L., Dunfee, R.L., Schwartzman, L.M., Ozinsky, A., Bell, G.L., Dalton, R.M., Lo, A., Efsthathiou, S., Atkins, J.F., Firth, A.E., Taubenberger, J.K., and Digard, P.** (2012). An overlapping protein-coding region in influenza A virus segment 3 modulates the host response. *Science* **337**, 199-204.
- Jefferson, T., Demicheli, V., Rivetti, D., and Deeks, J.** (1999). Cochrane reviews and systematic reviews of economic evaluations. Amantadine and rimantadine in the prevention and treatment of influenza. *Pharmacoeconomics* **16 Suppl 1**, 85-89.

- Jefferson, T., Jones, M.A., Doshi, P., Del Mar, C.B., Heneghan, C.J., Hama, R., and Thompson, M.J.** (2012). Neuraminidase inhibitors for preventing and treating influenza in healthy adults and children. *Cochrane Database Syst Rev* **1**, CD008965.
- Jobling, S.A., Jarman, C., Teh, M.M., Holmberg, N., Blake, C., and Verhoeyen, M.E.** (2003). Immunomodulation of enzyme function in plants by single-domain antibody fragments. *Nature biotechnology* **21**, 77-80.
- Johansson, B.E., and Brett, I.C.** (2008). Recombinant influenza B virus HA and NA antigens administered in equivalent amounts are immunogenically equivalent and induce equivalent homotypic and broader heterovariant protection in mice than conventional and live influenza vaccines. *Hum Vaccin* **4**, 420-424.
- Johansson, B.E., Bucher, D.J., and Kilbourne, E.D.** (1989). Purified influenza virus hemagglutinin and neuraminidase are equivalent in stimulation of antibody response but induce contrasting types of immunity to infection. *J Virol* **63**, 1239-1246.
- Johansson, B.E., Matthews, J.T., and Kilbourne, E.D.** (1998). Supplementation of conventional influenza A vaccine with purified viral neuraminidase results in a balanced and broadened immune response. *Vaccine* **16**, 1009-1015.
- Johansson, B.E., Moran, T.M., Bona, C.A., Popple, S.W., and Kilbourne, E.D.** (1987). Immunologic response to influenza virus neuraminidase is influenced by prior experience with the associated viral hemagglutinin. II. Sequential infection of mice simulates human experience. *J Immunol* **139**, 2010-2014.
- Johnson, N., Cunningham, A., and Fooks, A.R.** (2010). The immune response to the rabies infection and vaccination. In *Vaccine*, pp. 3896-3901.
- Johnson, N.P., and Mueller, J.** (2002). Updating the accounts: global mortality of the 1918-1920 "Spanish" influenza pandemic. *Bulletin of the history of medicine* **76**, 105-115.
- Josset, L., Frobert, E., and Rosa-Calatrava, M.** (2008). Influenza A replication and host nuclear compartments: many changes and many questions. *J Clin Virol* **43**, 381-390.
- Kang, A.S., Jones, T.M., and Burton, D.R.** (1991). Antibody redesign by chain shuffling from random combinatorial immunoglobulin libraries. *Proc Natl Acad Sci U S A* **88**, 11120-11123.
- Kawaoka, Y., Krauss, S., and Webster, R.G.** (1989). Avian-to-human transmission of the PB1 gene of influenza A viruses in the 1957 and 1968 pandemics. *J Virol* **63**, 4603-4608.
- Kido, H., Yokogoshi, Y., Sakai, K., Tashiro, M., Kishino, Y., Fukutomi, A., and Katunuma, N.** (1992). Isolation and characterization of a novel trypsin-like protease found in rat bronchiolar epithelial Clara cells. A possible activator of the viral fusion glycoprotein. *J Biol Chem* **267**, 13573-13579.
- Kilbourne, E.D., Pokorny, B.A., Johansson, B., Brett, I., Milev, Y., and Matthews, J.T.** (2004). Protection of mice with recombinant influenza virus neuraminidase. *J Infect Dis* **189**, 459-461.
- Kim, C.U., Lew, W., Williams, M.A., Liu, H., Zhang, L., Swaminathan, S., Bischofberger, N., Chen, M.S., Mendel, D.B., Tai, C.Y., Laver, W.G., and Stevens, R.C.** (1997). Influenza neuraminidase inhibitors possessing a novel hydrophobic interaction in the enzyme active site: design, synthesis, and structural analysis of carbocyclic sialic acid analogues with potent anti-influenza activity. *Journal of the American Chemical Society* **119**, 681-690.
- Kobasa, D., Kodihalli, S., Luo, M., Castrucci, M.R., Donatelli, I., Suzuki, Y., Suzuki, T., and Kawaoka, Y.** (1999). Amino acid residues contributing to the substrate specificity of the influenza A virus neuraminidase. *J Virol* **73**, 6743-6751.
- Krug, R.M., and Aramini, J.M.** (2009). Emerging antiviral targets for influenza A virus. *Trends Pharmacol Sci* **30**, 269-277.

- Lackenby, A., Hungnes, O., Dudman, S.G., Meijer, A., Paget, W.J., Hay, A.J., and Zambon, M.C.** (2008). Emergence of resistance to oseltamivir among influenza A(H1N1) viruses in Europe. *Euro Surveill* **13**.
- Lafon, M., Edelman, L., Bouvet, J.P., Lafage, M., and Montchatre, E.** (1990). Human monoclonal antibodies specific for the rabies virus glycoprotein and N protein. In *J Gen Virol*, pp. 1689-1696.
- Lalezari, J., Campion, K., Keene, O., and Silagy, C.** (2001). Zanamivir for the treatment of influenza A and B infection in high-risk patients: a pooled analysis of randomized controlled trials. *Arch Intern Med* **161**, 212-217.
- Lauwereys, M., Arbadi Ghahroudi, M., Desmyter, A., Kinne, J., Holzer, W., De Genst, E., Wyns, L., and Muyldermans, S.** (1998). Potent enzyme inhibitors derived from dromedary heavy-chain antibodies. In *EMBO J*, pp. 3512-3520.
- Laver, W.G., and Valentine, R.C.** (1969). Morphology of the isolated hemagglutinin and neuraminidase subunits of influenza virus. *Virology* **38**, 105-119.
- Lawrence, M.C., and Colman, P.M.** (1993). Shape complementarity at protein/protein interfaces. *J Mol Biol* **234**, 946-950.
- Lawrenz, M., Wereszczynski, J., Amaro, R., Walker, R., Roitberg, A., and McCammon, J.A.** (2010). Impact of calcium on N1 influenza neuraminidase dynamics and binding free energy. *Proteins* **78**, 2523-2532.
- Le, Q.M., Kiso, M., Someya, K., Sakai, Y.T., Nguyen, T.H., Nguyen, K.H., Pham, N.D., Ngyen, H.H., Yamada, S., Muramoto, Y., Horimoto, T., Takada, A., Goto, H., Suzuki, T., Suzuki, Y., and Kawaoka, Y.** (2005). Avian flu: isolation of drug-resistant H5N1 virus. *Nature* **437**, 1108.
- Lee, J.T., and Air, G.M.** (2006). Interaction between a 1998 human influenza virus N2 neuraminidase and monoclonal antibody Mem5. *Virology* **345**, 424-433.
- Li, Q., Qi, J., Zhang, W., Vavricka, C.J., Shi, Y., Wei, J., Feng, E., Shen, J., Chen, J., Liu, D., He, J., Yan, J., Liu, H., Jiang, H., Teng, M., Li, X., and Gao, G.F.** (2010). The 2009 pandemic H1N1 neuraminidase N1 lacks the 150-cavity in its active site. *Nat Struct Mol Biol* **17**, 1266-1268.
- Lindstrom, S.E., Hiromoto, Y., Nerome, R., Omoe, K., Sugita, S., Yamazaki, Y., Takahashi, T., and Nerome, K.** (1998). Phylogenetic analysis of the entire genome of influenza A (H3N2) viruses from Japan: evidence for genetic reassortment of the six internal genes. *J Virol* **72**, 8021-8031.
- Lingwood, D., McTamney, P.M., Yassine, H.M., Whittle, J.R., Guo, X., Boyington, J.C., Wei, C.J., and Nabel, G.J.** (2012). Structural and genetic basis for development of broadly neutralizing influenza antibodies. *Nature* **489**, 566-570.
- Luke, C.J., and Subbarao, K.** (2006). Vaccines for pandemic influenza. *Emerg Infect Dis* **12**, 66-72.
- Malby, R.L., McCoy, A.J., Kortt, A.A., Hudson, P.J., and Colman, P.M.** (1998). Three-dimensional structures of single-chain Fv-neuraminidase complexes. *J Mol Biol* **279**, 901-910.
- Malby, R.L., Tulip, W.R., Harley, V.R., McKimm-Breschkin, J.L., Laver, W.G., Webster, R.G., and Colman, P.M.** (1994). The structure of a complex between the NC10 antibody and influenza virus neuraminidase and comparison with the overlapping binding site of the NC41 antibody. *Structure* **2**, 733-746.
- Marcelin, G., Sandbulte, M.R., and Webby, R.J.** (2012). Contribution of antibody production against neuraminidase to the protection afforded by influenza vaccines. *Rev Med Virol* **22**, 267-279.
- Matrosovich, M., Matrosovich, T., Garten, W., and Klenk, H.D.** (2006). New low-viscosity overlay medium for viral plaque assays. *Virol J* **3**, 63.
- Matrosovich, M.N., Matrosovich, T.Y., Gray, T., Roberts, N.A., and Klenk, H.D.** (2004a). Neuraminidase is important for the initiation of influenza virus infection in human airway epithelium. *J Virol* **78**, 12665-12667.

- Matrosovich, M.N., Matrosovich, T.Y., Gray, T., Roberts, N.A., and Klenk, H.D.** (2004b). Human and avian influenza viruses target different cell types in cultures of human airway epithelium. *Proc Natl Acad Sci U S A* **101**, 4620-4624.
- Matsumoto, K., Ogawa, N., Nerome, K., Numazaki, Y., Kawakami, Y., Shirato, K., Arakawa, M., Kudoh, S., Shimokata, K., Nakajima, S., Yamakido, M., Kashiwagi, S., and Nagatake, T.** (1999). Safety and efficacy of the neuraminidase inhibitor zanamivir in treating influenza virus infection in adults: results from Japan. GG167 Group. *Antivir Ther* **4**, 61-68.
- Matsuoka, Y., Swayne, D.E., Thomas, C., Rameix-Welti, M.A., Naffakh, N., Warnes, C., Altholtz, M., Donis, R., and Subbarao, K.** (2009). Neuraminidase stalk length and additional glycosylation of the hemagglutinin influence the virulence of influenza H5N1 viruses for mice. *J Virol* **83**, 4704-4708.
- McKimm-Breschkin, J.L., Selleck, P.W., Usman, T.B., and Johnson, M.A.** (2007). Reduced sensitivity of influenza A (H5N1) to oseltamivir. *Emerg Infect Dis* **13**, 1354-1357.
- McLellan, J.S., Yang, Y., Graham, B.S., and Kwong, P.D.** (2011). Structure of respiratory syncytial virus fusion glycoprotein in the postfusion conformation reveals preservation of neutralizing epitopes. In *J Virol*, pp. 7788-7796.
- Mendel, D.B., Tai, C.Y., Escarpe, P.A., Li, W., Sidwell, R.W., Huffman, J.H., Sweet, C., Jakeman, K.J., Merson, J., Lacy, S.A., Lew, W., Williams, M.A., Zhang, L., Chen, M.S., Bischofberger, N., and Kim, C.U.** (1998). Oral administration of a prodrug of the influenza virus neuraminidase inhibitor GS 4071 protects mice and ferrets against influenza infection. *Antimicrob Agents Ch* **42**, 640-646.
- Mishin, V.P., Hayden, F.G., and Gubareva, L.V.** (2005). Susceptibilities of antiviral-resistant influenza viruses to novel neuraminidase inhibitors. *Antimicrob Agents Chemother* **49**, 4515-4520.
- Mitnaul, L.J., Matrosovich, M.N., Castrucci, M.R., Tuzikov, A.B., Bovin, N.V., Kobasa, D., and Kawaoka, Y.** (2000). Balanced hemagglutinin and neuraminidase activities are critical for efficient replication of influenza A virus. *J Virol* **74**, 6015-6020.
- Mochalova, L., Kurova, V., Shtyrya, Y., Korchagina, E., Gambaryan, A., Belyanchikov, I., and Bovin, N.** (2007). Oligosaccharide specificity of influenza H1N1 virus neuraminidases. *Arch Virol* **152**, 2047-2057.
- Montano-Hirose, J.A., Lafage, M., Weber, P., Badrane, H., Tordo, N., and Lafon, M.** (1993). Protective activity of a murine monoclonal antibody against European bat lyssavirus 1 (EBL1) infection in mice. In *Vaccine*, pp. 1259-1266.
- Monto, A.S., Fleming, D.M., Henry, D., de Groot, R., Makela, M., Klein, T., Elliott, M., Keene, O.N., and Man, C.Y.** (1999). Efficacy and safety of the neuraminidase inhibitor zanamivir in the treatment of influenza A and B virus infections. *The Journal of infectious diseases* **180**, 254-261.
- Moscona, A.** (2005a). Neuraminidase inhibitors for influenza. *N Engl J Med* **353**, 1363-1373.
- Moscona, A.** (2005b). Oseltamivir resistance--disabling our influenza defenses. *N Engl J Med* **353**, 2633-2636.
- Moscona, A.** (2008). Medical management of influenza infection. *Annu Rev Med* **59**, 397-413.
- Munier, S., Larcher, T., Cormier-Aline, F., Soubieux, D., Su, B., Guigand, L., Labrosse, B., Cherel, Y., Quere, P., Marc, D., and Naffakh, N.** (2010). A genetically engineered waterfowl influenza virus with a deletion in the stalk of the neuraminidase has increased virulence for chickens. *J Virol* **84**, 940-952.
- Murti, K.G., Webster, R.G., and Jones, I.M.** (1988). Localization of RNA polymerases on influenza viral ribonucleoproteins by immunogold labeling. *Virology* **164**, 562-566.

- Muyldermans, S., Atarhouch, T., Saldanha, J., Barbosa, J.A., and Hamers, R.** (1994). Sequence and structure of VH domain from naturally occurring camel heavy chain immunoglobulins lacking light chains. In *Protein Eng*, pp. 1129-1135.
- Muyldermans S, B.T., Retamozzo VC, De Baetselier P, De Genst E, Kinne J, Leonhardt H, Magez S, Nguyen VK, Revets H, Rothbauer U, Stijlemans B, Tillib S, Wernery U, Wyns L, Hassanzadeh-Ghassabeh G and Saerens D.** (2008). Camelid immunoglobulins and nanobody technology. In *Vet Immunol Immunopathol*, pp. 178-183.
- Nagata, K., Kawaguchi, A., and Naito, T.** (2008). Host factors for replication and transcription of the influenza virus genome. *Rev Med Virol* **18**, 247-260.
- Nair, H., Nokes, D.J., Gessner, B.D., Dherani, M., Madhi, S.A., Singleton, R.J., O'Brien, K.L., Roca, A., Wright, P.F., Bruce, N., Chandran, A., Theodoratou, E., Sutanto, A., Sedyaningsih, E.R., Ngama, M., Munywoki, P.K., Kartasmita, C., Simoes, E.A., Rudan, I., Weber, M.W., and Campbell, H.** (2010). Global burden of acute lower respiratory infections due to respiratory syncytial virus in young children: a systematic review and meta-analysis. *Lancet* **375**, 1545-1555.
- Nedyalkova, M.S., Hayden, F.G., Webster, R.G., and Gubareva, L.V.** (2002). Accumulation of defective neuraminidase (NA) genes by influenza A viruses in the presence of NA inhibitors as a marker of reduced dependence on NA. *J Infect Dis* **185**, 591-598.
- Neiryneck, S., Deroo, T., Saelens, X., Vanlandschoot, P., Jou, W.M., and Fiers, W.** (1999). A universal influenza A vaccine based on the extracellular domain of the M2 protein. *Nature medicine* **5**, 1157-1163.
- Neumann, G., Hughes, M.T., and Kawaoka, Y.** (2000). Influenza A virus NS2 protein mediates vRNP nuclear export through NES-independent interaction with hCRM1. *Embo J* **19**, 6751-6758.
- Newcomb, L.L., Kuo, R.L., Ye, Q., Jiang, Y., Tao, Y.J., and Krug, R.M.** (2009). Interaction of the influenza A virus nucleocapsid protein with the viral RNA polymerase potentiates unprimed viral RNA replication. *J Virol* **83**, 29-36.
- Nguyen, H.T., Fry, A.M., Loveless, P.A., Klimov, A.I., and Gubareva, L.V.** (2010). Recovery of a multidrug-resistant strain of pandemic influenza A 2009 (H1N1) virus carrying a dual H275Y/I223R mutation from a child after prolonged treatment with oseltamivir. *Clin Infect Dis* **51**, 983-984.
- Nguyen, V.K., Muyldermans, S., and Hamers, R.** (1998). The specific variable domain of camel heavy-chain antibodies is encoded in the germline. *J Mol Biol* **275**, 413-418.
- Nidom, C.A., Takano, R., Yamada, S., Sakai-Tagawa, Y., Daulay, S., Aswadi, D., Suzuki, T., Suzuki, Y., Shinya, K., Iwatsuki-Horimoto, K., Muramoto, Y., and Kawaoka, Y.** (2010). Influenza A (H5N1) viruses from pigs, Indonesia. *Emerg Infect Dis* **16**, 1515-1523.
- Nimmerjahn, F., and Ravetch, J.V.** (2006). Fcγ receptors: old friends and new family members. *Immunity* **24**, 19-28.
- Nimmerjahn, F., and Ravetch, J.V.** (2008). Fcγ receptors as regulators of immune responses. *Nat Rev Immunol* **8**, 34-47.
- Oakley, A.J., Barrett, S., Peat, T.S., Newman, J., Streltsov, V.A., Waddington, L., Saito, T., Tashiro, M., and McKimm-Breschkin, J.L.** (2010). Structural and Functional Basis of Resistance to Neuraminidase Inhibitors of Influenza B Viruses. *J Med Chem* **53**, 6421-6431.
- Osterhaus, A.D., Rimmelzwaan, G.F., Martina, B.E., Bestebroer, T.M., and Fouchier, R.A.** (2000). Influenza B virus in seals. *Science* **288**, 1051-1053.
- Ozawa, M., Fujii, K., Muramoto, Y., Yamada, S., Yamayoshi, S., Takada, A., Goto, H., Horimoto, T., and Kawaoka, Y.** (2007). Contributions of two nuclear localization signals of influenza A virus nucleoprotein to viral replication. *J Virol* **81**, 30-41.

- Palese, P., and Schulman, J.L.** (1976). Mapping of the influenza virus genome: identification of the hemagglutinin and the neuraminidase genes. *P Natl Acad Sci USA* **73**, 2142-2146.
- Palese, P., Tobita, K., Ueda, M., and Compans, R.W.** (1974). Characterization of temperature sensitive influenza virus mutants defective in neuraminidase. *Virology* **61**, 397-410.
- Parrish, C.R., and Kawaoka, Y.** (2005). The origins of new pandemic viruses: the acquisition of new host ranges by canine parvovirus and influenza A viruses. *Annu Rev Microbiol* **59**, 553-586.
- Pinto, L.H., Holsinger, L.J., and Lamb, R.A.** (1992). Influenza-Virus M2 Protein Has Ion Channel Activity. *Cell* **69**, 517-528.
- Plotch, S.J., Bouloy, M., and Krug, R.M.** (1979). Transfer of 5'-terminal cap of globin mRNA to influenza viral complementary RNA during transcription in vitro. *P Natl Acad Sci USA* **76**, 1618-1622.
- Plotch, S.J., Bouloy, M., Ulmanen, I., and Krug, R.M.** (1981). A unique cap(m7GpppXm)-dependent influenza virion endonuclease cleaves capped RNAs to generate the primers that initiate viral RNA transcription. *Cell* **23**, 847-858.
- Poland, G.A., Jacobson, R.M., and Targonski, P.V.** (2007). Avian and pandemic influenza: an overview. *Vaccine* **25**, 3057-3061.
- Rameix-Welti, M.A., Zarantonelli, M.L., Giorgini, D., Ruckly, C., Marasescu, M., van der Werf, S., Alonso, J.M., Naffakh, N., and Taha, M.K.** (2009). Influenza A virus neuraminidase enhances meningococcal adhesion to epithelial cells through interaction with sialic acid-containing meningococcal capsules. *Infection and immunity* **77**, 3588-3595.
- Rasmussen, S.G., Choi, H.J., Fung, J.J., Pardon, E., Casarosa, P., Chae, P.S., Devree, B.T., Rosenbaum, D.M., Thian, F.S., Kobilka, T.S., Schnapp, A., Konetzki, I., Sunahara, R.K., Gellman, S.H., Pautsch, A., Steyaert, J., Weis, W.I., and Kobilka, B.K.** (2011). Structure of a nanobody-stabilized active state of the beta(2) adrenoceptor. *Nature* **469**, 175-180.
- Rohde, W., and Scholtissek, C.** (1980). On the origin of the gene coding for an influenza A virus nucleocapsid protein. *Arch Virol* **64**, 213-223.
- Rohm, C., Zhou, N., Suss, J., Mackenzie, J., and Webster, R.G.** (1996). Characterization of a novel influenza hemagglutinin, H15: criteria for determination of influenza A subtypes. *Virology* **217**, 508-516.
- Rudge, J.S., Holash, J., Hylton, D., Russell, M., Jiang, S., Leidich, R., Papadopoulos, N., Pyles, E.A., Torri, A., Wiegand, S.J., Thurston, G., Stahl, N., and Yancopoulos, G.D.** (2007). VEGF Trap complex formation measures production rates of VEGF, providing a biomarker for predicting efficacious angiogenic blockade. *Proc Natl Acad Sci U S A* **104**, 18363-18370.
- Ruiz-Arguello, M.B., Martin, D., Wharton, S.A., Calder, L.J., Martin, S.R., Cano, O., Calero, M., Garcia-Barreno, B., Skehel, J.J., and Melero, J.A.** (2004). Thermostability of the human respiratory syncytial virus fusion protein before and after activation: implications for the membrane-fusion mechanism. *J Gen Virol* **85**, 3677-3687.
- Russell, R.J., Haire, L.F., Stevens, D.J., Collins, P.J., Lin, Y.P., Blackburn, G.M., Hay, A.J., Gamblin, S.J., and Skehel, J.J.** (2006). The structure of H5N1 avian influenza neuraminidase suggests new opportunities for drug design. *Nature* **443**, 45-49.
- Rust, M.J., Lakadamyali, M., Zhang, F., and Zhuang, X.** (2004). Assembly of endocytic machinery around individual influenza viruses during viral entry. *Nat Struct Mol Biol* **11**, 567-573.
- Saerens, D., Pellis, M., Loris, R., Pardon, E., Dumoulin, M., Matagne, A., Wyns, L., Muyldermans, S., and Conrath, K.** (2005). Identification of a universal VHH framework to graft non-canonical antigen-binding loops of camel single-domain antibodies. *J Mol Biol* **352**, 597-607.
- Sandbulte, M.R., Gao, J., Straight, T.M., and Eichelberger, M.C.** (2009). A miniaturized assay for influenza neuraminidase-inhibiting antibodies utilizing reverse genetics-derived antigens. *Influenza Other Respi Viruses* **3**, 233-240.

- Sauter, N.K., Hanson, J.E., Glick, G.D., Brown, J.H., Crowther, R.L., Park, S.J., Skehel, J.J., and Wiley, D.C. (1992). Binding of influenza virus hemagglutinin to analogs of its cell-surface receptor, sialic acid: analysis by proton nuclear magnetic resonance spectroscopy and X-ray crystallography. *Biochemistry* **31**, 9609-9621.
- Schepens, B., Ibanez, L.I., Hultberg, A., Bogaert, P., De Bleser, P., De Baets, S., Vervalle, F., Verrips, T., Melero, J., Vandeveld, W., Vanlandschoot, P., and Saelens, X. (2011). Nanobodies specific for Respiratory Syncytial Virus Fusion protein protect against infection by inhibition of fusion. In *J Inf Dis*.
- Schmidt, P.M., Attwood, R.M., Mohr, P.G., Barrett, S.A., and McKimm-Breschkin, J.L. (2011). A generic system for the expression and purification of soluble and stable influenza neuraminidase. *PLoS One* **6**, e16284.
- Scholtissek, C., Burger, H., Kistner, O., and Shortridge, K.F. (1985). The nucleoprotein as a possible major factor in determining host specificity of influenza H3N2 viruses. *Virology* **147**, 287-294.
- Schotsaert, M., De Filette, M., Fiers, W., and Saelens, X. (2009). Universal M2 ectodomain-based influenza A vaccines: preclinical and clinical developments. *Expert review of vaccines* **8**, 499-508.
- Schotsaert, M., Ysenbaert, T., Neyt, K., Ibanez, L.I., Bogaert, P., Schepens, B., Lambrecht, B.N., Fiers, W., and Saelens, X. (2012). Natural and long-lasting cellular immune responses against influenza in the M2e-immune host. *Mucosal Immunol*.
- Schulman, J.L., Khakpour, M., and Kilbourne, E.D. (1968). Protective effects of specific immunity to viral neuraminidase on influenza virus infection of mice. *J Virol* **2**, 778-786.
- Seif, I., Coulon, P., Rollin, P.E., and Flamand, A. (1985). Rabies virulence: effect on pathogenicity and sequence characterization of rabies virus mutations affecting antigenic site III of the glycoprotein. In *J Virol*, pp. 926-934.
- Shoji, Y., Chichester, J.A., Palmer, G.A., Farrance, C.E., Stevens, R., Stewart, M., Goldschmidt, L., Deyde, V., Gubareva, L., Klimov, A., Mett, V., and Yusibov, V. (2011). An influenza N1 neuraminidase-specific monoclonal antibody with broad neuraminidase inhibition activity against H5N1 HPAI viruses. *Hum Vaccin* **7 Suppl**, 199-204.
- Smith, G.J., Vijaykrishna, D., Bahl, J., Lycett, S.J., Worobey, M., Pybus, O.G., Ma, S.K., Cheung, C.L., Raghvani, J., Bhatt, S., Peiris, J.S., Guan, Y., and Rambaut, A. (2009). Origins and evolutionary genomics of the 2009 swine-origin H1N1 influenza A epidemic. *Nature* **459**, 1122-1125.
- Stech, J., Stech, O., Herwig, A., Altmeppen, H., Hundt, J., Gohrbandt, S., Kreibich, A., Weber, S., Klenk, H.D., and Mettenleiter, T.C. (2008). Rapid and reliable universal cloning of influenza A virus genes by target-primed plasmid amplification. *Nucleic Acids Res* **36**, e139.
- Steel, J., Lowen, A.C., Wang, T.T., Yondola, M., Gao, Q., Haye, K., Garcia-Sastre, A., and Palese, P. (2010). Influenza virus vaccine based on the conserved hemagglutinin stalk domain. *Mbio* **1**.
- Steinhauer, D.A., and Skehel, J.J. (2002). Genetics of influenza viruses. *Annu Rev Genet* **36**, 305-332.
- Stevens, J., Blixt, O., Glaser, L., Taubenberger, J.K., Palese, P., Paulson, J.C., and Wilson, I.A. (2006). Glycan microarray analysis of the hemagglutinins from modern and pandemic influenza viruses reveals different receptor specificities. *J Mol Biol* **355**, 1143-1155.
- Stiehm, E.R., Keller, M.A., and Vyas, G.N. (2008). Preparation and use of therapeutic antibodies primarily of human origin. *Biologicals* **36**, 363-374.
- Subbarao, K., Klimov, A., Katz, J., Regnery, H., Lim, W., Hall, H., Perdue, M., Swayne, D., Bender, C., Huang, J., Hemphill, M., Rowe, T., Shaw, M., Xu, X., Fukuda, K., and Cox, N. (1998). Characterization of an avian influenza A (H5N1) virus isolated from a child with a fatal respiratory illness. *Science* **279**, 393-396.
- Swanson, K.A., Settembre, E.C., Shaw, C.A., Dey, A.K., Rappuoli, R., Mandl, C.W., Dormitzer, P.R., and Carfi, A. (2011). Structural basis for immunization with postfusion respiratory syncytial virus

- fusion F glycoprotein (RSV F) to elicit high neutralizing antibody titers. *Proc Natl Acad Sci U S A* **108**, 9619-9624.
- Takasuka, N., Enami, M., Itamura, S., and Takemori, T.** (2002). Intranasal inoculation of a recombinant influenza virus containing exogenous nucleotides in the NS segment induces mucosal immune response against the exogenous gene product in mice. *Vaccine* **20**, 1579-1585.
- Taubenberger, J.K., Hultin, J.V., and Morens, D.M.** (2007). Discovery and characterization of the 1918 pandemic influenza virus in historical context. *Antiviral therapy* **12**, 581-591.
- Taubenberger, J.K., Reid, A.H., Krafft, A.E., Bijwaard, K.E., and Fanning, T.G.** (1997). Initial genetic characterization of the 1918 "Spanish" influenza virus. *Science* **275**, 1793-1796.
- Taubenberger, J.K., Reid, A.H., Lourens, R.M., Wang, R., Jin, G., and Fanning, T.G.** (2005). Characterization of the 1918 influenza virus polymerase genes. *Nature* **437**, 889-893.
- Tayyari, F., Marchant, D., Moraes, T.J., Duan, W., Mastrangelo, P., and Hegele, R.G.** (2011). Identification of nucleolin as a cellular receptor for human respiratory syncytial virus. *Nature medicine*.
- Teh, Y.H., and Kavanagh, T.A.** (2010). High-level expression of Camelid nanobodies in *Nicotiana benthamiana*. *Transgenic research* **19**, 575-586.
- Thompson, J.D., Higgins, D.G., and Gibson, T.J.** (1994). Improved sensitivity of profile searches through the use of sequence weights and gap excision. *Comput Appl Biosci* **10**, 19-29.
- Throsby, M., van den Brink, E., Jongeneelen, M., Poon, L.L., Alard, P., Cornelissen, L., Bakker, A., Cox, F., van Deventer, E., Guan, Y., Cinatl, J., ter Meulen, J., Lasters, I., Carsetti, R., Peiris, M., de Kruif, J., and Goudsmit, J.** (2008). Heterosubtypic neutralizing monoclonal antibodies cross-protective against H5N1 and H1N1 recovered from human IgM+ memory B cells. *PLoS One* **3**, e3942.
- Tomar, N.R., Singh, V., Marla, S.S., Chandra, R., Kumar, R., and Kumar, A.** (2010). Molecular docking studies with rabies virus glycoprotein to design viral therapeutics. *Indian J Pharm Sci* **72**, 486-490.
- Tominack, R.L., and Hayden, F.G.** (1987). Rimantadine hydrochloride and amantadine hydrochloride use in influenza A virus infections. *Infect Dis Clin North Am* **1**, 459-478.
- Tompkins, S.M., Zhao, Z.S., Lo, C.Y., Misplon, J.A., Liu, T., Ye, Z., Hogan, R.J., Wu, Z., Benton, K.A., Tumpey, T.M., and Epstein, S.L.** (2007). Matrix protein 2 vaccination and protection against influenza viruses, including subtype H5N1. *Emerg Infect Dis* **13**, 426-435.
- Tran, T.H., Nguyen, T.L., Nguyen, T.D., Luong, T.S., Pham, P.M., Nguyen, V.C., Pham, T.S., Vo, C.D., Le, T.Q., Ngo, T.T., Dao, B.K., Le, P.P., Nguyen, T.T., Hoang, T.L., Cao, V.T., Le, T.G., Nguyen, D.T., Le, H.N., Nguyen, K.T., Le, H.S., Le, V.T., Christiane, D., Tran, T.T., Menno de, J., Schultsz, C., Cheng, P., Lim, W., Horby, P., and Farrar, J.** (2004). Avian influenza A (H5N1) in 10 patients in Vietnam. *N Engl J Med* **350**, 1179-1188.
- Treanor, J.J., Hayden, F.G., Vrooman, P.S., Barbarash, R., Bettis, R., Riff, D., Singh, S., Kinnersley, N., Ward, P., and Mills, R.G.** (2000). Efficacy and safety of the oral neuraminidase inhibitor oseltamivir in treating acute influenza: a randomized controlled trial. *US Oral Neuraminidase Study Group. Jama* **283**, 1016-1024.
- Tulip, W.R., Harley, V.R., Webster, R.G., and Novotny, J.** (1994). N9 neuraminidase complexes with antibodies NC41 and NC10: empirical free energy calculations capture specificity trends observed with mutant binding data. *Biochemistry* **33**, 7986-7997.
- Tulip, W.R., Varghese, J.N., Laver, W.G., Webster, R.G., and Colman, P.M.** (1992). Refined crystal structure of the influenza virus N9 neuraminidase-NC41 Fab complex. *J Mol Biol* **227**, 122-148.

- Tulip, W.R., Varghese, J.N., Baker, A.T., van Donkelaar, A., Laver, W.G., Webster, R.G., and Colman, P.M.** (1991). Refined atomic structures of N9 subtype influenza virus neuraminidase and escape mutants. *J Mol Biol* **221**, 487-497.
- Tumpey, T.M., Basler, C.F., Aguilar, P.V., Zeng, H., Solorzano, A., Swayne, D.E., Cox, N.J., Katz, J.M., Taubenberger, J.K., Palese, P., and Garcia-Sastre, A.** (2005). Characterization of the reconstructed 1918 Spanish influenza pandemic virus. *Science* **310**, 77-80.
- Van Borm, S., Thomas, I., Hanquet, G., Lambrecht, B., Boschmans, M., Dupont, G., Decaestecker, M., Snacken, R., and van den Berg, T.** (2005). Highly pathogenic H5N1 influenza virus in smuggled Thai eagles, Belgium. *Emerg Infect Dis* **11**, 702-705.
- van der Vries, E., van den Berg, B., and Schutten, M.** (2008). Fatal oseltamivir-resistant influenza virus infection. *N Engl J Med* **359**, 1074-1076.
- van der Vries, E., Veldhuis Kroeze, E.J., Stittelaar, K.J., Linster, M., Van der Linden, A., Schrauwen, E.J., Leijten, L.M., van Amerongen, G., Schutten, M., Kuiken, T., Osterhaus, A.D., Fouchier, R.A., Boucher, C.A., and Herfst, S.** (2011). Multidrug resistant 2009 A/H1N1 influenza clinical isolate with a neuraminidase I223R mutation retains its virulence and transmissibility in ferrets. *PLoS Pathog* **7**, e1002276.
- Van Droogenbroeck, B., Cao, J., Stadlmann, J., Altmann, F., Colanesi, S., Hillmer, S., Robinson, D.G., Van Lerberge, E., Terry, N., Van Montagu, M., Liang, M., Depicker, A., and De Jaeger, G.** (2007). Aberrant localization and underglycosylation of highly accumulating single-chain Fv-Fc antibodies in transgenic Arabidopsis seeds. *Proc Natl Acad Sci U S A* **104**, 1430-1435.
- Van Reeth, K.** (2007). Avian and swine influenza viruses: our current understanding of the zoonotic risk. *Vet Res* **38**, 243-260.
- Varghese, J.N., Laver, W.G., and Colman, P.M.** (1983). Structure of the influenza virus glycoprotein antigen neuraminidase at 2.9 Å resolution. *Nature* **303**, 35-40.
- Varghese, J.N., McKimm-Breschkin, J.L., Caldwell, J.B., Kortt, A.A., and Colman, P.M.** (1992). The structure of the complex between influenza virus neuraminidase and sialic acid, the viral receptor. *Proteins* **14**, 327-332.
- Varghese, J.N., Colman, P.M., van Donkelaar, A., Blick, T.J., Sahasrabudhe, A., and McKimm-Breschkin, J.L.** (1997). Structural evidence for a second sialic acid binding site in avian influenza virus neuraminidases. *Proc Natl Acad Sci U S A* **94**, 11808-11812.
- Vene, S., Haglund, M., Vapalahti, O., and Lundkvist, A.** (1998). A rapid fluorescent focus inhibition test for detection of neutralizing antibodies to tick-borne encephalitis virus. In *J Virol Methods*, pp. 71 - 75.
- Venkatramani, L., Bochkareva, E., Lee, J.T., Gulati, U., Graeme Laver, W., Bochkarev, A., and Air, G.M.** (2006). An epidemiologically significant epitope of a 1998 human influenza virus neuraminidase forms a highly hydrated interface in the NA-antibody complex. *J Mol Biol* **356**, 651-663.
- Verheesen, P., Roussis, A., de Haard, H.J., Groot, A.J., Stam, J.C., den Dunnen, J.T., Frants, R.R., Verkleij, A.J., Theo Verrips, C., and van der Maarel, S.M.** (2006). Reliable and controllable antibody fragment selections from Camelid non-immune libraries for target validation. *Biochim Biophys Acta* **1764**, 1307-1319.
- Vonitzstein, M., Wu, W.Y., Kok, G.B., Pegg, M.S., Dyason, J.C., Jin, B., Phan, T.V., Smythe, M.L., White, H.F., Oliver, S.W., Colman, P.M., Varghese, J.N., Ryan, D.M., Woods, J.M., Bethell, R.C., Hotham, V.J., Cameron, J.M., and Penn, C.R.** (1993). Rational Design of Potent Sialidase-Based Inhibitors of Influenza-Virus Replication. *Nature* **363**, 418-423.
- Vu, K.B., Ghahroudi, M.A., Wyns, L., and Muyldermans, S.** (1997). Comparison of llama VH sequences from conventional and heavy chain antibodies. *Mol Immunol* **34**, 1121-1131.

- Wagner, R., Herwig, A., Azzouz, N., and Klenk, H.D.** (2005). Acylation-mediated membrane anchoring of avian influenza virus hemagglutinin is essential for fusion pore formation and virus infectivity. *J Virol* **79**, 6449-6458.
- Wang, K., Shun-Shin, M., Gill, P., Perera, R., and Harnden, A.** (2012). Neuraminidase inhibitors for preventing and treating influenza in children (published trials only). *Cochrane Database Syst Rev* **4**, CD002744.
- Wang, M.Z., Tai, C.Y., and Mendel, D.B.** (2002a). Mechanism by which mutations at his274 alter sensitivity of influenza a virus n1 neuraminidase to oseltamivir carboxylate and zanamivir. *Antimicrob Agents Chemother* **46**, 3809-3816.
- Wang, M.Z., Tai, C.Y., and Mendel, D.B.** (2002b). Mechanism by which mutations at his274 alter sensitivity of influenza a virus n1 neuraminidase to oseltamivir carboxylate and zanamivir. *Antimicrob Agents Chemother* **46**, 3809-3816.
- Wang, P., and Yang, X.** (2010). Neutralization efficiency is greatly enhanced by bivalent binding of an antibody to epitopes in the V4 region and the membrane-proximal external region within one trimer of human immunodeficiency virus type 1 glycoproteins. In *J Virol*, pp. 7114-7123.
- Ward, E.S., Gussow, D., Griffiths, A.D., Jones, P.T., and Winter, G.** (1989). Binding activities of a repertoire of single immunoglobulin variable domains secreted from *Escherichia coli*. *Nature* **341**, 544-546.
- Watowich, S.J., Skehel, J.J., and Wiley, D.C.** (1994). Crystal structures of influenza virus hemagglutinin in complex with high-affinity receptor analogs. *Structure* **2**, 719-731.
- Webster, R.G., and Hulse, D.J.** (2004). Microbial adaptation and change: avian influenza. *Rev Sci Tech* **23**, 453-465.
- Webster, R.G., Brown, L.E., and Laver, W.G.** (1984). Antigenic and biological characterization of influenza virus neuraminidase (N2) with monoclonal antibodies. *Virology* **135**, 30-42.
- Webster, R.G., Yakhno, M., Hinshaw, V.S., Bean, W.J., and Murti, K.G.** (1978). Intestinal influenza: replication and characterization of influenza viruses in ducks. *Virology* **84**, 268-278.
- Webster, R.G., Kawaoka, Y., Taylor, J., Weinberg, R., and Paoletti, E.** (1991). Efficacy of nucleoprotein and haemagglutinin antigens expressed in fowlpox virus as vaccine for influenza in chickens. *Vaccine* **9**, 303-308.
- Webster, R.G., Bean, W.J., Gorman, O.T., Chambers, T.M., and Kawaoka, Y.** (1992). Evolution and ecology of influenza A viruses. *Microbiol Rev* **56**, 152-179.
- Webster, R.G., Air, G.M., Metzger, D.W., Colman, P.M., Varghese, J.N., Baker, A.T., and Laver, W.G.** (1987). Antigenic structure and variation in an influenza virus N9 neuraminidase. *J Virol* **61**, 2910-2916.
- Wei, G., Meng, W., Guo, H., Pan, W., Liu, J., Peng, T., Chen, L., and Chen, C.Y.** (2011). Potent neutralization of influenza A virus by a single-domain antibody blocking M2 ion channel protein. *PLoS One* **6**, e28309.
- Wenzel, R.P.** (2000). Expanding the treatment options for influenza. *Jama* **283**, 1057-1059.
- White, N.J., Webster, R.G., Govorkova, E.A., and Uyeki, T.M.** (2009). What is the optimal therapy for patients with H5N1 influenza? *PLoS Med* **6**, e1000091.
- Wiley, D.C., Wilson, I.A., and Skehel, J.J.** (1981). Structural identification of the antibody-binding sites of Hong Kong influenza haemagglutinin and their involvement in antigenic variation. *Nature* **289**, 373-378.
- Wilson, I.A., Skehel, J.J., and Wiley, D.C.** (1981). Structure of the Hemagglutinin Membrane Glycoprotein of Influenza-Virus at 3-Å Resolution. *Nature* **289**, 366-373.

- Winichayakul, S., Pernthaner, A., Scott, R., Vlaming, R., and Roberts, N.** (2009). Head-to-tail fusions of camelid antibodies can be expressed in planta and bind in rumen fluid. *Biotechnology and applied biochemistry* **53**, 111-122.
- Wise, H.M., Foeglein, A., Sun, J., Dalton, R.M., Patel, S., Howard, W., Anderson, E.C., Barclay, W.S., and Digard, P.** (2009a). A complicated message: Identification of a novel PB1-related protein translated from influenza A virus segment 2 mRNA. *J Virol* **83**, 8021-8031.
- Wise, H.M., Foeglein, A., Sun, J.C., Dalton, R.M., Patel, S., Howard, W., Anderson, E.C., Barclay, W.S., and Digard, P.** (2009b). A Complicated Message: Identification of a Novel PB1-Related Protein Translated from Influenza A Virus Segment 2 mRNA. *J Virol* **83**, 8021-8031.
- Wrigley, N.G., Skehel, J.J., Charlwood, P.A., and Brand, C.M.** (1973). The size and shape of influenza virus neuraminidase. *Virology* **51**, 525-529.
- Wu, S.J., Schmidt, A., Beil, E.J., Day, N.D., Branigan, P.J., Liu, C., Gutshall, L.L., Palomo, C., Furze, J., Taylor, G., Melero, J.A., Tsui, P., Del Vecchio, A.M., and Kruszynski, M.** (2007). Characterization of the epitope for anti-human respiratory syncytial virus F protein monoclonal antibody 101F using synthetic peptides and genetic approaches. *J Gen Virol* **88**, 2719-2723.
- Wu, T.T., Johnson, G., and Kabat, E.A.** (1993). Length distribution of CDRH3 in antibodies. In *Proteins*, pp. 1-7.
- Wu, Z.L., Ethen, C., Hickey, G.E., and Jiang, W.** (2009). Active 1918 pandemic flu viral neuraminidase has distinct N-glycan profile and is resistant to trypsin digestion. *Biochem Biophys Res Commun* **379**, 749-753.
- Yamada, S., Suzuki, Y., Suzuki, T., Le, M.Q., Nidom, C.A., Sakai-Tagawa, Y., Muramoto, Y., Ito, M., Kiso, M., Horimoto, T., Shinya, K., Sawada, T., Kiso, M., Usui, T., Murata, T., Lin, Y., Hay, A., Haire, L.F., Stevens, D.J., Russell, R.J., Gamblin, S.J., Skehel, J.J., and Kawaoka, Y.** (2006). Haemagglutinin mutations responsible for the binding of H5N1 influenza A viruses to human-type receptors. *Nature* **444**, 378-382.
- Yen, H.L., Ilyushina, N.A., Salomon, R., Hoffmann, E., Webster, R.G., and Govorkova, E.A.** (2007). Neuraminidase inhibitor-resistant recombinant A/Vietnam/1203/04 (H5N1) influenza viruses retain their replication efficiency and pathogenicity in vitro and in vivo. *J Virol* **81**, 12418-12426.
- Yoshida, R., Igarashi, M., Ozaki, H., Kishida, N., Tomabechei, D., Kida, H., Ito, K., and Takada, A.** (2009). Cross-protective potential of a novel monoclonal antibody directed against antigenic site B of the hemagglutinin of influenza A viruses. *Plos Pathog* **5**, e1000350.
- Yuen, K.Y., and Wong, S.S.** (2005). Human infection by avian influenza A H5N1. *Hong Kong Med J* **11**, 189-199.
- Zhou, B., Zhong, N., and Guan, Y.** (2007). Treatment with convalescent plasma for influenza A (H5N1) infection. *N Engl J Med* **357**, 1450-1451.
- Zimmer, S.M., and Burke, D.S.** (2009). Historical perspective--Emergence of influenza A (H1N1) viruses. *N Engl J Med* **361**, 279-285.

ADDENDUM

PATENT APPLICATION No. EP 12196499.3.

ANTI-INFLUENZA ANTIBODY

The present invention relates to an antibody that confers protection against influenza. More specifically, it relates to an anti-neuraminidase antibody, protecting against highly pathogenic H5N1 influenza strains. The invention relates further to the use of the antibody for prophylactic and/or therapeutic treatment of influenza virus infections, and to a pharmaceutical composition comprising the antibody.

The zoonotic influenza infections in humans present a persistent and great burden worldwide to health, academic and pharmaceutical entities. The possibility of a highly pathogenic influenza pandemic in humans had been recognized, which, if present, not only can present a high toll to human society, but could also change the importance and perceived danger of infectious diseases in the social and cultural context. In less than 10 years, two zoonotic outbreaks had a major global impact: the Avian Influenza Virus (IAV) (Tran et al., 2004) and the swine flu (H1N1) or “Mexican flu”, confirmed the lack of preparedness against a highly pathogenic pandemic (Ilyushina et al., 2010). Among these zoonotic influenza outbreaks, the avian H5N1 influenza virus is one of the most concerning because of the vast animal reservoir for this virus (domesticated as well as wild water fowl) and the high lethality rate in humans. Indeed, infection of humans with highly pathogenic H5N1 (HPAIV H5N1) influenza virus results in a 60% mortality rate (Chotpitayasunondh et al., 2005). This high pathogenicity and lethality of the HPAIV H5N1 in humans can be attributed to a high replication rate and a broad cellular tropism that can lead to a systemic spread. During severe infections, a deregulated induction of proinflammatory cytokines and chemokines (sometimes called “cytokine storm”) is associated with HPAIV H5N1

infections that can result into an excessive immunological response and autoimmune symptoms (de Jong et al., 2006).

The treatments reported and available against HPAIV H5N1 are far from optimal. The currently licensed influenza antiviral drugs remain the most used treatment against HPAIV H5N1, even though they were developed against seasonal human influenza viruses. These drugs target only two viral proteins: the proton ion channel M2 (amantadine and rimantadine) and the sialidase Neuraminidase (NA) (oseltamivir, zanamivir and peramivir). The efficacy of these drugs depends greatly of the severity of the H5N1 infection, that itself depends on several factors like: patient age, activity, previous vaccination and previous exposure to similar Influenza strains. In addition, the use of influenza antiviral drugs for hospitalized patients is often characterized by long term treatment and high concentrations are used in severe clinical cases. Such treatment regimes represent a major concern because they favor selective pressure causing the appearance of reported and emerging drug-resistant mutants. Moreover, bacterial secondary infections are associated with influenza and complicate the clinical outcome (Hebert et al., 1992; Rameix-Welti et al., 2009). On the other hand, the vaccination strategy used against seasonal influenza is not efficient in preventing or controlling zoonotic or pandemic Influenza virus treatment, due the unpredictability in their occurrence, the antigenic mismatch between such vaccines and pandemic viruses and the lack of immunological memory in human. The recent reports of experimental adaptation of H5N1 virus for airborne transmission in ferrets, confirm the possibility of human to human transmission of zoonotic HPAIV H5N1 (Herfst et al., 2012; Imai et al., 2012). Treatment of patients with convalescent plasma from influenza HPAIV H5N1 (Zhou et al., 2007) and H1N1 (Hung et al., 2011) survivors patients has been shown to be protective. However, those data are based on a limited number of patients, treatment with convalescent plasma is certainly not generally accepted as a therapy and there are practical limitations in collecting convalescent plasma (Wong et al., 2010). Influenza NA best known function is to

prevent aggregation of the newly produced virions by cleaving the sialic acids from the infected cell and from the viral glycoproteins. In addition, other functions had been reported for the NA, pointing out its relevance in several parts of the replicative cycle of Influenza (Air et al., 2012). The immunogenicity of the influenza virion depends mainly of the two major proteins in its surface, the Hemagglutinin (HA) and the NA. It has been reported that the HA is immunodominant over the NA with respect to T- and B- cell priming (Johansson et al., 1987), but their disassociation re-established an equal immunogenic potential of both viral proteins (Johansson and Kilbourne 1993). A high immunogenic potential of the NA had been reported, and it has been proposed to depend in some degree of defective ribosomal products (DRiP) by presenting NA peptides to the MHC class I molecules for T cell activation, enabling rapid immunosurveillance (Dolan et al., 2010). Nowadays, the evidence of the importance in the immune response dependent of NA, leads to the proposal of standardize the NA content in the seasonal vaccine formulation (Johansson et al., 1998) (Kilbourne et al., 2004). In addition, the pace with which HA and NA drift in human influenza A viruses is similar, suggesting the selection pressure of the human host directed against the two glycoproteins of influenza viruses is comparable. Besides the immunogenicity of NA and its receptor destroying activity that avoids virion aggregation, there are another NA roles reported: cleavage of decoy receptors in the mucins, which is necessary during the initiation of infection (Matrosovich et al., 2004); limitation of influenza superinfections and possible reassortment (Huang et al., 2008); possibility of increased infectivity (Goto and Kawaoka 1998). Interestingly, Influenza virus sensitive to NA inhibitory drugs resulted in a crippled or absence of NA activity (Ilyushina et al., 2012). These data confirms that the fitness of these mutant virus can be rescued by decreased HA binding to Neu5Ac receptors, which had been reported due to insertions of mutations or glycosylations that affect the receptor binding site (Gubareva et al., 2002). Such compensatory effect in the HA and NA activities towards fitness had been widely reported (Gubareva et al., 2002; Mitnaul et al.,

2000; Nedyalkova et al., 2002), demonstrating that the NA activity can be compromised, but not necessarily results in a replication deficient virus. These pieces of evidence highlight the complexity of the mechanism of Influenza escape mutants under selective pressure. There also important roles of the NA function that do not depend of the catalytic site: enhancement of neurovirulence (e.g. the glycan at position 130, Li et al., 1993); enhanced pathogenicity (length of NA stalk; Matsuoka et al., 2009; Yamada et al., 2006). Taken together, these data demonstrate the major importance of the NA in influenza A virus infection, indicating that targeting NA may result in a global effective antiviral strategy, dependent or independent of the NA catalytic activity. Several authors have disclosed methods for passive immunization using monoclonal antibodies. WO2009035420 discloses monoclonal antibodies against H5N1 hemagglutinin and neuraminidase, and the use of the hemagglutinin antibodies in treatment of influenza infection. However, whereas protection using the hemagglutinin antibodies is demonstrated, no evidence for protection using the neuraminidase antibodies is shown. Shoji et al. (2011) and WO2010037046 describe a humanized neuraminidase antibody, its production in plants and the use of this antibody for treatment of influenza virus infection. However, a high amount of antibody is needed and even then, the survival after challenge is only 50% in their animal model. There is still need for antibodies that can be effectively used in passive immunization, resulting in a high protection and survival after lethal challenge.

Surprisingly we found that high affinity camelid heavy chain antibodies or nanobodies (VHHs) can be generated targeting the Influenza NA. The high affinity of these monomeric VHH to bind a recombinant N1 (N1rec), results also in highly potent H5N1 inhibitors *in vitro*. The introduction of bivalent formats in the VHH increased the antiviral potential *in vitro* and rescued H5N1 lethality challenged mice. Even more surprisingly, bivalent VHHs, either by fusion of the VHH to an Fc tail or by linking the VHHs to an IgG2c hinge resulted in an unexpected increase in potency of the nanobodies, giving full protection against a lethal challenge in a mouse model,

while using low amounts of antibodies. A first aspect of the invention is a variable domain of camelid heavy chain antibodies (VHH) specifically binding influenza neuraminidase. Preferably, said neuraminidase is an influenza type N1 neuraminidase. Preferably, said VHH is inhibiting the neuraminidase activity. Even more preferably, said VHH comprises a CDR1 loop sequence selected from the group consisting of SEQ ID N°1 and SEQ ID N° 2, a CDR2 loop sequence selected from the group consisting of SEQ ID N° 3 and SEQ ID N° 4 and a CDR3 loop sequence consisting of SEQ ID N° 5 and SEQ ID N°6.

Another aspect of the invention is an influenza neuraminidase binding construct, comprising a VHH according to the invention. Preferably, said neuraminidase is a type N1 neuraminidase. Said influenza binding construct may be any construct; preferably it is a fusion protein, even more preferably it is a bivalent or multivalent construct, comprising more than one influenza neuraminidase binding VHHs. In one preferred embodiment, the VHH according to the invention is fused to an Fc tail. In another preferred embodiment, two VHHs are linked by an IgG2c hinge. Preferably, the construct according to the inventions comprises a sequence; even more preferably consist of a sequence selected from the group consisting of SEQ ID N° 7, SEQ ID N° 8, SEQ ID N° 9 and SEQ ID N° 10.

BRIEF DESCRIPTION OF THE FIGURES

Figure 1. Characterization and production of recombinant H5N1 NA. Soluble recombinant NA derived from A/crested eagle/Belgium/01/2004 was produced in Sf9 cells using the Baculovirus expression platform. **A.** Diagram of the expression cassette in the pACMP2 vector: Promoter, Baculovirus basic protein promoter; ssHA, secretion signal of Hemagglutinin; tGCN4, tetramerizing leucine zipper; H5N1 NA, extracellular domain of the H5N1 NA. **B.** Sialidase activity in crude culture supernatant of infected Sf9 cells. Supernatants of different amounts of

Baculovirus N1rec infected cells and mock infected cells were measured in a MUNANA based NA activity test. **C.** Chromatographic elution profile of the fractions of N1rec after superdex 200 gel filtration. The highest NA activity was localized in the fractions F19 – F26. **D.** Coomassie stained SDS-PAGE and immunoblot against N1rec, of F19 - F26 from D: 18 µl and 9 µl of eluted fractions from the gel filtration were loaded on the SDS-PAGE and immunoblot, respectively.

Figure 2. Characterization of the H5N1 NA-binding VHHs. **A.** Alignment of the VHH amino acid sequence of the 13 VHHs that were isolated by phage-display generated from a N1-rec immunized Alpaca. The four framework regions are separated by 3 Complementary Determining Regions (CDRs, left-right arrows). The VHH CDR3 is the most variable region in the VHH candidates. **B.** *In silico* predicted 3D-structure of the VHHs, showing electropositive (blue) and electronegative (red) potential. The white ribbon represents the CDR3. Note that N1-1-VHH, N1-3-VHH, N1-4-VHH, N1-5-VHH and N1-6-VHH CDR3 present an electronegative protruding topology. **C.** Coomassie-blue stained reducing SDS-PAGE of the purified *E. coli*-produced N1-VHHm candidates. Twenty µg of SA-VHHm was loaded as control VHH. The VHH size ranges from 14 – 15 kDa. Purified BSA standards were loaded for quantification and comparison.

Figure 3. Bivalent formats of the N1-3-VHH and N1-5-VHH, design and production. **A.** Diagram of the expression cassette of the N1-VHHb, which consist of two n1-vhhm moieties in tandem, fused by a linker: *pelB*, signal peptide to the periplasmic compartment; *n1-vhhm*, n1-3/5-vhhm genes; *hinge IgG2c*, hinge sequence of the llama IgG2c immunoglobulin; *his-tag*, hexahistidine sequence. **B.** Schematic diagram of the plant produced bivalent format N1-VHH-Fc T-DNA region in the binary vector pPhas: 3' *ocs*: 3' end of the octopine synthase gene; *npt II*, neomycin phosphotransferase II open reading frame; *Pnos*, nopaline synthase gene promoter; *Pphas*: β-phaseolin gene promoter; 5' *utr*: 5' UTR of *arc5-I* gene; *SS*: signal peptide of the Arabidopsis thaliana 2S2 seed storage protein gene; *n1-vhh-fc*: coding sequence of the N1-3/5/7-VHH-Fc;

KDEL: ER retention signal; 3' *arc*, 3' flanking regulatory sequences of the *arc5-l* gene; *RB* and *LB*: T-DNA right and left border, respectively. **C.** PCR amplification of the *n1-vhhm* (357 bp) and the *n1-vhhb* (763 bp) genes inserted in the pHEN6c vector, resolved in an agarose 1% gel. **D.** BamHI digested empty "E" or *n1-vhh-fc* gene inserted pPhasGW.*arc* vector. The 1066 bp band indicates an *n1-vhh-fc* gene insert. **E.** Cartoon representation of the 2 N1-VHH bivalent formats. The bacteria-produced N1-VHHb consists of two moieties in tandem of N1-VHHm linked by a llama IgG2c hinge of 17 amino acid residues. The plant-produced bivalent N1-VHH-Fc comprises two N1-VHH-Fc moieties, each consist of one N1-VHHm fused to a mouse IgG2a Fc, dimerized through a disulphide bond. **F.** The llama IgG2c-derived hinge is sensitive to trypsin. Coomassie stained reducing SDS-PAGE of purified N1-3-VHHm, N1-5-VHHm, N1-3-VHHb and N1-5-VHHb incubated for 37 min at 37 °C in the presence or absence of 1 µg/ml or 10 µg/ml trypsin. The N1-VHHb molecules migrate at ca. 32 kDa, and the N1-VHHm and the cleavage products of N1-VHHb migrate as bands of ca. 17 kDa (arrows). **G.** Coomassie stained reducing SDS-PAGE of the eluted fractions from a protein G column purification step using seed extracts of pPhas transformed *A. thaliana* T3 plants. The N1-VHH-Fc constructs migrate at ca. 42 kDa (arrow). A degradation product (*) of ca. 28 kDa corresponds to the Fc moiety only, as was confirmed by immunoblotting (data not shown).

Figure 4. Single intranasal administration of N1-3-VHHm, N1-5-VHHm, N1-3-VHHb and N1-5-VHHb decrease the morbidity during the first four days after challenge with H5N1 virus. **A.** Groups of 6-8 week-old Balb/c mice were given 100 µg of indicated VHH, administered intranasally at 4 hours before challenge with 4 LD50 of NIBRG-14ma virus. Thirty µg of intranasal administered H5-VHHb and daily oral administration of oseltamivir (45/kg/day, from 4 hrs before challenge) were included as positive controls. Body weight was monitored daily after challenge and expressed as the percentage of initial body weight. The groups of mice treated with N1-3-VHHm and N1-5-VHHm displayed significantly less morbidity than the groups treated

with PBS ($P < 0.001$), N1-7-VHHm ($P < 0.001$) at 72 and 96 hours post infection. **B.** Mice were sacrificed on day 4 after challenge and lung homogenates were prepared. A viral genome specific RT-qPCR was used as readout for the viral load. The obtained Ct values for the individual mice are plotted and a horizontal line indicates the mean. The Ct value H5-VHHb group was significantly different (indicative for lower virus load), compared to all other groups (***: $P < 0.001$). The oseltamivir treated group was only slightly different from the groups treated with the N1-3-VHHm, N1-5-VHHm and N1-7-VHHm (*: $P < 0.05$). **C.** The bivalent format of the N1-3-VHH and N1-5-VHH increases the potency to reduce the morbidity in H5N1-challenged mice. Four hours before challenge with 4 LD₅₀ of NIBRG-14 ma virus, groups of Balb/c mice were treated intranasally with 60 µg of N1-3-VHHb, 60 µg of N1-5-VHHb, 60 µg of BL-VHHb, 84 µg of N1-3-VHH-Fc, 84 µg of N1-5-VHH-Fc or 84 µg of GP4-Fc. Mice treated with neutralizing H5-VHHb (30 µg) or oseltamivir (45 mg/kg/day, daily by gavage) were included as positive controls. The groups treated with both bivalent formats of the N1-3-VHH and N1-5-VHH were significantly different compared with groups treated with: BL-VHHb and GP4-Fc at 60 hpi ($P < 0.05$), 72 and 96 hpi ($P < 0.001$); PBS, 36 and 60 hpi ($P < 0.05$), and at 72 and 96 hpi ($P < 0.001$).

Figure 5. The N1-VHH bivalent formats protect against morbidity and mortality in a dose-dependent way in H5N1-challenged mice. Groups of 4 Balb/c mice were given the indicated amount of N1-VHH and administered 24 hours before challenge with 4 LD₅₀ of NIBRG-14 ma virus. One group of mice was treated with one dose of oseltamivir (45 mg/day/kg) as positive control at 24 hrs before challenge, followed by daily boost from 6-14 days after challenge. A boost was given at 6 dpi only to the highest doses of each treatment, including the oseltamivir.

A. The group of mice treated with 60 µg of N1-3-VHHb presented significant increase in morbidity compared to the oseltamivir group at: 10 – 11 dpi ($P < 0.001$), 12-13 dpi ($P < 0.01$) and 14 dpi ($P < 0.05$). The difference of the morbidity between the different N1-3-VHHb treated

groups was not significant ($P > 0.05$). **B.** The survival of the N1-3-VHHb 60 μg group was 100 %, highly significantly different from the control groups BL-VHHb 60 μg and PBS (***, $P < 0.001$). In the group treated with 12 μg N1-3-VHHb survival was 50%, but still significantly different from the PBS groups (**, $P < 0.01$). The survival of the groups treated with N1-3-VHHb 2.5 μg (25 %) and 0.5 μg (0 %) was not different to the control groups ($P > 0.05$). **C.** The morbidity of the N1-5-VHHb 60 μg treated group was different from the N1-5-VHHb 12, 2.5 and 0.5 μg groups at days 10 – 14 ($P < 0.001$), but not different from the oseltamivir group ($P > 0.05$). **D.** The survival and significance of the N1-5-VHHb treated groups was similar to the N1-3-VHHb treatment in C. dpi, days post infection. **E.** Groups of 6 Balb/c mice were treated with different amounts of N1-3-VHH-Fc, but the difference in morbidity was not significant between them or compared with the oseltamivir treated group ($P > 0.05$). **F.** The survival and statistical significance of the N1-3-VHH-Fc treated groups treated with different doses and compared to the control groups PBS and GP4-Fc 84 μg : N1-3-VHH-Fc 84 μg and 17 μg , 100% (both ***, $P < 0.001$); N1-3-VHH-Fc 3.5 μg , 66.6 % (both, **, $P < 0.01$); 0.7 μg , 33.3 % (PBS, , $P < 0.05$,). **G.** The morbidity of the groups treated with N1-5-VHH-Fc was not significantly different between them, but different compared to the oseltamivir treated group. **H.** The survival of the groups treated with N1-5-VHH-Fc 84, 17 or 3.5 μg was 100%, being highly significantly different from survival in the groups GP4-Fc 84 μg and PBS (***, $P < 0.001$). The treatment with N1-5-VHH-Fc 0.7 μg resulted in a survival of 75 %, significantly different from the groups GP4-Fc 84 μg and PBS (**, $P < 0.01$).

Figure 6. Treatment with N1-3-VHHb or N1-3-VHH-Fc, but not with N1-5-VHHb/N1-5-VHH-Fc, rescues mice from a H5N1 H274Y 1 LD_{50} challenge. Twenty-four hours before challenge with 4 LD_{50} of NIBRG-14 or 1 LD_{50} H274Y H5N1 virus, groups of 6 Balb/c were given: 60 μg of N1-3-VHHb, N1-5-VHHb or BL-VHHb; 84 μg of the N1-3-VHH-Fc, N1-5-VHH-Fc or GP4-Fc. Groups of 6 mice were treated with oseltamivir (1 mg/day/kg) as positive control. **A.** There was no significant difference in the morbidity between the groups treated with N1-3-VHHb and N1-5-

VHHb, or compared to the Oseltamivir group during the NIBRG-14 infection ($P > 0.05$). **B.** In NIBRG-14 infected mice, the N1-3-VHHb, N1-5-VHHb and oseltamivir treated groups showed a survival of 100%, being significantly different from the control groups BL-VHHb and PBS (***, $P < 0.001$). **C.** The morbidity of H5N1 H274Y infected groups was severe, with all groups close to a body weight loss of 70 %, only the N1-3-VHHb treated group showed an increase of body weight at 10 dpi. **D.** The treatment with N1-3-VHHb rescued all the H5N1 H274Y infected mice (survival of 100 %), with high statistical significance compared with the rest of the groups (***, $P < 0.001$). The N1-5-VHHb and oseltamivir treatments failed to rescue H274Y infected mice. **E.** In NIBRG-14 infected mice, the difference in morbidity of the N1-5-VHH-Fc group compared with the N1-3-VHH-Fc, N1-7-VHH-Fc, GP4-Fc or oseltamivir groups is significant at days: 8-13 dpi ($P < 0.001$) and 14 dpi ($P < 0.01$). **F.** The treatment of N1-3-VHH-Fc, N1-5-VHH-Fc and oseltamivir in NIBRG-14 infected mice results in a highly significant (***, $P < 0.001$) survival of 100%. The group treated with N1-7-VHH-Fc presented a survival of 83.3 %, being significantly different compared to PBS (**, $P < 0.01$) and GP4-Fc ($P < 0.05$). **G.** In the same way as in C., the body weight loss was severe in the H5N1 H274Y infected mice, but the groups treated with N1-3-VHH-Fc and N1-7-VHH-Fc presented an increased in the body weight at 10 dpi. **H.** In H5N1 H274Y infected mice, the survival of the groups treated with N1-3-VHHb and N1-7-VHH-Fc was significant, 100 % (***, $P < 0.001$) and 66.6 % (**, $P < 0.05$), respectively. The N1-5-VHH-Fc and oseltamivir treatments failed to rescue H5N1 H274Y infected mice.

Figure 7. The treatment with N1-5-VHHb and N1-5-VHH-Fc decrease significantly the morbidity in NIBRG-14 challenged FcγRI / FcγRIII K.O. mice. Twenty-four hours before challenge with 4 LD₅₀ of NIBRG-14 virus, groups of 4 FcγRI / FcγRIII K.O. mice were given: 60 µg of N1-5-VHHb or 84 µg of the N1-5-VHH-Fc/N1-7-VHH-Fc/GP4-Fc. The N1-5-VHH-Fc treated group showed no morbidity and was statistically different to: the N1-5-VHHb group at 8 dpi ($P < 0.01$) and 9 dpi ($P < 0.05$); the N1-7-VHH-Fc group at 7- 11 dpi ($P < 0.001$), 12 dpi ($P < 0.01$) and 13 dpi ($P <$

0.05). The morbidity of the N1-5-VHHb treated group was statistically different to: GP4-Fc group, at 9 dpi ($P < 0.05$), 10 dpi ($P < 0.01$), 11– 12 dpi ($P < 0.001$) and 13 dpi ($P < 0.05$); PBS group, at 9-10 dpi ($P < 0.01$), 11 dpi ($P < 0.01$) and 12 dpi ($P < 0.05$). The morbidity between the N1-5-VHHb and the N1-7-VHH-Fc groups was not statistically different.

EXAMPLES

Materials and methods to the examples

H5N1 Influenza Virus

H5N1 influenza A virus NIBRG-14 and NIBRG-23 were obtained from the UK National Institute for Biological Standards and Control, a center of the Health Protection Agency. NIBRG-14 and NIBRG-23 are 2:6 reverse genetics–derived reassortant of NA and HA derived from (H5N1) A/Vietnam/1194/2004 or A\turkey\Turkey\2005 respectively, and (H1N1) A/PR/8/34 viruses, respectively. The H5N1 H274Y is a 1:1:6 reverse genetics-derived reassortant with the NA derived from A/crested eagle/Belgium/09/2004 (with the H274Y mutation introduced by site-specific mutagenesis), the HA from A/Vietnam/1194/2004 and the rest of the influenza genes from PR8. All of the HA segments lacks the polybasic cleavage site to allow their use in BioSafety level 2 (BSL-2) facilities. The NIBRG-14 and the H5N1 H274Y virus were passaged 7 times in specific pathogen–free Balb/c mice to obtain a mouse-adapted derivative (NIBRG-14 ma and H5N1 H274Y ma) and propagated in Madin-Darby canine kidney (MDCK) cells. The HA and NA coding region was sequenced and found to be identical in NIBRG-14 and H5N1 H274Y and NIBRG-14 ma H5N1 H274Y ma viruses (except the H274Y mutation). The median tissue culture infectious dose (TCID₅₀) and median lethal dose (LD₅₀) of NIBRG-14 ma, NIBRG-23 and H5N1 H274Y ma virus were determined using the method of Reed and Muench. All experiments with the previously described viruses were performed in BSL-2 rooms with negative pressure relative to adjoining rooms.

Baculovirus production of the N1rec

The N1rec expression cassette gene (*n1rec*) consisted of: hemagglutinin type 1 signal sequence (ssHA, 16 residues), a tetramerizing leucine zipper derived from transcription factor GCN4 (tGCN4, 32 residues) (Harbury et al. 1993), and the extracellular part of the H5N1 NA derived from A/crested eagle/Belgium/09/2004 (53–449 amino acid residues) (Van Borm et al. 2005). This expression cassette was cloned into a pAcMP2 Baculovirus transfer vector (BD Biosciences®), resulting in the pAcMP2*n1rec* vector. The *Autographa californica* nuclear polyedrosis virus (AcNPV) derived BaculoGold Linearized Baculovirus DNA (BD Biosciences®), and the pAcMP2*n1rec* were cotransfected in the clonal tissue culture line Sf9 derived from *Spodoptera frugiperda*, by the ESCORT IV Transfection Reagent (Sigma®), resulting in the recombinant AcNPVN1rec virus. The transfected Sf9 cells were incubated at 28 ° C in rolling tubes for 4 days. Then, 4 X 10⁸ cells Sf9 cells were infected with a multiplicity of infection (moi) of 10. After 7 days the supernatant was centrifuged 1 hr at 50000 g, and the NA activity was measured.

Neuraminidase activity assay.

The Neuraminidase (NA) activity was quantified by the cleavage of the fluorogenic substrate 4-MUNANA (2'-4-Methylumbelliferyl- α -D-N-acetylneuraminic acid, sodium salt hydrate, 50 mM, dissolved in deionized water, Sigma-Aldrich®) into free 4-methylumbelliferone, and measured with a excitation at 365 nm and fluorescence emission at 450 nm in a Optima Fluorostar®. The NA activity reaction mixture consisted of: 200 mM NaAc, 2 mM CaCl₂, 1 % butanol and 1 mM 4-MUNANA. The amount of NA was measured as NA units: 1 NA unit = 1 nmol of 4-methylumbelliferone / min.

N1rec purification

Two parts of n-butanol were added to 3 parts of cleared AcNPVN1rec infected Sf9 cells supernatant. An aqueous phase, containing the soluble N1rec, was extracted from a lipid phase,

and was 2.5 times diluted in 5 mM KH₂PO₄ pH 6.6 and 0.22 µm filtered. The diluted aqueous phase was applied to a HA Ultrogel® Hydroxyapatite Chromatography Sorbent (Pall®) packed XK26\70 column (GE Healthcare®), and eluted with a gradient of 5 - 400 mM KH₂PO₄ pH 6.6, 4 % butanol to KH₂PO₄ pH 6.6, 4 % butanol. Eluted fractions that scored positive to NA activity were pooled and loaded into a 50 mM MES pH 6.6, 5 % glycerol, 8 mM CaCl₂ equilibrated 10 ml column packed with Blue Sepharose (Sigma-Aldrich®). A single step elution was done with 50 mM MES pH 6.6, 5 % glycerol, 8 mM CaCl₂, 1.5 NaCl. A desalting step was performed by gel filtration in XK70 packed with HiLoad 16/60 Superdex 200 pg (GE Healthcare®) column equilibrated with 50 mM MES pH 6.6, 5 % glycerol, 8 mM CaCl₂, 150 mM NaCl. All the chromatography steps were performed on an Akta purification station (GE Healthcare®).

Camelid immunization and phage library construction

An alpaca (*Vicugna pacos*) was weekly injected subcutaneously with 125 µg of N1rec during 35 days. On day 39, anticoagulated blood was collected for the preparation of lymphocytes. Lymphocytes were isolated using a UNI-SEP density gradient separation kit (NOVAmed®), and total RNA was extracted. cDNA was prepared using using oligo (dT) primers, and the VH and VHH genes were amplified with: primer call 01 (GTCCTGGCTGCTCTTCTACAAGG) and primer call 02 (GGTACGTGCTGTTGAACTGTTCC). The PstI and NotI restriction sites were inserted into the amplified sequences using the primers: A6E (GAT GTG CAG CTG CAG GAG TCT GGR GGA GG) and 38 (GGA CTA GTG CGG CCG CTG GAG ACG GTG ACC TGG GT). The PCR 550 bp product and the vector pHEN4 were PstI and NotI digested and ligated (Arbabi Ghahroudi et al. 1997). This ligation was used for the transformation of electrocompetent TGI *E. coli* cells, and was growth in 2xTY (supplemented with 100 µg/ml ampicilin and 1% glucose) into the exponential phase, and the helper phage M13K07 was added. The library was subjected to 4 consecutive rounds of panning, performed in solid-phase coated N1rec (200 µg/ml) to select N1rec-binding phages.

N1-VHHm production and purification.

The VHH genes of the selected N1rec binding phages, contained in the pHEN4 phagemid, were amplified by PCR amplification with the primers: A6E (GAT GTG CAG CTG CAG GAG TCT GGR GGA GG) and 38 (GGA CTA GTG CGG CCG CTG GAG ACG GTG ACC TGG GT). A 400 bp PCR product and the pHEN6c vector were *Pst*I and *Bst*EII digested and purified with the PCR product purification kit (Roche®) and ligated. Competent *E. coli* WK6 strains were transformed with the ligation mix. Positive colonies were screened by PCR amplification for a 550 bp fragment using the primers: universal reverse primer (TCACACAGGAAACAGCTATGAC) and the universal forward primer (CGCCAGGGTTTTCCCAGTCACGAC). The VHH gene cloned in the pHEN6c vector contains *PeIB* signal sequence at the N-terminus and a hexahistidine tag at the C - terminus. WK6 cells transformed with the pHEN6c harboring the VHH genes were growth in TB medium supplemented with ampicillin (100 µg/ml), 2 mM CaCl₂ and 0.1% glucose. The production of the VHH was induced with 1 mM of IPTG. The periplasmic extracts were obtained by osmotic shock using TES (0.2 M Tris pH 8.0, 0.5 mM EDTA and 0.5 M sucrose). Periplasmic extracts were centrifuged at 8000 rpm at 4 °C and the supernatant was applied to a His Select Nickel Affinity gel (Sigma®), washed with PBS and the soluble VHH was eluted with 0.5 Imidazole and dialyzed at 4 °C with PBS by ultrafiltration (cutoff 3.5 kDa). Concentration of the monomeric VHH (VHHm) was performed in a Vivaspin 5000 MW (Vivascience®). Total protein concentration was determined with BCA protein Assay kit (Thermo Scientific®).

Theoretical N1-VHHm structure prediction

The amino acid sequence of the 13 different candidates VHH directed against NA were loaded in the ESyPred3D Web Server 1.0 Molecular Biology Research Unit, The University of Namur, Belgium (<http://www.fundp.ac.be/sciences/biologie/urbm/bioinfo/esypred/>) and retrieved as PDB

files. The structures of the 13 N1-VHHm were modeled with DeepView/Swiss-PdbViewer (<http://spdbv.vital-it.ch/>).

VHH Surface Plasmon resonance analysis

The affinity of the N1-3-VHHm, N1-5-VHHm and N1-7-VHHm elicited against N1rec were determined by surface plasmon resonance (SPR) on a Biacore3000. N1rec antigen was first immobilized (2000 RU) into a Series S sensor chip CM5 (GE Healthcare®) (coupling was in 10 mM NaAc, pH 4.5), with regeneration in 0.02% SDS. Subsequently, each N1-VHHm was diluted in HBS buffer (0.01 M HEPES, 0.15 M NaCl, 0.005% Tween 20, pH 6.4) to arrive at a concentration between 1.95 and 1000 nM and was injected over the CM5 chip to record its binding kinetics with the N1rec. Binding sensograms were used to calculate the K_{on} and K_{off} values with the Biacore T100 evaluation software and to determine the equilibrium dissociation constant (K_D) and the epitome analysis.

Construction of the N1-VHH bivalent

The genes encoding the N1-3-VHHm or the N1-5-VHHm were amplified with primers MH (5'-CATGCCATGGGAGCTTTGGGAGCTTTGGAGCTGGGGGTCTTCGCTGTGGTGCGCTGAGGAGACGGTGACCTGGGT-3') and A4 short (5'-CATGCCATGATCCGCGGCCAGCCGGCCATGGCTGATGTGCAGCTGGTGGAGTCT-3') to introduce a *NcoI* restriction enzyme site at both extremities of the amplified fragment. The MH primer also added the hinge sequence of llama γ 2c (AL-His-His-Ser-Glu-Asp-Pro-Ser-Ser-Lys-Ala-Pro-Lys-Ala-Pro-Met-Ala) (Hmila et al. 2010) to the 3' end of the VHH. The PCR amplified product was then purified with PCR product purification kit (Roche®). The PCR product and the pHEN6c plasmid containing the *n1-3-vhh* or the *n1-5-vhh* genes were digested for several hours with *NcoI* enzyme and treated with alkaline phosphatase, and then purified. Finally, the pHEN6c recombinant plasmid and the PCR fragment were ligated with T4 DNA ligase (Fermentas®). The ligated product was used to transform *E. coli* WK6 electrocompetent cells. Clones were

screened by PCR using the universal forward and reverse sequencing primers for the presence of the bivalent construct. The amplification products of ca 1000 bp were sequenced to ensure the absence of unintended mutations. After expression, the encoded protein was tested for binding to N1rec by ELISA. To obtain larger amounts of the tandemly linked bispecific N1-VHH construct, the protocols for the expression and purification conditions of the N1-VHHm were followed (see above).

Plant produced N1-VHH-Fc expression cassette

The *n1-vhh-fc* expression cassette was designed as follows, from 5' to 3': *LB* (left border of TDNA); *3' ocs* (3' end of the octopine synthase gene); *npt II* (neomycin phosphotransferase II open reading frame); *Pnos* (nopaline synthase gene promoter); *Pphas* (β -phaseolin gene promoter); *5' utr* (5' UTR of *arc5-I* gene); *SS* (signal peptide of the *Arabidopsis thaliana* 2S2 seed storage protein gene); *KDEL* (ER retention signal); *n1-3-vhh* (coding sequence of the N1-3-VHH); *3' arc* (3' flanking regulatory sequences of the *arc5-I* gene); *n1-3-vhh* (coding sequence of the N1-3-VHH fused to the mouse CH2 and CH3 IgG2a hinge sequence); *RB*, DNA right border (De Jaeger et al. 2002) (Van Droogenbroeck et al. 2007). This expression cassette was synthesized in the commercial vector pUC57 (GenScript®), and cloned into a pPhasGW binary T-DNA vector, resulting in the *pPhasGWn1-vhh-fc* vector.

Production and purification of soluble N1-VHH-Fc

The *pPhasGWn1-vhh-fc* was used for transformation of *Agrobacterium* C58C1RifR(pMP90). This *Agrobacterium* strain was grown on YEB medium supplemented with rifampicin (100 mg/L), gentamycin (40 mg/L), spectinomycin (100 mg/L) and streptomycin (300 mg/L). *Arabidopsis* transformants are obtained via *Agrobacterium*-mediated floral dip transformation (Clough and Bent 1998). Seeds from T1 segregating plants were crushed and total protein was extracted with: 50 mM Tris-HCl, pH 8.0, 200 mM NaCl, 5 mM EDTA, 0.1% (v/v) of Tween 20 and

Complete® protease inhibitor tablets (Roche®). The seed extracts were applied to a protein G sepharose column (GE Healthcare®) and eluted fractions were analyzed.

Inhibitory immune plaque assay

Monolayers of MDCK cells were grown in DMEM supplemented with 10% Fetal Bovine Serum, 1% penicillin/streptomycin, 1% glutamine at 37 °C with 5% CO₂. MDCK TMPRSS2 medium was supplemented with geneticin (0.3 mg/ml) and puromycin (2 µg/ml) and the expression of TMPRSS2 was induced with doxycycline (0.5 µg/ml). At 70% of confluency, the MDCK cells were infected with a moi of 10 with the corresponding virus. The antiviral treatment was mixed with 0.8% of Avicel RC-591 as an overlay (Matrosovich et al. 2006). After different times of incubation, cells were fixed with 4% paraformaldehyde in PBS for 30 min. The cells were permeabilized with 20 mM glycine, 0.5% (v/v) Triton X-100. After blocking, the cells were incubated for 2 hrs with polyclonal α-NIBRG-14 (1:1000) and α-M2e (mAb 148, 1:5000). After washing, α mouse IgG-HRP conjugated was used to visualize plaques using the substrate TrueBlue™ Peroxidase Substrate (KPL®).

Neuraminidase sequences alignment

The phylogenetic tree and aminoacids substitutions of the aligned sequences of the H5N1 NA of: A/crested eagle/Belgium/01/2004 (accession number: ABP52007), A/Vietnam/1194/2004 (ABA70757) and A/turkey/Turkey/01/2005 (ABQ58915), were obtained by the Clustal W method, in the MegAlign software (DNASTAR®).

Prophylactic Efficacy Studies in Mice

Specific-pathogen-free female Balb/c mice, 7–9 weeks old, were purchased from Charles River (Germany) and used for all experiments. Mice were housed in cages individually ventilated with high-efficiency particulate air filters in temperature-controlled, air-conditioned facilities with food and water *ad libitum*. Mice were anesthetized by intraperitoneal injection of xylazine (10 µg/g) and ketamine (100 µg/g) before intranasal administration of N1-VHH or challenge virus (50 µl,

divided equally between the nostrils). The N1-VHH in any format were diluted in endotoxin-free phosphate-buffered saline (PBS) with 1% (weight/volume) bovine serum albumin and administered as a single dose, ranging from 100 to 0.5 µg per mouse (5–0.25 mg/kg). To determine the effect of intranasal N1-VHH delivery on lung virus titer production, mice were challenged with 4 LD₅₀ of NIBRG-14ma virus. Lung homogenates were prepared in PBS, cleared by centrifugation at 4°C, and used for virus titration. Monolayers of MDCK cells were infected with 50 µl of serial 1:10 dilutions of the lung homogenates, in a 96-well plate in serum-free Dulbecco's modified Eagle medium (Invitrogen®) supplemented with penicillin and streptomycin. After 1 h, the inoculum was replaced by medium containing 2 µg/ml of L-(tosylamido-2-phenyl) ethyl chloromethyl ketone–treated trypsin (Sigma®). End-point virus titers were determined by hemagglutination of chicken red blood cells and expressed as TCID₅₀ per milliliter. Influenza RNA levels were determined with quantitative polymerase chain reaction (PCR). RNA was isolated from 150 µl of cleared lung homogenate using the Nucleospin RNA virus kit (Machery-Nagel®). The relative amount of NIBRG-14 ma genomic RNA was determined by preparing viral cDNA and performing quantitative PCR with M-genomic segment primers 5'TCGAAAGGAACAGCAGAGTG3' and 5'CCAGCTCTATGCTGACAAAATG3' and probe 5'GGATGCTG3' (probe no. 89; Universal ProbeLibrary, Roche) and the LightCycler 480 Real-Time PCR System (Roche®). To determine the degree of protection against mortality, mice were challenged with 4 LD₅₀ of NIBRG-14 ma virus and subsequently monitored for 14 days. A 30% loss in body weight drop was the end point at which moribund mice were euthanized. All animal procedures were approved by the Institutional Ethics Committee on Experimental Animals.

Statistical Analysis

Graphpad (Graphpad Prism®, version 5) was used for statistical analysis. Differences between groups were tested using the 2-way ANOVA. When this test demonstrated a significant

difference between groups ($P < .05$), t tests were used to compare 2 groups. Kaplan-Meier survival curves were plotted and evaluated.

Example 1: Production of recombinant tetrameric Neuraminidase

A Baculovirus Expression Vector System was used to produce a recombinant H5N1 NA derived from A/crested eagle/Belgium/09/2004. The N1rec expression cassette gene (*n1rec*) (Figure 1A) was cloned into a pAcMP2 expression vector (pAcMP2*n1rec*), under the control of the AcNPV basic protein promoter, an infectious cycle late phase promoter preferred for the production of proteins with post-translational modifications (BD Biosciences®). Infection of *Spodoptera frugiperda* (Sf9) cells with a recombinant baculovirus containing the N1rec expression cassette resulted in sialidase activity in the cell supernatant suggesting that the N1rec product was soluble and enzymatically active tetrameric NA (Figure 1B). The N1rec in the culture supernatant was purified from the culture supernatant. Following a final size exclusion chromatography step, we obtained 90% pure N1rec (Figure 1C). The theoretical molecular weight of N1rec is 49.5 kDa. The relative electrophoretic mobility in SDS-PAGE suggested a size of approximately 60 kDa (Figure 1D), presumably due to the presence of glycosylations; there are predicted 3 N-glycosylation and 2 O-glycosylation sites in the N1rec. The purified protein had a specific activity of 56850.9 NA units/mg of total protein.

Example 2: Immunization and VHH phage library construction

N1rec was next used as an immunogen for the generation and selection of NA-specific VHH. An alpaca (*Vicunia pacos*) was immunized at day 0 with 125 µg of N1rec, followed by 6 weekly boosts. One week after the last immunization, blood was collected and peripheral blood lymphocytes were isolated. From the lymphocytes, total RNA was extracted and used as template for cDNA synthesis. The VH and VHH genes were amplified by PCR, and the VHH genes were isolated and cloned into the phagemid vector pHEN4 (Arabi Ghahroudi et al.

1997). We obtained a VHH phage library of 2×10^8 independent transformants. Fifty seven % of these transformants harbored a pHEN4 with a VHH cDNA insert of the correct size (550 bp). The VHH phage display library was then subjected to four consecutive rounds of panning, performed on solid-phase coated N1rec antigen. From the panning, 78 positive clones were retained. Subsequent Restriction fragment Length Polymorphism analysis narrowed down the N1rec-specific VHH candidates to 24 colonies, encoding 13 different VHHs. Sequences analysis of these 13 VHHs allowed classifying them into 9 clonally related groups, with differences mainly in the CDR3 domain sequence (Figure 2A). We named these N1rec-binding VHHs N1-(1-13)-VHH. The *in silico* predicted topology of the 13 N1-VHH, suggested that they covered a diverse range of CDR3 structures (Figure 2B). Some of the N1-VHH structures showed a protruding electronegatively charged CDR3 (e.g. N1-3-VHHm, Figure 2B).

Example 3: Production and characterization of soluble N1-VHHm

The coding information for each of the 13 N1-VHH candidates was transferred into the bacterial expression vector pHEN6 under the control of a lac operon, for expression and purifications purposes (Kang et al., 1991). The transformation of amber suppressor *E. coli* strain WK6 with the pHEN6 $n1-vhh$ produced a monomeric N1-VHH (N1-VHHm) that is targeted to the periplasm and C-terminally tagged with hexahistidine. Following osmotic shock, periplasmic extracts were prepared and loaded onto a nickel sepharose column, to purify a set of 13 N1-VHH proteins (Figure 2C). The binding of each of the 13 N1-VHHm to the NA part of N1rec, but not to the tGCN4 moiety, was confirmed by ELISA (data not shown). We next assessed the capacity of our monovalent N1-VHHm candidates to inhibit the enzymatic activity of N1rec. For this, we used a small substrate-based fluorogenic assay to evaluate the potential inhibitory activity of our N1-VHHm. Interestingly, 4 candidates; N1-1-VHHm, N1-3-VHHm, N1-5-VHHm and N1-6-VHHm could inhibit the N1rec catalytic activity. The N1-3-VHHm and the N1-5-VHHm were the most potent inhibitors of the N1rec catalytic activity (data not shown), and together with N1-7-VHHm,

were analyzed by surface plasmon resonance using immobilized N1rec. The N1-7-VHHm was included in this analysis as a binding but non-inhibitory N1-VHHm control. Both N1-3-VHHm and N1-5-VHHm presented a high affinity for N1rec, with an equilibrium dissociation constant (K_D) in the low nanomolar (N1-5-VHHm) to picomolar (N1-3-VHHm) range. N1-7-VHHm showed an approximately 10- to 100-fold lower affinity K_D than N1-5-VHHm and N1-3-VHHm, respectively (data not shown). These binding affinities of N1-3-VHHm and N1-5-VHHm for N1rec are comparable to the maximal affinities reported for a monomeric VHH (De Genst et al., 2006). Competitive surface plasmon resonance analysis also showed that prior binding of N1-3-VHHm to N1rec abolished subsequent binding of N1-5-VHHm and vice versa. On the other hand, N1-7-VHHm binding to N1rec was not affected by prior binding of N1-3-VHHm or N1-5-VHHm to N1rec (data not shown). This observation suggests that N1-3-VHHm and N1-5-VHHm bind an overlapping epitope in N1rec, while the N1-7-VHHm targets a different epitope.

We next analyzed the antiviral potential of the N1rec inhibitory VHHs, N1-3-VHHm and N1-5-VHHm. A/crested eagle/Belgium/09/2004 is a highly pathogenic H5N1 virus that we could not handle in our BLS-2 facilities. Therefore, we used the laboratory strain NIBRG-14 virus, generated by reverse genetics and containing NA and HA (lacking the polybasic maturation sequence) segments derived from A/Vietnam/1194/2004. The NA sequences of these two H5N1 viruses are highly homologous with only 13 amino acid sequence differences. In the presence of N1-3-VHHm or N1-5-VHHm the size and number of NIBRG-14 plaques in monolayers of infected MDCK cells were reduced in a concentration dependent manner (data not shown). In contrast, the N1-7-VHHm did not affect the size or number of NIBRG-14 plaques in this assay (data not shown). These results suggest that the *in vitro* antiviral potential of the N1-3-VHHm and N1-5-VHHm depends of their NA-inhibitory activity.

Example 4: A bivalent format of the N1-VHH enhances their NA-inhibitory and antiviral activity

It has been reported that multivalent formats of VHHs increases their affinity, by introducing avidity, for their target antigen and often also their functional activity (Hultberg et al., 2011) (Ibanez et al., 2011) (Schepens et al., 2011). For example, the introduction of avidity drastically decreased the dissociation constant (K_{off}) of the VHH molecules directed against lysozyme, and significantly improved their enzyme inhibitory activity as compared to their monovalent counterpart formats (Els Conrath et al. 2001) (Hmila et al. 2010). To increase the avidity of the N1-VHHm, two different bivalent formats were produced. As a first approach to obtain bivalent VHH, we used the llama IgG2c hinge (17 amino acid residues) as flexible linker to fuse 2 identical inhibitory N1-VHHm in a tandem configuration resulting in N1-3-VHHb and N1-5-VHHb (Figure 3C). N1-3-VHHb and N1-5-VHHb were expressed and purified from *E. coli* and their *in vitro* NA inhibitory and antiviral activities were compared with those of their monovalent counterparts. We found that N1-3-VHHb and N1-5-VHHb displayed a 500-2000 fold enhanced N1rec inhibition activity as compared with the corresponding monovalent N1-3-VHHm and N1-5-VHHm format. Surprisingly, in a plaque assay using NIBRG-14 virus infected MDCK cells, both N1-3-VHHb and N1-5-VHHb had an antiviral activity that was comparable to the levels of their monovalent counterparts (data not shown). We reasoned that the integrity of the bivalent format is necessary to present an enhanced antiviral potency in both N1-VHHb. However, in the plaque assay with H5N1 infected MDCK cells, exogenous trypsin is used to facilitate maturation of HA in newly produced virions to allow multicycle replication of the recombinant NIBRG-14 virus. We found that the dimerizing llama IgG2c hinge linker in the N1-VHHb was sensitive to trypsin cleavage (Figure 3F). Therefore, in the presence of relatively low amounts of trypsin N1-3-VHHb and N1-5-VHHb were effectively severed into monovalent VHH. To circumvent the use of

exogenously added trypsin we took advantage of the TMPRSS2 MDCK cells, which are stably transformed with the doxycycline inducible serine protease TMPRSS2 and allow multicycle replication of influenza A viruses in the absence of trypsin (Bottcher et al., 2009). Using monolayers of TMPRSS2 MDCK cells for infection with NIBRG-14, the antiviral effect of N1-3-VHHb and N1-5-VHHb was 240 and 58 fold increased, respectively, compared with their monovalent format (data not shown). These results obtained with N1-VHHb indicate that (i) there is a significantly enhanced NA-inhibitory and antiviral activity of both N1-VHHb compared with the N1-VHHm format and (ii) the 10-fold difference between the increase of the N1rec inhibition compared to the plaque assay, suggests that there are other factors that account for the *in vitro* antiviral effect of the N1-VHHb than just their inhibitory potential.

Example 5: Transgenic plant produced bivalent N1-VHH (N1-VHH-Fc)

The previously described N1-VHH monovalent or bivalent molecules are relatively simple molecules that are stable and small sized, feasible for production in prokaryotic and yeast systems. For more complex protein molecules, other production platforms are available and have to be considered. We used a plant-based approach, with reported high-end yield results for recombinant antibodies (Van Droogenbroeck et al., 2007). In particular, targeting the protein of interest as a seed storage protein, we were able to produce a second bivalent N1-VHH format. For this, the *n1-3-vhh*, *n1-5-vhh* and the *n1-7-vhh* genes were fused to the sequence encoding the hinge and Fc tail of a mouse IgG2a (*n1-vhh-fc*). The resulting N1-VHH-Fc consists of two identical N1-VHH-Fc moieties linked by a disulphide bridge (Figure 3B). These *n1-vhh-fc* constructs were cloned into the binary vector pPhas as a T-DNA expression cassette (Figure 3E). Subsequently, transgenic *Arabidopsis thaliana* plants were generated by *Agrobacterium*-mediated floral dip transformation. Seed extract of segregating T3 *Arabidopsis* clones were used for screening to identify the highest expressers of the recombinant dimeric protein N1-VHH-Fc (data not shown). Coomassie stained, reducing SDS-PAGE analysis showed that the

N1-VHH-Fc monomers migrated at ca. 42 kDa band (Figure 3F). We also found a good correlation between the expression level of the N1-VHH-Fc and the NA inhibitory activity in crude seed extracts from different T3 transformants (data not shown). The N1-3-VHH-Fc, N1-5VHH-Fc and N1-7-VHH-Fc were purified from seed extracts by protein G affinity chromatography (Figure 3G). We found stronger N1rec inhibition and *in vitro* antiviral activity by N1-3-VHH-Fc and N1-5-VHH-Fc compared with the monovalent N1-3-VHHm and N1-5-VHHm (data not shown). Nevertheless, the N1-3-VHHb and N1-5-VHHb still proved to be 2 to 8 times more potent in NA inhibition compared with N1-3-VHH-Fc and N1-5-VHH-Fc. In addition, inhibition of replication of NIBRG-14 virus by either N1-3-VHH-Fc or N1-5-VHH-Fc was 80- and 30-fold stronger, respectively, compared with their monovalent counterparts. We conclude that the *in vitro* NA inhibition and antiviral activity against NIBRG-14 virus is strongly enhanced by bivalent N1-VHH formats with the highest improvement observed for tandemly linked copies of VHH molecules.

Example 6: *In vitro* antiviral activity of N1-VHH against clade 2.2 and oseltamivir-resistant H5N1 virus

The NA derived from A/crested eagle/Belgium/01/2004 belongs to the clade 1 of the H5N1 NAs, which also includes NA of the NIBRG-14 (derived from A/Vietnam/1194/2004). H5N1 NA derived from A/turkey/Turkey/01/2005 belongs to the clade 2.2. These 3 different NAs shared a high homology between them (> 95%) and were used as targets in the present study. Although the number of laboratory confirmed human cases of H5N1 virus infection remain limited, it appears that clade 2 H5N1 viruses comprise a majority of these zoonotic infections with highly pathogenic avian influenza viruses. We therefore evaluated the antiviral potential of N1-3-VHH and N1-5-VHH in the three formats available (*i.e.* monovalent, bivalent without and with Fc) against the clade 2.2 virus NIBRG-23. Monovalent N1-3-VHHm and N1-5-VHHm reduced *in vitro* growth of NIBRG-23 virus on MDCK with an IC₅₀ in the low micromolar range. Both

bivalent formats of these NA-inhibitory VHH, (N1-3-VHHb, N1-5-VHHb, N1-3-VHH-Fc and N1-5-VHH-Fc) displayed an approximately 150-fold higher *in vitro* antiviral activity against this clade 2 virus as judged by a plaque size reduction assay, compared with their monovalent counterparts. Based on these findings, we conclude that the two NA-inhibitory VHH can inhibit H5N1 viruses, representative for clade 1 and clade 2 with a comparable efficiency *in vitro*, suggesting that they target an epitope that is shared in the NA of these viruses. Oseltamivir-resistant influenza viruses frequently emerge and spread in the human population. Several mutations had been reported to contribute to oseltamivir resistance but among these the mutation H274Y (N2 numbering) is the most commonly found in oseltamivir resistant viruses (Wang et al., 2002). Therefore, we wanted to determine if our N1-3-VHHb, N1-5-VHHb, N1-3-5 VHH-Fc and N1-5-VHH-Fc would be active against an oseltamivir-resistant H5N1 virus that carries this mutation. We used a reverse genetics method (Hoffmann et al., 2000) to generate a clade 1 H5N1 virus (harboring the H274Y mutation in NA derived from A/crested eagle/Belgium/09/2004, the HA segment from NIBRG-14 and the remaining 6 segments from PR/8), resulting in the H5N1 H274Y virus used in this study. Given that all of our formats of N1-3-VHH and N1-5-VHH performed similar in biochemical and *in vitro* antiviral activity assays, we were surprised to observe that only the N1-3-VHH in monovalent and both bivalent formats, but not any format of N1-5-VHH, reduced growth of oseltamivir-resistant H5N1 H274Y virus (data not shown). Compared to NIBRG-14 as a target, the H5N1 H274Y IC₅₀ values were 3 to 7-fold higher, but still in the low nM range. Even though the competitive surface Plasmon resonance experiment suggested that the epitope in NA is shared for both N1-3-VHHm and N1-5-VHHm, the contact residues necessary for their binding are not the same. The H274Y mutation seems to be sufficient to abolish the *in vitro* antiviral effect of the N1-5-VHH formats during the infection with the H5N1 H274Y mutant virus used here. We conclude that NA-specific VHH, such as N1-3-

VHHm, N1-3-VHHb and N1-3-VHH-Fc can inhibit growth of H5N1 viruses *in vitro*, even if such viruses are oseltamivir resistant.

Example 7: The treatment with N1-3-VHHm and N1-5-VHHm reduces morbidity in H5N1-challenged mice

We next evaluated the *in vivo* antiviral effect of the NA-specific VHH. In a first experiment we administered intranasally 100 µg of N1-3-VHHm, N1-5-VHHm, and N1-7-VHHm to Balb/c mice at 4 hours before challenge with 4 LD₅₀ of mouse-adapted NIBRG-14 virus (NIBRG-14ma). As positive controls we included a group of mice that received 30 µg of H5-VHHb, a bivalent NIBRG-14ma-neutralizing VHH (Ibanez et al., 2011) as well as daily oral administration of oseltamivir, at a high dose (45 mg/kg/day). The body weight was followed daily, and the groups treated with the inhibitory N1-3-VHHm or N1-5-VHHm showed a significant difference in morbidity at 72 and 96 hours after infection, compared with the groups treated with the N1-7-VHHm and PBS ($P < 0.001$) (Figure 4A). Four days after infection, the mice were sacrificed to determine lung virus titers. Assessment of the lung virus load by endpoint dilution in a TCID₅₀ assay, revealed that all mice had a high and comparable virus load between -4.75 to -6.48 TCID₅₀/ml in the lung homogenates (including the oseltamivir treated group)(data not shown). We therefore decided to quantify the amount of viral RNA in the lung homogenates using a genome strand-specific RT-qPCR method. Except for the samples derived from the H5-VHHb treated mice, all the N1-VHH treated groups showed high viral RNA levels at 96 h after infection, comparable to those in the PBS-treated group, even so for the high oseltamivir dose treated mice, which difference with the rest of the groups was significant ($P < 0.05$) (Figure 4B). We conclude that intranasal administration of monovalent N1-3-VHHm and N1-5-VHHm prevents body weight loss after challenge with NIBR-14 ma virus during the early stage of infection.

Example 8: Bivalent formats of N1-VHHb protect against H5N1 challenge

The *in vitro* results indicated that the bivalent formats of the NA-inhibitory VHH increased their potency against the tested H5N1 viruses at least 30-fold compared to the monovalent ones (Table 3). We therefore assessed if this increased antiviral effect would also be reflected in an *in vivo* challenge experiment. We first determined the protective potential during the early stages of viral infection. Four hours prior to challenge with 4 LD₅₀ of NIBRG-14 groups of Balb/c mice were intranasally given 60 µg of N1-3-VHHb, 60 µg of N1-5-VHHb, 60 µg of BL-VHHb (a bivalent VHH directed against the irrelevant bacterial target β-lactamase), 84 µg of N1-3-VHH-Fc, 84 µg of N1-5-VHH-Fc or 84 µg of GP4-Fc (a plant-produced Coronavirus-Fc fusion protein with an IgG2a Fc moiety, used here as an irrelevant control). Treatment with N1-3-VHHb or with N1-3-VHH-Fc significantly improved morbidity at 72 and 96 h after infection compared with the negative control groups GP4-Fc and PBS ($P < 0.001$). This protection against weight loss was comparable to that observed with the positive controls (H5-VHHb and oseltamivir) (Figure 4C). On the other hand, treatment with the bivalent formats of N1-5-VHH resulted in a decrease in morbidity that was significant at 60, 72 and 96 hpi compared with the negative controls ($P < 0.001$) (Figure 4C). Determination of the lung virus load on day 4 after challenge by a TCID₅₀-based assay using lung homogenates from sacrificed mice, revealed that all challenged groups, except the H5-VHHb-treated mice (no virus detectable), had a comparable lung virus load (data not shown). Taken together, both bivalent formats (tandem repeats and Fc-mediated) of N1-inhibitory N1-3-VHH and N1-5-VHH improve protection during the first four days following NIBRG-14 challenge.

Example 9: Bivalent NA inhibitory VHH protection against a lethal challenge with H5N1 virus is dose-dependent

In order to probe if mice that have been challenged with 4 LD₅₀ of NIBRG-14ma virus can be rescued by prior administration of N1-3-VHHb, N1-3-VHH-Fc, N1-5-VHHb or N1-5-VHH-Fc we

followed the morbidity and mortality over a 2-week period. For this, we focused on the bivalent formats and first assessed their protective efficacy in a dose-response experiment. Groups of four Balb/c mice were treated intranasally with 60, 12, 2.5 or 0.5 µg of N1-3-VHHb or N1-5-VHHb. In parallel a group was treated by oral administration of oseltamivir (45 mg/kg/day), and boost of oseltamivir were given at 6 – 14 days after challenged. In addition, one group of mice was treated with 60 µg of BL-VHHb or with PBS prior to challenge. In this experiment mice that had received 60 µg of N1-3-VHHb, N1-5-VHHb or BL-VHHb prior to challenge received a second intranasal dose with 60 µg of the same bivalent VHH at day 6 after challenge. All mice from the PBS and BL-VHHb treatment groups succumbed after challenge at 9 -10 days after challenged. In contrast, oseltamivir and high dose (60 µg) intranasal treatment with N1-3-VHHb or N1-5-VHHb displayed clear body weight loss following challenge (Figure 5A and C), but protected the mice against lethality (Figure 5B and D). Surviving N1-3-VHHb 60 µg treated group, but not the N1-5-VHHb 60 µg treated group, displayed a significant delay in recovery from weight loss after challenge compared with the oseltamivir treated group (Figure 5A and C). A single intranasal dose of 12 µg or 2.5 µg of either N1-3-VHHb or N1-5-VHHb provided partial protection against mortality but failed to reduce morbidity (Figure 5A-D). We next evaluated protection against a potentially lethal NIBRG-14 challenge by prior single intranasal administration of the plant-produced N1-3-VHH-Fc and N1-5-VHH-Fc formats. Eighty four and 17 µg of N1-3-VHH-Fc as well as oseltamivir treatment provided full protection against NIBRG-14 challenge but the survival of the mice treated with 3.5 and 0.7 µg was dose-dependent (Figure 5F and H). Nevertheless this protection was associated with significant body weight loss in all dosing used, including the oseltamivir group (Figure 5E and G). All PBS and GP4-Fc treated animals died after challenge by day 9 after challenge. On the other hand, the body weight loss was less severe in the treatment with all N1-5-VHH-Fc treated groups, and only the group treated with 0.7 µg failed to show a survival of 100% (Figure 5G and H). Finally, when

comparing the protective efficacy of the two bivalent formats of N1-3-VHH and N1-5-VHH, it appears that the Fc moiety in the N1-VHH-Fc formats provides an extra protective effect against morbidity and mortality following NIBRG-14ma challenge. This increased protective potential correlates with the somewhat higher NA inhibitory activity in a biochemical assay using purified N1rec but is not reflected in the plaque number/size reduction assay (data not shown). Taken together, we conclude that bivalent formats of N1-3-VHH and N1-5-VHH can protect mice against a potentially lethal challenge with an H5N1 virus, although this protection does not eliminate completely morbidity following challenge.

Example 10: N1-3-VHHb and N1-3-VHH-Fc protect against challenge with an oseltamivir-resistant

H5N1 virus

In vitro analysis demonstrated that N1-3-VHH but not N1-5-VHH in monovalent or bivalent format could reduce growth of oseltamivir-resistant H5N1 H274Y virus. Groups of 6 Balb/c mice received 30 µg of N1-3-VHHb, N1-5-VHHb or BL-VHHb by intranasal administration 24 hours before challenge with 4 LD₅₀ of either NIBRG-14 ma or H5N1 H274Y virus. A PBS-recipient group was included as negative control. In parallel, a group was treated by daily oral administration of oseltamivir (1 mg/kg/day), a dose that has been reported to protect laboratory mice against challenge with an H5N1 virus (Govorkova et al., 2001). All N1-3-VHHb, N1-5-VHHb and oseltamivir treated mice survived challenge with NIBRG-14 ma virus whereas PBS and BL-VHHb recipient mice succumbed after challenge (Figure 6A and B). This result demonstrates that a single intranasal administration of N1-3-VHHb or N1-5-VHHb is sufficient to protect against a subsequent (24 h later) potentially lethal challenge with an H5N1 virus that has an antigenically matching NA. Again all surviving mice suffered from substantial but transient weight loss after challenge (Figure 6B). From the mice that had been similarly treated as above but challenged with H5N1 H274Y virus, only those that had received N1-3-VHHb prior

to challenge survived. All other groups, including those that had been treated with an oseltamivir dose that fully protected against NIBRG14 ma challenge, died following challenge with H5N1 H274Y virus (Figure 6C and D). Finally, we evaluated the effect of prior intranasal instillation of bivalent Fc formatted N1-3-VHH-Fc, N1-5-VHH-Fc and now also N1-7-VHH-Fc in our lethal challenge model. We again included PBS and oseltamivir treatment groups as well as GP4-Fc recipients. Following challenge with 4 LD₅₀ of NIBRG-14 ma, all mice except 1 mouse in the PBS and 1 mouse in the GP4-Fc group died. In the N1-7-VHH-Fc group, only 1 of 6 mice died after challenge. In contrast, all mice in the N1-3-VHH-Fc, N1-5-VHH-Fc and oseltamivir groups survived this challenge and all displayed significant body weight loss, except for the mice that had received N1-5-VHH-Fc that appeared to be fully protected from morbidity following NIBRG-14 ma challenge (Figure 6E and F). Challenge with H5N1 H274Y virus proved lethal to all mice except for those that had been treated in advance with N1-3-VHH-Fc (all mice survived) or N1-7-VHH-Fc (4 out of 6 mice survived) although all animal suffered from substantial body weight loss after challenge (Figure 6G and H). We conclude that bivalent NA-specific VHH can protect against a potentially lethal challenge with oseltamivir-resistant H5N1 virus.

REFERENCES

- Arbabi Ghahroudi, M., A. Desmyter, et al. (1997). "Selection and identification of single domain antibody fragments from camel heavy-chain antibodies." *FEBS Lett* **414**(3): 521- 526.
- Bottcher, E., C. Freuer, et al. (2009). "MDCK cells that express proteases TMPRSS2 and HAT provide a cell system to propagate influenza viruses in the absence of trypsin and to study cleavage of HA and its inhibition." *Vaccine* **27**(45): 6324-6329.

- Chotpitayasunondh, T., K. Ungchusak, et al. (2005). "Human disease from influenza A (H5N1), Thailand, 2004." *Emerging infectious diseases* **11**(2): 201-209.
- Clough, S. J. and A. F. Bent (1998). "Floral dip: a simplified method for *Agrobacterium* mediated transformation of *Arabidopsis thaliana*." *The Plant journal : for cell and molecular biology* **16**(6): 735-743.
- Coppieters, K., T. Dreier, et al. (2006). "Formatted anti-tumor necrosis factor alpha VHH proteins derived from camelids show superior potency and targeting to inflamed joints in a murine model of collagen-induced arthritis." *Arthritis Rheum* **54**(6): 1856-1866.
- De Genst, E., K. Silence, et al. (2006). Molecular basis for the preferential cleft recognition by dromedary heavy-chain antibodies. *Proc Natl Acad Sci.* **103**: 4586-4591.
- De Jaeger, G., S. Scheffer, et al. (2002). "Boosting heterologous protein production in transgenic dicotyledonous seeds using *Phaseolus vulgaris* regulatory sequences." *Nature biotechnology* **20**(12): 1265-1268.
- de Jong, M. D., C. P. Simmons, et al. (2006). Fatal outcome of human influenza A (H5N1) is associated with high viral load and hypercytokinemia. *Nat Med.* **12**: 1203-1207.
- Decanniere, K., A. Desmyter, et al. (1999). A single-domain antibody fragment in complex with RNase A: non-canonical loop structures and nanomolar affinity using two CDR loops. *Structure.* **7**: 361-370.
- Decanniere, K., S. Muyldermans, et al. (2000). Canonical antigen-binding loop structures in immunoglobulins: more structures, more canonical classes? *J Mol Biol.* **300**: 83-91.
- Desmyter, A., S. Spinelli, et al. (2002). Three camelid VHH domains in complex with porcine pancreatic alpha-amylase. Inhibition and versatility of binding topology. *J Biol Chem.* **277**: 23645-23650.
- Desmyter, A., T. R. Transue, et al. (1996). Crystal structure of a camel single-domain VH antibody fragment in complex with lysozyme. *Nat Struct Biol.* **3**: 803-811.

- Dolan, B. P., L. Li, et al. (2010). "Defective ribosomal products are the major source of antigenic peptides endogenously generated from influenza A virus neuraminidase." *Journal of immunology* **184**(3): 1419-1424.
- Dooley, H., M. F. Flajnik, et al. (2003). "Selection and characterization of naturally occurring single-domain (IgNAR) antibody fragments from immunized sharks by phage display." *Mol Immunol* **40**(1): 25-33.
- Els Conrath, K., M. Lauwereys, et al. (2001). "Camel single-domain antibodies as modular building units in bispecific and bivalent antibody constructs." *J Biol Chem* **276**(10): 7346-7350.
- Goto, H. and Y. Kawaoka (1998). "A novel mechanism for the acquisition of virulence by a human influenza A virus." *Proceedings of the National Academy of Sciences of the United States of America* **95** (17): 10224-10228.
- Govorkova, E. A., I. A. Leneva, et al. (2001). "Comparison of efficacies of RWJ-270201, zanamivir, and oseltamivir against H5N1, H9N2, and other avian influenza viruses." *Antimicrobial agents and chemotherapy* **45**(10): 2723-2732.
- Gubareva, L. V., M. S. Nedyalkova, et al. (2002). "A release-competent influenza A virus mutant lacking the coding capacity for the neuraminidase active site." *The Journal of general virology* **83**(Pt 11): 2683-2692.
- Hamers-Casterman, C., T. Atarhouch, et al. (1993). "Naturally occurring antibodies devoid of light chains." *Nature* **363**(6428): 446-448.
- Harbury, P. B., T. Zhang, et al. (1993). "A switch between two-, three-, and four-stranded coiled coils in GCN4 leucine zipper mutants." *Science* **262**(5138): 1401-1407.
- Herfst, S., E. J. Schrauwen, et al. (2012). "Airborne transmission of influenza A/H5N1 virus between ferrets." *Science* **336**(6088): 1534-1541.
- Hmila, I., D. Saerens, et al. (2010). "A bispecific nanobody to provide full protection against lethal scorpion envenoming." *Faseb J* **24**(9): 3479-3489.

- Hoffmann, E., G. Neumann, et al. (2000). "A DNA transfection system for generation of influenza A virus from eight plasmids." *Proceedings of the National Academy of Sciences of the United States of America* **97**(11): 6108-6113.
- Huang, I. C., W. Li, et al. (2008). "Influenza A virus neuraminidase limits viral superinfection." *Journal of virology* **82**(10): 4834-4843.
- Hubert, B., L. Watier, et al. (1992). "Meningococcal disease and influenza-like syndrome: a new approach to an old question." *The Journal of infectious diseases* **166**(3): 542-545.
- Hultberg, A., N. J. Temperton, et al. (2011). "Llama-derived single domain antibodies to build multivalent, superpotent and broadened neutralizing anti-viral molecules." *PLoS One* **6**(4): e17665.
- Hung, I.F.N, To, K.K.W. et al. (2011). "Convalescent plasma treatment reduced mortality in patients with severe pandemic influenza A (H1N1^o 2009 virus infection. *CID* **52**: 447-456.
- Ibanez, L. I., M. De Filette, et al. (2011). "Nanobodies with in vitro neutralizing activity protect mice against H5N1 influenza virus infection." *J Infect Dis* **203**(8): 1063-1072.
- Ilyushina, N. A., N. V. Bovin, et al. (2012). "Decreased neuraminidase activity is important for the adaptation of H5N1 influenza virus to human airway epithelium." *Journal of virology* **10** **86**(9): 4724-4733.
- Ilyushina, N. A., M. F. Ducatez, et al. (2010). "Does pandemic A/H1N1 virus have the potential to become more pathogenic?" *mBio* **1**(5).
- Imai, M., T. Watanabe, et al. (2012). "Experimental adaptation of an influenza H5 HA confers respiratory droplet transmission to a reassortant H5 HA/H1N1 virus in ferrets." *Nature* **486**(7403): 420-428.
- Ismaili, A., M. Jalali-Javaran, et al. (2007). "Production and characterization of anti-(mucin MUC1) single-domain antibody in tobacco (*Nicotiana tabacum* cultivar Xanthi)." *Biotechnology and applied biochemistry* **47**(Pt 1): 11-19.

- Jobling, S. A., C. Jarman, et al. (2003). "Immunomodulation of enzyme function in plants by single-domain antibody fragments." *Nature biotechnology* **21**(1): 77-80.
- Johansson, B. E. and E. D. Kilbourne (1993). "Dissociation of influenza virus hemagglutinin and neuraminidase eliminates their intravirionic antigenic competition." *Journal of virology* **67**(10): 5721-5723.
- Johansson, B. E., J. T. Matthews, et al. (1998). "Supplementation of conventional influenza A vaccine with purified viral neuraminidase results in a balanced and broadened immune response." *Vaccine* **16**(9-10): 1009-1015.
- Johansson, B. E., T. M. Moran, et al. (1987). "Immunologic response to influenza virus neuraminidase is influenced by prior experience with the associated viral hemagglutinin. II. Sequential infection of mice simulates human experience." *Journal of immunology* **139**(6): 2010-2014.
- Kang, A. S., T. M. Jones, et al. (1991). "Antibody redesign by chain shuffling from random combinatorial immunoglobulin libraries." *Proceedings of the National Academy of Sciences of the United States of America* **88**(24): 11120-11123.
- Kilbourne, E. D., B. A. Pokorny, et al. (2004). "Protection of mice with recombinant influenza virus neuraminidase." *The Journal of infectious diseases* **189**(3): 459-461.
- Lauwereys, M., M. Arbadi Ghahroudi, et al. (1998). Potent enzyme inhibitors derived from dromedary heavy-chain antibodies. *EMBO J.* **17**: 3512-3520.
- Li, S., J. Schulman, et al. (1993). "Glycosylation of neuraminidase determines the neurovirulence of influenza A/WSN/33 virus." *Journal of virology* **67**(11): 6667-6673.
- Matrosovich, M., T. Matrosovich, et al. (2006). "New low-viscosity overlay medium for viral plaque assays." *Virology journal* **3**: 63.

- Matrosovich, M. N., T. Y. Matrosovich, et al. (2004). "Neuraminidase is important for the initiation of influenza virus infection in human airway epithelium." *Journal of virology* **78**(22): 12665-12667.
- Matsuoka, Y., D. E. Swayne, et al. (2009). "Neuraminidase stalk length and additional glycosylation of the hemagglutinin influence the virulence of influenza H5N1 viruses for mice." *Journal of virology* **83**(9): 4704-4708.
- Mitnaul, L. J., M. N. Matrosovich, et al. (2000). "Balanced hemagglutinin and neuraminidase activities are critical for efficient replication of influenza A virus." *Journal of virology* **74**(13): 6015-6020.
- Muyldermans, S., T. Atarhouch, et al. (1994). Sequence and structure of VH domain from naturally occurring camel heavy chain immunoglobulins lacking light chains. *Protein Eng.* **7**: 1129-1135.
- Nedyalkova, M. S., F. G. Hayden, et al. (2002). "Accumulation of defective neuraminidase (NA) genes by influenza A viruses in the presence of NA inhibitors as a marker of reduced dependence on NA." *The Journal of infectious diseases* **185**(5): 591-598.
- Nguyen, V. K., S. Muyldermans, et al. (1998). "The specific variable domain of camel heavy-chain antibodies is encoded in the germline." *J Mol Biol* **275**(3): 413-418.
- Rameix-Welti, M. A., M. L. Zarantonelli, et al. (2009). "Influenza A virus neuraminidase enhances meningococcal adhesion to epithelial cells through interaction with sialic acid-containing meningococcal capsules." *Infection and immunity* **77**(9): 3588-3595.
- Rasmussen, S. G., H. J. Choi, et al. (2011). "Structure of a nanobody-stabilized active state of the beta(2) adrenoceptor." *Nature* **469**(7329): 175-180.
- Saerens, D., M. Pellis, et al. (2005). "Identification of a universal VHH framework to graft non-canonical antigen-binding loops of camel single-domain antibodies." *J Mol Biol* **352**(3): 597-607.

- Schepens, B., L. I. Ibanez, et al. (2011). Nanobodies specific for Respiratory Syncytial Virus Fusion protein protect against infection by inhibition of fusion. *J Inf Dis*. **In press**.
- Shoji, Y., J. A. Chichester, et al. (2011). "An influenza N1 neuraminidase-specific monoclonal antibody with broad neuraminidase inhibition activity against H5N1 HPAI viruses." *Human vaccines* **7 Suppl**: 199-204.
- Teh, Y. H. and T. A. Kavanagh (2010). "High-level expression of Camelid nanobodies in *Nicotiana benthamiana*." *Transgenic research* **19**(4): 575-586.
- Tran, T. H., T. L. Nguyen, et al. (2004). "Avian influenza A (H5N1) in 10 patients in Vietnam." *The New England journal of medicine* **350**(12): 1179-1188.
- Van Borm, S., I. Thomas, et al. (2005). "Highly pathogenic H5N1 influenza virus in smuggled Thai eagles, Belgium." *Emerging infectious diseases* **11**(5): 702-705.
- Van Droogenbroeck, B., J. Cao, et al. (2007). "Aberrant localization and underglycosylation of highly accumulating single-chain Fv-Fc antibodies in transgenic *Arabidopsis* seeds." *Proceedings of the National Academy of Sciences of the United States of America* **104**(4): 1430-1435.
- Wang, M. Z., C. Y. Tai, et al. (2002). "Mechanism by which mutations at his274 alter sensitivity of influenza a virus n1 neuraminidase to oseltamivir carboxylate and zanamivir." *Antimicrob Agents Chemother* **46**(12): 3809-3816.
- Ward, E. S., D. Gussow, et al. (1989). "Binding activities of a repertoire of single immunoglobulin variable domains secreted from *Escherichia coli*." *Nature* **341**(6242): 544-546.
- Wei, G., W. Meng, et al. (2011). "Potent neutralization of influenza A virus by a single domain antibody blocking M2 ion channel protein." *PloS one* **6**(12): e28309.
- Winichayakul, S., A. Pernthaner, et al. (2009). "Head-to-tail fusions of camelid antibodies can be expressed in planta and bind in rumen fluid." *Biotechnology and applied biochemistry* **53**(Pt 2): 111-122.

- Wong, H.K., Lee, C.K. et al. (2010). "Practical limitations of convalescent plasma collection: a case scenario in pandemic preparation for influenza A (H1N1) infection. *Transfusion* **50**: 1967-1971.
- Yamada, S., Y. Suzuki, et al. (2006). "Haemagglutinin mutations responsible for the binding of H5N1 influenza A viruses to human-type receptors." *Nature* **444**(7117): 378-382.
- Zhou, B., N. Zhong, et al. (2007). "Treatment with convalescent plasma for influenza A (H5N1) infection." *N Engl J Med* **357**(14): 1450-1451.

CLAIMS

1. A VHH specifically binding influenza neuraminidase.
2. The VHH according to claim 1, comprising a CDR1 loop sequence selected from the group consisting of SEQ ID N°1 and SEQ ID N° 2, a CDR2 loop sequence selected from the group consisting of SEQ ID N° 3 and SEQ ID N° 4 and a CDR3 loop sequence consisting of SEQ ID N° 5 and SEQ ID N°6
3. An influenza neuraminidase binding construct comprising a VHH according to claim 1 or 2.
4. The neuraminidase binding construct according to claim 3, wherein said construct is bivalent.
5. The neuraminidase binding construct according to claim 4, wherein said VHH is fused to an Fc tail.
6. The neuraminidase binding construct according to claim 4, wherein said VHHs are linked by an IgG2c hinge.
7. The neuraminidase binding construct according to claim 5 or 6, wherein said construct comprises a sequence selected from the group consisting of SEQ ID N°7, SEQ ID N° 8, SEQ ID N° 9 and SEQ ID N° 10.

ANTI-INFLUENZA ANTIBODY

ABSTRACT

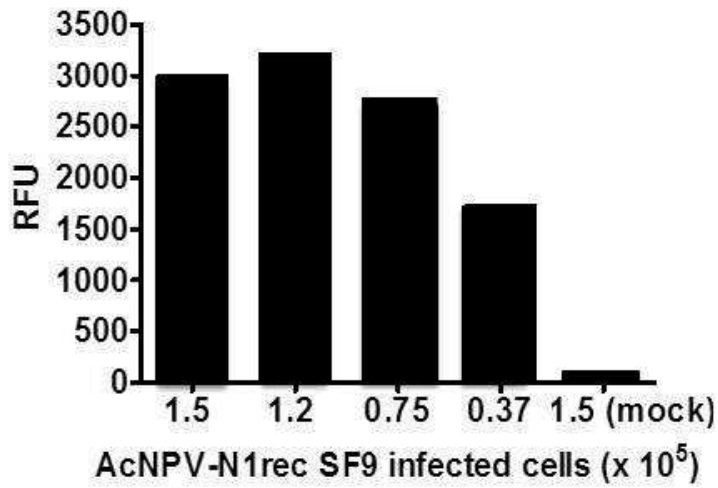
The present invention relates to an antibody that confers protection against influenza virus infection. More specifically, it relates to an anti-neuraminidase antibody, protecting against highly pathogenic H5N1 influenza strains. The invention relates further to the use of the antibody for prophylactic and/or therapeutic treatment of influenza virus infections, and to a pharmaceutical composition comprising the antibody.

FIGURE 1

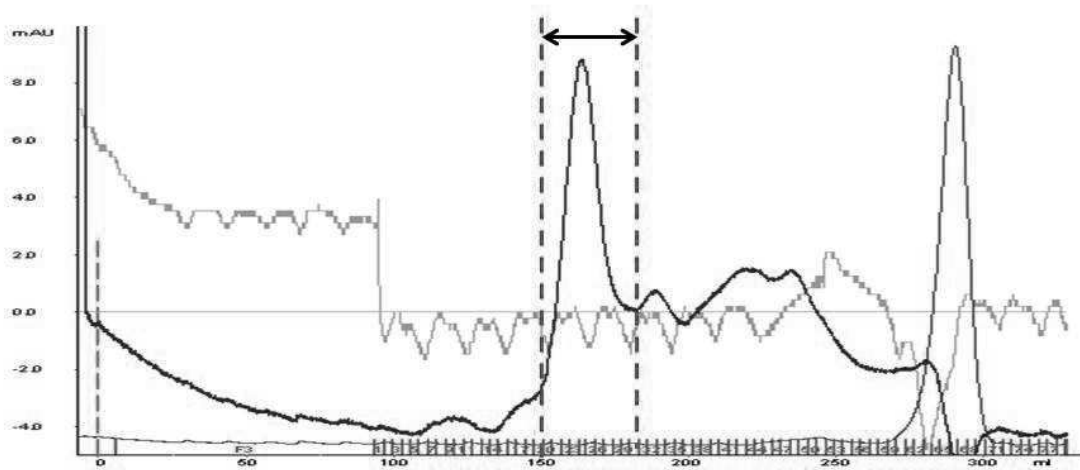
A



B



C



D

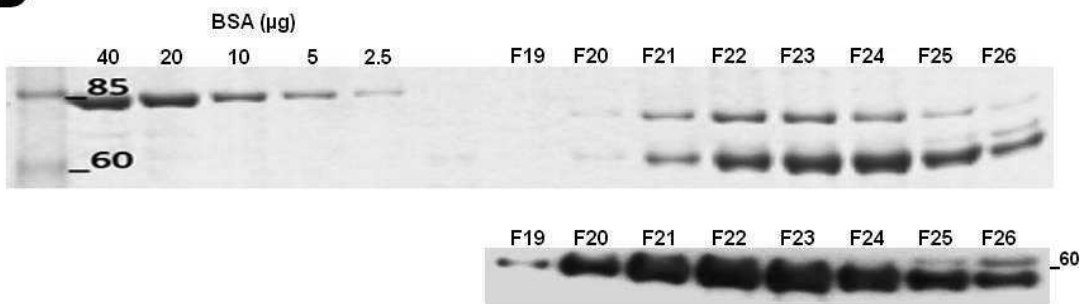


FIGURE 2

A

	10	20	30	40	50	60	70	80
	CDR1				CDR2			
N1-1-VHH	QVQLQESGGGLVQAGGSLR	LSC	TA	SGGTFSSYP	MGWFRQAPGK	REFVAAISWSGGSTNYADSVKGRFTISR	DN	AKTTVY
N1-2-VHH	QVQLQESGGGLVQAGGSLR	LSCAASGR	TSSYAMGWFRQAPGK	REFVAAISWSGLSTYYADSVKGRFSISR	DN	AKNMVY		
N1-3-VHH	QVQLQESGGGLVQPGGSLR	LSCAASG	SIFSIHDMGWYRRAPGKQRELVA	AITS-GGSTNYADSVKGRFTISR	DN	AKNTVS		
N1-4-VHH	QVQLQESGGGLVQPGGSLR	LSCAASGN	IFSLYSMAWYRQAPGKQRELVA	DITS-GGATNYADSVKGRFTISR	DN	AKNTVY		
N1-5-VHH	QVQLQESGGGLVQPGGSLR	LSCAASG	SDISYEMGWYRQAPGKQRELVA	AITS-GGTNYADSVKGRFTISR	DN	AKNTVY		
N1-6-VHH	QVQLQESGGGLVQPGGSLR	LSCAASG	IIFSIYVMGWYRQAPGKQRELVA	AITE-GGSTNYADSVKGRFTISR	DN	AMNTVY		
N1-7-VHH	QVQLQESGGGLVQPGGSLR	LSCAASG	SFRSRYDMGWYRQAPGKQRELVA	TITS-GGITNYADSVKGRFTISR	DN	TKNTVY		
N1-8-VHH	QVQLQESGGGMVQPGGSLR	VS	CAASGSRFSRYDMGWYRQAPGKQRELVA	TITS-GGITNYADSVKGRFTISR	DN	TKNTVY		
N1-9-VHH	QVQLQESGGGLVQPGGSLR	LSCAASG	FPSSYVMGWYRQAPGKERELVAEISSRGGTTNYADPVKGRFTISR	DN	NFKNMVY			
N1-10-VHH	QVQLQESGGGLVQPGGSLR	LSCAASG	FPSSYVMGWYRQAPGKERELVAEISSRGGTTNYADSVKGRFTISR	DN	NFRNMVY			
N1-11-VHH	QVQLQESGGGLVQPGGSLR	LSCAASG	FPSSYVMGWYRQAPGKERELVAEISSRGGTTNYADSVKGRFTISR	DN	NIKNMVY			
N1-12-VHH	QVQLQESGGGLVQPGGSLR	LSCAASG	FPSSYVMGWYRQAPGKERELVAEISSRGGTTNYADSVKGRFTISR	DN	NIKNMVY			
N1-13-VHH	QVQLQESGGGMVQPGGSLR	LTC	CAASGTFSSYDMSWYRQAPGKGP	PERVSAIDIGGGSTYYANSVKGRFTISR	DN	AKNTLY		

	90	100	110	120
	CDR3			
N1-1-VHH	LQMNSLKPEDTAVYYCNAEGDSD--SPALG-MDYWGKGTQVTVSS			
N1-2-VHH	LQMNSLKPEDTAVYYCNAADPRAR--TTGWAPSGDNGQGTQVTVSS			
N1-3-VHH	LQMNSLKPEDTAVYYCNAWG-E---DYGLGEYDSNGQGTQVTVSS			
N1-4-VHH	LHMNNLKPEDTAVYYCNAADASS---DYGLSFFDSNGQGTQVTVSS			
N1-5-VHH	LQMNSLKPEDTAVYYCNAAD-F---D--LWEYDYNQGTQVTVSS			
N1-6-VHH	LQMNSLKPEDTAVYYCNAIT-P---DGSLWEADYNGQGTQVTVSS			
N1-7-VHH	LQMNSLKPEDTAVYYCNAEDPLRAIQLGSLTYEYNGQGTQVTVSS			
N1-8-VHH	LQMNSLKPEDTAVYYCNAEDPLRAIQLGSLTYEYNGQGTQVTVSS			
N1-9-VHH	LQMNSLKPEDTAVYYCNRPH-----P-DYWGRTQVTVSS			
N1-10-VHH	LQMNSLKPEDTAVYYCNRPH-----P-DYNGQGTQVTVSS			
N1-11-VHH	LQMNSLKPEDTAVYYCNRPH-----P-DYNGQGTQVTVSS			
N1-12-VHH	LQMNSLKPEDTAVYYCNRPH-----P-DYNGQGTQVTVSS			
N1-13-VHH	LQMNSLKPEDTALYYCVRDWTYG-----LARRYRQGTQVTVSS			

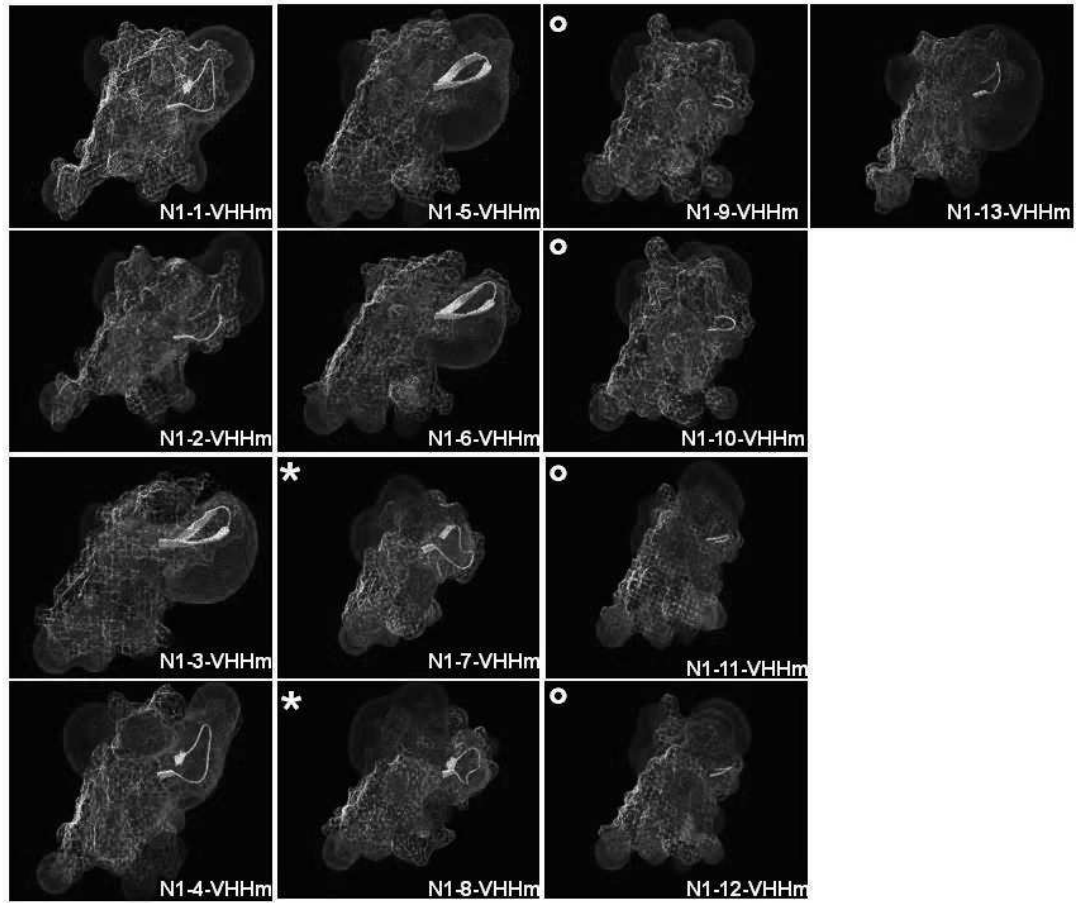
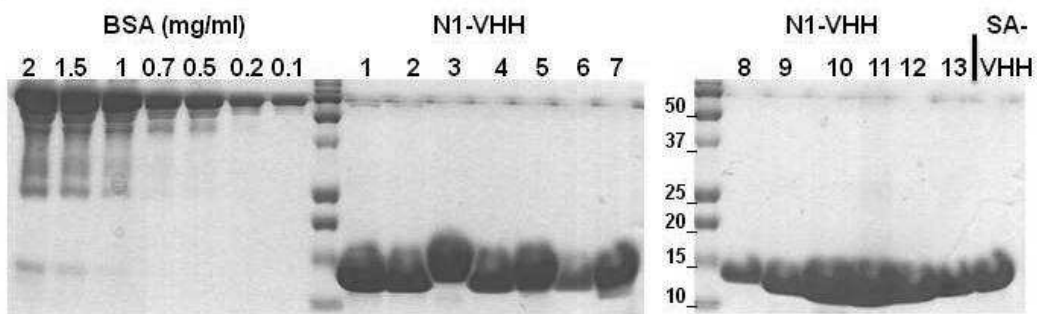
B**C**

FIGURE 3

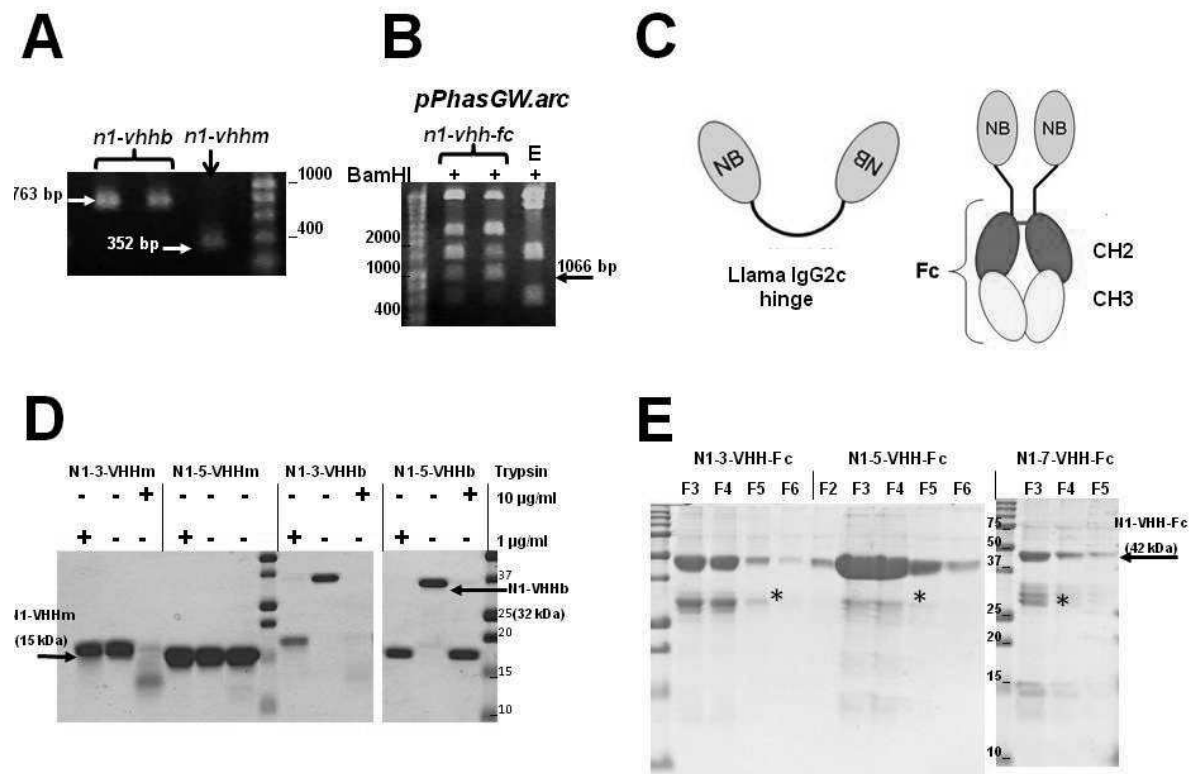
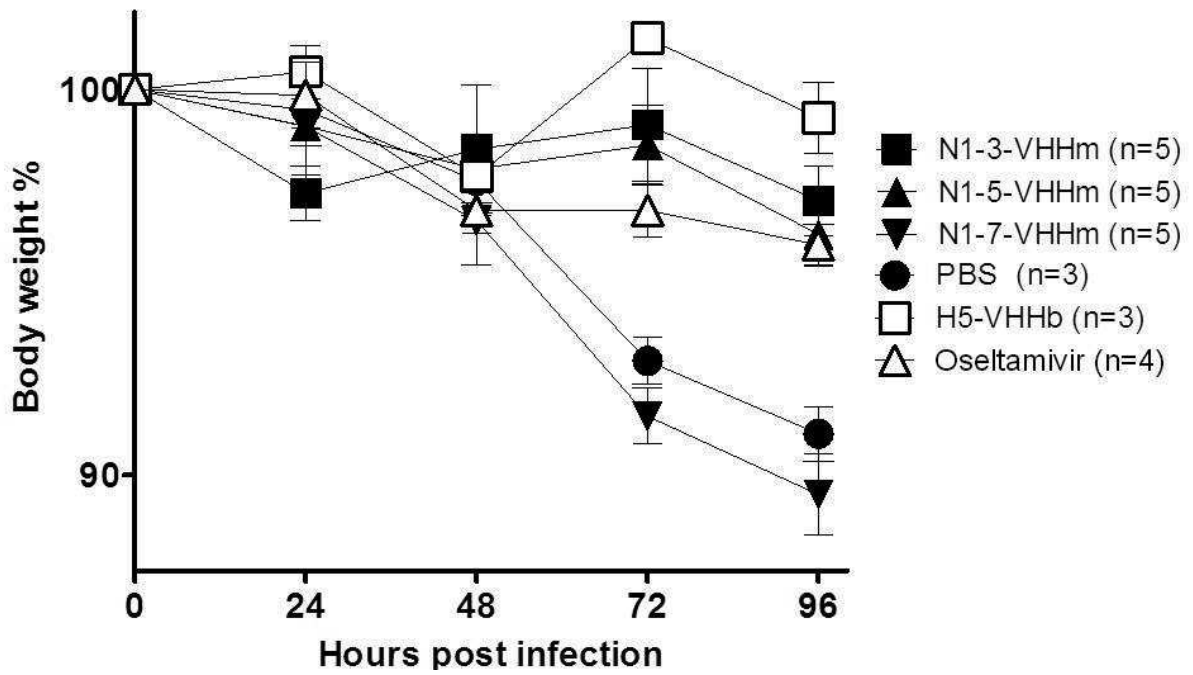
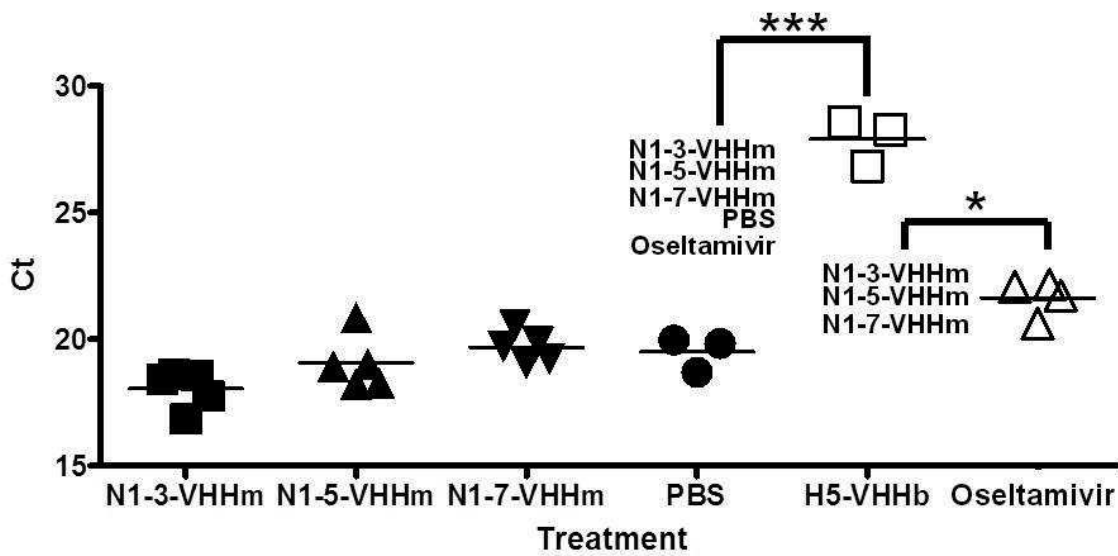


FIGURE 4

A



B



C

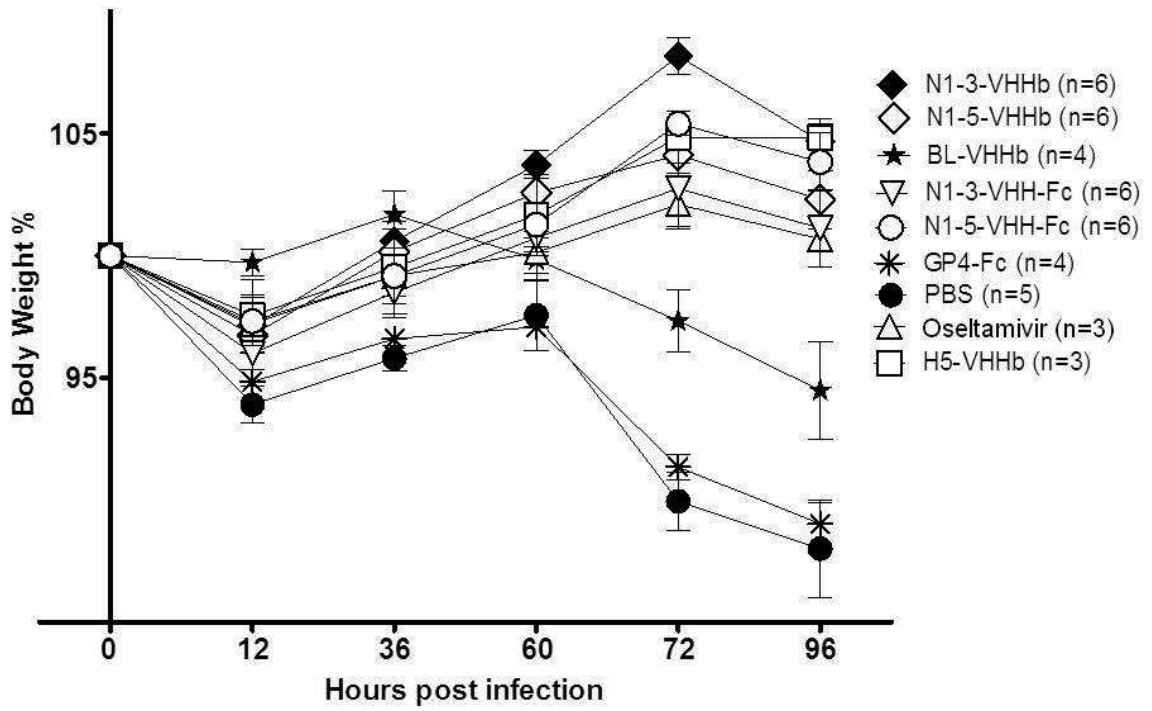
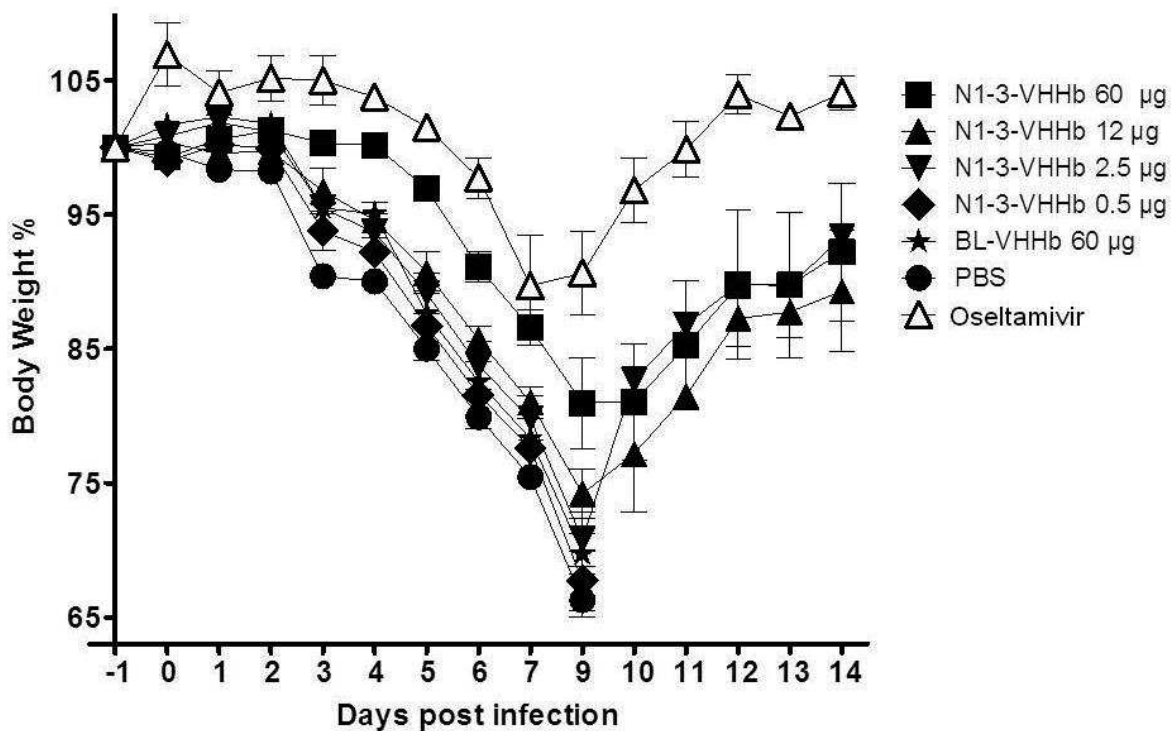


FIGURE 5

A



B

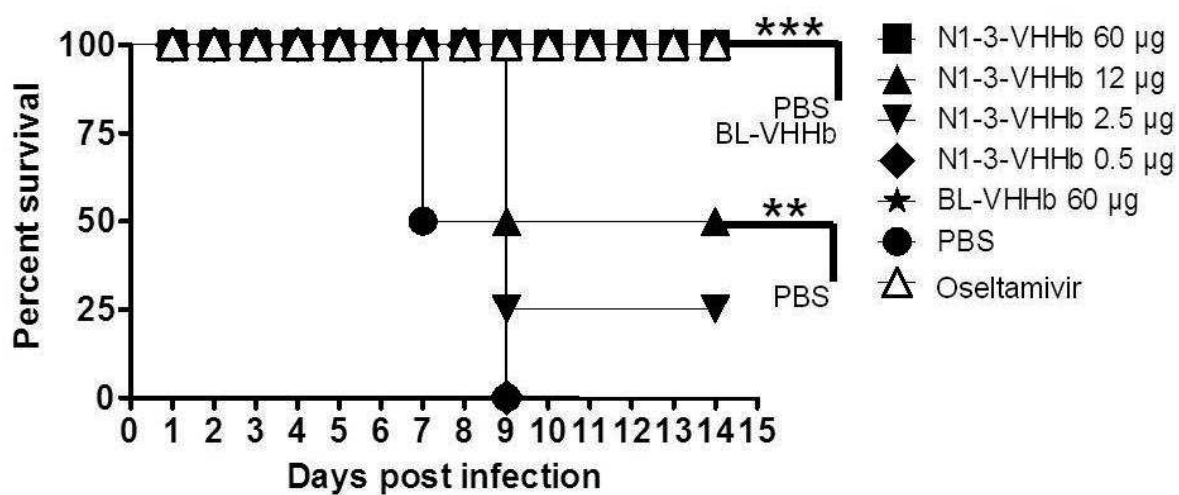
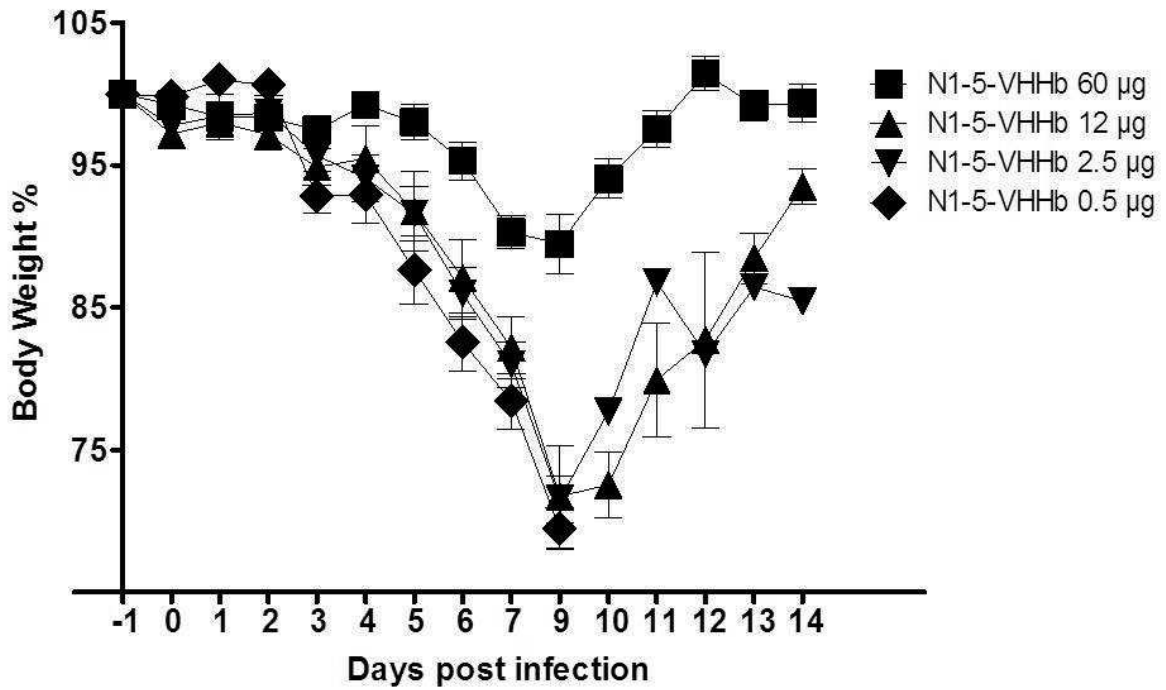


FIGURE 5 cont

C



D

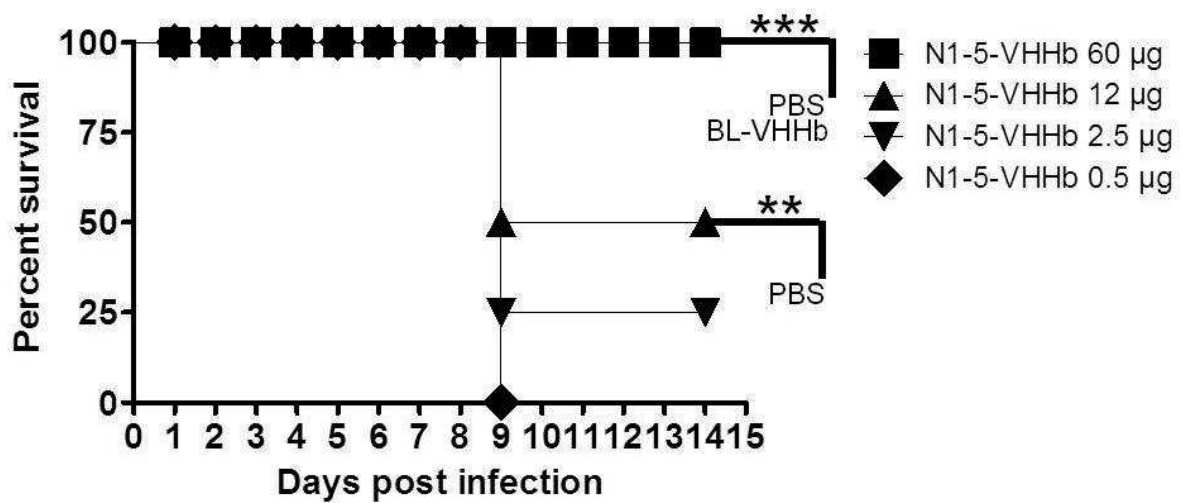
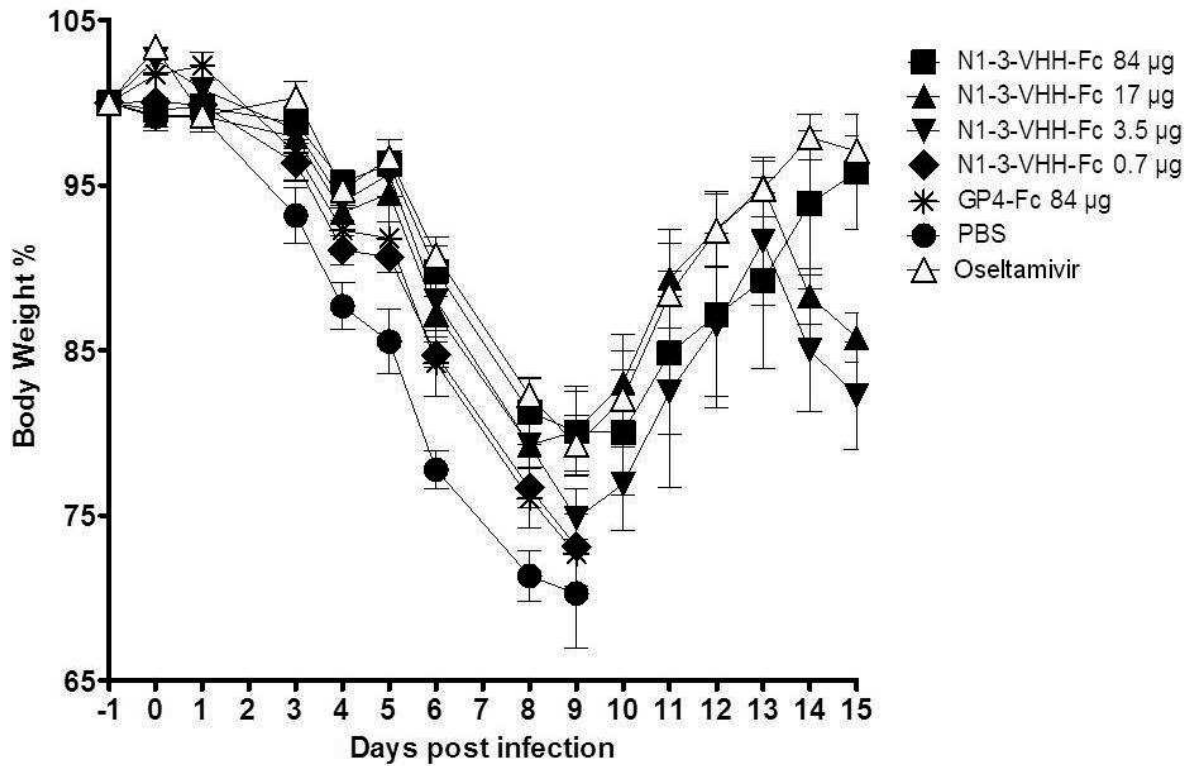


FIGURE 5 cont

E



F

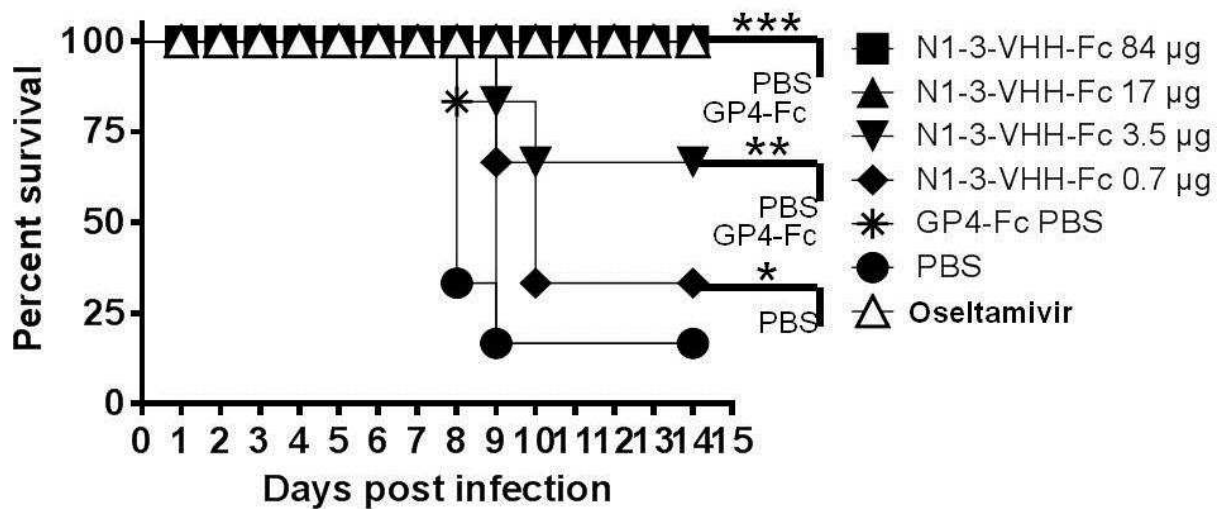
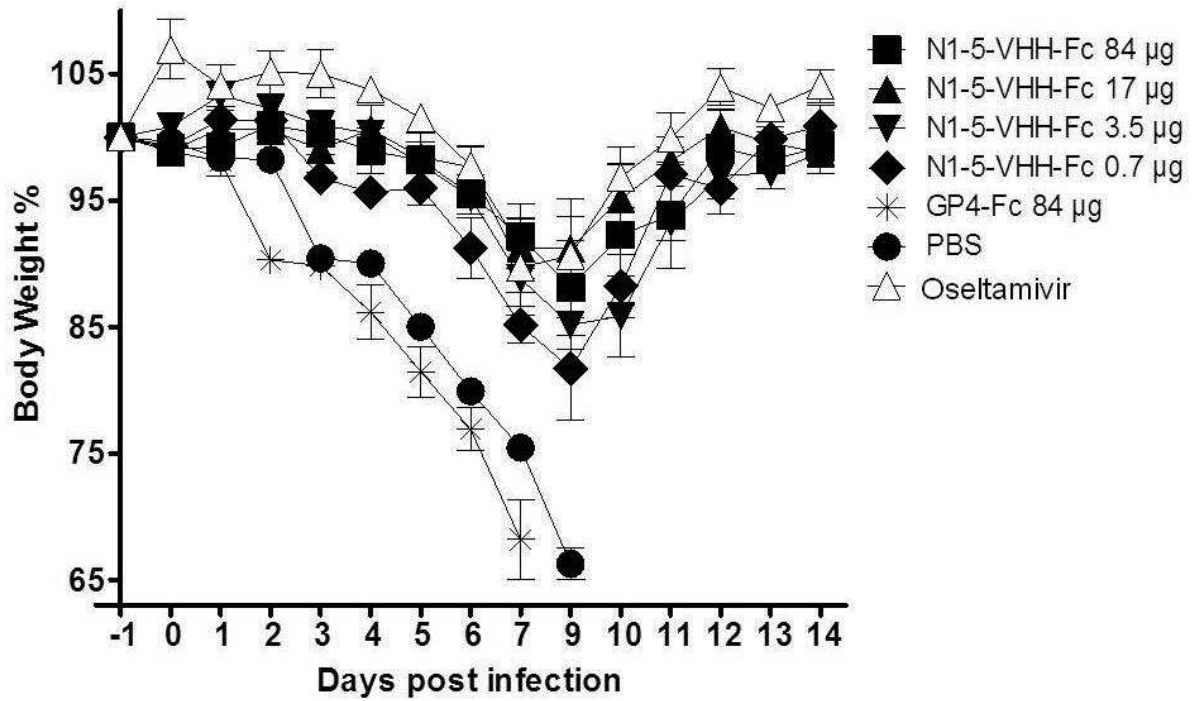


FIGURE 5 cont.

G



H

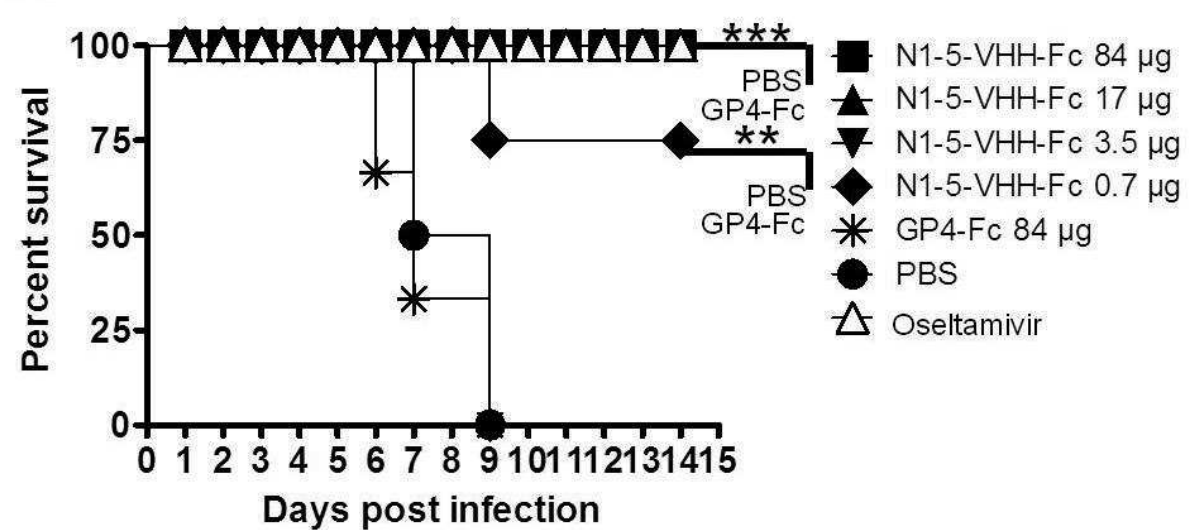
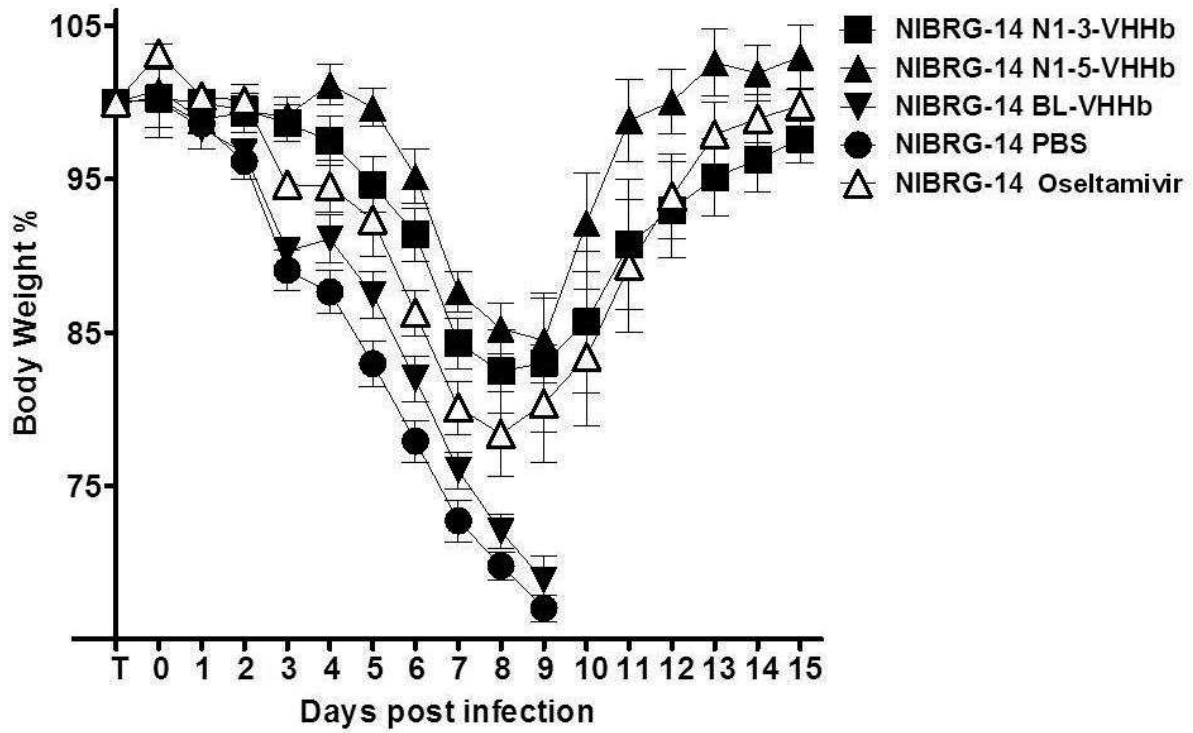


FIGURE 6

A



B

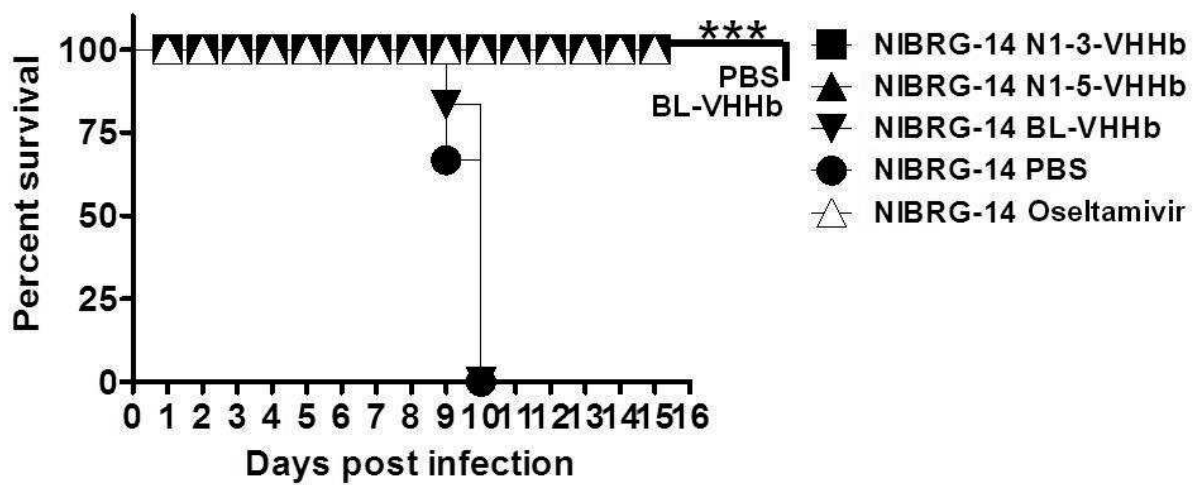
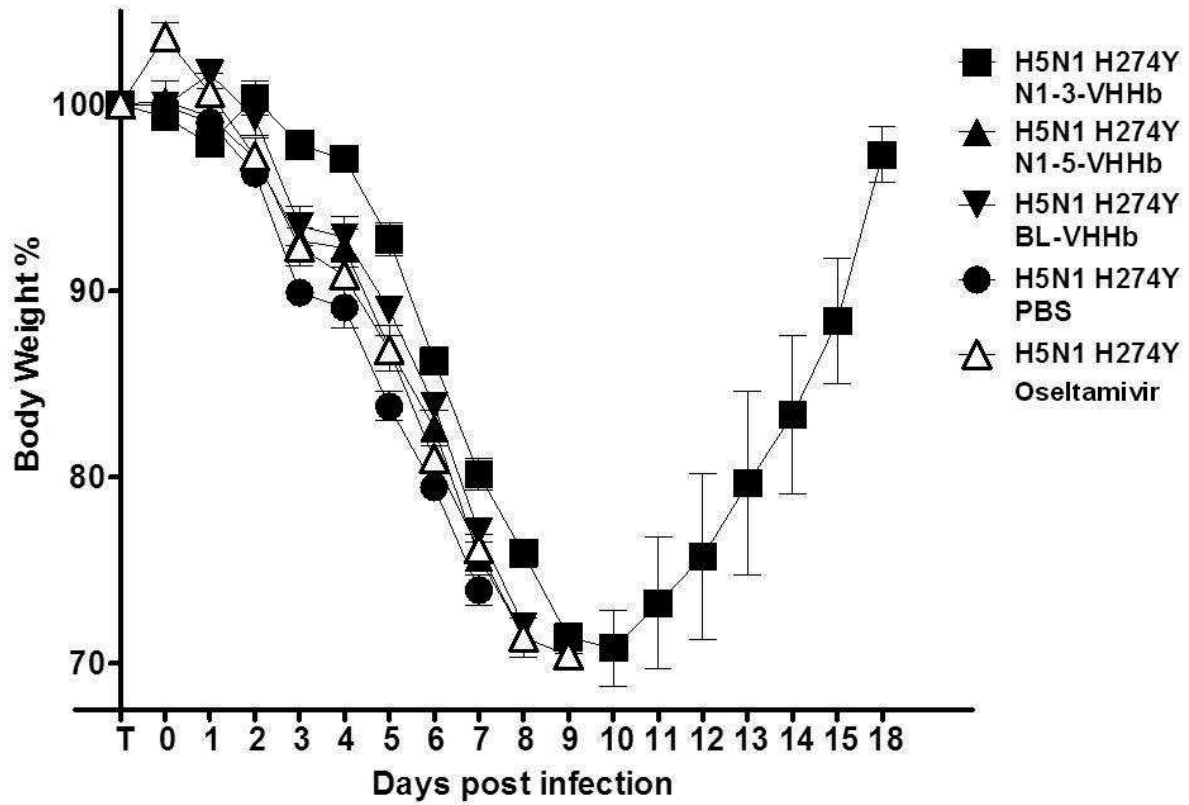


FIGURE 6 cont.

C



D

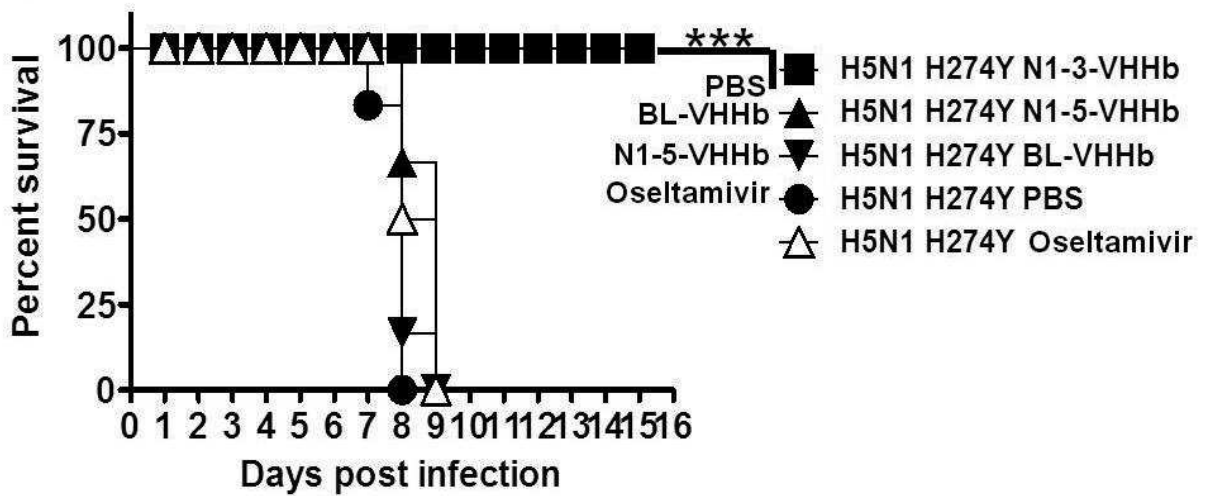


FIGURE 6 cont.

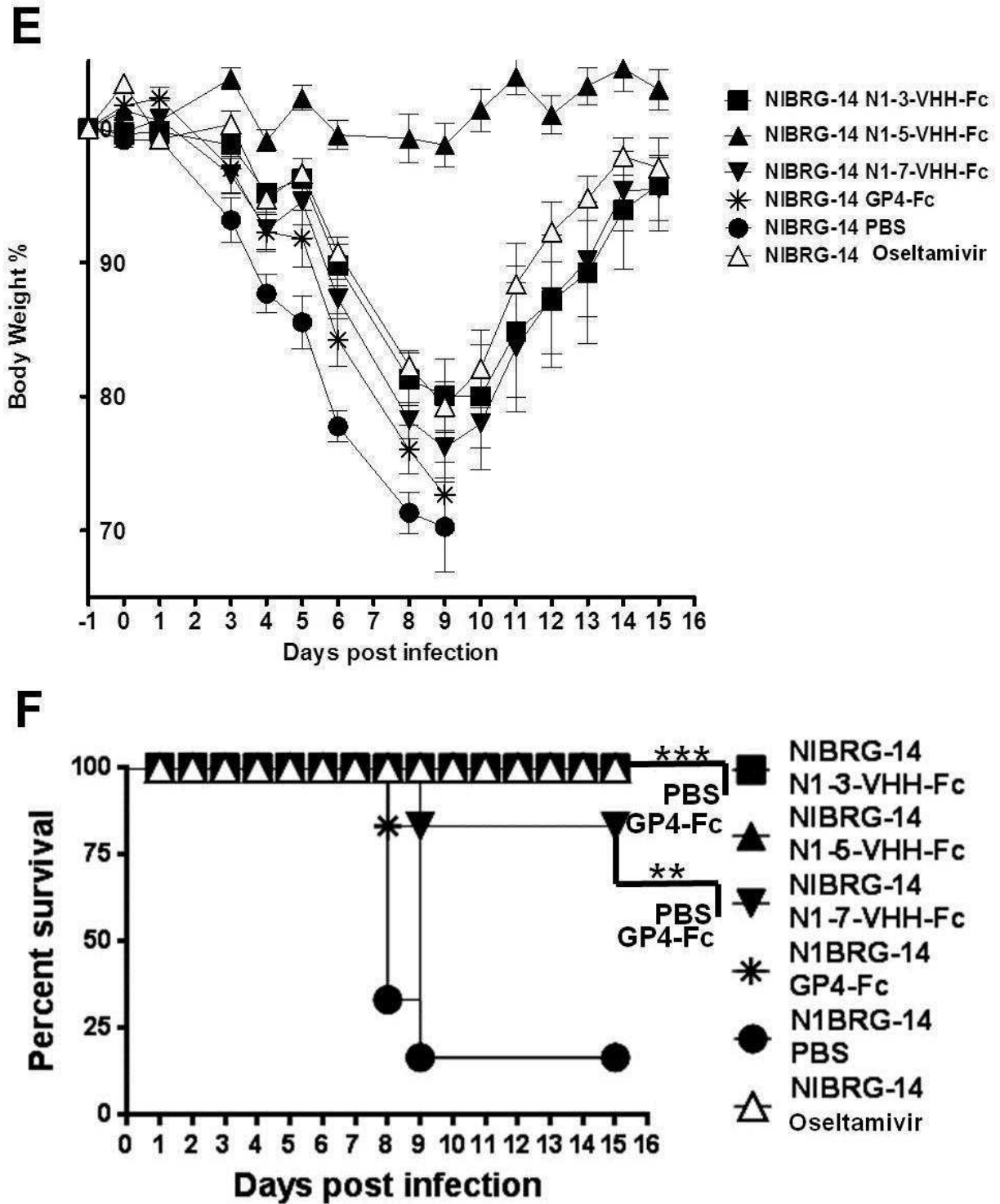
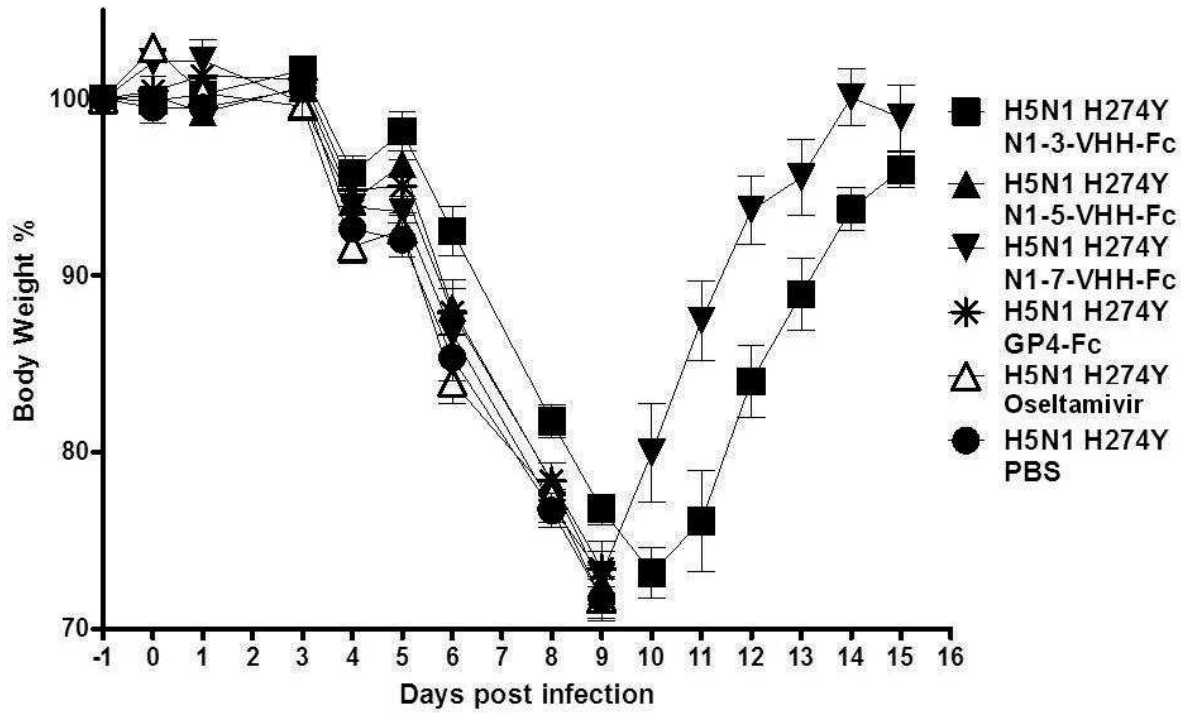
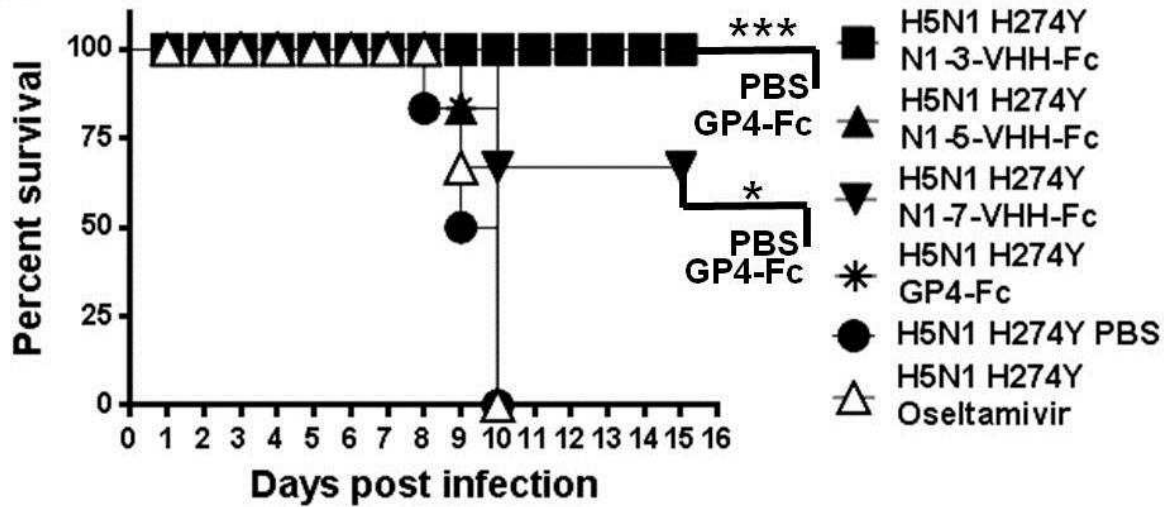


FIGURE 6 cont.

G



H



Single domain camelid antibodies that neutralize negative strand viruses

Francisco Miguel Lopez Cardoso, Lorena Itatí Ibañez, Bert Schepens and Xavier Saelens

Department for Molecular Biomedical Research, VIB Technologiepark 927, Ghent;

Department of Biomedical Molecular Biology, Ghent University, Technologiepark 927, Ghent.

Belgium.

1. Introduction

1.1 Conventional Antibodies

Recombinant antibodies are widely regarded as one of the main, if not the most promising tools against cancer and auto-immune, inflammatory, neurodegenerative and infectious diseases (Stiehm et al., 2008). Conventional antibodies (Abs) are complex molecules consisting of pairs of heavy and light chains, whose N-terminal domain is more variable than the rest of the protein sequence. The antibody heavy chain consists of three constant domains (CH1, CH2 and CH3) and a variable domain (VH). The light chain has only two domains, the constant light (CL) and the variable light (VL). Important Glycosylations on the CH2 domain are necessary for antibody effector functions, such as Antibody-Dependent Cellular Cytotoxicity (ADCC) and Complement-Dependent Cytolysis (CDC), and for regulating antibody half time in serum (Fig. 1, A). Antigen-binding is determined by the three hypervariable Complementary Determining Regions (CDR1, CDR2 and CDR3) present in both the VH and VL domains. These regions are located in juxtaposed loops, creating a continuous surface of $\sim 1000 \text{ \AA}^2$ that specifically binds to the epitope in an antigen. Although all CDRs can potentially make contact with the antigen, CDR3 contacts with the epitope are generally more extensive. The structural diversity of the antigen-binding sites of a conventional antibody depends on the size of the CDR3 in the VH and the conjunction with the VL at different angles and distances. These are grouped in three different classes, according to the size and type of an antigen: cavities (fitting haptens), grooves (fitting peptides) and planar sites (fitting surface patches of proteins) (Johnson et al., 2010).

1.2 The Single variable domain of the heavy chain antibodies

In 1993 a surprising observation was made in members of the Artiodactyl Tylopoda family (camelids). Next to conventional IgG antibodies, camelids also naturally produce Heavy Chain antibodies (HCAbs) that lack the light chain (Hamers-Casterman et al., 1993). Two years later, similar single chain antibodies were discovered in cartilaginous fish (sharks) (Greenberg et al., 1995). Although the CH2 and CH3 of the HCAbs and the conventional antibodies are highly homologous, there is no CH1 domain in the camelid HCAbs. The single variable domain, called VHH, is the only domain of HCAbs that makes contact with the antigen. Surprisingly, although the VHH have only three CDR regions, their affinity for antigens reaches the low nanomolar to even picomolar range, matching the best affinities of classical antibodies. When expressed as single domains (often referred to as nanobodies, Nb), the VHHs retain their strong epitope specificity and affinity, a feature that might be explained by the VHH architecture (Fig. 1, B). Just like the VHs of conventional antibodies, the amino acid (AA) sequence of VHHs is organized in three hypervariable regions (CDR1, CDR2 and CDR3) separated by four Framework regions (FR1-FR4) (Muyldermans et al., 1994). As the AA sequence of the VHH FRs is highly similar to those of conventional VHs it was not surprising that the overall architecture of VHHs closely resembles that of VHs (Muyldermans et al., 1994). Both VHH and VH domains fold into two β -sheets with the three CDRs that link these two sheets at one end of the barrel (or domain) (Desmyter et al., 1996; De Genst et al., 2006) (Fig. 1, C,E). However, there are striking structural differences between VHHs and conventional VH. Evidently, VHHs lack an interacting VL domain. Associated with this lack, the hydrophobic amino acids present at the VH surface that is normally interacting with the VL, are substituted by hydrophilic AA (Fig.1, D). This enhances the solubility of VHH single domain proteins have an enhanced solubility compared to engineered VH single domain proteins.

The absence of the additional CDRs in VHHs is likely compensated by structural features. First, the CDR3 regions of camelid VHHs are generally longer (13-17 amino acids) than the CDR3 regions of mouse and human VHs (9-12 and 9-17 AA respectively) (Wu et al., 1993). In contrast to conventional Abs, in which the antigen binding surface is often a flat surface, a cavity or a groove, the long CDR3 loop may extend from the antigen binding surface (Desmyter et al., 1996). This enlarges the paratope surface and hence the potential affinity and repertoire of camelid HcAbs. In addition, especially in dromedaries, the CDR1 and CDR3 regions contain a cysteine, which allows formation of a second disulfide bridge next to the single disulfide bridge in conventional VHs (Muyldermans et al., 1994). This extra bridge likely stabilizes the CDR loops, thereby reducing their flexibility. This probably also contributes to the affinity (less entropy is lost upon antigen binding) and structural diversity of VHHs. Long extending CDR3 loops that are stabilized by an extra disulfide bridge can explain the tendency of VHHs to bind to clefts and concave surfaces more readily than conventional antibodies do (Fig. 1, F) (De Genst et al., 2006). Indeed comparison of multiple structures of hen egg white lysozyme interacting with either several conventional human antibodies or several camelid VHHs clearly illustrated that VHHs tends to bind to the concave substrate-binding pocket, whereas conventional antibodies favor epitopes on the "flat" surface of the antigen (Fig. 1, C). In addition, whereas each of the three CDRs of conventional VHs contributes considerably to the interaction with antigen, VHHs depended mainly on the CDR 3 loop for this interaction. Other antigens that are hard to target by conventional antibodies, but can be targeted by cameloid VHHs are ion channels, GPCRs, haptens and enzymatic sites (Lauwereys et al., 1998) (Rasmussen et al., 2011).

Next to an extended CDR3, the AA sequence of the H1 loop that precedes and comprises CDR1 appears to be particularly more variable in camelid VHHs than in conventional VHs. This might be interpreted as an extension of the VHH CDR1 (Vu et al., 1997). Associated with this high variability in camelid VHHs, CH1 loops adopt conformations that deviate from the canonical H1 structures of conventional VHs (Barre et al., 1994); (Decanniere et al., 1999; Decanniere et al., 2000). Camelid VHH CH1 loops appear to fold into a more diverse repertoire of structures. The high variability in the AA sequence and conformations of the CH1 loop contribute to the VHH paratope size (850-1150 Å²), which approaches that of conventional antibodies (VH + VL) (Desmyter et al., 2002). Clearly, different biochemical and structural features of camelid VHHs compensate for the lack of a VL domain and allowing a broad repertoire of specific high affinity antigen interactions. In addition, due to their small size and typical extruding CDR3 regions, camelid VHH tend to bind in cavities that are not readily accessible for conventional antibodies. Next to these particular features, VHH single domain protein is exceptionally stable and soluble, even in stringent conditions. As VHH are small and naturally monomeric, they can be easily formatted. In addition, the small size of VHHs allows them penetrate deeper into tissue (e.g. tumor tissue) and to occasionally cross the blood-brain barrier. On the down side, the small size of single domain VHH contributes to their rapid clearance from circulation.

Using display technologies, it is possible to select VHHs from large, synthetic or naive libraries (Verheesen et al., 2006). Nevertheless, the phage display generated from an immune VHH repertoire is the most widely and powerful technique used nowadays to rapidly select VHHs with the desired specificity (Arbabi Ghahroudi et al., 1997). VHH are easily produced in bacterial or yeast systems in miligram quantities per liter of culture. Their stability, solubility, ease of production and small size make them excellent candidates for multivalent formatting. Tailor-made constructions using VHHs as building blocks enhance the avidity of the molecule even in a 3 log scale, and several constructions are being tested in clinical trials (Els Conrath et al., 2001; Hmila et al., 2010). Their high potential as therapeutics had prompted the creation in Belgium of the company Ablynx in 2001. Because of the publicity surrounding nanotechnology and the small size of the VHH, Ablynx named the VHH as “Nanobody (Nb)”, and retains full intellectual property rights of the use of Nbs in therapeutics and diagnosis. The combined features of VHHs potential tools for many applications. In this chapter, we focus on the development and use of VHHs for anti-viral therapy. It is interesting to point that in the field of therapy, only one monoclonal antibody is used today (Synagis) against infectious disease (Groothuis and Simoes, 1993).

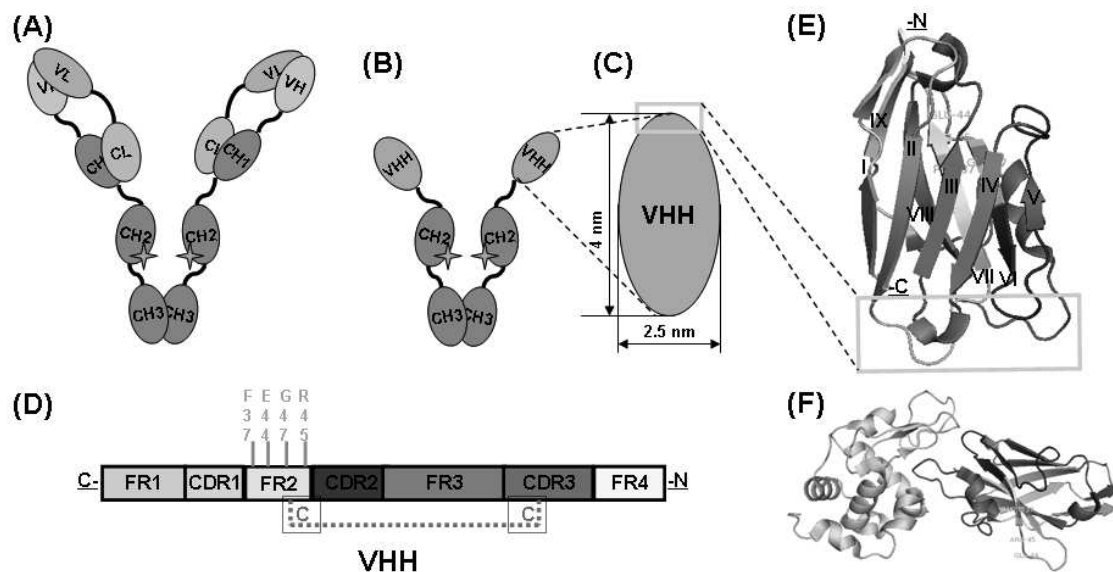


Figure 1. Representative diagrams of a conventional antibody, an HCAb, and a VHH. (A) A conventional antibody is a dimeric molecule, and each monomer comprising a heavy chain and a light chain. The heavy chain consists of the constant domains (CH1, CH2 and CH3) and the variable domain (VH). The light chain has only one conserved domain (CL) and a variable domain (VL). Important glycosylation sites (orange stars) are present in CH2, which is responsible for effector functions and the flexibility of the molecule. (B) The HCAb devoid of the light chain and CH1 is the paratope (yellow box) present only in the single variable domain (VHH). (C) The VHH can be expressed as a prolate-shaped, soluble molecule of ~15 kDa, with. The yellow square shows the antigen binding site. (D) The VHH sequence is made of four Framework Regions (FR1, light gray; FR2, cyan; FR3, magenta and FR4, yellow), and three Complementary Determining Regions (CDR1, green; CDR2, blue and CDR3, red). Residues F37, E44, G47 and R45 (orange) are located in the FR2 and mask a hydrophobic patch. C, C- terminal; N, N-terminal. The dotted red line represents a disulfide bond between the FR2 and the CDR3; this bond stabilizes the molecule and is present in dromedaries. (E) A three-dimensional structure of an anti lysozyme VHH, showing the Ig folding of β sheets, five strands in the front (roman numerals: I - V) and four strands in the back (VI - IX). The enlarged yellow square shows the antigen binding site, formed by juxtaposition of three CDRs. (F) The VHH shown in (F) is drawn in complex with lysozyme (light blue). A protruding paratope consisting mainly of CDR3 (red) recognizes and binds the catalytic cleft of lysozyme, inhibiting its activity.

2. Influenza virus

Nowadays, the main prophylactic measure against Influenza is vaccination. Therapeutic options for influenza are small molecule drugs targeting the viral proteins Neuraminidase (NA) or matrix protein 2 (M2). Influenza virus poses a great and continuous threat to humans and zoonotic infections also pose a dangerous challenge to human. In the last six years, two important viruses have risen as pandemic or potential pandemic outbreaks: the recent pandemic outbreak in the 2009 by the swine-derived H1N1 influenza virus (also called the Mexican Flu) and Highly Pathogenic Avian Influenza (HPAV) viruses of the H5N1 subtype, mainly in Asiatic countries. The 2009 H1N1 pandemic presents an interesting case. It was a zoonotic infection that could be transmitted between humans, but had a low mortality rate. On the other hand, the HPAV H5N1 virus infections present a high replication efficiency, broader cell tropism and possible systemic spread in patients. Fulminant pneumonia, multi-organ failure caused by a

high viral load and an intense inflammatory response (cytokine storm) are responsible of a mortality rate of 60 % (de Jong et al., 2006). Vaccines to prevent HPAV infection are not available, but NA inhibitors (oseltamivir) are used as antiviral drugs. A combination of antiviral drugs and immunomodulators was used to control infection by HPAV H5N1 in patients, but its use was considered as a risk. On the other hand, passive immunization has been a successful alternative. Immunoglobulins in immune sera derived from animals or humans exposed to a homologous virus had been used to treat HPAV-infected humans (Luke and Subbarao, 2006; Zhou et al., 2007). In addition, the genetic shift and drift of the influenza virus underline the need for new antiviral approaches. In addition, the emergence of drug resistant strains poses an extra concern. The Tamiflu Resistant strain (conferred mainly by the H274Y mutation, (Wang et al., 2002a) is evidence of the urgent need of new anti-influenza tools. It is also urgent to develop new and better antiviral tools against the zoonotic Influenza virus, including HPAV. The characteristics of Nbs mentioned above makes them a potentially effective antiviral approach. Several attempts have been made to target conserved epitopes of proteins in the capsid of Influenza viruses. The main antigenic target in Influenza virus is the HA protein. However, the genetic shift of this viral protein, especially in its antigenic regions and including the binding site, complicates this approach. Even though this strategy has been successful in current seasonal vaccines, it is a costly and far from optimal: it is not suitable for emerging pandemic viruses, as has been proven not suitable by the Mexican flu in 2009.

2.1 Targeting Influenza HA: the Nb approach

The work of Hultberg and colleagues (Hultberg et al., 2011) is the first report of the use of Nb technology as an antiviral tool against influenza. That study proved the binding of the Nb to an Influenza protein and the neutralization of the binding of the virion to its cellular receptor in human transformed mammalian cells. These results are the proof of principle of the use of Nbs as antivirals. We discuss the most relevant results in scope of the potential further use of Nbs. To obtain Nanobodies directed against H5N1 viruses, llamas were immunized with recombinant H5N1 Hemagglutinin (H5, A/Vietnam/1203/2004). The nanobody repertoire of the hyperimmune animals was cloned into a phage display library, and two promising HA-binding Nbs were isolated. The VHH of the HCab or Nb was cloned, produced as monovalent molecules, purified and screened for specific binding to the antigen, using as competitor the HA surrogate receptor fetuin. Two of the specific binders (B12 and C8) had high affinity to HA ($K_D = 9.91$ and 30.1 nM) as determined by surface plasmon resonance. In addition, in a MLV (H5) pseudotyped neutralization assay both Nbs neutralized the parental virus A/Vietnam/1203/04 and also another clade 1 virus (A/Vietnam/1194/04) with a minimal inhibition concentration (IC_{50}) of 75 nM. The possibility of cross reactivity among different H5N1 clades was also tested. The Nbs efficiency in neutralizing other clades of Influenza virus decreased proportionally with the antigenic distance from the virus A/Vietnam/1203/04. Three viruses from clade 2.2 were inhibited by the monovalent Nbs in a similar range as clade 1 ($IC_{50} = 50$ – 150 nM). On the other hand, one virus of clade 2.3.4 and one virus from clade 2.5 showed little or no inhibition. As mentioned above, Nbs are potentially good building blocks for multivalent molecules due their small size, high affinity, and efficacy as a

production platform. Based on Nbs C-8, bivalent and trivalent constructs were made, using Gly4/Ser linkers (GS) of different lengths. As expected, the neutralization potential of the bivalent and trivalent constructions was greatly enhanced against the A/Vietnam/1194/04 virus ($IC_{50} \leq 1$ pM). Inhibition of this clade 1 virus was confirmed by a microneutralization assay in NIBRG-14 infected cells. NIBRG-14 is an engineered recombinant virus whose HA and NA are derived from the A/Vietnam/1194/04 virus. Surprisingly, the IC_{50} in the bivalent and trivalent Nbs neutralization activity (9 and 3 pM, respectively) decrease by more than 3 logs compared to the monovalent Nb. These results show that NIBRG-14 outperforms a previously developed monoclonal antibody CR 261 (Throsby et al., 2008). These results were also confirmed in a hemagglutination inhibition assay, which showed an IC_{50} of 2 nM for the bivalent and trivalent construction, compared to 156 nM of the monovalent.

The multivalency format also resulted in the potential for neutralization of Influenza virus of different clades. For three clade 2.2 viruses, two bivalent constructions of the Nb C-8 (9GS and 15 GS) did not show any decrease in the IC_{50} . On the other hand, the 10 GS linker trivalent molecule showed a 10 - 40 fold increase in the neutralization potential, but the 20 GS linker trivalent showed only two fold decrease in the IC_{50} , or none at all. Nevertheless, using the monovalent Nb the neutralization of virus from clades 2.3.4 or 2.5 was in the high nM range or absent, respectively. This result confirms the previous result showing that both bivalent and one trivalent (10GS) constructions decrease the IC_{50} to a low nM range. It is worth mentioning that the retroviral pseudovirus A/Vietnam/1194/04 and the Influenza virus NIBRG-14 share the same HA, but different results were obtained using the MLV pseudotyped neutralization assay and the infected cells microneutralization. Using the microneutralization, the reported IC_{50} of the monovalent; bivalent and trivalent molecules was reduced by ten-fold compared to the IC_{50} obtained by the pseudotyped neutralization. The difference in sensitivity of the assays emphasize the need to confirm the results of the different influenza clades by NBs by using infected cells based assays. The validation of the anti HA Nbs in an *in vivo* model was performed in a mouse model by Ibañez (Ibanez et al., 2011).

To confirm the efficacy of the Nbs *in vivo*, Ibañez et al. used an H5N1 NIBRG-14 mouse adapted (NIBRG-14 ma) virus strain. It is important to point out that the Nbs were administered intranasally in all mouse experiments, in order to enhance penetration in the respiratory tract. Initially, to evaluate the antiviral potential using the bivalent Nb (C-8, 15 GS) *in vivo*, a dose of 5 mg/kg (100 µg) was used in mice. This dose completely prevented loss of body weight at 4, 24 and 48 h before a challenge of 1 LD₅₀ of NIBRG-14 ma, compared to the controls after 4 days of monitoring. Using the same set up, on day 4 after challenge, any detectable lung virus titers were observed at 4 and 24 hrs before challenge, and at 48 hrs the titer was 50-fold lower than in controls. These results suggested that the bivalent Nbs provide strong protection against 1 LD₅₀, but it is important to consider the half life of the molecule. In previous *in vitro* results, the bivalent Nb neutralization activity was even 3 logs higher than that of the monovalent Nb, but *in vivo* also there was a significant improvement using the bivalent. The difference in the virus neutralization capacity between the monovalent and bivalent Nbs and the minimal protective dose was assessed by administration of different doses of Nbs 24 h before challenge with 1 LD₅₀ NIBRG-14. The doses of Nb ranged from 3 to 0.025 mg/kg, and complete neutralization was confirmed for the highest doses of both constructions. In addition, administration of the highest dose (60 µg, 3 mg/kg) of bivalent Nb 24 h before challenge with 4 LD₅₀ also resulted in complete protection. The monovalent neutralization activity was dependent on the amount of Nb, but it was statistically also for doses of 6 or

1.2 µg of Nb per mouse. Remarkably, very low or any lung virus titer was detected in mice treated with the bivalent Nb, even for the lowest doses used (2.5–0.5 µg). These results strongly confirmed the neutralization efficacy of the bivalent Nb when used as prophylactic tool against a NIBRG-14 ma, a highly pathogenic Influenza virus model.

In addition, the therapeutic efficacy of the bivalent Nb was also tested in the same model. The administration of 60 µg of bivalent Nb prevented the drop in body weight and showed a reduction in the lung viral titers when administered 4, 24 and 48 h after 1 LD₅₀ challenge. On the other hand, 72 h after challenge, the drop in body weight was similar to that of the controls, but statistically significant reduction in lung viral titers was observed. The decrease in viral titers was also confirmed by measuring the amount of viral RNA by RT-PCR. In addition, 48 h after challenge of mice (treated with this dose of bivalent Nb) with 4 LD₅₀ of NIBRG-14 ma, weight loss was observed and also a delay in mortality compared with the controls.

The antigenic site of the HA was mapped by escape mutants in presence of the monovalent or bivalent Nbs. Three escape mutants were selected in the presence of monovalent Nb, K189E/N and N154D/S mutations were found, they are contiguous in the antigenic B site of the HA (Wiley et al., 1981; Yamada et al., 2006). It is noteworthy to mention that N154D/S remove an N glycosylation site, a possible adaptation to mask an antigenic site (Fig.2). The escape mutants selected in presence of the bivalent Nb presented not only the K189E/N mutation, but an additional D145N mutation located in the stalk of HA, 40 residues upstream of the membrane anchor. The results of the hemagglutination assays and microneutralization experiments suggest that mutation K189N/E is necessary and sufficient to abolish binding to the Nb in a monovalent or bivalent conformation, indicating a close proximity between the antigenic B site and the receptor binding domain. Those results are the first one reported of the potential antiviral activity of a Nb against the Influenza virus.

The Nb viral neutralization activity against a trimeric HA molecule (HA) was greatly enhanced when presented as bivalent and trimeric molecule, but the dynamics and details of the binding are not clear. It has been demonstrated that in intramolecular binding, a multivalent molecule has greater avidity than its monovalent counterpart. But a very interesting question is whether intermolecular binding occurs during Nb binding to the HA. In recent reports, the existence of intermolecular binding was proved to enhance an antiviral effect (Wang and Yang, 2010). Intermolecular binding could explain the increase in the neutralization activity: steric, the hindrance of the HA for its cellular receptor is enhanced, and the flexibility of the HA is decreased.

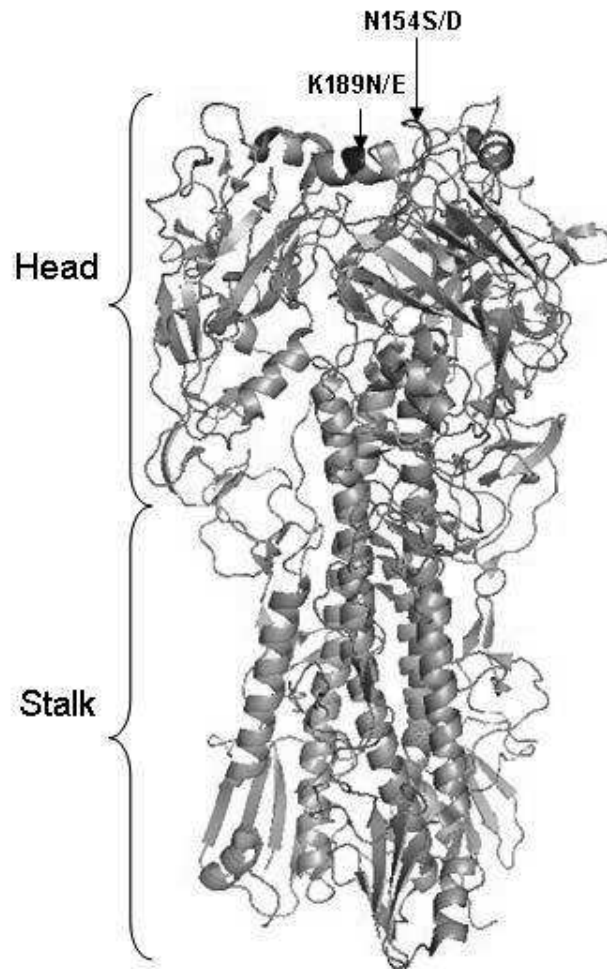


Figure 2. Ribbon representation of the H5N1 HA trimeric protein. Two mutations in the head of the trimer confer resistance to the monovalent and bivalent VHH C-8. The mutation K189N/E was necessary and sufficient to prevent binding of both mono and bivalent proteins. (PDB : 2IBX)

3. RSV virus

Respiratory Syncytial Virus (RSV) infections are the leading cause of acute lower respiratory tract infections (ALRI) in children and associated hospitalizations world wide (Falsey et al., 2005; Nair et al., 2010). There is no specific antiviral therapy for RSV infection available. Each year 66, 000 – 199,000 children die worldwide due to RSV ALRI. Most pediatric cases of fatal RSV infections occur in developing countries. As RSV infections do not evoke protective immunity, infections occur throughout life, causing severe morbidity in young infants, the elderly, and immune-comprised adults (Boyce et al., 2000; Falsey et al., 2005).

Although high levels of RSV neutralizing antibodies correlate with lower frequencies of RSV-associated ALRI, no RSV vaccine is available (Glezen et al., 1981). However, monthly administration of large amounts of a humanized RSV neutralizing antibody, palivizumab (Synagis), reduces RSV-associated hospitalization of high risk infants by about 78-39% (Groothuis and Simoes, 1993). Palivizumab is currently the sole monoclonal antibody that is approved

for preventing viral infection. Palivizumab blocks fusion of the RSV membrane with the membrane of the target cell by binding to the RSV fusion protein (F) (Huang et al., 2010). However, due to the high cost of Palivizumab, there is an urgent need for new anti-virals that can prevent or treat RSV infections. RSV neutralizing Nbs have been developed as an alternative to antibodies (Hultberg et al., 2011).

3.1 RSV binding VHHs antiviral effect: comparison with Synagis Mab.

To investigate if Nbs could be used for antiviral therapy, Nbs that bind to the palivizumab epitope were developed. For this purpose, two llamas were immunized with recombinant RSV A F protein (RSV F_{TM-}) lacking the transmembrane region (Hultberg et al., 2011). This protein folds into trimers that resemble the native RSV F protein in its post-fusion conformation (Ruiz-Arguello et al., 2004). Remarkably, RSV F_{TM-} proteins can be readily recognized by RSV F neutralizing antibodies that, just like palivizumab, bind to the antigenic site II (McLellan et al., 2011; Swanson et al., 2011). In this way, RSV F_{TM-} immunization can potentially induce RSV F antigenic site II specific camelid HCabs. HcAbs that specifically bind to the RSV F antigenic region II were enriched by biopanning using RSV F_{TM-} protein and competitive elution in the presence of excess of palivizumab antibody. From these HCabs, VHHs were produced and tested for binding to the RSV F_{TM-} protein. Twelve VHHs that bound to the RSV F protein were tested for neutralization of RSV Long strain (RSV A subtype) virus in a micro-neutralization assay. Two VHHs (RSV-C4 and the RSV-D3) could neutralize RSV in the high nanomolar range (IC₅₀: 640 nM and 300 nM, respectively), which is similar to the neutralization activity than the Synagis Fab (IC₅₀: 549.2 nM) and about 100-fold less effective as the Synagis Mab (IC₅₀: 3.02 nM). However, in contrast to palivizumab, neither RSV-C4 nor RSV-D3 VHHs could neutralize RSV B subtype virus *in vitro*. On the contrary, another VHH (RSV-E4) could neutralize RSV B infection to some extent.

The epitopes of different VHHs were determined by antibody competition assays and diverse antibody escape RSV mutants. Whereas RSV-C4 and RSV-D3 VHHs readily competed with palivizumab for binding to recombinant RSV F_{TM-} or inactivated RSV virions, RSV-E4 competed with 101 Fab, which is known to bind to the antigenic region IV-VI (Wu et al., 2007). These data are in line with the observation that AA substitutions within antigenic regions II and IV-VI, respectively, affected the binding of both RSV-D4 and RSV-C3 VHHs and RSV-E4 VHH. These data strongly suggest that both RSV-C3 and RSV-D4 bind to antigenic region II (palivizumab epitope) (Crowe et al., 1998) whereas RSV-E4 VHH binds to antigenic region IV-VI, explaining the observed differences in neutralization.

The affinity of the three VHHs, Synagis Mab and Synagis Fab was determined by Surface Plasmon Resonance using recombinant RSV F_{TM-} as bait. The K_D of RSV-D3, RSV-E4 and RSV-E4 were in the low nanomolar range: 9.24 nM, 1.78 nM and 0.45 nM, respectively. Although RSV-D3 was more effective than RSV-C4 at neutralizing RSV A, it had a lower affinity for F_{TM-} than RSV-C4. Moreover, the efficient binding of RSV-E4 VHH to a neutralizing epitope (antigenic region IV-VI) was not associated with neutralization of RSV A. This suggests that the affinity of VHHs for

the recombinant RSV F_{TM}, which likely represents the F protein in its post-fusion conformation, does not correlate directly with neutralization of living RSV (Table 1.)

It has been reported before that the avidity of a binding molecule can be increased in a multivalent format (Rudge et al., 2007; Wang and Yang, 2010). In order to increase its antiviral potential, the RSV-D3 was selected and formatted in a bivalent molecule, by a flexible linker of Gly₄/Ser (GS). Surprisingly, bivalent RSV-D3 VHH's with GC linkers of different size neutralized RSV A Long virus between 2421 and 4181 times more efficient than monovalent RSV-D3 VHH's, reaching picomolar range (190 - 110 pM). In contrast, Synagis Mab was only 200 times (IC₅₀: 6.5 nM) more efficient in neutralizing RSV A virus than its corresponding Fab fragment. In this way bivalent RSV F specific VHHs outperform the Synagis antibody in RSV neutralization. Moreover, in contrast to its monovalent format, bivalent RSV-D3 could also neutralize RSV B1 strain virus. Also linking two different VHHs, RSV-D3 and RSV-E4 targeting two different epitopes, notably boosted neutralization of both RSV A and B virus subtypes. Likely the profound enhancement in activity by linking two VHHs is enabled by the flexibility of the linker. Experiments aiming to characterize the binding dynamics of the RSV-D3 to the F protein are necessary for characterize an intra- or intermolecular binding.

Table 1. Inhibition and protection of the RSV virus A binding RSV-D3.

	F-RSV-D3m	F-RSV-D3b	Synagys
In vitro neutralization (IC ₅₀ , nM)	300	0.05 - 0.14 nM*	1.03 - 5.5 nM*
Prophylactic minimal protective dose (mg/kg)	ND	12 µg	ND
Prophylactic protective extension (mg/kg)	ND	48 hrs	ND
Therapeutisch protection extension	ND	24 hrs	ND

* Obtained from two different cell based assays, microneutralization and plaque assay

The RSV protein F is responsible of the fusion of the viral lipid membrane with the host membrane, but also participates in the attachment of the RSV virions to target cells. Moreover it was recently demonstrated that RSV F protein can bind to nucleolin expressed at the surface of target cells and that this interaction is crucial for RSV infection *in vitro* and *in vivo* (Tayyari et al., 2011). After viral attachment, the RSV F protein mediates fusion of the viral membrane with the plasma membrane of the target cell, thereby releasing the viral genome into the cytoplasm of the host cell. This process involves a series of conformational changes of the F protein from a metastable pre-fusion to a stable post-fusion conformation. We recently demonstrated that bivalent RSV-D3 VHHs can prevent RSV infection both before and after viral attachment, can inhibit syncytia formation but cannot hamper RSV attachment (Schepens et al., 2011). Together observations constantly indicate that in a similar mechanism that palivizumab, bivalent RSV-D3 VHHs prevent RSV infection by blocking fusion. Although the conformations of the RSV F antigenic regions II and IV-VI are maintained in the post-fusion form, it is more plausible that the RSV VHHs block viral fusion and syncytia formation by binding to the RSV F protein in either its pre-fusion or intermediate conformations (Fig. 3). Possibly, binding of the VHHs to the antigenic region II interferes with the conformational changes of the F protein that are required for fusion.

Immune compromised (cyclophosphamide treatment) Balb/c mice were used to test whether bivalent RSV-D3 VHHs could protect against RSV infection *in vivo* (Schepens et al., 2011). As VHHs are known to remain active in the respiratory tract after nebulisation, bivalent RSV-D3 and control VHHs were administered intranasally (patent application WO 2009/147248). Prophylactic treatment of mice with 5mg/kg bivalent RSV-D3 VHH or palivizumab reduced RSV pulmonary titers below the detection limit of the RSV plaque assay. This strong reduction was confirmed by quantitative PCR analysis. Remarkably, as low as 0.6 mg/kg bivalent RSV-D3 could either prevent or strongly reduce (at least 100-fold) pulmonary RSV replication. In comparison, monovalent RSV-D3 VHH could protect against pulmonary RSV replication about 25 times less efficient than their bivalent counterpart. In order to be valuable, even an easy to administer prophylactic treatment should have a long-lasting effect. We could demonstrate that intranasal administration of bivalent RSV-D3 VHHs can protect at least for 48 hours against RSV infection. Although prophylactic treatment with palivizumab in high risk infants reduces RSV associated hospitalization, there is currently no effective therapeutic treatment available. Therefore RSV-D3 VHHs were also evaluated as therapeutic treatment. Intranasal administration of RSV-D3 VHHs 4 or 24 hours after infection strongly reduced (at least 100-fold) pulmonary RSV replication. Plaque assays also indicated that administration of bivalent RSV-D3 VHHs 72 hours after RSV treatment can reduce pulmonary RSV replication. However, as lung homogenates used to quantify the pulmonary RSV titer in mice (treated 72 hours after infection) still contained neutralizing RSV VHHs, it is not clear to which extend treatment at this time point reduced RSV replication *in vivo*. The potential of bivalent VHHs to prevent morbidity and pulmonary inflammation upon RSV infection was assessed in a non immunocompromised mice model. Prophylactic administration of bivalent RSV-D3 VHHs (1 mg/kg) could completely prevent body weight loss and pulmonary cell infiltration that was observed in mice treated with control VHHs. Therapeutic treatment with bivalent RSV-D3 VHHs 24 hours after infection partially reduced body weight loss and pulmonary cell infiltration. These observations confirm the *in vivo* antiviral potential of neutralizing VHHs.

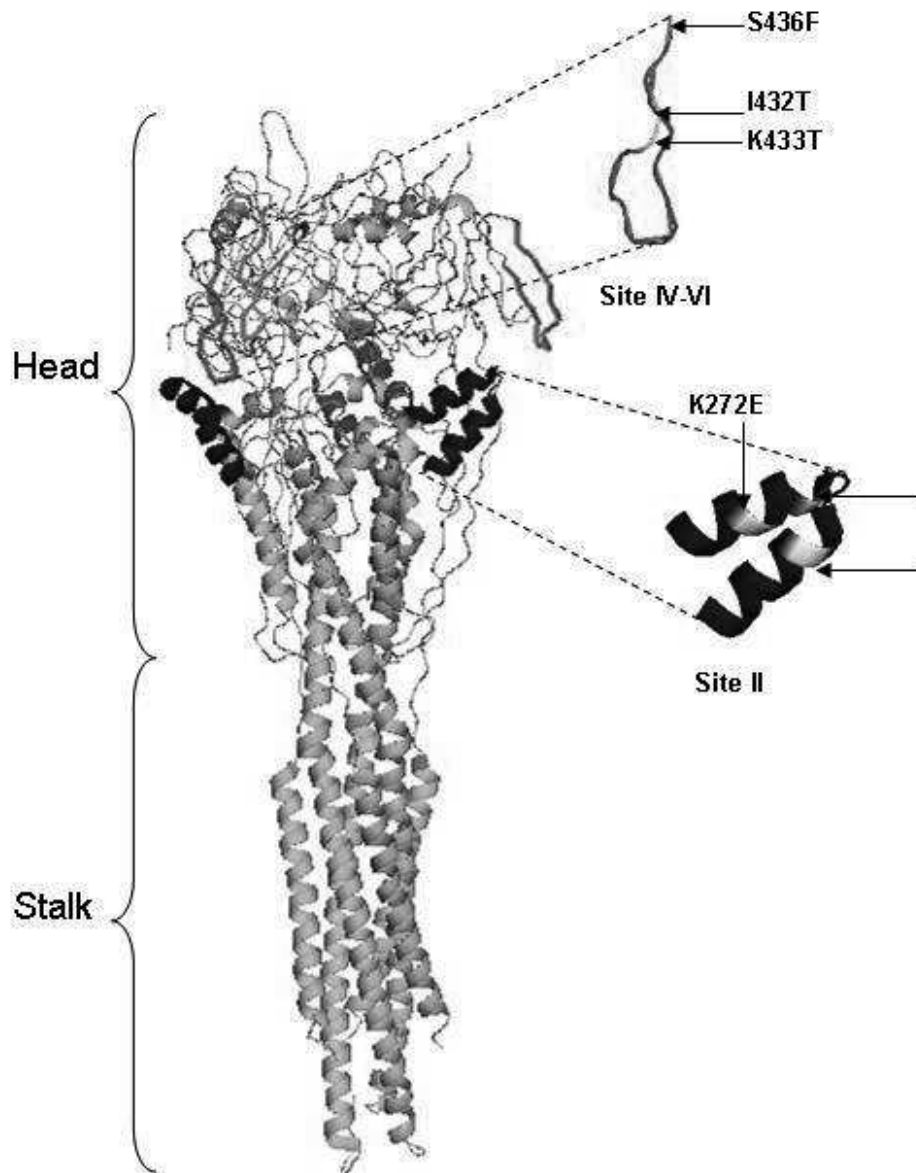


Figure 3. Ribbon representation of the RSV F protein trimer structure, in the post-fusion form. In this recombinant protein the head and stalk are depicted of the protein, and lacking the fusion peptide, the transmembrane region and the cytoplasmic domain. The immunogenic epitopes recognized by the 101F Mab (site II) and the palimuzab (site IV-VI) are shown in red and blue respectively, the rest of the F protein in green. The RSV-D3 and RSV-C4 resistant escape mutants are shown in yellow. The mutations I432T, K433T and S436F localized in the site II disrupt the binding of the RSV-C4. The K262Y, N268I and K272E in the site IV-IV, resulting in loss of binding of the RSV-D3 molecule. (PDB: 3RKI).

Currently Ablynx is preparing a phase I clinical trial to evaluate the safety of a trivalent RSV neutralizing VHH format which consists of 3 identical VHHs. Preclinical evaluation of this lead candidate illustrated its potential to

readily neutralize a broad spectrum of clinical RSV A and RSV B subtype viruses, more efficiently than Synagis (abstract, 7th international RSV symposium). *In vivo* studies demonstrated that both prophylactic and therapeutic treatment with this RSV neutralizing VHH can readily reduce RSV replication in the upper and lower respiratory tract of cotton rats (abstract, 7th international RSV symposium).

In summary, neutralizing RSV VHHs are exciting new candidates for anti-RSV therapeutics for different reasons. First, VHHs allow versatile formatting including the creation of multivalent formats by the use of flexible linkers. This feature enabled the creation of bivalent and trivalent VHH which can neutralize RSV at picomolar range, more than 1000 fold more efficient than their monovalent counterpart. Second, by linking two different VHHs which neutralize different virus strains (such as the RSV A versus the RSV B subtype strains) cross-reactive VHH constructs can be obtained. Moreover, as a result of avidity effects, cross linking VHH with different specificity can considerably improve the neutralizing activity. Third, the VHHs small size and protruding paratopes can contribute to its neutralizing activity. As structural models and electron microscopic analysis indicate that the antigenic region II is located at the side of the RSV F protein trimer, at the dense surface of RSV virions this region is reasonably more accessible for small and flexible VHH formats rather than for large more rigid antibodies (Ruiz-Arguello et al., 2004; McLellan et al., 2011) (Fig. 3). Fourth, due to their high stability at stringent conditions, VHHs can be administered via nebulisation, which allows a rapid accumulation of high amounts of neutralizing VHH at the site of respiratory viral infections. In addition, due to the high stability of VHHs and the ease of intranasal or pulmonary administration, VHH therapy could be applied more generally, even in developing countries.

4. Rabies Virus

Rabies virus (RV) is a single stranded RNA virus, from the *Rhabdoviridae* family, genus *Lyssavirus*. The infection with RV in humans causes acute encephalitis, with a mortality rate of almost 100 %. It is transmitted to humans by bite from a carnivore or quiroptera vector and the majority of cases occur in Asia or Africa. The long incubation period following infection by RV presents a paradigm, because of the absence or very weak immune response (Johnson et al., 2010). The small amount of virus inoculated after infection and the neurotropism of RV have been considered as factors that contribute to the lack of effective antibodies in the patient. After the bite, wound cleaning is a highly and low cost means to lower the chances of a productive infection in human. Passive immunization and vaccination promptly after exposure remains the only efficient therapeutic tool nowadays. Modern vaccines are inactivated virus produced from continuous cell lines, like the human -diploid -cell vaccine by Aventis Pasteur. Nevertheless, in underdeveloped countries, the high cost of established RV therapy (attenuated virus, Mab anti RV) represents a non affordable approach for the majority of the population. The RV has a genome of 12 kDa coding for 5 proteins: the nucleoprotein, phosphoprotein, matrix, a RNA-dependent RNA polymerase and the Glycoprotein (RVG). In the virus particle, the RVG is the only viral protein exposed as a trimeric spike, responsible of: i) recognition of cellular receptors; ii) the determination of the virulence; iii) antigenicity.

4. 1 Nbs present a broad protection against Rabies Virus

For more than 25 years, two well-defined antigenic sites in the RVG had been characterized by Mabs, the antigenic site II and III (Lafon et al., 1990). Other epitopes are also been characterized, but their contribution to the antigenicity is minor. The antigenic site III extends from 330 to 340 amino acids and is linear (Seif et al., 1985). The mutations in this site affect the virulence and the host range of the virus. On the contrary, the antigenic site II is conformational and discontinuous, determined by two regions, amino acids 34 -42 and 198-200. This site is responsible of approximately 70 % of the known MABs against RVG (Benmansour et al., 1991).

The RGV is an interesting target for the Nb platform, because of the need of alternative cost effective antirabies tools. In a similar approach as those previously discussed for the Influenza and RSV, a llama was immunized with recombinant RVG and 5 VHHs were obtained (Rab - E8, H7, F8, E6 and C12). Those VHHs were validated in their neutralizing activity against 10 Rabies genotype 1 viruses: 3 laboratory strains (CVS-11 as prototype, ERA, CB-1) and 7 field isolates. Also one rabies genotype 5 virus (EBL-V1) was included to validate broad cross neutralization. The data of the virus neutralization relies on one cell based assay, the Rapid Fluorescent Focus Inhibition Test (RFFIT) (Vene et al., 1998). This assay has been internationally recognized as the *in vitro* standard for virus neutralizing antibodies. The Mab 8-32, which recognizes the RVG protein antigenic site II, was also included as positive control (Montano-Hirose et al., 1993). The VHHs F8, E6, H7 and C12 neutralized the genotype 1 strains: CB-1 and ERA, with an IC₅₀ in the low nanomolar range; the CVS-11 strain from the low to high nanomolar range. Also they were able to neutralize several field isolates. On the other hand, the E8 was efficient in the neutralization only of the CB-1 and CVS-11, in the low and high nanomolar range, respectively. When compared with MAb 8-2, the C12 and E6 presented better neutralization activity, against the strains ERA and CB-1. Using the same reasoning of the previous sections, the authors also use the bivalent approach against the Rabies genotype 1 CVS -11 and the genotype 5 EBLV-1. Bivalent monoparatopic VHHs (H7, E8 and F8) were constructed using a Gly4/Ser linker. The neutralization IC₅₀ of these constructions was reduced from a 2 fold - 180 fold, compared with the monovalent protein, indicating the previously seen enhancement of the neutralization. Nevertheless, the best results were obtained when biparatopic molecules were used. The E6/H7 and the H7/F8 molecules increase the neutralization potency by a 2 log factor, while the E8/H7 reach an increase of 3 log fold, compared with the monovalents. The E8/H7 even outperformed the Mab 8 -2 against the CVS-11. On the contrary, in the case of the genotype 5 strain EBLV-1, the monovalent molecules showed no or modest neutralization potency. But confirming the tendency shown above, the biparatopic molecule E8/C12 presented an increase in the neutralization potential of 147 fold (IC₅₀ = 3.76 nM) compared with the monovalent moiety, but not as low as Mab 8 - 2 (IC₅₀ = 0.12 nM). The results of competition assays of the 5 VHHs against the Mab 8- 2 shown that the E6, E8, F8 and H7 compete for the same epitope. On the other hand, the C12 did not compete with the Mab 8-2, which indicates the recognition of a different epitope. The difference in epitope recognition can be one of the causes of the high and broad effect of biparatopic molecules, specially the E8/C12, which recognize different epitopes in the RVG. Experiments using those VHHs with Rabies mutant virus, carrying substitutions in the known residues in the antigenic site II, could define the exact place of binding of these new

antibodies. For example it is reported that the substitution K198E of the glycoprotein abolish the binding of the Mab 8 - 2 (Montano-Hirose et al., 1993). Unfortunately, the crystallographic structure of the RVG protein has not been reported. For modelling of the RVG structure, the vesicular stomatitis virus glycoprotein is often using as template and surrogate (Cibulski et al., 2009; Tomar et al., 2010). We are using the alignment of this protein with the RVG as reference, to show the possible structure representation of the antigenic site II (Fig. 4). The purpose of this estimate is to show the tendency of the VHHs to recognize conformational epitopes, over linear epitopes. In line with the results of the neutralizing VHHs against Influenza and RSV, the results of the broadness and the high potency against both RV genotypes indicate these RV neutralizing VHHs as a promising tool. Nevertheless, in contrast with the previous cases of the Influenza and RSV VHHs, there is not *in vivo* validation of the RV neutralizing VHHs available.

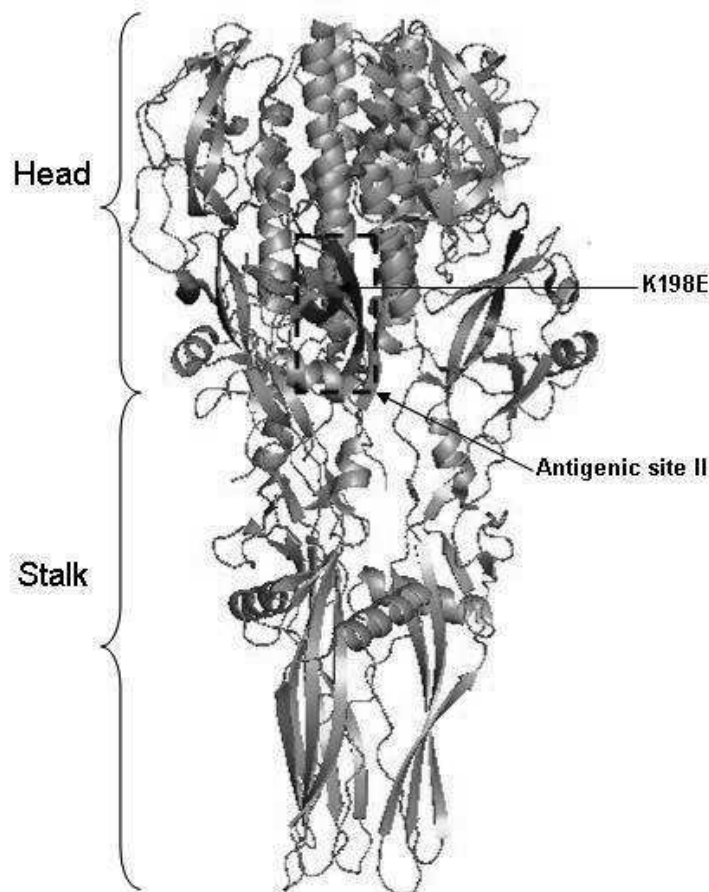


Figure 4. Schematic representation of the trimeric vesicular stomatitis vesicular virus protein G trimer. This protein is taken as reference to depict the amino acids corresponding with the antigenic site II of the Rabies Virus glycoprotein (residues 34-42, and 198-200, in blue). The localization of the K198E mutation that prevents the binding of the Mab 8-2 is shown in red. The VHHs E8, F8, E6 and H7 compete with the MAb 8- 2 for the binding, mapping their possible epitope within the antigenic site II. (PDB: 2CMZ)

5. Conclusion

The Nb platform as an antiviral agent is a new and promising antiviral tool. The ease to produce Nbs in bacterial and lower eukaryotic cells and the possibility to produce tailor made construction makes them an attractive and cost effective alternatives compared to established antiviral means. This approach may be useful for the treatment of infectious orphan diseases (including viral) and in developing countries, where the “standard” prophylaxis or therapy is prohibitively expensive or not available. In this work we discussed the data of recently developed Nanobodies directed against 3 human viruses: the generation and *in vitro* validation of the VHHs against Influenza H5N1, RSV and RV (Hultberg et al., 2011); the *in vivo* validation of the Influenza HA binding VHH (Ibanez et al., 2011) and RSV (Schepens et al., 2011). In the case of protection against Influenza infection the bivalent format of the Nbs proved superior *in vitro* and *in vivo*. But, as indicated by the successful *in vivo* validation of one of the H5N1 strains, it is imperative to extend this validation to the others Influenza strains. Furthermore, it would be very interesting to isolate and characterize Nbs that recognize conserved domains in HA, such as the stalk. In line with the Influenza results, the RSV and RVG neutralizing Nbs activity was significantly higher in the bivalent compared to the monovalent format, increasing both the cross neutralization activity and potency. Those results manifest the advantages of using a multimeric format against multimeric viral targets. As stated before, the increase in avidity and the intra or inter molecular binding can be part of the explanation of the enhancement in the antiviral potential. Experiments to assess this could lead to a better design of multivalent antiviral antibodies. The surprising results confirm two important points: the high potential of the Nbs as prophylactic and therapeutic tools, and the development of Nbs directed against other infectious diseases. The similarity among the three proteins used as antigens (HA, RSVF and RVG) besides their trimeric architecture and antigenicity, is limited. The functionally similar HA and the RVG proteins are involved in the cellular receptor binding, whereas RSVF participates in virion binding to the receptor, its main function is in membrane fusion. In all three cases Nbs with the capacity to neutralize the viral target by blocking binding or hampering necessary conformational changes indicates the great versatility and efficiency of the antiviral Nbs here discussed. In competition assays, the recognition of non – conventional epitopes by these antiviral Nbs was not observed, but could be focused on in the future. In the three cases, the Nbs recognized well known antigenic sites that are also targeted by Mabs. The described viral proteins are not enzymes, and lack extensive antigenic clefts. This could be one reason why recognition of the Nbs of “classical” epitopes in the viral proteins appeared to be preferred. If the presence of antigenic clefts could lead to recognition of none “classical” epitopes in the viral proteins, targeting viral enzymes could be an interesting approach. Enzymes like the Influenza Neuraminidase could be an interesting target. This viral sialidase presents a catalytic cleft, in which framework and substrate contact residues are conserved in most of the Influenza strains. The coming years will probably bring potent novel anti-viral Nbs directed against different viruses and it is likely that some of these Nbs will reach clinical trials.

6. Acknowledgement

We are grateful to Dr. Amin Bredan for editing the text. M.C. holds a VIB international PhD fellowship. L.I.I. was a beneficiary of the Belgian Federal Sciences Administration (Federale Wetenschapsbeleid, BELSPO) and was supported by Ghent University IOF grant Stepstone IOF08/STEP/001. B.S. is a postdoctoral fellow of FWO-Flanders.

7. References

7. References

- Arbabi Ghahroudi, M., Desmyter, A., Wyns, L., Hamers, R. & Muyldermans, S. (1997). Selection and identification of single domain antibody fragments from camel heavy-chain antibodies. *FEBS letters* 414, 521-526.
- Barre, S., Greenberg, A. S., Flajnik, M. F. & Chothia, C. (1994). Structural conservation of hypervariable regions in immunoglobulins evolution. In *Nat Struct Biol*, pp. 915-920.
- Benmansour, A., Leblois, H., Coulon, P., Tuffereau, C., Gaudin, Y., Flamand, A. & Lafay, F. (1991). Antigenicity of rabies virus glycoprotein. In *J Virol*, pp. 4198-4203.
- Boyce, T. G., Mellen, B. G., Mitchel, E. F., Wright, P. F. & Griffin, M. R. (2000). Rates of hospitalization for respiratory syncytial virus infection among children in medicaid. In *J Pediatr*, pp. 865-870.
- Cibulski, S. P., Sinigaglia, M., Rigo, M. M., Antunes, D. A., Vieira, G. F., Fulber, C. C., Chies, J. A. B., Franco, A. C. & Roehe, P. M. (2009). Structure modelling of Rabies Virus Glycoprotein. In *5th International Conference of the Brazilian Association for Bioinformatics and Computational Biology*. Rio de Janeiro.
- Crowe, J. E., Firestone, C. Y., Crim, R., Beeler, J. A., Coelingh, K. L., Barbas, C. F., Burton, D. R., Chanock, R. M. & Murphy, B. R. (1998). Monoclonal antibody-resistant mutants selected with a respiratory syncytial virus-neutralizing human antibody fab fragment (Fab 19) define a unique epitope on the fusion (F) glycoprotein. *Virology* 252, 373-375.
- De Genst, E., Silence, K., Decanniere, K., Conrath, K., Loris, R., Kinne, J., Muyldermans, S. & Wyns, L. (2006). Molecular basis for the preferential cleft recognition by dromedary heavy-chain antibodies. In *Proc Natl Acad Sci*, pp. 4586-4591.
- de Jong, M. D., Simmons, C. P., Thanh, T. T., Hien, V. M., Smith, G. J., Chau, T. N., Hoang, D. M., Chau, N. V., Khanh, T. H., Dong, V. C., Qui, P. T., Cam, B. V., Ha do, Q., Guan, Y., Peiris, J. S., Chinh, N. T., Hien, T. T. & Farrar, J. (2006). Fatal outcome of human influenza A (H5N1) is associated with high viral load and hypercytokinemia. In *Nature medicine*, pp. 1203-1207.
- Decanniere, K., Desmyter, A., Lauwereys, M., Ghahroudi, M. A., Muyldermans, S. & Wyns, L. (1999). A single-domain antibody fragment in complex with RNase A: non-canonical loop structures and nanomolar affinity using two CDR loops. In *Structure*, pp. 361-370.
- Decanniere, K., Muyldermans, S. & Wyns, L. (2000). Canonical antigen-binding loop structures in immunoglobulins: more structures, more canonical classes? In *J Mol Biol*, pp. 83-91.
- Desmyter, A., Spinelli, S., Payan, F., Lauwereys, M., Wyns, L., Muyldermans, S. & Cambillau, C. (2002). Three camelid VHH domains in complex with porcine pancreatic alpha-amylase. Inhibition and versatility of binding topology. In *The Journal of biological chemistry*, pp. 23645-23650.
- Desmyter, A., Transue, T. R., Ghahroudi, M. A., Thi, M. H., Poortmans, F., Hamers, R., Muyldermans, S. & Wyns, L. (1996). Crystal structure of a camel single-domain VH antibody fragment in complex with lysozyme. In *Nat Struct Biol*, pp. 803-811.
- Els Conrath, K., Lauwereys, M., Wyns, L. & Muyldermans, S. (2001). Camel single-domain antibodies as modular building units in bispecific and bivalent antibody constructs. *The Journal of biological chemistry* 276, 7346-7350.

- Falsey, A. R., Hennessey, P. A., Formica, M. A., Cox, C. & Walsh, E. E. (2005). Respiratory syncytial virus infection in elderly and high-risk adults. In *The New England journal of medicine*, pp. 1749-1759.
- Glezen, W. P., Paredes, A., Allison, J. E., Taber, L. H. & Frank, A. L. (1981). Risk of respiratory syncytial virus infection for infants from low-income families in relationship to age, sex, ethnic group, and maternal antibody level. In *J Pediatr*, 708-15 edn.
- Greenberg, A. S., Avila, D., Hughes, M., Hughes, A., McKinney, E. C. & Flajnik, M. F. (1995). A new antigen receptor gene family that undergoes rearrangement and extensive somatic diversification in sharks. *Nature* 374, 168-173.
- Groothuis, J. R. & Simoes, E. A. (1993). Immunoprophylaxis and immunotherapy: role in the prevention and treatment of respiratory syncytial virus. In *Int J Antimicrob Agents*, pp. 97-103.
- Hamers-Casterman, C., Atarhouch, T., Muyldermans, S., Robinson, G., Hamers, C., Songa, E. B., Bendahman, N. & Hamers, R. (1993). Naturally occurring antibodies devoid of light chains. *Nature* 363, 446-448.
- Hmila, I., Saerens, D., Ben Abderrazek, R., Vincke, C., Abidi, N., Benlasfar, Z., Govaert, J., El Ayeb, M., Bouhaouala-Zahar, B. & Muyldermans, S. (2010). A bispecific nanobody to provide full protection against lethal scorpion envenoming. *Faseb J* 24, 3479-3489.
- Huang, K., Incognito, L., Cheng, X., Ulbrandt, N. D. & Wu, H. (2010). Respiratory syncytial virus-neutralizing monoclonal antibodies motavizumab and palivizumab inhibit fusion. In *J Virol*, pp. 8132-8140.
- Hultberg, A., Temperton, N. J., Rosseels, V., Koenders, M., Gonzalez-Pajuelo, M., Schepens, B., Ibanez, L. I., Vanlandschoot, P., Schillemans, J., Saunders, M., Weiss, R. A., Saelens, X., Melero, J. A., Verrips, C. T., Van Gucht, S. & de Haard, H. J. (2011). Llama-derived single domain antibodies to build multivalent, superpotent and broadened neutralizing anti-viral molecules. *PLoS one* 6, e17665.
- Ibanez, L. I., De Filette, M., Hultberg, A., Verrips, T., Temperton, N., Weiss, R. A., Vandeveld, W., Schepens, B., Vanlandschoot, P. & Saelens, X. (2011). Nanobodies with in vitro neutralizing activity protect mice against H5N1 influenza virus infection. *The Journal of infectious diseases* 203, 1063-1072.
- Johnson, N., Cunningham, A. & Fooks, A. R. (2010). The immune response to the rabies infection and vaccination. In *Vaccine*, pp. 3896-3901.
- Lafon, M., Edelman, L., Bouvet, J. P., Lafage, M. & Montchatre, E. (1990). Human monoclonal antibodies specific for the rabies virus glycoprotein and N protein. In *The Journal of general virology*, pp. 1689-1696.
- Lauwereys, M., Arbadi Ghahroudi, M., Desmyter, A., Kinne, J., Holzer, W., De Genst, E., Wyns, L. & Muyldermans, S. (1998). Potent enzyme inhibitors derived from dromedary heavy-chain antibodies. In *EMBO J*, pp. 3512-3520.
- Luke, C. J. & Subbarao, K. (2006). Vaccines for pandemic influenza. *Emerging infectious diseases* 12, 66-72.
- McLellan, J. S., Yang, Y., Graham, B. S. & Kwong, P. D. (2011). Structure of respiratory syncytial virus fusion glycoprotein in the postfusion conformation reveals preservation of neutralizing epitopes. In *J Virol*, pp. 7788-7796.
- Montano-Hirose, J. A., Lafage, M., Weber, P., Badrane, H., Tordo, N. & Lafon, M. (1993). Protective activity of a murine monoclonal antibody against European bat lyssavirus 1 (EBL1) infection in mice. In *Vaccine*, pp. 1259-1266.
- Muyldermans, S., Atarhouch, T., Saldanha, J., Barbosa, J. A. & Hamers, R. (1994). Sequence and structure of VH domain from naturally occurring camel heavy chain immunoglobulins lacking light chains. In *Protein Eng*, pp. 1129-1135.
- Nair, H., Nokes, D. J., Gessner, B. D., Dherani, M., Madhi, S. A., Singleton, R. J., O'Brien, K. L., Roca, A., Wright, P. F., Bruce, N., Chandran, A., Theodoratou, E., Sutanto, A., Sedyaningsih, E. R., Ngama, M., Munywoki, P. K., Kartasmita, C., Simoes, E. A., Rudan, I., Weber, M. W. & Campbell, H. (2010). Global burden of acute lower respiratory infections due to respiratory syncytial virus in young children: a systematic review and meta-analysis. *Lancet* 375, 1545-1555.
- Rasmussen, S. G., Choi, H. J., Fung, J. J., Pardon, E., Casarosa, P., Chae, P. S., Devree, B. T., Rosenbaum, D. M., Thian, F. S., Kobilka, T. S., Schnapp, A., Konetzki, I., Sunahara, R. K., Gellman, S. H., Pautsch, A., Steyaert, J., Weis, W. I. & Kobilka, B. K. (2011). Structure of a nanobody-stabilized active state of the beta(2) adrenoceptor. *Nature* 469, 175-180.
- Rudge, J. S., Holash, J., Hylton, D., Russell, M., Jiang, S., Leidich, R., Papadopoulos, N., Pyles, E. A., Torri, A., Wiegand, S. J., Thurston, G., Stahl, N. & Yancopoulos, G. D. (2007). VEGF Trap complex formation measures production rates of VEGF, providing a biomarker for predicting efficacious angiogenic blockade. *Proceedings of the National Academy of Sciences of the United States of America* 104, 18363-18370.
- Ruiz-Arguello, M. B., Martin, D., Wharton, S. A., Calder, L. J., Martin, S. R., Cano, O., Calero, M., Garcia-Barreno, B., Skehel, J. J. & Melero, J. A. (2004). Thermostability of the human respiratory syncytial virus fusion protein

- before and after activation: implications for the membrane-fusion mechanism. *The Journal of general virology* 85, 3677-3687.
- Schepens, B., Ibanez, L. I., Hultberg, A., Bogaert, P., De Bleser, P., De Baets, S., Vervalle, F., Verrips, T., Melero, J., Vandeveld, W., Vanlandschoot, P. & Saelens, X. (2011). Nanobodies specific for Respiratory Syncytial Virus Fusion protein protect against infection by inhibition of fusion. In *J Inf Dis*.
- Seif, I., Coulon, P., Rollin, P. E. & Flamand, A. (1985). Rabies virulence: effect on pathogenicity and sequence characterization of rabies virus mutations affecting antigenic site III of the glycoprotein. In *J Virol*, pp. 926-934.
- Stiehm, E. R., Keller, M. A. & Vyas, G. N. (2008). Preparation and use of therapeutic antibodies primarily of human origin. *Biologicals* 36, 363-374.
- Swanson, K. A., Settembre, E. C., Shaw, C. A., Dey, A. K., Rappuoli, R., Mandl, C. W., Dormitzer, P. R. & Carfi, A. (2011). Structural basis for immunization with postfusion respiratory syncytial virus fusion F glycoprotein (RSV F) to elicit high neutralizing antibody titers. *Proceedings of the National Academy of Sciences of the United States of America* 108, 9619-9624.
- Tayyari, F., Marchant, D., Moraes, T. J., Duan, W., Mastrangelo, P. & Hegele, R. G. (2011). Identification of nucleolin as a cellular receptor for human respiratory syncytial virus. *Nature medicine*.
- Throsby, M., van den Brink, E., Jongeneelen, M., Poon, L. L., Alard, P., Cornelissen, L., Bakker, A., Cox, F., van Deventer, E., Guan, Y., Cinatl, J., ter Meulen, J., Lasters, I., Carsetti, R., Peiris, M., de Kruif, J. & Goudsmit, J. (2008). Heterosubtypic neutralizing monoclonal antibodies cross-protective against H5N1 and H1N1 recovered from human IgM+ memory B cells. *PloS one* 3, e3942.
- Tomar, N. R., Singh, V., Marla, S. S., Chandra, R., Kumar, R. & Kumar, A. (2010). Molecular docking studies with rabies virus glycoprotein to design viral therapeutics. *Indian journal of pharmaceutical sciences* 72, 486-490.
- Vene, S., Haglund, M., Vapalahti, O. & Lundkvist, A. (1998). A rapid fluorescent focus inhibition test for detection of neutralizing antibodies to tick-borne encephalitis virus. In *J Virol Methods*, pp. 71 - 75.
- Verheesen, P., Roussis, A., de Haard, H. J., Groot, A. J., Stam, J. C., den Dunnen, J. T., Frants, R. R., Verkleij, A. J., Theo Verrips, C. & van der Maarel, S. M. (2006). Reliable and controllable antibody fragment selections from Camelid non-immune libraries for target validation. *Biochimica et biophysica acta* 1764, 1307-1319.
- Vu, K. B., Ghahroudi, M. A., Wyns, L. & Muyldermans, S. (1997). Comparison of llama VH sequences from conventional and heavy chain antibodies. *Molecular immunology* 34, 1121-1131.
- Wang, M. Z., Tai, C. Y. & Mendel, D. B. (2002). Mechanism by which mutations at his274 alter sensitivity of influenza a virus n1 neuraminidase to oseltamivir carboxylate and zanamivir. *Antimicrobial agents and chemotherapy* 46, 3809-3816.
- Wang, P. & Yang, X. (2010). Neutralization efficiency is greatly enhanced by bivalent binding of an antibody to epitopes in the V4 region and the membrane-proximal external region within one trimer of human immunodeficiency virus type 1 glycoproteins. In *J Virol*, pp. 7114-7123.
- Wiley, D. C., Wilson, I. A. & Skehel, J. J. (1981). Structural identification of the antibody-binding sites of Hong Kong influenza haemagglutinin and their involvement in antigenic variation. *Nature* 289, 373-378.
- Wu, S. J., Schmidt, A., Beil, E. J., Day, N. D., Branigan, P. J., Liu, C., Gutshall, L. L., Palomo, C., Furze, J., Taylor, G., Melero, J. A., Tsui, P., Del Vecchio, A. M. & Kruszynski, M. (2007). Characterization of the epitope for anti-human respiratory syncytial virus F protein monoclonal antibody 101F using synthetic peptides and genetic approaches. *The Journal of general virology* 88, 2719-2723.
- Wu, T. T., Johnson, G. & Kabat, E. A. (1993). Length distribution of CDRH3 in antibodies. In *Proteins*, pp. 1-7.
- Yamada, S., Suzuki, Y., Suzuki, T., Le, M. Q., Nidom, C. A., Sakai-Tagawa, Y., Muramoto, Y., Ito, M., Kiso, M., Horimoto, T., Shinya, K., Sawada, T., Kiso, M., Usui, T., Murata, T., Lin, Y., Hay, A., Haire, L. F., Stevens, D. J., Russell, R. J., Gamblin, S. J., Skehel, J. J. & Kawaoka, Y. (2006). Haemagglutinin mutations responsible for the binding of H5N1 influenza A viruses to human-type receptors. *Nature* 444, 378-382.
- Zhou, B., Zhong, N. & Guan, Y. (2007). Treatment with convalescent plasma for influenza A (H5N1) infection. *The New England journal of medicine* 357, 1450-1451.

CURRICULUM VITAE

Mr. Francisco Miguel Lopez Cardoso

Address: Iepenstraat 41, bus 4, Ghent, 9000 Belgium



Date of birth: 30/05/1981

Nationality: Mexican

Marital status: single

Telephone: +32 933 13623 (Work)

+32 488 617614 (Mobile)

e-mail: miguelc@dibr.ugent.be

miguelmofo@gmail.com

Key words: Influenza virus, neuraminidase, single chain antibodies, vaccine design

Professional profile

I am a positive, dedicated and self-motivated professional, with experience in Molecular and Cellular Biology, and more specifically Virology: viral and cellular regulation mechanisms; and vaccine design and validation. I am flexible and responsible enough to work as part of a team as well as an individual. I am a hard-working person who is able to manage workloads in a very busy international working environment, and who is quick to assimilate new concepts, ideas and cutting-edge technologies, while demonstrating a logical and analytical approach to solving complex problems and issues.

Education

- **PhD in Sciences (in progress)** **Sep. 2008 – Present**
University of Ghent

Ghent, Belgium

Promotor: Prof. Dr. Xavier Saelens

Funding: Flanders Institute for Biotechnology (VIB), Belgian Government

The aim of the project was to obtain camelid single chain antibodies with antiviral activity against highly pathogenic H5N1 Influenza virus, by targeting the neuraminidase. The techniques used: Recombinant Protein production, Chromatography Purification, Enzymatic Kinetic assays, Gene Cloning, Sequences Alignment analysis, Phage Libraries construction, Immunoassays, Protein Modelling, Transgenic Plant-based Vaccines, Vaccine validation in animal model in BSL-2 facilities.

- **MSc in Biotechnology (Grade 9.0 out of 10.0)** **Feb. 2006 – Jun. 2008**

Biotechnology Institute, Autonomous National University of Mexico

Cuernavaca, Mexico.

Promotor: Prof. Dr. Ramon Gonzalez Garcia-Conde.

Funding: National Commission for Sciences and Technology, Mexican Government.

The aim of the project was to study the p53 dependent apoptosis pathway during the early phase of the replication cycle of Adenovirus. The techniques used: Cell culture, Virus amplification and titration, Luminogenic assays, Western Blot, Flow Cytometry and quantitative RT-PCR.

- **BSc in Biology (Grade 8.3 out of 10.0)** **Feb. 2000 - Jan. 2006**
Autonomous University of the state of Morelos

Cuernavaca, Mexico.

Promotor: Dr. Ramón Gonzalez Garcia-Conde.

Funding: School of Sciences, Autonomous University of the state of Morelos

The aim of the study was to investigate the altered replication and localization of Adenovirus E1B gene mutants, in normal epithelial human cells. The techniques used: SDS-PAGE, Immunofluorescence microscopy.

Professional development

Present:

Full time contract as a pre-doctoral researcher (PhD in Sciences), from the Flanders Institute for Biotechnology (VIB), Belgian Government. **Sep. 2008 – Dec. 2012**

Scholarships and awards:

- Awarded a scholarship to study the Master in Sciences from the National Commission for Sciences and Technology. Autonomous National University of Mexico. **Feb. 2006 – Feb. 2008**
- Awarded a scholarship to study for the Bachelor degree from the School of Sciences. Autonomous University of the state of Morelos. **Apr. 2005 – Jun. 2005**
- Awarded a scholarship to study the High School from the Autonomous National University of Mexico. **Sep. 1996 – May. 1999**
- Awarded a scholarship for the National Contest of Academic Excellence. Mexican Government. **Sep. 1992 – Sep. 1993**

Teaching experience

- Master thesis supervision: Silve Van Den Hoecke. **Feb. 2011 – July 2011**
- Master thesis research stay: Alicja Sochacka. **Oct. 2010 – Dec. 2010**

Other experiences

- Social service. **Feb. 2004 – July 2004**
Human Cell Culture and Virus Amplification.
Tutor: Dr. Ramón Gonzalez Garcia-Conde.
School of Sciences, Autonomous University of the state of Morelos.
Cuernavaca, Mexico.
- Waiter. **Apr. 2004 – Sep. 2005**
"Las Mañanitas" Hotel and Restaurant. Cuernavaca, Mexico.
- Receipt Department. **Oct. 1999 – Sep. 2000**
Walt-Mart. Cuautla, Mexico.
- Carpentry and dining room. **Sep. 1996 – May. 1999**
"Meritorious from the Americas" High School. Mexico City, Mexico.

National and international scientific diffusion

Publication in International Scientific Journals:

- **Cardoso, F.M.**, Ibanez, L.I., De Baets, S., Smet, A., Schepens, B., Fiers, W., Myuldermans, S., Depicker, A. and Saelens, X. (2012). Camelid single chain antibodies directed against neuraminidase protect H5N1 challenged mice. In preparation.
- **Cardoso, F.M.**, Ibanez, L.I., Schepens, B. and Saelens, X. (2012). Single domain camelid antibodies that neutralize negative strand viruses. Book chapter in "**Antiviral drugs – aspects of clinical use and recent advances**". Published by InTech.
- **Cardoso, F.M.**, Kato, S., Huang, W., Flint, S.J. and Gonzalez, R.A. (2008). An early function of the adenoviral E1B 55 kDa protein is required for the nuclear relocalization

of the cellular p3 protein in adenovirus-infected normal human cells. **Virology** 378(2): 339-46.

Work Diffusion through Conferences and Presentations

- **Cardoso, F.M.**, Ibanez, L.I., Hultberg, A., Temperton, N., Vanlandschoot, P. and Saelens, X. Nanobodies® with in vitro neutralizing activity protect mice against H5N1 influenza virus. Poster presentation in the: **Fourth ESWI Influenza Conference. Malta. Sep. 2011.**
- **Cardoso, F.M.**, Ibanez, L.I., Hultberg, A., Temperton, N., Vanlandschoot, P. and Saelens, X. Nanobodies® with in vitro neutralizing activity protect mice against H5N1 influenza virus. Oral presentation in the: **Antivirals Congress 2010. Amsterdam, Netherlands. Nov. 2010**
- **Cardoso, F.M.**, Gonzalez, R.A. Studies of the p53 dependent apoptosis in the early phase of the replication cycle of Adenovirus, in normal human cells. Poster presentation in the: **V National Virology Congress, Queretaro, Mexico. Oct. 2007.**
- **Cardoso, F.M.**, Gonzalez, R.A. Analysis of the E1B 55 kDa and the E4 Orf6 Adenovirus proteins interaction on apoptosis, in presence of p53. Poster presentation in the: **IV National Virology Congress. Veracruz, Mexico. Mar. 2006.**
- **Cardoso, F.M.**, Gonzalez, R.A. “Construct your own virus”. Workshop during the **Scientific Fair of the School of Sciences. Autonomous University of the state of Morelos. Cuernavaca, Mexico. Oct. 2005.**

Personal details

Languages

- Spanish (Mother tongue).
- English. (Professional).

Interest - hobbies

- Culture: Museums and alternative ways of expression.

- Sports: Football and martial arts.
- Food: International and Mexican cuisine.
- Music: Classic rock, reggae and blues.
- Motocyclism and traveling.
-

References

Prof. Dr. R.A. Gonzalez

Cellular Biology Laboratory

School of Sciences

Autonomous University of the

state of Morelos

Cuernavaca, 62209, Mexico

Tel.: +52 777 329 7020

Fax.: +52 777 329 7040

e-mail: rgonzalez@uaem.mx

Prof. Dr. Xavier Saelens

Molecular Virology Unit

VIB Department for Molecular

Biomedical Research, UGent

'Fiers-Schell-Van Montagu' building

Technologiepark 927

B-9052 Ghent (Zwijnaarde), Belgium

Tel : +32-9-33 13 620

Fax : +32-9-33 13609

e-mail: Xavier.Saelens@dmbr.UGent.be

Acknowledgments:

The persons who gave me the opportunity to come to Belgium by the VIB international PhD program: Mark Veugelers, Marijke Lein and Jo Bury.

Specially to my Xavier Saelens for all his support and teachings, thank you for stand me...

To Prof. Fiers for his advices.

To all the people of my animal lab: Anouk, Fred, Kenny, Tine, Sara, Judith, Koen, Iebe, Liesbeth; to (Michel and Bert for all the dirty Jokes and help); the foreign mafia Farzaneh, Lei and Joon. Specially to the cutest, Silvie.

To Ann Depicker for all the support, and the molecular farming lab: Mr Nolf, Els, Annelies, Thomy, and specially to Vikram.

To Wilson Ardiles for gave me shelter and friendship.

To Itati Ibanez and Gustavo for their moral advices and true friendship.

To my carnal Ricardo and Claudia, always in so many adventures.

To my carnalation Robin and Patricia for so many experiences.

To Andres, Pepe, Fabiola for all the support.

To Peter and Maria.

To Gloria and Alien.

To my comadre Karen Vazquez.

My comadre Yadira for the good vibes...

To the DMBR people that were friendly to me: Mathias, Connor, Lars, Magdalena, Rene, Morgane, Mouna. Specially to Annelies Demeyer and Michael de Vos. To my carnal Miguel the good one...

To all the VIBes 2012 crew!!!!, specially to Tina Mueller, Lynn Elton and Nathan.

To all my Blue Family, specially the Ghent chapter: Rebel, Eddy, Johan, Bart, Stone (RIP), Scream, Luke, Kwak and Pat. Also to Dave, Jos, Koentjes, Mark, Pascal, Gabor, Chief, Walter, Bokky. 21 forever...

To Rebeca, my mother and Pui for being part of me.

Dedicated to my partner in crime, Stephanie....

Corrigendum to:

“Antiviral Activity of Camelid Single Domain Antibodies targeting the Neuraminidase of H5N1 Influenza virus”.

Author: Francisco Miguel Lopez Cardoso.

Thesis submitted in partial fulfilment of the requirements for the degree of Doctor in Sciences, Biotechnology.

Promoter: Prof. Dr. Xavier Saelens. Co-promoters: Prof. Dr. Ann Depicker, Prof. Dr. Serge Muyldermans

This corrigendum should be considered as a replacement for paragraph “N1-5-VHHm ESCAPE MUTANTS” on pages 132-134 and Figure 23 in said PhD thesis. This Figure 23 and the accompanying text were based on preliminary data and, in hindsight, ambiguous sequence data. The text and corrected figure shown below, are based on additional experiments and sequencing results, performed after the PhD thesis was submitted and successfully defended. These additional data and the resulting figure, have been published:

“Single domain antibodies targeting neuraminidase protect against an H5N1 influenza virus challenge” by: Francisco Miguel Cardoso^{1,2}, Lorena Itatí Ibañez^{1,2§}, Silvie Van den Hoecke^{1,2}, Sarah De Baets^{1,2}, Anouk Smet^{1,2}, Kenny Roose^{1,2}, Bert Schepens^{1,2}, Francis J. Descamps^{1,2#}, Walter Fiers^{1,2}, Serge Muyldermans^{3,6}, Ann Depicker^{4,5}, Xavier Saelens^{1,2}

¹VIB Inflammation Research Center, Technologiepark 927, Ghent, Belgium

²Department for Biomedical Molecular Biology, Ghent University, Technologiepark 927, Ghent, Belgium

³Structural Biology Research Center, VIB, Pleinlaan 2, B-1050 Brussels, Belgium

⁴Department of Plant Systems Biology, VIB, Technologiepark 927, Ghent, Belgium

⁵Department of Biotechnology and Bioinformatics, Technologiepark 927, Ghent, Belgium

⁶Laboratory of Cellular and Molecular Immunology, Vrije Universiteit Brussel, Pleinlaan 2, 1050 Brussels, Belgium

[§]Current address: ICT-Milstein – CONICET, Ciudad Autónoma de Buenos Aires, Argentina

[#]Current address: Ablynx NV, Ghent, Belgium

Published on *Journal of Virology* and published online ahead of print on 14 May 2014

J. Virol. doi:10.1128/JVI.03178-13

On pages 132 – 134, the text regarding N1-5-VHHm escape mutants and Fig.23 should be as following:

N1-5-VHHm escape mutants

To identify the amino acid residues involved in the binding of N1-3HHm and N1-5-VHHm to H5N1 NA, escape viruses were selected and plaque purified after serial passage of NIBRG-14 ma virus in MDCK cells, in the presence of 10 IC₅₀ of N1-3-VHHm or N1-5-VHHm, essentially as described before (1). After nine passages, candidate escape mutants were plaque purified and the NA sequences of four (N1-5-VHHm selection) and three (N1-3-VHHm selection) isolated escape viruses were determined. One of the escape viruses that was selected with N1-5-VHHm contained a mutation in the NA coding region that resulted in a change from isoleucine to threonine at position 437 in the deduced amino acid sequence (Fig 8C). This substitution is located on the NA surface, relatively close to the active site (Fig. 8A). A conserved NA epitope that is recognized by HCA-2 under denaturing conditions (2, 3) and localized within the NA catalytic site, and the amino acids necessary for binding a recently reported set of mAbs that recognize H1N1 and H5N1 NA (4) do not overlap with this N1-5-VHHm escape mutations (Fig. 8A). Sequence alignment of a set of representative N1 influenza A viruses, including human H1N1, other H5N1 viruses and an avian H6N1 virus showed that I437 is conserved in these NA sequences (Fig. 8B).

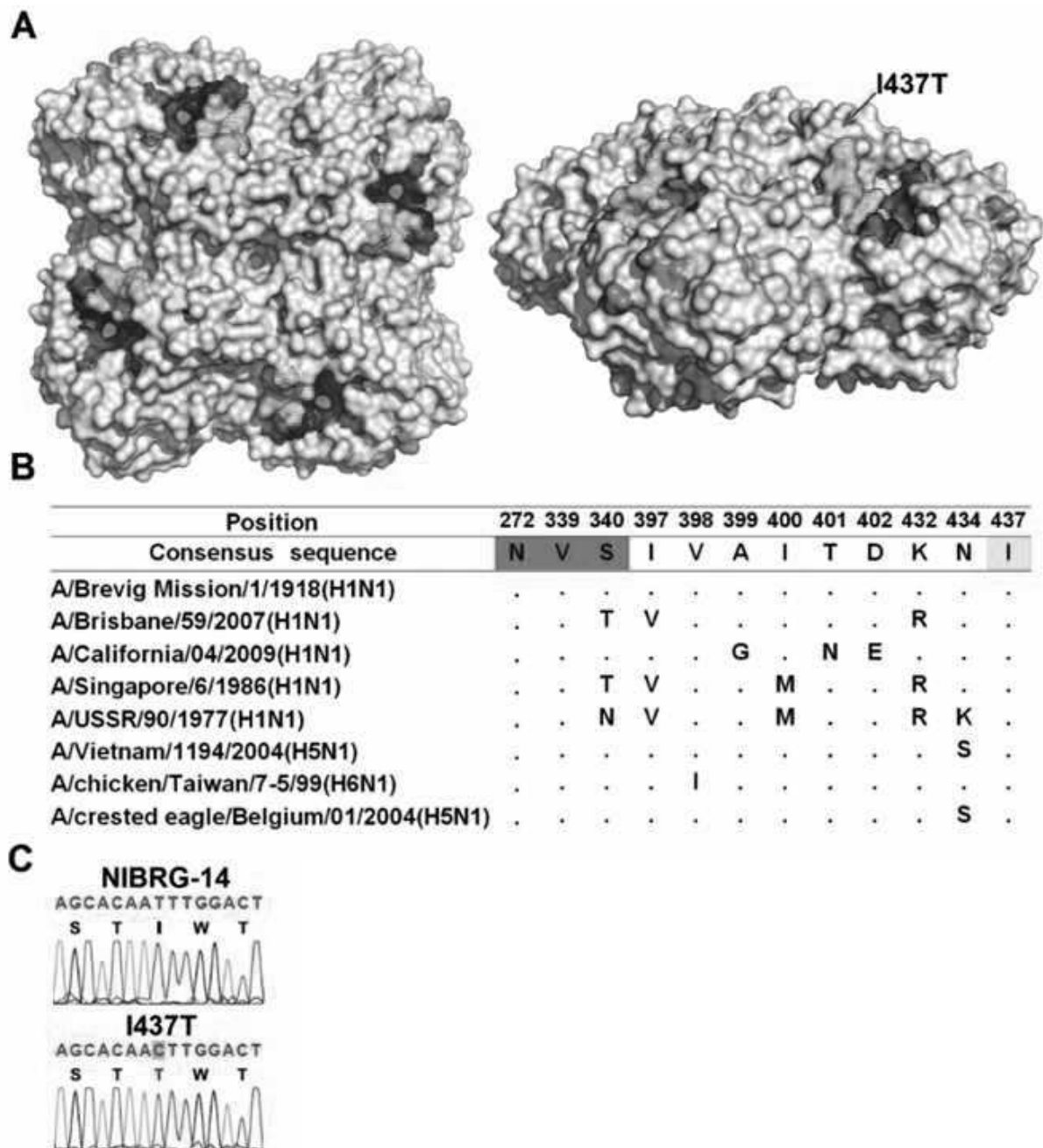


Figure 8. Epitope mapping of N1-5-VHHm escape mutants in NIBRG-14 ma NA. MDCK cells were infected with NIBRG-14 ma in the presence of 3.7 μ M N1-5-VHHm. Evidence for resistant viruses was based on cytopathic effect in infected cell culture and was followed by plaque purification of candidate escape viruses. The NA coding sequence of the resultant escape viruses was amplified by RT-PCR and sequenced. One selected escape virus carried an Ile to Thr change at position 437. The deduced amino acid sequence in NA was modeled with with PyMol (Delano Scientific, <http://www.pymol.org>) using the H5N1 NA structure derived from A/Vietnam/1194/2004 (PDB code 2HTY). A. Top (left) and later view (right) of

surface exposed amino acid residues of the NA dimer. The I437T amino acid substitution of the NA of N1-5-VHHm escape mutant is surface exposed and marked in yellow. Residues that form the catalytic site framework are depicted in red. The N1 “150 loop” is shown in green. For comparison, residues involved in mAb HCA-2 binding are shown in dark blue (residues 222–230) and those in mAb 3H10 binding in orange (N272, V339 and T340). B. Sequence alignment of relevant N1 NAs. The I437T change in one of the N1-5-VHHm escape viruses is highlighted in yellow. The residues highlighted in red are important for mAb 3H10 binding. C. Fluorogram showing the T to C substitution in the cloned cDNA of the N1-5-VHHm escape virus.

References:

1. Ibanez, L. I., M. De Filette, A. Hultberg, T. Verrips, N. Temperton, R. A. Weiss, W. Vandeveld, B. Schepens, P. Vanlandschoot, and X. Saelens. 2011. Nanobodies with *in vitro* neutralizing activity protect mice against H5N1 influenza virus infection. *The Journal of infectious diseases* 203:1063-1072.
2. Doyle, T. M., B. Jaentschke, G. Van Domselaar, A. M. Hashem, A. Farnsworth, N.E. Forbes, C. Li, J. Wang, R. He, E. G. Brown, and X. Li. 2013. The universal epitope of influenza A viral neuraminidase fundamentally contributes to enzyme activity and viral replication. *The Journal of biological chemistry* 288:18283-18289.
3. Gravel, C., C. Li, J. Wang, A. M. Hashem, B. Jaentschke, K. W. Xu, B. Lorbetskie, G. Gingras, Y. Aubin, G. Van Domselaar, M. Girard, R. He, and X. Li. 2010. Qualitative and quantitative analyses of virtually all subtypes of influenza A and B viral neuraminidases using antibodies targeting the universally conserved sequences. *Vaccine* 28:5774-5784.
4. Wan, H., J. Gao, K. Xu, H. Chen, L. K. Couzens, K. H. Rivers, J. D. Easterbrook, K. Yang, L. Zhong, M. Rajabi, J. Ye, I. Sultana, X. F. Wan, X. Liu, D. R. Perez, J. K. Taubenberger, and M. C. Eichelberger. 2013. Molecular basis for broad neuraminidase immunity: conserved epitopes in seasonal and pandemic H1N1 as well as H5N1 influenza viruses. *Journal of Virology* 87:9290-9300.